#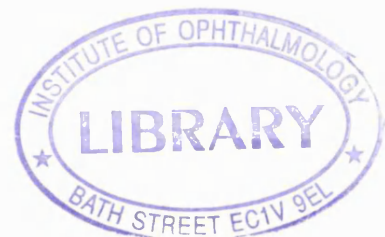 Towards positional cloning of the autosomal dominant Doyne honeycomb retinal dystrophy (DHRD) gene localised to chromosome 2p16.

Sana Kermani
B.Sc.

A thesis submitted to the University of London
for the Degree of Doctor of Philosophy

Department of Molecular Genetics
Institute of ophthalmology
University of London
Bath Street
London EC1V 9EL

September 1999

1

ProQuest Number: U538569

ProQuest U538569

Abstract

Inherited retinal dystrophies are genetically diverse with a large number of gene defects implicated in a variety of clinical phenotypes. This thesis aims to investigate the molecular genetic basis of Doyne honeycomb retinal dystrophy (DHRD) which principally affects the central retina with the aim of discovering the underlying molecular pathology of this ocular disease.

DHRD is an autosomal dominant disease that is characterised by the presence of drusen deposits in the macula of affected individuals leading to decreased visual acuity and eventually blindness.

Mapping a disease to a chromosome is a prerequisite for the application of positional cloning strategies, leading to the characterisation of candidate gene(s) and its putative protein, addressing questions of its functional role and finally studying the pathophysiology of the disease phenotype with which it is associated. A similar strategy has been applied to DHRD that was initially mapped to the 2p16-21 region using the technique of linkage analysis thus placing the disease between the interval of D2S2316 and D2S378, of approximately 5 cM. Subsequent haplotype analysis, narrowed the critical region between the interval D2S2739 and D2S378 of approximately 4 cM. The highest lod score calculated (9.49 at $\theta = 0.06$) was obtained with marker D2S378. Current genetic refinement has been achieved by haplotyping new members of the family that provided new recombination events placing the disease gene telomeric to D2S2352 and centromeric to D2S2251 in a 1 cM genetic interval. Additionally, two dominant drusen families were also mapped to the disease locus confirming the flanking markers previously published. These families did not refine the locus, but their haplotypes differed from the original DHRD haplotype, indicating the occurrence of 3 independent mutational events.

Following linkage of DHRD, the construction of a YAC contig was initiated in order to map genes in the critical region. The previous disease interval was defined by markers D2S2739 and D2S378 was spanned by a YAC tiling path of approximately 3 Mb consisting of YAC clones from three different libraries. The contig physically ordered 17 STSs in 29 YAC clones. Following the construction of the contig, 2 ESTs and a gene (D2S1848E, D2S1981E, and β-fodrin (*SPTBN1*)) were mapped to this interval.

2

As *SPTBN1* is expressed in rat retinal pigment epithelium (RPE) it was considered to be a good candidate gene to screen for DHRD. Thus immediate work concerned screening a partial region of *SPTBN1* and mapping ESTs in the region in the hope of discovering the disease causative gene for DHRD. This work was later pre-empted due to the genetic refinement of the disease, excluding *SPTBN1*, D2S1848E and D2S1981E from the critical region. Meanwhile, PACs were isolated to reinforce the YAC contig and to provide non-chimaeric clones in a relatively narrow genetic region (between markers D2S2352 and D2S2251, of approximately 1 cM). Following the exclusion of obvious candidate genes a retinally expressed EST (WI-31133) was mapped to the refined genetic region.

Subsequent work involved genomic characterisation of this gene in order to screen for mutations in the DHRD family and dominant drusen families in this region. The full-length coding sequence of this gene was capable of translating one exon which was screened but failed to reveal any single base pair mutations or polymorphism. Interestingly, a single variant (Arg345Trp) in the *EFEMP1* has been demonstrated as the disease-causing gene for DHRD and Malattia (Stone *et al.*, 1999). Although this change has been verified in the DHRD family, this gene lies external to our recent genetic refinement. It is proposed that this change is probably due to a polymorphism that was present in a common ancestor. Thus further work must be performed to reinforce that that *EFEMP1* is the gene for DHRD. We are currently awaiting blood samples from a Japanese family that are affected with DHRD. It is of interest to screen their DNA with exon 10 of the *EFEMP1* gene to demonstrate whether they possess the disease-causing (Arg345Trp) variant. If the affected individuals do not demonstrate this change, then the entire coding region of the *EFEMP1* gene must be screened in search of a second mutation, thus reinforcing that is *EFEMP1* the disease-causing gene for DHRD.

Declaration

I declare that this thesis submitted for the degree of Doctor of Philosophy is my own composition and save as otherwise stated the data presented herein is my own original work.

Sana Kermani B.Sc.

Dedication

I dedicate this thesis to my parents who have faced some hard times and had to live separately to provide me with the best; something they could not achieve themselves.

I hope you are proud of me.

Acknowledgements

Publications

Kermani, S., Gregory-Evans, K., Tartellin, E.E., Bellingham, J., Plant, C., Bird, AC., Fox, M., Bhattacharya, S.S., and Gregory-Evans, C.Y. Refined genetic and physical positioning of the gene for Doyne honeycomb retinal dystrophy (DHRD). 1999 *Hum Genet,* **104 (1),** 77-82.

Kermani, S., Evans, K., Bhattacharya, S.S., and Gregory, C.Y. Genetic refinement of the Doyne's honeycomb retinal dystrophy (DHRD) spanning the disease region. 1997 *Am. J. Hum. Genet.,* **61(4),** 1377.

Evans, K., Gregory, C.Y., **Kermani, S.,** Bhattacharya, S.S. and Bird, A.C. Doyne honeycomb retinal dystrophy (DHRD): Genotype-phenotype correlation. 1997 *IOVS,* **38(4),** 3681.

Evans, K., Gregory, C.Y., Wijesuriya, S.D., **Kermani, S.,** Jay, M.R., Plant, C. and Bird, A.C. Assessment of the phenotypic range seen in Doyne honeycomb retinal dystrophy. 1997 *Archives of Ophthalmology,* **115(7),** 904-910.

Gregory, C.Y., Evans, K., Wijesuriya, S.D., **Kermani, S.,** Jay, M.R., Plant, C., Cox, N., Bird, A.C. and Bhattacharya, S.S. The gene responsible for autosomal dominant Doyne's honeycomb retinal dystrophy maps to chromosome 2p16. 1996 *Hum. Mol. Genet.,* **5(7),** 1055-1059.

Table of Contents

List of figures

16

List of tables

Amino acid codes

Amino acid	Three letter abbreviation	One letter symbol
Alanine	Ala	A
Argnine	Arg	R
Asparagine	Asn	N
Aspartic acid	Asp	D
Asparagine or aspartic acid	Asx	B
Cysteine	Cys	C
Glutamine	Gln	Q
Glutamic acid	Glu	E
Glutamine or glutamic acid	Glx	Z
Glycine	Gly	G
Histidine	His	H
Isoleucine	Ile	I
Leucine	Leu	L
Lysine	Lys	K
Methionine	Met	M
Phenylalanine	Phe	F
Proline	Pro	P
Serine	Ser	S
Threonine	Thr	T
Tryptophan	Trp	W
Tyrosine	Tyr	Y
Valine	Val	V

19

CHAPTER 1

Introduction

1.0   General introduction

The work presented in this thesis describes an approach to the positional cloning of a gene responsible for an autosomal dominantly inherited disease called Doyne honeycomb retinal dystrophy (DHRD). In the following sections an overview of the basic genetic concepts behind the project will be described emphasising strategies employed for identification of disease genes through a positional cloning approach. The contents are presented in an orderly fashion providing a detailed outline of the structure and physiology of the retina, the photochemistry of visual transduction, retinal disorders of the macula and advances made in the field of retinal degeneration research with the advent of recombinant DNA technology.

All molecular genetic projects of this kind contribute to the scientific understanding of the human genome and biology. Successful identification of a gene predisposing to human illness allows an insight into the understanding of that disease that opens avenues for further development of diagnostic tools and therapeutic progression for patients. At present all positional cloning projects are essentially in symbiosis with the collaborative international effort known as the Human Genome Mapping Project and have been accelerated due to many technologies that have arisen from this colossal project.

1.1   The Human Genome Project

The Human Genome Project is a leading internationally co-ordinated effort in the history of biological research. The goal is to determine the complete nucleotide sequence of the nearly 3 billion base pairs of DNA that constitutes the human genome, thus identifying the 100 thousand or so genes that define the human genome. The project was initiated in the late 80's and was intended as a three-step program to produce genetic maps, physical maps and ultimately the complete sequence of the genome by the year 2005. The first two mile stones have essentially been reached and sequencing project is well under way (Lander, 1996).

While achieving these goals the human genome project has been responsible for the development of several molecular biology techniques and reagents. Polymorphic DNA markers, dense genetic maps, variety of cloning vectors and physical maps that were developed as prerequisite to obtaining the entire human genomic sequence have been essential for many positional cloning projects and also constitute their driving forces. The greatest advantage is that this information is easily accessible via the Internet. Several electronic databases have been established to record the genetic and physical mapping information that is continuously generated. The central data resource for the human gene mapping effort is the Genome Data Base (GDB), which collects, organises, stores and distributes human genome mapping information and also offer interaction with other data bases maintained by major laboratories i.e. Généthon/CEPH and Co-operative Human Linkage Centre (CHLC).

In light of the work presented in this thesis that describes a positional cloning approach, it is only appropriate to analyse the progress of the Genome Project. Hence, the following sections describe the concept of linkage analysis, the use of polymorphic markers to localise disease genes, the evolution of polymorphic DNA markers, genetic maps and physical maps will be described.

1.2 Single gene disorders mapped by linkage analysis

1.2.1 Classical linkage analysis

The arrangement of genes on the chromosome of an organism can be determined by following the segregation pattern of two variable phenotypic traits through successive generations and analysing how frequently the different forms of the two traits are co-inherited. From this study, it can be deduced whether the genes for the two traits are on the same chromosome (linked) or located on separate chromosomes. For the latter case Mendels law of independent assortment applies, resulting in a 50% recombination rate of phenotypic traits since the chromosomes on which the genes reside are inherited independently. Linked pairs of genes or loci are co-inherited and there is a deviation from the independent assortment of traits, and any recombinants observed are due to meiotic events called cross overs. During meiosis the homologous chromosomes align allowing the exchange of corresponding segments of DNA between non-sister

chromatids. This process leads to formation of gametes that possess chromosomes containing new combinations of alleles, or recombinant chromosomes. Progeny resulting from these gametes are known as recombinants due to their recombinant phenotypic traits.

1.2.2 Recombination fraction (θ), genetic distance and order

Cross over events are more likely to occur between loci that are far apart than between two loci close together on the same chromosome (syntenic). Therefore the recombination fraction (θ), which is the probability of producing a recombinant, is related to the genetic distance separating the loci of the linked genes. These distances are measured in map units (m.u) referred to as 'centi-Morgans' (cM), where 1 cM is equal to a 1% chance of recombination between two loci during a meiotic event. This simple relationship only applies when the genetic interval is too small to allow multiple cross over events, which in reality do occur between loci that are further apart. Therefore mapping functions that relate recombination fraction with genetic distance have been derived to take in to account such multiple cross over events and also the phenomenon of interference. Interference is the negative effect of an already existing crossover has on the formation of a second one nearby. The Kosambi mapping function (1944), which takes interference and multiple cross over events into account, has been widely used in human genetic calculations since it produces more realistic map distance values.

Recombination fractions derived for linked pairs of loci can also be used to produce linkage groups. A linkage group is a set of gene pairs, each of which has been linked to at least one other member in the set. Since recombination fraction increases with the distance separating the loci of the two gene pairs, it can be used to derive the order of linked loci and produce a linkage map for a given chromosome.

1.2.3 Polymorphic DNA marker used as a tool for linkage analysis

Linkage analysis is mainly used for the mapping of inherited diseases, which are prominent among the variable single-gene traits of humans. It differs from classical linkage analysis in that at the end, linked loci are also given a "genomic address" or an actual physical location in the genome, as well a linkage order. In order to do so, linkage

analysis employs the use of a large number of polymorphic DNA markers of known genomic localisation, in a random search throughout the genome in a particular family within which the disease segregates. Polymorphic markers are variable regions in the DNA that exhibit a limited number of sequence variations (or alleles) among the population. The purpose of such a genome scan is to detect co-segregation between the disease locus, represented by the disease phenotype, and an allele of a DNA marker. Establishing such segregation of a known marker locus with the disease phenotype will infer linkage between the two loci and therefore localise the disease to the region where the marker maps. Once linkage has been established, more DNA markers that map at close proximity to the disease locus are typed in the family to establish a haplotype, which is the combination of alleles at the linked locus. It is easy to identify a haplotype for the disease phenotype, as they should co-segregate. Moreover any recombination events that occur during meiosis in the affected parent would be reflected in the haplotype of the resulting offspring. This would lead to refinement of the disease locus provided that the offspring still has the disease phenotype.

1.2.4 Statistical evaluation of linkage

The conventional approach to evaluate whether two given loci are linked is to apply the maximum likelihood analysis (Morton, 1955). This estimates the "most likely" value of the recombination fraction (θ) as well as the odds in favour of linkage versus non-linkage. The ratio of likelihood or the odds ratio is the ratio of the probability of observing a segregation pattern of two loci if they are linked at a given recombination value (θ) where $\theta < 0.5$, versus the probability of such segregation if they are not linked ($\theta = 0.5$). This ratio is calculated at a series of recombination values (from $\theta = 0$ to $\theta = 0.5$). The logarithm of the odds ratio called the lod score (Z) is what geneticists normally use to report results of linkage analysis. These calculations can be summarised in the following equation

$$Z\ (\theta) = Log_{10}[L(\theta)/L(0.5)]$$

Where:

L (θ) = the likelihood of obtaining the data if the two loci are linked and have a recombination fraction of θ

L (0.5) = the likelihood of obtaining data when the two loci are unlinked

The recombination value that gives the maximum lod score (Z) is the best estimate of the degree of linkage between two loci. Positive lod scores suggest the presence of linkage and a lod score of 3, which corresponds roughly to 1000 to 1 odds that two loci are linked, or higher is considered definitive evidence for linkage. Similarly a negative lod score of –2 at a given θ value is regarded as evidence against linkage within an interval equal to θ from either side of the marker locus.

1.2.5 Markers used in linkage analysis

The advantages of polymorphic markers and their value for mapping genes were discussed in the previous sections. To conduct a cost effective linkage analysis it is fundamental to have genetic maps, which are dense in informative DNA markers. The nature of naturally occurring DNA polymorphism used in linkage analysis has changed dramatically over the years. Before the advent of recombinant DNA technology, linkage studies were performed using blood group and other biochemical (protein) polymorphisms.

1.2.6 RFLPs and mini satellites

Recombinant DNA technology enabled the definition of a variety of scorable DNA polymorphisms. The first such DNA polymorphisms to be detected were differences in the length of DNA fragments after digestion with sequence specific restriction endonucleases, the so called restriction fragment length polymorphisms (RFLPs) (Botstein *et al.*, 1980). RFLPs were based on a variety of polymorphisms at the sequence level such as single nucleotide changes, insertions and deletions. Then came the variable number of tandem repeat polymorphisms (VNTRs), also known as minisatellites, which are due to variation in number of head to tail repeats, usually >10bp, at a given locus (Jeffreys *et al.*, 1985). RFLPs and VNTRs were both assayed by

southern blotting (Southern *et al.*, 1975) followed by hybridisation with the specific DNA probe.

The most useful markers in linkage analysis are those that are very polymorphic with a high heterozygosity value. Heterozygosity of a marker is directly proportional to the number of alleles each marker exhibits and the frequency of each allele in the general population. In this the multi-allelic VNTRs have the advantage over RFLPs, which are usually bi-allelic. But VNTRs do not have as even a distribution in the genome as RFLPs, as they are more frequent at telomeric ends of chromosomes. The first RFLP map of the human genome produced by Donis-Keller *et al.* (1987) was a landmark publication. It characterised 393 RFLP loci with an average spacing of 10 cM. Given that the human genome is approximately 4000 cM in length, the distance between each RFLP was 10Mb (on average 1 cM approximates 1 Mb of DNA across the human genome) on average, which was too great to be of use for gene isolation. Nevertheless, these markers made human molecular genetics a reality and led to the mapping of number of important Mendelian diseases. To overcome the limitations posed by RFLPs new generation of markers, with high incidence and greater informativeness were identified. These markers known as microsatellites not only fulfil both criteria required of an ideal DNA marker for linkage analysis, they could also be assayed by PCR thus obviating the need for laborious and time consuming blotting techniques.

1.2.7   Short Tandem Repeat polymorphisms (STRP)

Microsatellites are tandem repeats of simple sequence that occur abundantly and at random throughout most eukaryotic genomes with the exception of yeast (Weber and May, 1989; Litt and Luty, 1989). In human 76% of repeats are of the types A, AC, AAAN, AAN or AG, in decreasing order of abundance (Beckmann and Weber, 1992). On average AC is the most common type of microsatellite as they occur on average every 30 kb. The CA repeats are equally distributed in the 5'- and 3'-untranslated regions and introns. The informativeness of a microsatellite marker is indicated by its polymorphic information content (PIC). The PIC value of a marker is calculated from the number of alleles and their frequencies in the population and is related to the mean repeat length of the marker (Weber, 1990). For use in linkage analysis the PIC of a

microsatellite must be >0.7. The equation to calculate the PIC value is given below, where p_i and p_j are population frequencies of the ith and the jth alleles.

$$PIC = 1 - \left(\sum_{i=1}^{n} p_i^{2}\right) - \sum_{i=1}^{n-1} . \sum_{j=i+1}^{n} 2 p_i^{2} p_j^{2}$$

$$Heterozygosity = 1 - \left(\sum_{i=1}^{n} p_i^{2}\right)$$

The abundance and ease of typing by PCR has made microsatellites ideal genetic markers for linkage analysis. Furthermore, the advent of fluorescent labelling technology has enabled the typing of several markers in a single run (multiplex PCR) leading to lower costs and a greater degree of automation of marker typing (Ziegle *et al.*, 1992). Several genetic maps composed of microsatellites have been published, and the publication of the final Généthon map in 1996 marked the end of genetic mapping phase of the Genome mapping Project (Dib *et al.*, 1996).

Even though microsatellites are seen as the best DNA markers, the need to run electrophoretic gels to separate microsatellite marker products by size makes it hard to fully automate the genotyping process. Improvements can still be made in mapping technology and the answer may be provided by the use of single nucleotide polymorphisms, which could be scored by DNA chip technology, which may enable complete automation of linkage analysis.

1.2.8 Single nucleotide polymorphisms (Biallelic markers)

Lately, attention has focused on the use of single nucleotide polymorphisms (SNPs) as genetic markers where, the polymorphism is based on a single nucleotide change at the DNA sequence level. SNPs only have two alleles, hence the term biallelic, therefore genotyping them only requires a plus/minus assay. Biallelic markers vary in their polymorphism rates, the common allele could range in frequency from 50% to

26

nearly 100% (Kruglyak, 1997). At first glance it appears to be a step back in to the days of low polymorphism rates characteristic of RFLPs. However modern technology is said to allow efficient assays of SNPs in sufficient numbers to overcome the low polymorphism rates (Kruglyak, 1997). The main advantage offered by SNPs over microsatellites is their great abundance in the genome, which is estimated to be 1 every kilobase pair, and also the fact that the assay technique is more amenable for automation. To overcome the lower polymorphism rates of SNPs, maps based on SNPs need to be denser than maps of microsatellite markers (Kruglyak 1997). On the whole, maps of biallelic markers need to be about 2.25-2.5 times the density of microsatellites to provide a comparable information content.

As yet facts do not argue in favour of SNPs but with improvements in technology, screening of denser biallelics may prove to be more cost effective than the use of microsatellites. These dense maps could be used for homozygosity mapping and would also enable genome scans for linkage disequilibrium (LD) and association required for the analysis of complex genetic disorders. The most promising outlook for biallelics is the fact that functional biallelic polymorphisms, found within coding regions of genes, can be included for direct association studies for both monogenic and polygenic disorders.

1.2.9   Evolution of genetic maps and future prospects

Genetic markers and maps of human chromosomes are essential for localising Mendelian traits and disease-susceptibilty genes to precise chromosomal regions. Since 1987 several genetic maps have been published. The "genetic composition" of these maps has changed with the evolution of polymorphic markers. The early maps had uneven coverage, with larger gaps especially at the telomeric and centromeric regions of most chromosomes. However with the development of more markers, the marker density gradually increased to meet the final goal set by the Human Genome Mapping Project, which was to have a genetic map of 1cM density. Table 1.1 summarises the evolution of these genome maps.

Early maps were composed of RFLP or VNTR polymorphisms detected by DNA hybridisation (Donis-Keller *et al.*, 1987). Some maps integrated RFLP and VNTR

markers with microsatellites (STRPs) (NIH/CEPH Collaborative Mapping Group 1992). The most recent publications of genetic maps of the human genome have been composed entirely of microsatellites or STRPs. The three genome maps published by Généthon stand as the best example (Weissenbach *et al.*, 1992; Gyapay *et al.*, 1994; Dib *et al.*, 1996). Apart from this, other groups have also created genome maps from independent collection of markers (The Utah Marker Development Group, 1994).

The lack of integration was the major draw back with maps created independently. In principle marker data from individual laboratories can be used to integrate genetic maps, provided that they have been genotyped using a common set of reference families. The most widely used set of reference families is that distributed through CEPH (Centre d'Etude du Polymorphisme Humaine). In the beginning two integrated maps were published by NIH/CEPH collaborative mapping group (1992) and Cooperative Human linkage Centre (CHLC) using the CEPH reference panel (Buetow *et al.*, 1994). However these maps became outdated as soon as they appeared in print due to the rapid pace of new marker development within the human genetic community. Integration of markers has now become easier with the increased physical map information for these markers from independent sets. Since markers from different sources are being extensively integrated into a physical map by means of radiation hybrid panels and overlapping YAC clones, more integrated maps are now available for each chromosome through electronic sources such as the World Wide Web (WWW). CEPH/Généthon (http://www.genethon.fr/genethon-cu.html) Whitehead Institute for Biomedical Research/MIT Centre for Genome Research (http://www-genome.wi.mit.edu/), Sanger Centre (http://webace.sanger.ac.uk/HGMP/) and Stanford Human Genome Centre (SHGC) (http://shgc-www.stanford.edu) can be sited as being some of the main Genome Centres, which offer collated mapping information most essential to gene hunters.

Year	Marker type	Average resolution (cM) and Total map distance	Total no Of markers	Mapping group	Reference
1987	RFLP+VNTR	10 cM	403 (393RFLP)	Collaborative Research	Donis-Keller *et al.*, 1987
1992	(CA/TG)n	4.4 cM 3576 cM	814	Genethon	Weissenbach *et al.*, 1992
1992	RFLP/(CA)n	<5 cM	1416 (279 genes)	NIH/CEPH	NIH/CEPH Collaborative Mapping Group, 1992
1994	(CA/TG)n	4.9 cM 4798.3 cM	1123	CHLC	Buetow *et al.*, 1994
1994	(CA/TG)n	2.9 cM 3690cM	2066	Genethon	Gyapay *et al.*, 1994
1996	(CA/TG)n	1.6 cM 3699 cM	5264	Genethon	Dib *et al.*, 1996

Table 1.1:

The evolution of genetic maps.

The evolution of these dense and highly informative genetic maps has been most beneficial for mapping of susceptibility loci involved in complex traits such as juvenile onset diabetes, schizophrenia and hypertension. They also provide a key tool for positional cloning of disease genes by providing ready access to all chromosomal regions, moreover such a map is a necessity in order to obtain the complete genomic sequence. Even though the genome-mapping phase is essentially complete, marked by the publication of the last Généthon map, with the development of SNPs, the genetic mapping arena still appears to be dynamic. So the next question is whether a high-density map based on SNPs will replace the current genetic map?

1.3   Mapping of genes for recessive disorders

Although conventional linkage mapping can be applied to recessive disorders, the following section describes an alternate approach.

1.3.1   Homozygosity mapping

Mapping of autosomal dominant disorders through traditional linkage analysis has been discussed previously. For mapping of recessive disorders a different approach is used, which obviates the use of traditional family mapping, referred to as homozygosity mapping (Lander and Botstein, 1987). It requires polymorphic markers of high heterozygosity and DNA of affected children from consanguineous marriages. The

29

method essentially involves the detection of the disease locus by virtue of the fact that the adjacent region will preferentially be homozygous by descent in such inbred children. The main advantage of homozygosity mapping is that it provides a way to map a recessive disease even when families with multiple affecteds are scarce. When affected individuals from different families are used in the analysis, the disease is assumed to be homogeneous i.e. caused by mutation at a single locus.

Given the fact dense maps of highly polymorphic markers are now available they facilitate the detection of homozygosity by descent, by detecting regions in which a contiguous stretch of markers are homozygous. Specifically homozygosity mapping would be performed as follows. To test the hypothesis that the disease gene maps to a given interval, the DNA of each affected inbred child is examined for homozygosity at say six consecutive loci, three on either side of the interval. Then for each possible outcome, the probability of it occurring due to linkage (P_1) and chance (P_2) is calculated. In which case the odds ratio in favour of linkage is $P_1 : P_2$. Computer programs called HOMMAP has been develop to do these calculations (Lander and Green, 1987)

1.4 Physical mapping

The path from the closely linked genetic marker to the gene is laborious and requires physically mapping techniques. A physical map is a representation of the locations of identifiable landmarks on DNA. Physical mapping technologies can be categorised according to the level of resolution achieved with each technique, the complete sequence of the genome being the physical map of the highest possible resolution or greatest molecular detail. An arbitary distinction is made between the two classes of physical mapping (low and high resolution physical mapping, see proceeding sections). The physical mapping phase of the Human Genome Project has been responsible for the development and improvement of many of these techniques, therefore this section will be dedicated to the detailed description of a variety of these methods giving close attention to those techniques of more recent evolution.

1.4.1 Low resolution physical mapping

This is the smallest map unit that can be resolved and is typically one to several megabases of DNA (cytogenetically). The traditional methods of physical mapping to complement genetic localisation have been cytogenetic techniques, which include the use of somatic cell hybrids (rodent-human hybrid cells) and *in situ* hybridisation. Although considered traditional both techniques in recent times have improved considerably.

1.4.2 Cytogenetic techniques

Somatic cell hybrids are formed by fusing the cells of the two different species and applying conditions that select against the two donor cells. If hybrid cells are grown under non-selective conditions after the initial selection, chromosomes from one of the parents tend to be lost more or less at random. In the case of human/rodent fusions, which are the most common, the human chromosomes are preferentially lost. In this manner rodent cell lines containing one or a few human chromosomes have been constructed. Such rodent-human hybrid cell lines that contain individual human chromosomes in whole or part can localise a marker of interest to the level of a cytogenetic band on a chromosome and provide mapping at a resolution of about 10 Mb. Individual chromosomes can also be tagged with selectable genes (i.e. thymidine kinase gene that allows growth in HAT medium) (Tunnacliffe *et al.*, 1983; Saxon *et al.*, 1985), fractionated by separation into microcells, and fused with rodent cell lines. Selection allows for the recovery of hybrid cell lines with a choice of intact chromosome (Warburton *et al.*, 1990). These chromosomes maintain their integrity and can be propagated indefinitely and can also be subfractionated by the introduction of interstitial or terminal deletions by radiation (Dowdy *et al.*, 1990). Development of chromosome or chromosomal region-specific libraries and *in situ* hybridisation analysis are some of the uses of hybrid cell lines. Further extensions of hybrid cells are the radiation hybrids used to generate genetic/physical maps at increasing levels of resolution.

In situ hybridisation allows comparison to be made between high-resolution physical map such as contigs assembled from cloned DNA and the genetic linkage map. Provided that hybridisation to repetitive sequences is suppressed and that no DNA chimaeras are present, a cloned fragment or restriction fragment should anneal to a single

31

location on the cytogenetic map. Furthermore, the physical map order should match that found by *in situ* hybridisation. Where genetic markers have been located on the cytogenetic map by in situ hybridisation they also can be positioned on the physical map. Conventional fluorescent *in situ* hybridisation (FISH) as applied to metaphase chromosomes has a resolving power of approximately 1 Mb. For higher resolution mapping, FISH has been applied to interphase cell nuclei where DNA is less condensed than in metaphase chromosomes, which permits resolution in the 50-100 kb range (Trask *et al.*, 1989,1991). A new technique has been developed that allows even greater resolution (Parra and Windle, 1993) combination of this procedure with differential fluorescent labelling of individual probes enables the arrangement of DNA probes along an extended strand of DNA to be observed. The images observed are recorded through a fluorescent microscope and used to construct a direct visual hybridisation (DIRVISH) DNA map. DIRVISH mapping has been used to determine orientation and distance between two different cosmid clones and have facilitated chromosome walking.

1.4.3 Pulse-field Gel Electrophoretic mapping

Physical maps have been constructed in the mega base range with the use of pulsed-field gel electrophoresis (PFGE) (Schwartz and Cantor, 1984), which allows the separation of DNA molecules as large as 10 Mb, and rare cutting restriction enzymes such as *Sfi*I and *Not*I. Markers which hybridise to a common restriction fragment of DNA separated by PFGE gel are assumed to be linked and a restriction map of a region can be constructed in this manner provided that the region of interest has an adequate supply of markers and the cutting sites of the enzyme are conveniently spaced. Such long range restriction maps have successfully been constructed of the 12 Mb Cystic Fibrosis (CF) region (Fulton *et al.*, 1989) and the Duchenne muscular dystrophy (DMD) locus (Burmeister *et al.*, 1988). The complications associated with this technique are comigration of fragments and the partial methylation of sites for many methylation-sensitive restriction enzymes in uncloned human DNA. However the major limitation of this method is that it does not provide the DNA in the form that facilitates further study and this technique is now mostly used for further analysis of 'contigs' assembled from cloned DNA.

1.4.4 High resolution physical mapping

The mapping resolution is typically high resulting in several hundreds of kilobases to a single nucleotide. Physical mapping at high resolution involves the assembling of cloned DNA fragments in the same linear order as found in the corresponding chromosomal DNA and such an assembly is described as a 'contig'. In the human genome-mapping endeavour the ultimate purpose of this process is to sequence the overlapping fragments of DNA and obtain the physical map at its highest possible resolution i.e. the DNA sequence of the entire genome. However in a positional cloning endeavour the purpose of contig construction across a candidate interval is to have the genomic segment that harbours the disease gene in an accessible form for subsequent use in gene identification protocols. There are several aspects to physical mapping, which include the choice of vector for cloning, the methods for assembling clones and detecting overlaps between the assembled DNA fragments.

1.4.5 Yeast Artificial chromosomes (YACs)

Many different types of vector have been developed to propagate DNA, to enable it to be mapped and ultimately sequenced. Yet only a few are suitable for large scale mapping projects. The early human genomic libraries were constructed in bacteriophage λ and cosmid vectors both hosted in *E. coli* with respective insert capacities of 25 and 50 kb (Murray, 1986; Whittaker *et al.*, 1988). While the cloning efficiency of these systems was high they were also associated with several disadvantages. These included the requirement of a great number of clones to cover a given human region and unclonability of certain human sequences such as repetitive sequences. The advent of the second high molecular weight DNA cloning system, Yeast Artificial Chromosomes (YACs), greatly expanded the ability to clone and characterise large segments of DNA since fragments as large as 1 Mb in size could be isolated (Burke *et al.*, 1987; Anand *et al.*, 1990). Despite the many advantages of YACs, low cloning efficiencies, difficulties in isolating cloned DNA and chimaeric cloning artefacts have led to the development of other large-fragment cloning systems to supplant YACs.

33

1.4.6 P1 Alternative vectors to YACs

1.4.6.1 The bacteriophage P1 cloning system

The P1 cloning system complements cosmid and YAC cloning systems by offering an intermediate range of clonable genomic fragment sizes along with the ability to isolate from *E. coli* large amounts of plasmid DNA by standard molecular techniques. Furthermore unlike YAC clones P1 clones are also less prone to chimaerisms (Sternberg, 1994). The P1 vector system, based on the P1 bacteriophage that mediates generalised transduction, contains a packaging site (pac) necessary for in vitro packaging of recombinant molecules into phage particles and two *lox*P sites. These sites are recognised by the phage recombinase; the product of the host *cre* gene, and lead to the circularisation of the packaged DNA after it has been injected into an *E. coli* host expressing the recombinase. The clones are maintained in *E. coli* as low copy number plasmids by selection for a vector kanamycin-resistance marker. However, high copy number can be induced by exploitation of the P1 lytic replicon (Sternberg, 1990). The original cloning vector p*Ad*10 employs a unique *Bam*H1 site for the insertion of genomic fragments as large as 100 kb. The second-generation vector p*Ad*10-*sac*BII also contains rare cutting restriction sites and T7 and SP6 phage promoters that directly border the *Bam*HI cloning site. These elements are useful for the isolation, characterisation and analysis of plasmid DNA from P1 clones (Sternberg, 1990, Pierce *et al.*, 1992). The limitation of co-cloning events (found in YACs) due to the ability of P1 phages to package DNA by a headful mechanism and the recovery of cloned DNA in a pure form are other attractive features of P1 vector system. However since P1 phage amplifies in bacteria, as with cosmids, certain regions may also be difficult to clone in P1 vector.

1.4.6.2 Bacterial Artificial Chromosomes (BACs)

The BAC vector (Shizuya *et al.*, 1992) is based on the single-copy sex factor F of *E. coli* and includes the λ cosN and P1 *lox*P sites, two cloning sites (*Hind*III and *Bam* HI) and several restriction enzyme sites for potential excision of the inserts. Similar to P1 clones the cloning site is also flanked by T7 and SP6 promoters for generating RNA probes. BACs can be transformed into *E. coli* very efficiently without the use of packaging extracts required for the P1 system. Moreover reports claim that BACs are

34

capable of maintaining human and plant genomic fragments of greater than 300 kb for over 100 generations with a high degree of stability (Woo *et al.*, 1994). However currently there are two disadvantages associated with BACs. First, as yet there is no method for positively selecting clones with foreign DNA inserts and secondly it is difficult to isolate large amounts of DNA.

1.4.6.3 P1- derived artificial chromosomes (PACs)

PACs developed by combining features of both P1 and F-factor systems (Ioannou *et al.*, 1994) can handle inserts in the 100-300 kb range. As yet no chimaeras or clone instability have been reported for this vector. The advantages with the use of this vector are ease of manipulation and isolation of insert DNA in moderate quantities.

1.4.7 Contig assembly

There are several methods for assembling contigs, which include more traditional methods such as chromosome walking and restriction enzyme fingerprinting and more popular methods such as marker sequence and hybridisation assays.

1.4.7.1 Chromosome walking

This was originally developed for the isolation of gene sequences whose function is unknown but whose genetic location was known, i.e in positional cloning ventures (Bender *et al.*, 1983). The principle of this method is as follows. For the purpose of map generation a single cloned fragment is selected and used as a probe to detect other clones in the library with which this clone will hybridise and therefore represent clones overlapping with it. The overlap could be in both direction and this single walking step is repeated many times with the newly identified clones to extend the contig. A potential problem with chromosome walking is created by the existence of repeated sequences, which will lead to the isolation of non-contiguous fragments with a clone that contain such sequences. Hence, probes used for stepping from one genomic clone to the next must be a unique sequence clone. Furthermore use of large fragments of DNA for walking also minimises the number of steps required to achieve coverage of a given region. Although inherently attractive, chromosome walking is too laborious and time

consuming to be of value for mapping whole genomes. Therefore other methodologies have been developed as alternatives to chromosome walking.

1.4.7.2 Restriction enzyme fingerprinting

The principle of restriction enzyme fingerprinting was originally developed for the nematode *Caenorhabditis elegans* (Coulson *et al.*, 1986) and yeast (Olson *et al.*, 1986) and has been successfully used for the mapping of the *E. coli* genome (Kohara *et al.*, 1987). The original fingerprinting method devised by Coulson *et al.* (1986) is as follows. Cloned DNA is first digested with a 6 base pair cutter that leaves staggered ends (e.g. *Hind*III) and labelled by end-filling. After deactivation of the original enzyme the fragments are re-cleaved with a restriction enzyme with tetranucleotide recognition sequence (e.g. *Sau*3A), followed by separation on a high-resolution gel and detection by autoradiography. The fingerprint is prepared by determining the size of each band from each clone. In the fingerprinting technique used for mapping *E. coli*. Each clone within the genomic library of *E. coli* was restriction mapped using eight different restriction enzymes and the resulting restriction fingerprint of each clone was compared with that of all other clones. Overlapping clones were detected on the basis of a match of at least five consecutive cleavage sites. In the two previous methods two clones had to overlap at least 50% in order to declare with a high degree of certainty that the clones do indeed overlap and was a significant rate limiting factor in map completion. It was soon realised that increasing the information content in each clone fingerprint would enable the detection of small overlaps and therefore increase the rate at which the contigs increase in length. As a result in the whole human genome approach of Bellanné-Chantelot *et al.* (1992) used a different method for assembling contigs. To enable small overlaps to be detected YAC clones were digested by *Pvu*II separated by gel electrophoresis and a fingerprint was prepared by hybridisation with probes prepared from a LINE-1 repeated sequence and an *Alu* consensus sequence. Overlaps between YACs are identified by observation of fragments of the same size in the two YACs.

However there are a number of disadvantages with the fingerprinting approach. It is highly labour intensive and involves extensive handling of clones. Although the method generates large number of small contigs it is increasingly difficult to extend and

join these contigs. Finally the method only works well with phage clones but gives poor results with YACs and is susceptible to chimaera problems. Therefore restriction fingerprint mapping was superseded by sequence tagged sites (STSs) mapping.

1.4.7.3 STS content mapping

The concept of sequence tagged site was first developed by Olson *et al.* (1989) in an attempt to systematise landmarking of the genome. An STS is a short region of DNA about 200-300 bases long whose sequence is unique to the target region. The idea behind STS content mapping is simple, if two or more clones contain the same STS then they must overlap and the overlap must include the STS. A major advantage of this strategy is that it provides an ordered set of markers that can be stored as sequence information in a data base allowing reconstitution of contigs from different clone libraries. Operationally, an STS is defined by the sequence of the two primers that make its production possible and can be created from any unique sequence from the desired region. Polymorphic DNA markers with their specific amplimers (primers) are also classified as STSs, but with dual use since they are capable of acting as landmarks both in a genetic and a physical map. Expressed sequence tags (ESTs) which are partial cDNA sequences can serve the same purpose as the random genomic STSs but have the added advantage of pointing directly to an expressed gene. A physical map can easily be established if the region contains a high density of markers or STSs. Initially clones that span the region are isolated through screening of a genomic YAC, PAC or a BAC library by PCR using the primers for these STSs, then by the STS content of each isolated YAC (PAC or a BAC) overlaps between clones can also be detected. The use of STSs to generate physical maps has been authenticated by a number of workers. Green and Olson (1990) used 16 STS to isolate and overlap 30 YACs spanning 1.5 Mb of the region containing the cystic fibrosis trans-membrane regulator (*CFTR*) gene on chromosome 7, Chumakov *et al.* (1992) also constructed a continuous array of overlapping YAC clones that covered the entire chromosome 21q using the STS strategy. In our lab this has been achieved for the 7p13 region and as well as Xp11.3 region (Keen *et al.* 1995 and Thiselton *et al.* 1995)

1.4.7.4 *Alu*-PCR

This is another rapid method of detecting overlaps between YAC clones (Nelson *et al.*, 1989). Alu PCR utilises consensus primers derived from Alu repeat sequences and can be applied directly to YAC colonies. This generates an average of 10 bands between 0.1 and 2.0 kb per YAC. This method has been used to identify overlap between YACs in intron 1 of the dystrophin gene, where no STSs were available (Coffey *et al.*, 1992), and in a modified strategy to confirm overlap between two YAC clones in the class II region of MHC (Ragoussis *et al.*, 1991).

Physical maps that are composed entirely of overlapping YAC clones still need further characterisation to enable DNA sequencing or if one is to have the DNA in form that will enable easy purification essential for many a gene identification protocols. The required in-depth characterisation can be achieved through methods such as genome sequence sampling (GSS) and hybridisation mapping, which although highly laborious result in the production of a 'sequence ready' physical map.

1.4.7.5 Genome sequence sampling (GSS)

This method combines elements of restriction mapping and STS mapping and generates maps with resolution of 1-5 kb (Smith *et al.*, 1994). GSS also requires a chromosome specific cosmid library that represents the genome at 20-30-fold redundancy with reasonably random distribution of clone ends, which is produced by cloning using a variety of restriction enzymes and cloning sites. Initially a YAC clone is used as a hybridisation probe to select cosmid clones included in the YAC clone, which are then restriction mapped and arranged into contigs using methods previously described. STSs are generated and sequenced from the ends of cloned insert of each cosmid and aligned on the map. If a high density of cosmid map has been prepared then it also enables the preparation of high-density sequence map. Provided that the restriction sites used for cloning were evenly spaced, the DNA sequences determined would be spaced every kilobase on average. Using GSS Smith *et al.* (1994) studied the protozoan parasite *Giardia lamblia* with a genome size of 10.5 Mb.

1.4.7.6 Hybridisation mapping

This method is similar to chromosome walking but incorporates necessary steps to avoid the isolation of non-contiguous clones from the clone used as probe. This is achieved by first blocking the genomic library with five kinds of probe, representing known repetitive sequences (centromeric, telomeric, 17S and 5S ribosomal and the long terminal repeat (LTR) of retrotransposons) to identify those clones that only contain unique sequences. A number of these clones are selected at random and used as hybridisation probes to detect overlapping clones. From these clones which do not give a positive hybridisation signal another set is selected at random for use as probes in the next round of experiments. This process is continued until all clones show positive hybridisation at least once and in practice some clones containing repetitive DNA have to be used to join contigs. However a key feature of this technique is that clones are randomly chosen as probes based on the criterion that they have not yet given a positive hybridisation signal, which avoids a great number of redundant hybridisations. Any overlaps due to cross hybridisation between repetitive elements are avoided by demanding that all pairs of cosmid overlaps be reciprocal if both cosmids in the pair are used as probes. That is, if cosmid x hybridises to cosmid y then y must hybridise to x. The utility of hybridisation mapping has been shown by the construction of a map of the long arm of human chromosome 11 (Evans and Lewis, 1989) and a complete map of the fission yeast (*Schizosaccharomyces pombe*) (Maier *et al.*, 1992; Hoheisel *et al.*, 1993; Mizukami *et al.*, 1993).

1.4.7.7 Radiation hybrid mapping

Another powerful method for creating physical maps is the use of irradiation and fusion to gene transfer (IFGT) to produce radiation hybrid maps. This technology originally developed by Goss and Harris, (1975) demonstrated that chromosome fragments, generated by lethal irradiation of donor human cells could be rescued by fusion to rodent recipient. Radiation maps are based on breaks induced by radiation and the resolution of radiation hybrid mapping is a function of both fragment size and retention frequencies, which is the percentage of radiation hybrid cell lines containing a

given chromosome marker. The fragment size can be varied by altering the radiation dose and it is possible to construct panels designed either for map continuity with few markers or for high resolution with large number of markers. Information on localisation using radiation hybrids is obtained by determining linkage to markers of the framework. Such a linkage is expressed by a distance measured in breakage frequency accompanied by a likelihood estimate expressed as a lod score. Distances between markers in the radiation hybrid maps are expressed in cR_{3000} where 1 cR $_{(N\ rad)}$ correspond to a 1% frequency of breakage between two markers after exposure to "N" rad of X-rays (Cox *et al.*, 1990; Boehnke *et al.*, 1991).

Cox and co-workers (1990) modified the original approach by using somatic cell hybrid containing a single human chromosome as the donor cell instead of a diploid human cell. This approach is not feasible for mapping an entire genome, as it would require over 4000 hybrids. Walter and co-workers (1994) have found a solution to this problem by reverting to the original protocol of Goss and Harris (1975) and using a diploid human fibroblast as a donor. Using 44 radiation hybrids they constructed a map of the human chromosome 14 containing 400 ordered markers and concluded that a high resolution map of the whole genome is feasible with only a single panel of 100-200 radiation hybrids.

Radiation hybrid mapping complements both recombination maps and physical maps based on contigs. Whereas recombination maps are constrained by the recombination rate and only limited to polymorphic markers, radiation hybrid methods can be used to map both polymorphic markers and non-polymorphic STSs and ESTs. Therefore a radiation hybrid map of the human genome was developed to facilitate the completion of the YAC contig of the human genome as it presented an independent means of integrating STS with the polymorphic markers (Gyapay *et al.*, 1996). The limitations of YAC contig based maps, for example poor YAC coverage in some regions of the genome such as terminal parts of chromosomes and particularly GC-rich regions, which are more likely to be rich in genes, further emphasised the need for an independent method of mapping. The radiation hybrid map, which consisted of 168 whole–genome radiation hybrids, was constructed by irradiating donor human fibroblasts at 3000 rads, a relatively low dose to ensure continuity of the map, and fusing with recipient hamster

cells. A framework map of 404 markers was constructed by typing the panel with polymorphic markers and ordering them using standard methods (Cox *et al.*, 1990, Boehnke *et al.*, 1991). Even though the order of these markers in the genetic linkage map and the radiation map was the same there were some discrepancies in distances. Some gaps that correspond to 7-10 cM in the genetic map corresponded to very short distances on the radiation map and conversely some clusters on the genetic linkage map were split on the radiation map. Nevertheless the utility of the map has been demonstrated by mapping of 374 ESTs, whose accurate localisation on the radiation map was verified by assigning these ESTs to YACs that map to the same interval.

A subset of 93 hybrids from this panel has been made widely available for genome mapping projects under the panel name Genebridge4. Since the creation of Genebridge4 panel, which classifies as a lower resolution panel, two other radiation hybrid panels of higher resolution have been constructed. The Stanford G3 panel is a medium resolution 10,000-rad panel consisting of 83 clones and the Stanford TNG is a high resolution 50,000-rad panel consisting of 90 clones, the details of these panels are available from http://shgc-www.stanford.edu.

1.5   Physical maps and the current progress of the Human Genome Mapping Project

The physical mapping phase of the human genome project was officially completed with the landmark publication of the final YAC contig map of the human genome, which provided 75% coverage of the entire human genome (Chumakov *et al.*, 1995). This map although a major achievement, still fell short of the requirement set by the Human Genome Project (HGP) for a 'sequence ready' physical map. Therefore, since reaching this goal efforts have been directed at further map construction, integration and validation to meet the final goal set by HGP, which is to produce a physical map of the human genome containing 30,000 unique markers ordered with respect to each other and spaced on average every 1000,000 base pairs (1 Mb). The physical map constructed by Hudson *et al.* (1995) at the Whitehead Institute for Biomedical Research goes more than halfway to meet the criteria set by the human Genome Project. This map includes a large number of STSs previously generated and mapped by other groups. Approximately 7000

STSs on the map represent genetic markers that have been previously placed on meiotic linkage maps (Gyapay *et al.*, 1994; Dib *et al.*, 1996). Finally STSs developed from random genomic DNA and Expressed Sequence Tags (ESTs) from dbEST database (division of GenBank allocated for expressed sequences) have also been incorporated into the Whitehead physical map. Therefore this map integrates the locations of a large number of genes with meiotic linkage maps of the human genome. The two independent means used to order these STSs were radiation hybrid mapping (RH) using the Genebridge4 Radiation Hybrid panel and YAC-STS content mapping. Combining RH and YAC-STS content mapping information Hudson *et al.* (1995) estimate that they have achieved an effective resolution of 1 Mb and that their map provides RH coverage of 99% of the genome and physical coverage of 94% of the genome. Even though the Whitehead map is of immense use to disease gene hunters, in its present form this map does not provide adequate scaffold for sequencing the human genome. Presently, human DNA cloned as bacterial artificial chromosomes (BACs), with an average insert size of 100 kb appears to be the most likely source of template for large scale DNA sequencing. As such a contiguous map containing an ordered marker every 100 kb on average is required to isolate and order efficiently the 100-kb BAC sequencing templates. However as far as ordering of STSs is concerned, physical maps such as the Whitehead map with STSs ordered at an effective resolution of 1 Mb still represent a giant step forward in reaching this ultimate goal. The most up to date physical mapping information on this map can be obtained through the Whitehead Institute for Biomedical Research/MIT Centre for Genome Research's Human Physical Mapping Project World Wide Web server: (http://www-genome.wi.mit.edu/). Meanwhile further characterisation and sequencing of individual chromosomes have already been initiated at various genome centres that took up the task of constructing 'sequence ready' maps of a particular chromosome at the very outset of the human genome project. Information on these genome centres can be obtained from the World Wide Web server: (http://webace.sanger.ac.uk/HGP/). The most up to date physical mapping information on these chromosomes is available thorough the electronic genomic databases maintained by the respective genome centres.

1.6   Identification of genes

1.6.1   Identifying the gene of interest in positional cloning

In a positional cloning venture the physical characterisation of a disease candidate interval is usually followed by the isolation of transcripts to identify the disease causative gene. The methodologies used for such gene identification from cloned DNA can be categorised as either traditional or novel. Traditional methods include analysis of zoo blots, detection of CpG islands and newer approaches include exon amplification, cDNA selection, genome sequencing and computer analysis and analysis of regionally mapped candidate genes.

Zoo blot analysis is based on the conservation of coding regions between species (Monaco *et al.*, 1986). In this method hybridisation of a human genomic DNA clone to a Southern blot containing genomic DNA samples of a variety of species at low stringency is used to identify homologous genes present within the cloned DNA. However the genes that are species specific will not be detected by this method. By means of such zoo blots Sedlacek *et al.* (1993) isolated genomic DNA species conserved between humans, mice and pigs.

Identification of CpG islands is another traditional approach and has been instrumental in the localisation and subsequent isolation of many genes involved in human disease and mouse mutations (Gessler *et al.*, 1990; Herrman *et al.*, 1990). In mammals such islands are thought to mark transcriptionally active DNA sequences and are often located at the 5' end of house keeping genes (Craig and Bickmore, 1994). CpG islands are short stretches of DNA often 1 kb or less, containing CpG dinucleotides which are unmethylated and which are present at the expected frequency, unlike in the remainder of the genome. CpG islands can be recognised by diagnostic patterns of short and long-range restriction maps. For example the enzyme *Hpa*II cleaves at the recognition site CCGG but will not cleave CC^{M}GG. Thus *Hpa*II tend to cut selectively at CpG islands and as a consequence these islands are often referred to as HTF islands (*Hpa*II tiny fragments). In mammals CpG islands are generally also G + C rich and so are principle sites of cleavage for methylation sensitive enzymes with G + C rich recognition sequences such as BssHII, EagI and SacII. Rare cutter enzymes such as NotI

(GCGGCCGC) cut almost exclusively within islands. Clustering of such sites thus is commonly associated with CpG islands.

Conserved DNA fragments identified from Zoo blots and CpG island containing fragments can be tested for expression by hybridisation to Northern blots of RNA isolated from foetal and adult tissues. If a transcript is identified then the genomic fragment subsequently can be hybridised to cDNA libraries. Although Northern blotting and analysis of conserved DNA fragments and CpG islands have been particularly effective in the isolation of many human disease genes they are very labour intensive. An alternative approach is the direct selection method (Monaco, 1994) where whole YAC or cosmid inserts are directly hybridised to cDNA libraries on filters after suppression of repeated sequences in the radioactively labelled probe. Although associated with technical difficulties this method has enabled many new genes to be isolated.

In cDNA selection (Lovett *et al.*, 1991; Parimoo *et al.*, 1991), recognised as one of the newer approaches to gene isolation, an amplified cDNA library is hybridised to immobilised YAC or comid clones that cover part of the genome of interest. Of those cDNAs isolated at least one should correspond to the desired gene. As with direct selection this process is technically difficult (Lovett, 1994) due to simultaneous selection of cDNAs with homology to pseudogenes and low copy number repeat sequences.

In exon amplification (Buckler *et al.*, 1991) random segments of chromosomal DNA are inserted into an intron present within a mammalian expression vector. After transfection cytoplasmic mRNA is screened by PCR amplification for the acquisition of an exon from the genomic segment. The amplified exon is derived from the pairing of unrelated vector and genomic splicing signals. A number of human genes have successfully been isolated through this method (Monaco, 1994).

Sequencing of genomic segments from the region of interest and analysis of the assembled sequences for potential Open Reading Frames (ORFs) is another novel approach. This approach has been applied to the positional cloning of the human gene for Kallmann syndrome (Legouis *et al.*, 1991) and the identification of *RPGR* gene causing X-linked retinitis pigmentosa (Meindel *et al.*, 1996).

The success of Legouis *et al.* (1991) in identifying the Kallmann syndrome gene from DNA sequence data led to an alternative approach designated 'candidate gene' or

'positional candidate' approach for gene identification (Ballabio, 1993). Unlike functional and positional cloning this approach does not require the isolation of novel genes but relies on the availability of information regarding function and map position from previously isolated genes, which could have originated from either genomic sequencing or expressed sequence tags (EST)/ cDNA fingerprints. In fact most of the genes that have associated with various retinopathies have been identified by the positional candidate approach. The future expanding success of the positional candidate approach is predicted on the development of the increasingly dense transcript map, which is described in detail below.

1.6.2 Construction of the human transcript map

A comprehensive human gene map is a critical resource for the positional candidate approach to gene cloning (Wilcox *et al.*, 1991; Collins, 1995). Therefore as a prelude to the development of a gene map the tens of thousands of partial cDNA sequences of genes (or ESTs) produced by the Washington University/Merck & Co's public EST initiative and other groups that have been deposited in the public database (dbEST), were used by an international EST mapping consortium to develop a human transcript map (Schuler *et al.*, 1996; Marra *et al.*, 1998). Initially all the available ESTs in dbEST were clustered to identify novel, non-redundant mapping candidates for generating a transcript map. This 'UniGene collection' contains more than 48,000 clusters of sequences, each representing the transcription product of a distinct human gene (Schuler, 1997). With current estimates of 80,000 to 100,000 genes in the human genome, this is close to the 50% mark and the collaborative mapping effort has resulted in the placement of 15,000-20,000 of these transcripts on radiation hybrid (RH) and YAC maps. Previously other groups have also mapped cDNAs but mapping was at a limited scale and usually only to the resolution of a chromosome assignment (Wilcox *et al.*, 1991; Adams *et al.*, 1991, Khan *et al.*, 1992; Polymeropoulos *et al.*, 1992, 1993). However not all genes will be represented by ESTs, since some genes will either be poorly expressed or completely absent in the cDNA libraries analysed. These would include genes that show highly restricted tissue or cell expression patterns and genes that are expressed at certain developmental stages. Therefore it has been estimated that the

45

EST mapping effort will only identify sequences from about 80% of all the human genes. The remaining genes are to be identified as coding sequences in genomic DNA clones.

The UniGene collection and the transcript maps are an important resource for many investigators. Gene hunters can use the transcript maps to gain valuable clues to expected gene location and density in an area of interest. However the regional assignment of the ESTs in the gene map is still limited by the resolution of the radiation hybrid maps and, most ESTs that have been mapped to large genetic interval still have to be assayed in an ordered set of clones for a finer localisation. Therefore these ESTs represent a somewhat raw resource for positional cloning endeavours, requiring a further assay within DNA contig(s) of respective disease intervals for identification of potential candidate genes. The cDNA clones corresponding to the ESTs can be obtained from the IMAGE (integrated molecular analysis of gene expression) consortium at Lawrence Livermore National Laboratories (LLNL, USA), which maintains cDNA clones representing unique genes in gridded arrays.

UniGene clusters are also being studied to find gene polymorphisms. The Co-operative Human Linkage Centre (CHLC) has found ESTs to be a useful source of polymorphic markers for genetic mapping (Boguski and Schuler, 1995). Furthermore the recently developed techniques for assessing gene expression on a genomewide scale (e.g., microarray expression systems) take advantage of the abundance of unique EST sequences readily retrieved from GenBank (Strachan *et al.*, 1997). Finally the transcript map will be an important resource for genomic sequencing as gene-dense regions could be used as initial targets for sequencing. The gene map and the UniGene data set can be accessed through National Centre for Biotechnology Information's WWW service (http://www.ncbi.nlm.nih.gov/).

1.6.3 Cross species comparison for gene identification/ Comparative genomics

Characterisation and sequencing of genomes of model organisms (such as *E. coli*, *Saccharomyces cerevisiae*, *Drosophila*, *C. elegans*, *Fugu rubripes* and *Mus musculus*) is an essential part of the Human Genome Mapping effort and was undertaken to produce comparative maps to facilitate linkage predictions, disease gene identification, and studies of genome organisation and evolution. Gene identification strategies that rely on

cross species comparisons are based on the belief that functionally significant regions of the genome are highly conserved during evolution. Once identified comparison between homologous genes in distantly related species also provide remarkable insight into their function. In cases where orthologs and family members of genes mutated in human disease are cloned across several species, the experimental advantage in each organism can be applied synergistically to characterise the homologous gene products to understand the molecular mechanisms of the human disease process. Studies of the S. cerevisiae *MEC1* and *TEL1* genes, for example, have provided valuable insight into the function of the human *ATM* gene, which is mutated in ataxia telangiectasia, and further analysis is in progress using the yeast experimental system (Morrow *et al.*, 1995).

Traditionally gene identification based on cross–species comparison relied on the two major approaches, low stringency hybridisation of cDNA or genomic DNA libraries and PCR using degenerate oligonucleotides, both of which are technically difficult and time consuming. Therefore in an alternative approach the proliferating model organism sequence data and thousands of human partial cDNA sequences of genes (or ESTs) that have been deposited in the public database (dbEST), have been utilised to accelerate the identification of genes mutated in human diseases. This approach described as 'Genome cross referencing' is involved in systematically mapping novel human ESTs that show significant sequence similarity with model organism proteins (Bassett *et al.*, 1997). These mapped cDNAs cross-reference model organism protein function data with positions on the mammalian maps and allow application of the positional candidate approach to identify the genes mutated in human diseases that map to the same location in the genome. Through the cross-reference database (XREFdb) on the World Wide Web (http://www.ncbi.nlm.gov/XREFdb/), which also integrates the vast resource of EST mapping data generated by the Radiation hybrid mapping consortium (Schuler *et al.*, 1996), investigators can identify human homologues of model organism genes and establish links between model organism genes and human disease states, using either a protein query or/and map position–based query tool. Using this genome cross-referencing concept Banfi and co workers (1996) identified 66 human cDNAs with significant homology to previously identified *Drosophila* genes involved in the generation of mutant phenotypes and mapped these ESTs using FISH and radiation

47

hybrid mapping. Sequence data available for *D. melanogaster* is readily available from the database . So far, European Drosophila Genome Project (EDGP) has submitted 74 sequences or 2,722,019 bp to the public data libraries. 2.0 Mbp of non-redundant sequence has been analysed and annotated, resulting in 181 newly discovered genes plus 65 previously sequenced/studied ones. *C.elegans* (97 Mb of genomic sequence which represents >99% of the whole genome) of the genome has been sequenced and is available from the database (http://www.sanger.ac.uk/Projects/C_elegans/Genomic_Sequence.shtml). This suggests that the cross-referencing method will become increasingly valuable as more genome sequence from model multi-cellular eukaryotes becomes available (Bassett *et al.*, 1997). At present only *S. cerevisiae* and *E. coli* genomes have been completely sequenced (Goffeau *et al.*, 1996; Blattner *et al.*, 1997), and have already proved their utility by leading to the identification and functional analysis of several genes mutated in human disease (Hieter *et al.*, 1996; Goffeau *et al.*, 1996).

Similar to cross referencing a technique known as 'homology probing' is also capable of identifying genes mutated in human diseases and relies on the gene sequence and function data of the model organism as well as a robust collection of ESTs (Yahraus *et al.*, 1996). In this method a process or pathway is identified in humans that when defective result in disease. The genes that participate in this pathway are then identified in model organisms, and the EST database is screened for human cDNAs representing homologues of these model organism genes, which become candidates for genes mutated in the human disease. The potential of this technique is exemplified by the identification of human genes PXR1 (Yahraus *et al.*, 1996) and PXAAA1 (Dodt *et al.*, 1996) involved in peroxisome biogenensis and responsible for inherited defects in this process (Zellweger syndrome and related peroxisome biogenesis disorders).

As the techniques outlined above would indicate the future gene hunting process will soon be reduced to a mere computer exercise. When a new disease is assigned to a specific map position it may be possible to interrogate the genome database for that portion of the chromosome and obtain a list of all the genes assigned to the same region. By comparing the features of the gene with the features of the disease it will become relatively easy to select the most likely candidate gene(s).

1.7   Retinal Genetics

Inherited eye diseases constitute a substantial proportion of diseases classified as genetic defects (McKusick, 1992). Amongst these diseases retinal dystrophies constitute a major cause of blindness. Most of these diseases were originally defined based on the fundus appearance as seen through the ophthalmoscope, through histopathologic examination of autopsied eyes, and more recently through visual function assessments. Now biochemical studies and molecular genetic analyses have provided even newer approaches for, detecting these diseases, finding the underlying genetic defect, and defining pathogenetic mechanisms. The rapid development in gene cloning techniques that has been witnessed in recent years has led to the cloning of many of the genes associated with retinal degenerations and disorders (http://www.sph.uth.tmc.edu/RetNet/) leading to a greater understanding of the visual process and the functions of the retina. Moreover, through the identification of disease causative genes and mutations previously unrecognised associations between different clinical entities that share common gene mutations (gene sharing/ allelic effect) as well as distinctly different molecular alterations within the spectrum of what traditionally was believed to be the same disease (locus heterogeneity) has been revealed. Genetic heterogeneity suggests that retinal degeneration is a common end point for many biochemical abnormalities and allelic heterogeneity suggests that abnormalities at different sites within the same gene can have either similar or dissimilar consequences, depending upon the functional roles of these sites. More importantly however the identification of the precise genetic defect in a hereditary retinal disease helps to define its cause, allows new insights into pathogenesis and provides a framework for considering means of treatment.

1.8   Structure of the retina

The retina, which is one of the best-characterised parts of the central nervous system, in the most comprehensive sense, includes all the structures that are derived from the optic vesicle. Namely the sensory layers of the retina, the pigmented epithelium as well as the epithelial lining of the ciliary body and of the iris. However, put simply the retina can be said to have two compartments: a sensory layer (neural retina) and a pigmented layer derived from the inner and outer layers of the optic vesicle, respectively.

The two layers are attached loosely to each other by the extracellular matrix that fills the space between the apical villi of the retinal pigment epithelium (RPE) and the outer segment of the photoreceptors as well as inter photoreceptor space. The retinal pigment epithelium is firmly attached to the Bruch's membrane of the choroid.

1.8.1 The sensory (Neural) retina

The retina, when seen in cross section by light microscopy, is represented by 10 layers. The structure of the neural retina is best explained in the context of these layers of which, outer segments of photoreceptors and the internal limiting membrane represent the neural retina. The layers are as follows:

retinal pigment epithelium, outer segments of photoreceptors (rods and cones), external limiting membrane, outer nuclear layer, outer plexiform layer, inner nuclear layer, inner plexiform layer, ganglion cell layer, nerve fibre layer and an internal limiting membrane.

The mature vertebrate retina possesses five major neuronal cell types that form the visual pathway from retina to brain. The primary neurons in this visual pathway are the *photoreceptors*, which constitute the layer of rod and cone outer segments, the outer nuclear layer and the outer plexiform layer. The *horizontal*, *bipolar* and *amacrine* cells constitute the second order neurons and the *ganglion cells* constitute the third order neurons in the visual pathway. Photoreceptor axons synapse with the bipolar and horizontal cells in the outer plexiform layer, which marks the junction of the first and second order neurons in the retina. The flat horizontal cells serve to modulate and transform visual information received from photoreceptors and also form a network of fibres that integrate the activity of photoreceptor cells horizontally. The inner nuclear layer consists of nuclei of bipolar cells, amacrine cells and supporting Müller cells. Müller cells are the largest cells of the retina and extend from the external to the internal limiting membranes. As the principal glial cells they conserve the structural alignment of its neuronal elements. Müller cells also have an important role in the metabolism of the retina and they contribute to the b-wave of the electroretinogram. The axons of bipolar cells synapse with amacrine cells and dendrites of ganglion cells in the inner plexiform layer, which marks the junction of the second order neurons, the bipolar cells, with the third order neurons, the ganglion cells. The ganglion cell layer is composed mainly of the

cell bodies of the ganglion cells and the nerve fibre layer contains axons of these cells that join to form the optic nerve, which send the information gathered by the photoreceptors for further processing and interpretation by the visual cortex. The distribution of photoreceptors to optic nerve fibres is not uniform. In the fovea centralis approximately 200,000 cones are connected to at least as many optic nerve axons. However in the peripheral retina as many as 10,000 rods may connect in clusters to a single nerve fibre, with considerable overlapping, so that a single point of light may stimulate several clusters simultaneously. In the neural retina the photoreceptors cells are the percipient elements, required for the reception and conversion of light energy to neural impulses. All other neurons constitute the associative and conductive elements, which convey the nerve impulse to the visual cortex. Photoreceptors are of particular interest in this study as they are also commonly involved in retinal degenerations.

1.8.2 Photoreceptor cells

The two kinds of photoreceptors found in the vertebrate retina are morphologically and functionally distinct from each other. The rod photoreceptors possess thin cylindrical processes, function in dim light and are responsible for scotopic (night) vision and furthermore do not perceive colour. The cone photoreceptors are generally conical in shape, function in bright light (photopic) and are responsible for colour vision. There are on average 92 million rods and 4.6 million cones in the human eye. Individual variations in the density of both rods and cones occur in different regions in the eye. The greatest variability occurs near the fovea and at the very periphery of the retina (i.e. at the ora serrata).

1.8.2.1 Rods

Rods numbers far exceed that of cone photoreceptors and are at their greatest concentration in mid periphery of the retina. Rod concentration decreases as approaching the centre where they are completely absent in the fovea centralis. Extending from their cell bodies, the photoreceptors have two morphologically distinct regions: the inner and outer segments. In rods the inner and outer segments are 40-60 μm long throughout the retina. The slender outer segment (25-28 μm long and 1-1.5 μm in diameter) and the

slightly thicker inner segment of rods do not show much variation in morphology from the fovea to the periphery (Stryer, 1988). The major functions of the rod cell are highly compartmentalised. The function of the rod outer segment (ROS), which lies embedded in the interphotoreceptor matrix just internal to the retinal pigment epithelium, is the conversion of light energy into electrical impulses. The outer segments of the rods are cylindrical in shape and contain stacks of flattened double lamellae in the form of discs that are formed by the basal invagination of the outer segment plasma membrane. There are about 1000 discs in each human rod outer segment and the discs contain 90% of the visual pigment, rhodopsin, whereas the remaining pigment is scattered on the surface of the plasmalemma. Rhodopsin has the greatest sensitivity for blue-green light (λ_{max} 493nm) and allows scotopic (dim light) vision. The discs in the ROS are continually renewed throughout life by the "disc shedding" process in which the discs at the very apex of rods are removed in a light triggered rhythmic pattern and phagocytised by the RPE cells thus maintaining the outer segments at a relatively uniform length (Young and Bok, 1969; Bok, 1985). The outer segment is connected to the inner segment by a modified cilium, which functions in transmitting cellular components from the inner segment and cell nucleus to the discs and their plasma membrane. The rod inner segment is cylindrical and is composed of a finely granular cytoplasm. There are two histologically discernible regions: an outer eosinophilic ellipsoid and an inner basophilic myoid. The ellipsoid contains a large number of long and slender mitochondria and the cytoplasm contains smooth endoplasmic reticulum, neurotubules, free ribosomes and glycogen granules. The myoid, which is the site of major protein synthesis for new outer segment discs, contains high concentration of free ribosomes, a rough endoplasmic reticulum, glycogen granules and a golgi apparatus. The cytoplasm also contains microtubules and microfilaments that are arranged in parallel to the long axis of the cell and extend to the level of external limiting membrane and of the synapse, respectively. A thin cytoplasmic process (the outer fibre) connects the inner segment to the cell body that contains the nucleus. The rods synapse with second order neurons i.e. the bipolar and horizontal cells, through round or oval cytoplasmic expansions of 1 µm in diameter known as spherules at the synaptic body. The spherule contains numerous presynaptic vesicles filled with acetylcholine, mitochondria and neurotubules. Both horizontal and

bipolar cells make contact with the rod spherule. A horizontal cell only contacts a rod spherule once, but several different horizontal cells may contact each spherule. One to four bipolar cells contact an individual spherule at separate points and each bipolar cell may contact upto hundreds at the periphery of the retina.

1.8.2.2 Cones

The density of cones is maximal, with an average of 199, 000 cones per mm^2 at the fovea, where the visual resolution is at its greatest but this number reduces to 4500 per mm^2 towards the periphery. The morphology of cones differs depending on their location in the retina (Tripathy and Tripathy, 1984). Cone length is maximal (80 μm) at the fovea and gradually reduces to 40 μm at the periphery. Moreover, cones appear rod-like at the fovea and the inner region of the outer segment becomes wider towards the periphery. Cones located in the periphery have a conical shaped outer segment with the apex pointing towards the RPE cell layer. Ultrastructurally, the cone outer segments have more discs than (1000-1200 per cone) than do rod outer segments and are also arranged differently to rods. Unlike the rod discs, cone discs are attached to each other as well as to the surface plasma membrane and are not detached easily. Disc shedding also takes place in the cone photoreceptor cells in a process in which the cone outer segments remodel themselves after each shedding event, since most apical cone outer segments have a constant but smaller diameter than the basal ones (Hogan *et al.*, 1974; Anderson and Fisher, 1976).

Photopic (colour) vision originates in the cones by the presence of trichromatic pigments. Each cone contains one of three different iodopsin molecules that absorb light at three distinct peaks at 440 nm (blue), 540 nm (green) and 577 nm (orange) referred to as S- (short), M- (medium), and L- (long) wavelength cones, respectively (Dacey and Lee, 1994). Cone synapses have cytoplasmic expansions known as pedicles that are larger (5 μm in the fovea) than the rod spherules and are pyramidal in shape. At the fovea only one bipolar cell contacts one cone pedicle along with two different horizontal cells.

1.8.3 Retinal pigment epithelium

The retinal pigment epithelium (RPE) consists of a single layer of approximately five million cuboidal cells firmly attached to its basal lamina, the Bruch's membrane. RPE cells are joined to one another by tight junctions and constitute an important structural and functional part of the outer blood retinal barrier. Together with the endothelium of the choriocapillaries, it effectively excludes the exchange of potentially toxic substances between the choroidal circulation and the neural retina. The basal microfibrils of RPE are functionally linked to the choroid via the Bruch's membrane whereas apical region of the RPE is loosely attached to the sensory retina. The absence of specialised adhesion molecules in the interphotoreceptor matrix, and the lack of junctional complexes between apical microvilli of pigmented epithelial cells and the outer segments of the photoreceptor leave the sensory retina prone to detachment in pathological conditions. Despite the lack of any adherent functions the apical villi of the RPE are involved in phagocytosis of outer segment discs, and thus promote the renewal of photoreceptor discs (Young and Bok, 1969; Bok, 1985).

Another important function of the RPE is the uptake, processing, transport and release of vitamin A (retinol) and some of its visual cycle intermediates (retinoids) (Dowling, 1960; Bok, 1985). The purpose of this cycle is to regenerate 11-*cis* retinaldehyde, the retinoid that serves as the chromophore for the visual pigments in rod and cone outer segments. Retinol uptake occurs at both the basolateral and apical surfaces of RPE via a receptor mediated process. The release of a crucial retinoid, 11-*cis* retinaldehyde (11-*cis* retinal) occurs solely across the apical membrane. Delivery of retinol across the basolateral membrane is mediated by a retinol binding protein (RBP) that is secreted by the liver as a complex with retinol and through the receptors for RBP found on the basal and lateral plasma membrane of the RPE cells. Within the cell, retinol and its derivatives are solubilised by intracellular retinoid binding proteins that are selective for retinol (cellular retinol binding protein, CRBP) and 11-*cis* retinoids (cellular retinal binding protein, CRALBP). Release of 11-*cis* retinal across the apical membrane and re-uptake of retinol from the photoreceptors during the visual cycle is promoted by an
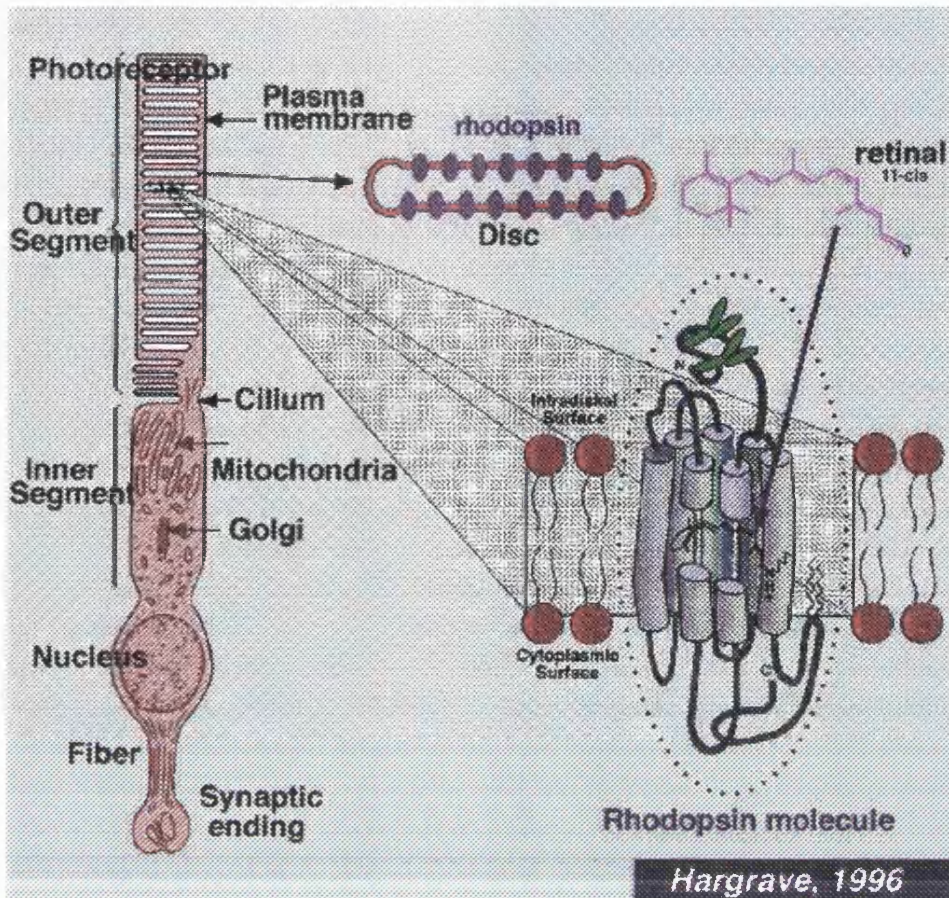
Figure 1.1:

A diagrammatic representation of a generalised photoreceptor cell and the relative orientation of rhodopsin molecule in the outer segments of the cell. The above diagram has been taken from Hargrave, 1996.

55
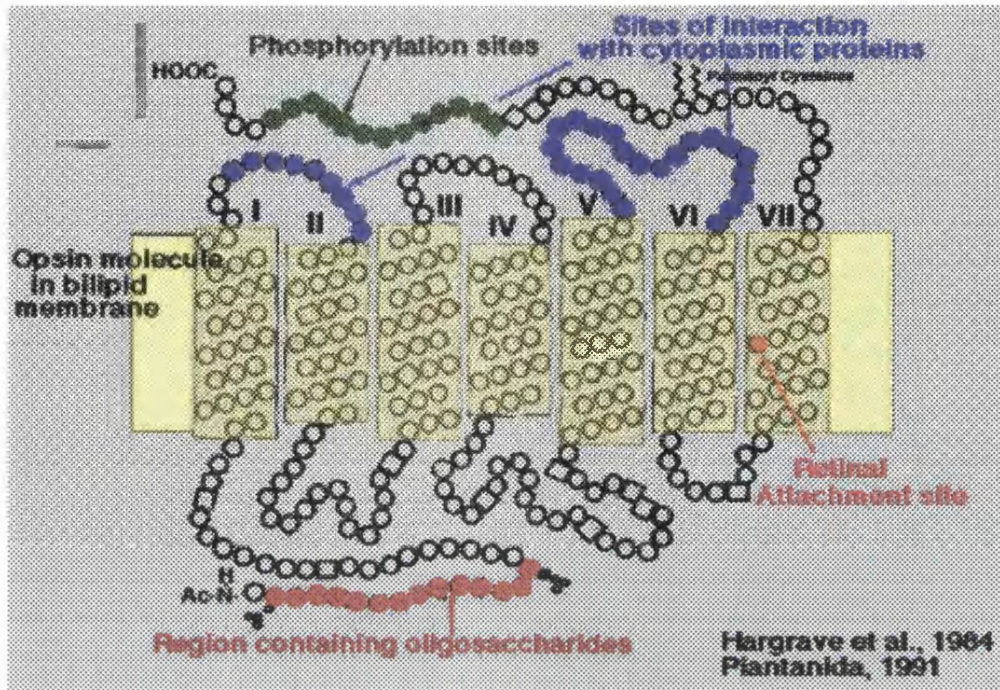
Figure 1.2:

A diagrammatic representation of the 7-transmembrane protein structure of Rhodopsin, showing its various components. The above diagram has been taken from Hargrave *et al.*, 1984 and Piantanida, 1991.

Intercellular retinoid binding protein (IRBP). In addition to disc renewal and recycling of vitamin A, the RPE is involved in the absorption of scattered light by the melanin granules, transport of nutrients and metabolites through this extra retinal-blood barrier, secretion of interphotoreceptor matrix (IPM) and maintenance of the photoreceptor microenvironment.

1.8.4 Phototransduction

A visual image enters the eye as light of different wavelengths and intensities and is captured by the two types of retinal cells, rods and cones, which exhibit distinct light sensitivities and response kinetics. The light signal captured by these cells stimulate a series of chemical reactions, called phototransduction, which is similar in both rods and cones and culminates in the generation of a neuronal signal that is transmitted via the optic nerve to the visual cortex where perception and interpretation occurs (for review see Koutalos and Yau, 1996). The outer segments of rods and cones which are the sites of visual transduction in vertebrate eyes can easily be isolated in pure forms and maintained in isolation for biochemical and electrophysiological studies. This has led to the elucidation of the intervening biochemical steps that comprise the phototransduction pathway. The visual pigment of the rod cell, rhodopsin ®, consists of the transmembrane protein opsin, chemically linked to the chromophore 11-*cis* retinal at Lys296. The primary event in the phototransduction cascade is the light triggered isomerisation of the 11-*cis* retinal of rhodopsin to its all *trans* isomer. This isomerisation alters the geometry of retinal and results in the release of all-*trans* from its membrane bound cofactor in to the disc membrane lipid (Wald, 1968). This conformational change results in the formation of the photoactivated or photolysed rhodopsin (R*), which is catalytically active.

The photoactivated rhodopsin binds a G protein called transducin (T), initiating a signal-amplifying cascade of reactions. G proteins are signal transducing guanosine nucleotide binding proteins whose function is to transmit signals between transmembrane receptors and cellular effectors. In the inactive state, transducin is a

57

Light photon

GDP

Tα
Tβ
Tγ

GDP

Tα

R

Rhodopsin

R*

ATP

Transducin

ATP

ADP

GTP

Ar (P)
R*

RK

Tβ Tγ

+

Tα*

Ar

ADP

ATP

Tβ
Tγ
Pho

GTPase

Pγ Pγ
Pα
Pβ

PDE

Pγ Pγ

Pα
Pβ

cGMP

Na⁺

cGMP

Cā

cGMP-gated channel

GC

↓[Ca]⁺²

GCAP

5'GMP

Na⁺

Ca⁺

DISC MEMBRANE SURFACE

CYTOPLASM

PLASMA MEMBRANE

INTERPHOTORECEPTOR SPACE
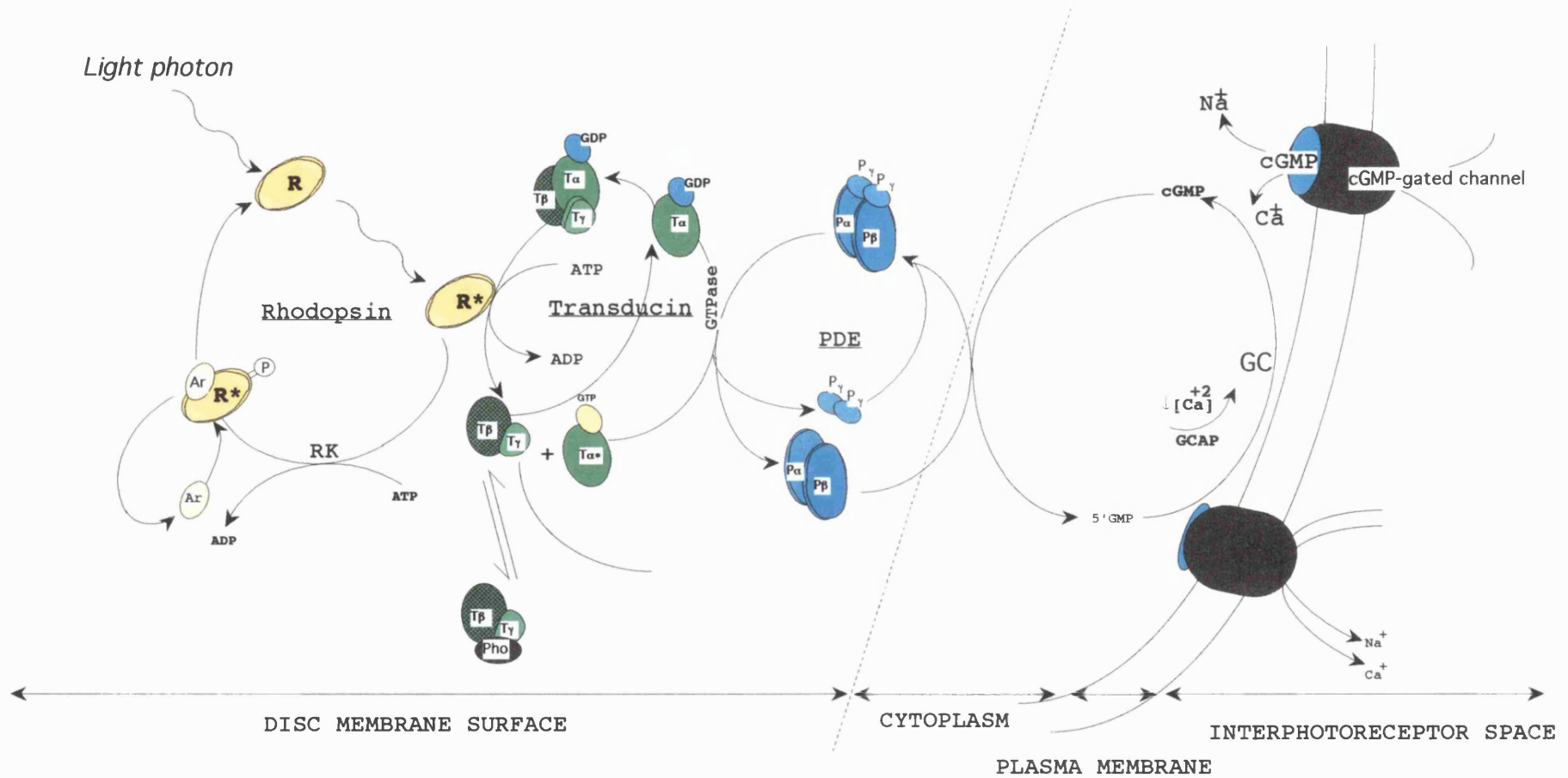
Figure 1.3:

Diagram of the biochemical events involved in the activation and inactivation of phototransduction. Ar: arrestin, Pho: phosducin, and other abbreviations are as described in text (modified from Farber, 1995).

Membrane-associated complex consisting of two functional subunits T_α and $T_{\beta\gamma}$ (T_β and T_γ) and non-covalently bound GDP (Baehr *et al.*, 1982; Fung, 1987). Interaction of R* with transducin catalyses the exchange of GDP bound to T_α subunit for GTP and the subsequent dissociation of the active GTP-T_α* complex from the $T_{\beta\gamma}$ heterodimer. In rods each photoactivated rhodopsin generates several hundred GTP-T_α * that persist in the active state long enough to find and activate membrane associated cGMP-PDE molecules (PDE).

In the dark rod cGMP-PDE is a heterotetrameric peripheral membrane protein composed of two catalytic α and β subunits and two smaller inhibitory γ subunits (Baehr *et al.*, 1979; Deterre *et al.*, 1988; Fung *et al.*, 1990). The interaction of PDE γ subunits with GTP-T_α * leads to the activation of PDE (PDE*) releasing its hydrolytic potential. PDE* hydrolyses 3', 5'-cGMP to 5'-GMP at a high rate which is limited only by the availability of the substrate through diffusion (Bourne *et al.*, 1990). PDE remains active until GTP associated with GTP-T_α * is hydrolysed by the intrinsic GTPase activity of T_α. Upon which T_α dissociates from PDE γ and re-associates with $T_{\beta\gamma}$ and the PDE γ subunits are released to form PDE complex once again and inhibit enzyme activity. The outer segment cation channels that control the influx of ions across the photoreceptor plasma membrane are gated directly by cGMP and the fall in cGMP that result from light triggered PDE activation changes the conformation of these cGMP activated cation channel proteins leading to channel closure. This channel protein consists of a 63 kd α subunit and 240 kd tightly linked β and γ subunits (Cook *et al.*, 1989; Molday *et al.*, 1990; Chen *et al.*, 1993; Illing *et al.*, 1994). Channel closure decreases the conductance of the plasma membrane to cations and results in the hyperpolarisation of the plasma membrane, inhibition of neurotransmitter release, and signalling of the light stimulus to adjacent neurons (Fesenko *et al.*, 1985; Stryer, 1986; Yau and Bayler, 1989).

1.8.5 Regulation of phototransduction and the retinal proteins involved

Mechanisms must exist in order for the photoreceptors to maintain their sensitivity and adaptability. In the dark-adapted state the photoreceptors are capable of responding to a single photon of light. Such sensitivity is achieved through signal amplification i.e. activated R* is able to activate over 500 transducin molecules and each

molecule of activated PDE is capable of hydrolysing approximately 1000 cGMP molecules (Stryer, 1986). Light adaptation is a process whereby absorption of each additional photon is less effective in activating the phototransduction pathway, thus producing smaller alterations in the conductance of the cell. It is a necessary process to maintain sensitivity of the receptor to flash of light in the presence of background illumination. Moreover modulation of light adaptation is required for the photoreceptors to respond to light stimuli that vary in intensity without response saturation.

1.8.6 Regulation by Ca^{2+}- binding proteins

In photoreceptors, Ca^{2+} play a crucial role in photorecovery and adaptation (Matthews *et al.*, 1988). Calcium ions regulate several stages of the phototransduction pathway by modifying the activity of different Ca^2 binding proteins that in turn interact with key enzymes in the pathway. In the dark, the concentration of Ca^{2+} is maintained at 300nM as the entry of Ca^{2+} through the cGMP-gated cation channels is balanced by efflux of calcium through the $Na^+/Ca^{2+}-K^+$ exchanger (Koch and Stryer, 1988). Upon light illumination, the closure of cGMP-gated cation channels and the continued efflux of calcium through the $Na^+/Ca^{2+}-K^+$ exchanger result in the drop of Ca^{2+} concentration to <70 nM. This decrease in $[Ca^{2+}]$ stimulates the enzyme guanylate cyclase (GC), the peripherally membrane bound enzyme that catalyses the conversion of GTP to cGMP. Following illumination, this key enzyme is responsible for the synthesis of cGMP, which in turn opens cation channels in the outer segment plasma membrane and re-establishes the dark potential of the cell. Two retina-specific membrane-associated guanylate cyclases have been cloned and sequenced (retGC1 and retGC2) (Shyjan *et al.*, 1992; Margulis *et al.*, 1993; Lowe *et al.*, 1995), however only retGC1 has been localised to outer segments by immunocytochemical localisations (Dizhoor *et al.*, 1994; Liu *et al.*, 1994). These GCs are activated and regulated by specific Ca^{2+}-binding proteins known as guanylate cyclase activating proteins (GCAPs) (Gorczyca *et al.*, 1995; Dizhoor *et al.*, 1995; Palczewski *et al.*, 1994). Two GCAP proteins have been isolated from retina (GCAP1 and GCAP2), but only GCAP1 have been localised definitively to both rod and cone outer segments and purified. Ca^{2+} free form of GCAP1 has been shown to regulate the activity of ROS guanylate cyclase as well as recombinant retGC1 (Subbaraya *et al.*,

1994; Gorczyca *et al.*, 1995). Therefore in summary GCAPs mediate Ca^{2+} sensitive regulation of guanylate cyclase, which by synthesising cGMP restores the open state of the channels, thus promoting recovery of the dark state of rod photoreceptors following light exposure. The entry of Ca^{2+} then leads to decreased activity of GC and the return of the dark state. This feed back loop involving Ca^{2+} is likely to be a major contributor in the maintenance of a constant cGMP level in the dark and to recovery following illumination (Koch and Stryer, 1988).

Originally a different photoreceptor-specific Ca^{2+}-binding protein, recoverin, was thought to be the regulator of rod outer segment guanylate cyclase activity (Dizhoor *et al.*, 1991; Lambrecht and Koch, 1991), but once cloned and expressed recoverin did not alter the activity of GC under *in vitro* conditions (Hurley *et al.*, 1993; Gray-Keller *et al.*, 1993). It was also demonstrated that raising the concentration of recoverin within rod cells slows recovery from photoexcitation. Moreover, Visinin and S-modulin (Gray-Keller *et al.*, 1993) the recoverin like proteins isolated from chicken cones and frog rods, respectively, were also shown to prolong the activation of cGMP phosphodiesterase (PDE) (Kawamura and Murakami, 1991). Since the proposed function for recoverin in the regulation of GC was not supported, the precise role of recoverin in the phototransduction pathway has been intensely investigated. Recent studies of rhodopsin phosphorylation has revealed a possible function for recoverin and related proteins. S-modulin was shown to inhibit phosphorylation at elevated levels of Ca^{2+} (Kawamura, 1993; Klenchin *et al.*, 1995). Because phosphorylation of rhodopsin and subsequent binding of arrestin block further activation of transducin, thus reducing the effective lifetime of photolysed rhodopsin, the inhibition of phosphorylation by S-modulin and recoverin would be expected to prolong the lifetime of activated rhodopsin. This is also an effect consistent with the longer lifetime of activated PDE and the prolonged photoresponse. Recoverin is now thought to function during light adaptation through its Ca^{2+}-dependent inhibition of rhodopsin kinase (Klenchin *et al.*, 1995; Gorodovikova and Philippov, 1993; Gorodovikova *et al.*, 1994), an idea further supported by the observation that recoverin binds to rhodopsin kinase in a Ca^{2+}-dependent manner (Chen *et al.*, 1995a). However the transgenic mouse in which recoverin expression has been eliminated does not show the expected response kinetics (Baylor, 1996). In addition there

is disagreement about the Ca^{2+} concentration at which recoverin might regulate the phosphorylation of rhodopsin, perhaps requiring a concentration elevated beyond physiological conditions. Furthermore recoverin immunoreactivity is most prevalent at photoreceptor terminals (Polans *et al.*, 1993; Milam *et al.*, 1993), and unlike other phototransduction-specific proteins which are sequestered in the outer segments, recoverin is distributed throughout the cell, indicating that it might be involved in functions distinct from phototransduction. Therefore the precise function of recoverin in phototransduction is still controversial. Aside from studies of phototransduction, recoverin was also identified as the protein previously known as CAR (cancer associated retinopathy) protein. The gene for the mouse recoverin protein was originally assigned to mouse chromosome 11, closely linked to trp53. In the paper, the human gene for recoverin was localized to human chromosome 17 by Southern analysis of restriction digests of the DNA from mouse/human somatic cell hybrids. Using a 7 kb subclone of the human recoverin gene, a positive fluorescence *in situ* hybridization signal was demonstrated near the terminus of the short arm of chromosome 17 at position p13.1. The mapping of recoverin to this region of human chromosome 17, which contained a number of cancer-related loci, suggested a possible mechanism by which cancer-associated retinopathy could occur in humans (McGinnis *et al.*, 1995).

Calmodulin is another cytosolic Ca^{2+}-binding protein that is expressed ubiquitously and found in the rod outer segments (Nagao *et al.*, 1987). It has been suggested that the cGMP-gated channels are also responsive to concentrations of Ca^{2+} and might be regulated by Calmodulin (Hsu and Molday, 1993). In vitro experiments have shown that in the dark, binding of Ca^{2+} bound calmodulin to the β-subunit of the channel protein lowers the apparent affinity of the channel for cGMP. In this low affinity state any decrease in cytosolic cGMP, as which occurs upon light illumination will lead to channel closure. The resultant lowering of intracellular Ca^{2+} levels due to channel closure will in turn increase the sensitivity of the channel to cGMP by uncoupling calmodulin from the channel, thus allowing the channel to reopen at lower cGMP levels, leading to recovery of the ROS to its dark state as cGMP synthesis proceeds with the activity of guanylate cyclase. The opening of the channel will in turn restore the $[Ca^{2+}]$ to dark levels and Ca^{2+} bound calmodulin will rebind the channel. All these have been

postulated upon *in vitro* experiments, however a Ca^{2+} binding protein other than calmodulin might contribute to channel sensitivity *in vivo* (Downing and Zimmerman, 1995).

Therefore in summary, the lowered Ca^{2+} levels due to photon absorption: (1) accelerate the synthesis of cGMP owing to GC stimulation by the Ca^{2+}-free form of GCAP1; (2) increase sensitivity of the channel to cGMP and accelerate the recovery of the dark current and Ca^{2+} by uncoupling calmodulin from the cGMP gated channel; and (3) shorten the life time of photolysed rhodopsin (R*) by uncoupling recoverin from rhodopsin kinase, thus allowing the inhibitory effect of rhodopsin phosphorylation to proceed as described in the following section. These Ca^{2+} sensitive steps represent the principle mechanisms of light adaptation in vertebrate photoreceptors.

1.8.7 Regulation by non Ca^{2+} binding proteins

Apart from regulation by the Ca^{2+} sensitive mechanisms described above other mechanisms exist for inactivation of photoactivated rhodopsin (R*), which help maintain the fast physiological response of photoreceptors to light. The deactivation of the phototransduction cascade is initiated by phosphorylation of R* by a cytosolic protein in the rod photoreceptors known as rhodopsin kinase (RK) (Shichi and Somers, 1978). It phosphorylates the threonine and serine residues located in the C-terminal domain of rhodopsin on the cytoplasmic surface of the disc membrane (Hargrave *et al.*, 1980). Thus phosphorylated rhodopsin has a decreased ability to activate transducin and enhanced ability to bind a 48 kd protein known as arrestin (Arr). Arrestin, also known as S-antigen is a cytoplasmic protein, which under dark conditions binds specifically to photolysed and phosphorylated rhodopsin (R*-P) and completes the deactivation of R* and quenches its activation of transducin (Wilden *et al.*, 1986). Ultimately, all-*trans*-retinal is reduced to all-*trans* retinol by the enzyme retinal dehydrogenase present in the disk membranes of the outer segments. This loss of the chromophore is the final step in the quenching process, since the resulting phosphorylated opsin is incapable of binding transducin, rhodopsin kinase or arrestin.

The intrinsic GTPase activity of T_α subunit is another contributory factor for terminating the signal initiated by photolysed rhodopsin. Like other G-proteins T_α

subunit is capable of hydrolysing the bound GTP to GDP and inactivate itself (Bourne *et al.*, 1990). As described earlier PDE remains active only until GTP associated with GTP-T_α * is hydrolysed by the intrinsic GTPase activity of T_α. Upon which T_α dissociates from PDE and re-associates with $T_{\beta\gamma}$ and the PDE γ subunits are released to form PDE complex, and once again inhibit enzyme activity.

Transducin may also be regulated by phosducin, which is a soluble 33kd phosphoprotein highly expressed in retinal photoreceptors and the pinealocytes of the pineal gland (Lolley *et al.*, 1992). Normally phosducin exists in photoreceptor cell in the form of phosducin/$T_{\beta\gamma}$ complex and unlike transducin which is concentrated in the rod outer segment, phosducin/$T_{\beta\gamma}$ complex is dispersed through out the cytosol of photoreceptor cells (Lee *et al.*, 1990). It has been suggested that phosducin/$T_{\beta\gamma}$ complex may be involved in the direct regulation of transducin function via inhibition of the GTPase activity of T_α chain (Bauer *et al.*, 1992).

1.9   Inherited retinal degenerations

Hereditary retinal degenerations and dysfunctions are an extremely heterogeneous group of diseases in terms of clinical description and genetic cause. This term encompasses: diseases of the peripheral retina, such as retinitis pigmentosa and congenital stationary blindness; diseases of the central retina, such as macular degenerations (solely confined to the macula region) and those that eventually also lead to involvement of the peripheral retina; and many others in which the pattern of degeneration is complex. The following sections will be dedicated to the description of a few of these disorders with more emphasis given to macular degenerations, the more relevant subgroup with regard to this thesis.

1.9.1   Retinal dystrophies

Retinal dystrophies can be classified into two distinct types, those that affect the peripheral retina e.g. retinitis pigmentosa (RP) and those that affect the central retina which can be further subdivided into those that are solely confined to the macula region, called macular dystrophies and those that eventually diverge into the peripheral retina e.g. Cone-rod dystrophy.

1.9.2 Diseases of the macula

Macular degeneration is a prominent feature of a number of hereditary retinal disorders and a common cause of legal blindness in older patients in developed countries. The damage caused to the macula is irreversible and is a general feature observed in a subset of inherited retinal disorders. Studies to date prove diseases of the macula to be genetically heterogeneous and clinically diverse group of disorders encompassing a variety of severe, early and late-onset diseases that prevent with progressive loss of central vision and colour vision. The extensive degenerative changes that are associated with these disorders not only affect the retinal surface, but often involve the subretinal layers including the retinal pigment epithelium (RPE) and choroid. Though the primary defect is thought to lie in the macula, in most cases the disease is not confined to this region, but progresses peripherally leading to progressive loss of peripheral vision. Although the macula is cone rich, mutations in cone degenerations (Nathans *et. al.*, 1992), unlike rhodopsin mutations, lead to rod and cone cell dystrophies. Despite the prevalence of the macular disease and the severity of its visual consequence the underlying molecular mechanisms are unknown. There is certain amount of similarity both clinically and histopathologically amongst the macular diseases and therefore elucidation of the molecular pathology underlying one or more of these diseases may shed light on the pathogenesis of others.

Various attempts have been made to create a classification system of inherited macular dystrophies based on a number of criteria but as yet none have proved to be completely satisfactory. In 1986, Noble created a classification system where four situations were observed. The **primary hereditary macular dystrophies** which primarily affect the macula, the **choroidoretinal dystrophies** which present with macular abnormalities as a part of a generalsied retinal dystrophy, **macular degenerations associated with other non-retinal ocular disorders** and the **inherited systemic disorders** which as a part of the constellation of abnormalities present with retinal and macular involvement. Macular degenerations or dystrophies are also associated with chromosomal abnormalities (Goldberg, 1986). It is hoped that with the

65

advent of molecular genetic techniques and the identification of disease genes that a more stringent classifation system will be established for macular dystrophies.

Inherited macular dystrophies	Pattern of inheritance	Location	Gene	References
(1) Primary hereditary macular dystrophies				
Stargardt disease (STGD1),	AR, AD	1p21-p13,	ABCR	Allikmets *etal* '97, Allikmets *etal* '97a, Anderson *etal* '94, Cremers *etal* '98, Gerber *etal* '95, Gerber *etal* '98, Kaplan *etal* '93, Kaplan *etal*'94,Lewis *etal* '99, Martínez-Mir *etal* '97, Martínez-Mir *etal* '98, Nasonkin *etal*'98,Rozet *etal* '98, Stone *etal*'98, Sun *etal* '97
(STGD2),		13q34,	-	Zhang *etal* '94
(STGD3)		6q11-q15	-	Greisinger *etal* '00, Stone *etal* '94, Kniazeva *etal* '99a, Zhang *etal* '99a
Best vitelliform macular macular disease	AD	11q12-q13	VMD2	Forsman *etal* '92, Graff *etal* '94, Petrukhin *etal* '98, Marquardt *etal* '98, Nichols *etal* '94, Stone *etal* '92a, Wadeilus *etal* '93, Weber *etal* '93, Weber *etal* ' 94a, Weber *etal* '94c, Zhaung *etal* '93
Pigment pattern dystrophhies	AD	6P21.1-CEN	RDS	Arikawa *etal* '92, Connell *etal* '90, Connell *etal* '91, Dryja *etal* '97, Farrar *etal* '91, Felbor *etal* '97a, Jordan *etal* '92a, Kajiwara *etal* '91, Kajiwara *etal* '94, Travis *etal* '91, Travis *etal* '91a
Central aeriolar choroidal dystrophy (CACD)	AD	17p, 6p21.2-cen	-	Lotery *etal* '96
North Carolina Macular dystrophy	AD	6q14-q16.2	-	Kelsell *etal* '95, Rabb *etal* '98, Sauer *etal* '97a, Small *etal* '92, Small *etal* '97
Dominant drusen	AD			
Pericentral choroidal dystrophy	AD, AR			
Dominant cystoid macular dystrophy	AD	7p15-p21		

Atypical vitelliform macular dystrophy (same as VMD1)	AD	Not 8q24 Linked previously, later excluded		Daiger *etal* '97, Ferrell *etal* '83, Leach *etal* '96, Sohocki *etal* '97
Familial exudative vitreoretinopathy (EVR1, FEVR)	AD	11q13-q23	-	Li *etal* '92 Li *etal* '92a, Müller *etal* '94
Rare hereditary macular dystrophies				
Adult foveomacular dystrophy		6p21-cen	RDS	Arikawa *etal* '92, Connell *etal* '90, Connell *etal* '91, Dryja *etal* '97, Farrar *etal* '91, Felbor *etal* '97a, Jordan *etal* '92a, Kajiwara *etal* '91, Kajiwara *etal* '94, Travis *etal* '91, Travis *etal* '91a
Benign concentric annular macular dystrophy	AD			
Central areolar pigment epithelial dystrophy	AD			
Congenital macular dystrophy				
Familial foveal retinischisis	AR			
Fenestrated sheen macular dystrophy	AD			
Sorsby fundus dystrophy	AD	22q12.1-q13.2	TIMP3	Felbor *etal* '95, Felbor *etal* '97, Jacobson *etal* '95, Peters *etal* '95, Stöhr *etal* '95, Weber *etal* ''94, Weber *etal* '94b Wijesuriya *etal* '96
Doyne honeycomb retinal dystrophy	AD	2p16		
Malattia leventinese	AD	2p16-p21		
Progressive bifocal chorioretinal atrophy (PBCRA)	AD	6q14-q16.2	-	Kelsell *etal* '95, Rabb *etal* '98, Sauer *etal* '97a, Small *etal* '92, Small *etal* '97
(2) Macular abnormalities with generalised choroidoretinal dystrophies				
Stargardt-like macular dystrophy,	AD	6q11-q15; (STGD3) 4p; (STGD)		Greisinger *etal* '98, Stone *etal* '94 Kniazeva 1999
Cone rod dystrophy	AD, X-linked	17q (CORD4), 18q21.1 (CORD1), 19q13.3 (CORD2)	- - CRX	Klystra etal '93 Manhant etal '95, Warburg etal '91 Bellingham *etal* '97, Evans *etal* '94, Evans *etal* '95, Freund *etal* '97, Freund *etal* '98,Gregory *etal* '94, Li *etal* '98, Sohocki *etal* '98, Swain *etal* '97, Swaroop *etal* ' 99
Progressive cone dystrophy	AD, X-linked	17p13-p12,	-	Balciuniene *etal* '95, Small *etal*

		(CORD5) 6q25-q26 (RCD1) Xq28		'95, Small *etal* '96
			-	
			-	Bergen *etal* '97
Leber's congenital amaurosis	AR	14q24 (LCA3)	-	Stockton *etal* ' 98
X-linked juvenile retinischisis	X-linked	Xp22.3-p22.1	XLRS1	Bergen *etal* '93a, Huopaniemi *etal* '97, Retinoschisis '98, Sauer *etal* '97, Sieving *etal* '90
Goldman-favre syndrome	AR	Xp22.2-22.1		Neetens *etal* '80

Table 1.2:

A selection of inherited macular degenerations belonging to 2 of the 4 classification groups as described by Noble (1986) and adapted from Zhang and coworkers (1995), indicating their mode of inheritance and chromosomal assignments where known. AD= autosomal dominant inheritance, AR= autosomal recessive inheritance, - denotes that the disease causative gene has not yet been cloned.

1.9.3 Macular dystrophy genes

Central retinal dystrophies can be subdivided into those that are solely confined to the macular region, termed macular dystrophies and those that eventually lead to involvement of the peripheral retina. Examples,of the latter group are cone dystrophy and cone-rod dystrophy. Some well-known examples of macular dystrophies are age related macular dystrophy (AMD), which is the most common cause of legal blindness in older patients in the developed countries, Stargardt's disease (fundus flavimaculatus), Sorsby's fundus dystrophy, North Carolina macular dystrophy, and Best's vitelliform macular dystrophy.

Central retinal dystrophies are characterised by loss of central vision (loss of visual acuity) and degeneration of the retinal pigment epithelium underlying the retina. In this group of retinopathies peripheral vision is either present indefinitely or retained long term. As observed with retinitis pigmentosa, central retinal dystrophies are genetically heterogeneous with autosomal dominant, recessive and X-linked inheritance patterns observed. Moreover in most subgroups there is extensive non-allelic heterogeneity even among families that show the same mode of inheritance.

1.9.4 Cone-rod dystrophy

Cone-rod dystrophy is a severe form of chorioretinal dystrophy characterised by loss of colour vision and visual acuity followed by night blindness and peripheral visual field loss with widespread advancing retinal pigmentation and chorioretinal atrophy of the central and peripheral retina (Moore, 1992). Autosomal dominant, X-linked and recessive modes of inheritance have been described for CRD.

Autosomal dominant forms have been associated with mutations in the peripherin/*RDS* gene on chromosome 6p21.2-cen (Nakazawa *et al.*, 1994; Nakazawa *et al.*, 1996), in the *CRX* gene on chromosome 19q13.3-q13.4 (Evans *et al.*, 1994; Gregory *et al.*, 1994; Freund *et al.*, 1997) and in the *GUCD2* gene on chromosome 17p (Kelsell *et al.*, 1997; Kelsell *et al.*, 1998).

The CRD gene on 19q13.3, *CRX*, is an *OTX*-like homeobox gene. The CRX homeodomain transcription factor regulates the expression of photoreceptor-specific genes such as rhodopsin, cone opsins, interphotoreceptor retinoid binding protein (IRBP), β-PDE, and arrestin, and in a dominant-negative form blocks photoreceptor morphogenesis (Furukawa *et al.*, 1997). The mutations identified to date include one missense mutation (Glu80Ala) and a 1-bp deletion (Glu168 [Δ1bp]) causing a frameshift. The authors have speculated that CRD patients carrying either a Glu80Ala or (Glu168 [Δ1bp]) *CRX* allele are most likely to have an overall reduction of *CRX* gene function, but that the loss-of-function will be greater than 50% if these alleles are dominant negative. This proposition is based on the premise that dominant negative alleles would bind to the target sequences and thus obstruct binding of normal CRX protein and other components of the transcription complex. The mechanisms by which these mutations cause premature death of photoreceptors are not known. Nevertheless it can be argued that the mutation induced reduction of CRX function would disrupt the turnover of photoreceptor outer segment discs and that this process may lead over time to the complete loss of outer segments and cell death.

Mutations in the *CRX* gene have also been associated with Leber's congenital amaurosis (LCA) (Freund *et al.*, 1998, Sohocki *et. al.* 1998). Since *CRX* is required for biogenesis of the outer segments it is appropriate that this gene be mutated in LCA which is essentially a photoreceptor developmental defect. LCA is a clinically heterogeneous

group of childhood retinal degenerations in which the affected infants have little or no retinal photoreceptor function from early infancy. Mutations in RPE65 also cause autosomal recessive childhood-onset severe retinal dystrophy (Gu *et. al.* 1997). The most severe cases are called LCA while the less aggressive cases are termed juvenile retinitis pigmentosa. The RPE65 gene expresses a tissue-specific and highly conserved 61 kD protein present in high levels *in vivo* (Gu *et. al.* 1997). LCA is also caused by a homozygous mutation (R90W) in the homeodomain of *CRX* (Swaroop, *et. al.,* 1998). As LCA is inherited in an autosomal recessive manner, a cohort of individuals were examined for *CRX* mutations. Observations indicated that the mutant *CRX* homeodomain demonstrated decresaed binding to the previously identified *cis* sequence elements in the rhodopsin promoter. Mutant protein reduced DNA binding and transcriptional regulatory activity and the subsequent changes in the gene expression tend to lead to early onset of severe visual impairment in LCA.

The third autosomal dominant CRD gene to be identified was *GUCD2*, which encodes retinal guanylate cyclase (RetGC1). Retinal guanylate cyclase restores the level of cGMP to the dark levels by converting GTP to 3', 5' cGMP which is an essential component in the recovery process of photoreceptors. The fact that cone photoreceptors are affected first in CRD is consistent with the observation that retinal guanylate cyclase is predominantly found in the cone outer segments of the retina (Polans *et al.,* 1996). Similar to *CRX*, mutations in *GUCD2* have also been identified in LCA where disease has been ascribed to an impaired production of cGMP in the retina (Perrault *et al.,* 1996).

Autosomal recessive forms of cone rod dystrophy in association with Bardet-Biedl syndrome have been linked, by homozygosity mapping to chromosome 3 (Sheffield *et al.,* 1994), 11q13 (Leppert *et al.,* 1994), 15 (Carmi *et al.,* 1995) and 16q21 (Kwitek-Black *et al.,* 1993). Recently mutations in the *ABCR* gene on chromosome 1p21-p13 have also been identified in a pedigree segregating autosomal recessive cone-rod dystrophy. In addition to this, two sporadic cases of cone-rod dystrophy have been reported; one in association with a cytogenetically visible deletion of chromosome 18q21.1-q21.3 (Warburg *et al.,* 1991) and the other in association with neurofibromatosis, suggestive of a cone-rod dystrophy gene situated close to the *NF1* gene on chromosome 17q11.2 (Kylstra and Aylsworth, 1993).

1.9.5 Cone dystrophy

The cone dystrophies are characterised by progressive degeneration of the cone photoreceptors with preservation of rod function. Affected individuals suffer from photophobia, loss of visual acuity, colour vision and central visual field (Weleber and Eisner, 1988). In the early stage of disease electrodiagnostic tests are required to distinguish cone dystrophy from cone rod dystrophies and macular dystrophies.

Cone dystrophies are genetically heterogeneous with autosomal dominant cone dystrophy loci localised on 17p12-p13 (Small *et al.*, 1996; Balciuniene *et al.*, 1995), on 6q25-q26 as identified by deletion mapping (McKusick, 1992), and on 6p21.1 (Payne *et al.*, 1998). X-linked cone dystrophy locus (COD1) has also been located on Xp11.4-p11.3 (Dash-Modi *et al.*, 1996) and pedigrees with autosomal recessive cone dystrophy have also been reported but no loci have yet been assigned by linkage analysis (Krill *et al.*, 1973).

The gene for the adCD locus on 6p21.1 has been identified as the guanylate cyclase activator 1A (*GUCA1A*) (Payne *et al.*, 1998). Guanylate cyclase activator 1A (GCAP1) is an important regulatory component of the phototransduction cascade, necessary for restoration of photoreceptors back to the dark state following activation. The disease mechanism associated with GCAP1 mutation (Tyr99Cys) in cone dystrophy is not known. However the mutation is predicted to lead to an aberrant change in the concentration of cGMP, either high or low, depending on whether the mutation causes GCAP to be permanently activated or lose functionality altogether. The fact that Tyr99Cys mutation only affects the cone cells suggests that this mutation is more deleterious in cone cells rather than in rods or that GCAP1 is more important to cones rather than rods. The second possibility is supported by the fact that GCAP1 has a greater expression in the cones than in rods (Polans *et al.*, 1996).

1.9.6 Age-related macular degeneration (AMD)

In order to identify genes responsible for a multifactorial disease, it is necessary to study diseases with similar clinical phenotypes. Mutations in peripherin (*RDS*), Rhodopsin (*RHO*) and tissue inhibitors of metalloproteinases (*TIMP-3*) give rise to disorders with certain phenotypic features of AMD (von Ruckman *et. al.*, 1997; Capon

et. al., 1988) but none of these genes have been shown to play a role in the pathogenesis of the age-related change to date (Silvestri *et. al.,* 1994; De la Paz *et. al.,* 1997).

In 1997 Allikmets and his group found mutations in unrelated individuals in *ABCR* (a photoreceptor gene) which is responsible for mutations in Stargardt disease. Stargardt is a recessive macular dystrophy with a characteristic juvenile to young to adult onset, central visual impairment, progressive bilateral atrophy of the macular RPE and neural epithelium and frequent appearance of orange-yellow flecks around the macula and the midretianl periphery. Mutations in *ABCR* suggested that it will permit presymptomatic testing of high-risk individuals and may lead to earlier diagnosis of AMD. The ABCR gene encodes for the Rim protein (RmP) of the rod outer segments. Characterisation of the ocular phenotype in abcr knockout mice displayed that mice lacking RmP show delayed dark adaptation, increased all-trans-retinaldehyde (all-trans-RAL) following light exposure, elevated phosphatidylethanolamine (PE) in outer segments, accumulation of the protonated Schiff base complex of all-trans-RAL and PE (N-retinylidene-PE), and striking deposition of a major lipofuscin fluorophore (A2-E) in retinal pigment epithelium (RPE). These data suggest that RmP functions as an outwardly directed flippase for N-retinylidene-PE. Delayed dark adaptation is likely due to accumulation in discs of the noncovalent complex between opsin and all-trans-RAL. Finally, ABCR-mediated retinal degeneration may result from "poisoning" of the RPE due to A2-E accumulation, with secondary photoreceptor degeneration due to loss of the RPE support role. Recently, AMD has been localised to chromosome 1q25-q31 as (ARMD1) a dominant trait in a large family with dry phenotype (Klein *et. al.* 1998).

Another good candidate for AMD is the *VMD*-2 gene which is mutated in Best vitelliform macular dystrophy. Best macular dystrophy is an autosomal disorder with an "egg yolk" lesion resulting from abnormal accumulation of lipofuscin in the thr retinal epithelium (RPE). The disorganization of the RPE eventually leads to vision loss. *VMD*-2 has been mapped to the long arm of (q13) of chromosome 11 (Graff *et. al.,* 1997, Hou *et. al.,* 1996, Stone *et. al.,* 1992). The *VMD*-2 gene encodes foe a 585-amino acid protein with a predicted size of 68 kDa and has 11 exons. The mutations reported resided in the 5' end of the *VMD*-2 mRNA (Petrukhin *et. al.,* 1998). Recently, Caldwell and his group reported three new observations that firstly, mutational hotspots were present within this

gene suggesting that particular regions of this proteins have greater functional significance than others and that secondly, a 2-bp deletion within the gene causes a frameshift and a subsequent premature termination of the protein. Also, they showed that some mutations are associated with variable expression of the disease, which could involve other factors or genes in the disease phenotype. Mutations have been found mainly to affect residues that are conserved from a family of genes in *C.elegans*. The function of bestrophin is so far unknown, and no reliable predictions can be made from sequence comparisons (Bakall *et al.*, 1999).

1.9.7 Mouse models

The *rd* mouse is a naturally occurring autosomal recessive animal model for retinal degeneration that has been studied in great detail The phenotype involves the degeneration of photoreceptors after the second week of life and virtually all rod cells disappear by postnatal day 20 Although cone receptors survive to this stage, subsequently they begin to degenerate but at a slower rate than the rods. Before the onset of cell degeneration elevated levels of cGMP are detected in the *rd* retina, which is followed by a steep decline in cGMP levels to barely detectable levels when all photoreceptors have disappeared. The initial rise in cGMP correlates with a deficiency in rod specific cGMP PDE (*pdeb*) as the *rd* locus (reviewed by Farber, 1995). The mutation in the *rd* mouse is recessive owing to a premature stop codon and an insertion of viral DNA in the *pdeb* gene, which results in no enzyme production (Bowes *et al.*, 1990, Pittler and Baehr, 1991; Farber 1995). Similarly, a homozygous nonsense mutation identified in the canine homolog of rod cGMP-*PDEB* was found mutated to cause the rod/cone dysplasia type 1 (*rcd1*) in Irish setter dogs (Suber *et al.*, 1993). The *rd* mouse is a good model for a subset of autosomal recessive RP caused by null mutations in the *PDEB* gene. The increased level of cGMP has now been proposed to trigger photoreceptor death as prior onset of cell degeneration elevated levels of cGMP are detected in the *rd* retina.

The retinal degeneration slow (*rds*) mouse is phenotypically characterised by the abnormal development of retinal photoreceptors followed by their slow degeneration without any of the other cell types of the retina being affected (Van Nie *et al.*, 1978).

This is also a naturally occurring animal model. In *rds/rds* homozygotes the retina undergoes normal development and differentiation until the first postnatal week when the photoreceptors normally appear. While the other retinal cells continue their normal development, *rds/rds* fail to form outer segment discs even though the inner segments, including the ciliary projections, appear morphologically normal (Sanyal 1987, Cohen 1983). The process of photoreceptor degeneration escalates then become s more gradual with significantly reduced thickness of the outer nuclear layer; by one year of age the degeneration is complete (Sanyal 1987). The defect in *rds/rds* mouse is a pure structural defect as all the components of the visual cascade are present even if at greatly reduced levels (Cohen 1983; Reuter and Sanyal 1984). The *rds* mutation is not recessive as originally thought since the *rds/+* heterozygote mice also exhibit mild phenotype abnormality. In contrast to homozygotes, heterozygotes do form outer segments, which are reduced in length and contain irregularly arranged discs that appear swollen and vacuolated with very slow degeneration (Sanyal, 1987). The phenotype observed in the *rds* mouse is caused by an insertion mutation that disrupts the gene encoding the rds/peripherin, which produces a *null* allele (Travis *et al.,* 1989, 1991). Peripherin is a photoreceptor specific transmembrane protein that is expressed in the rim region of the outer segment discs of both rods and cones. The phenotype of the *rds/rds* mice show peripherin is essential for the biogenesis of photoreceptor outer segments. Due to the phenotype in *rds* mice, the production of aberrant disc structure has been proposed as means of triggering photoreceptor degeneration.

Humphries and co-workers have recently generated mice carrying a targeted disruption of the rhodopsin gene (*Rho-/-*). The mice do not develop rod outer segments or develop any ERG response (electroretinograph) response after 8 weeks but lose their photoreceptors over 3 months. The heterozygous *Rho+/-* mice retain majority of their photoreceptors although the inner and outer segments of these cells display some structural disorganisation, the outer segment becoming shorter in older mice. Therefore, the *rho* knockout mouse appears as a good animal model for autosomal recessive RP caused by *null* mutations in the rhodopsin gene.

The *rho* mice can also be used for innumerable experiments, which include somatic gene therapy to see if the null phenotype can be rescued using one of the

recombinant viral delivery systems. Success of such experiments will pave for similar therapeutic intervention in the cognate human disease. Other experiments relate to the creation of transgenic mice that mimic human dominant RP disease. Previously when transgenic mice were created to develop theories concerning the pathological processes induced by certain rhodopsin, such as Pro23His (Roof *et al.*, 1994), Gln344Ter (Sung *et al.*, 1994) and Pro347Ser (Li *et al.*, 1996) by necessity the mutant transgenes were placed on a wild type genetic background. Now these transgenes can be placed in the *rho+/-* mice background to generate more faithful animal models of dominant RP since humans with Rhodopsin mediated dominant RP are also hemizygous for the wild type allele. Moreover the knockout mouse presents an opportunity to study the effects of mutations especially those mutations that affect the post-translational modification of rhodopsin, without the confounding presence of wild-type rhodopsin. Such an experiment carried out *in vivo* might also lead to the recognition of other proteins that interact with rhodopsin for the correct folding of rhodopsin which by virtue of their function be candidate genes for RP. Furthermore, experiments carried out on the null background can clarify some post-translational anomalies observed with certain rhodopsin mutations in different experimental systems.

1.9.7.1 Apoptosis

The mouse models (*rd, rds* and rhodopsin transgenic mice [either Pro347Ser or Gln344ter]) have been used in two independent studies to understand the pathway leading from the primary defect (i.e. mutation in gene) to photoreceptor cell death (Chang *et al.*, 1993; Portera-Calliau *et al.*, 1994). It was observed that even though the animal models represented different basic mutations, subsequent cell death was remarkably similar and bore all the biochemical hallmarks of death by apoptosis such as cytoplasmic condensation, nuclear chromatin condensation and inter-nucleosomal DNA fragmentation seen in agarose gels. Cleavage of DNA that link multiple nucleosomes gives rise to a DNA ladder, composed of fragments that are multiples of 180-200 bp and diagnostic for cell death by apoptosis. Apoptotic cell death is distinct from cell death by necrosis or accidental cell death that produce a spectrum of DNA fragment sizes without

evidence of a nucleosomal ladder (Collins *et al.*, 1992). Apotosis is normally used by retinal cells during development to fine-tune the number of cells in the retina and their interconnections (Young, 1984).

Even though apoptosis has been recognised as the final pathway the mechanisms by which each mutation trigger apoptosis is still not fully understood. However some aspects of the effects of these different mutations suggests certain possibilities. Internucleosomal DNA fragmentation, a hallmark of apoptotic cell death, is thought to be mediated by a nuclear endonuclease that can be stimulated by a rise in Ca^{2+} (McConkey *et al.*, 1989). Such a rise in Ca^{2+} can be induced in the *rd* mouse where cGMP accumulates as a result of the mutation (Yau and Baylor, 1989), thus activating the endonuclease. In *rds*/peripherin mice, failure to develop an outer segment may upset some internal mechanism of the photoreceptor thus activating the endonuclease. This situation is similar to that of a cell under stress, which might cause the cell to self-destruct. In the case of rhodopsin mutations (e.g. Pro347Ser) it could be that the presence of the mutant rhodopsin alters the normal cellular pathways and disrupts normal cell-cell interactions (Huang *et al.*, 1993), leading to the transmission of an incorrect signal to the photoreceptors and thus causing them to self-destruct.

1.10   Aims of this study

Inherited choroidoretinal dystrophies vastly contribute to the proportion of dystrophies that afflict the retina. Diseases that principally affect the macular region of the retina, eventually lead to central loss of vision. This study describes the positional cloning endeavours undertaken to identify the gene responsible for one such ocular disease known as autosomal dominant Doyne honeycomb retinal dystrophy (DHRD). The ultimate purpose of this study being to contribute to the understanding of the physiology of the retina and mechanisms that cause retinal degenerations.

Previously, a total genome search had been undertaken (by a former colleague) but significant linkage had not yet been achieved although tentative positive lodscores had been obtained on chromosome 2, 7, 8,14 and two regions on chromosome 1. These regions were further investigated with greater density of markers placed at 1-2 cM intervals in order of preference with those displaying the highest lodscores being

investigated first. Furthermore, an additional branch was incorporated to the original panel and regions of positive lodscores were re-analysed in the hope of linking DHRD to one of these chromosomes. Once linkage had been achieved to the 2p21-16 region, the entire family was haplotyped with linked markers in the disease interval further refining the linked region to a 4cM region (Evans, K. *et. al* 1997). Concurrently, two small families were also linked to the DHRD locus (Kermani, S. *et. al.* 1999) implying that this locus could be responsible for a proportion of families displaying the dominant drusen phenotype providing further refinement of the disease interval by obtaining new recombinants in the linked families (chapter 3).

Characterisation of the DHRD genetic interval was undertaken to establish a physical map of the region in the form of an overlapping YAC contig (Kermani, S. *et. al.* 1999). After coverage was obtained with YAC clones, PAC clones were further isolated in an attempt to substantiate the contig (Chapter 4)

Candidate gene screening is a well-established method of identifying disease genes and has led to the identification of numerous retinal genes. A retinally expressed gene that had been previously mapped to the 2p16 region (data from the Whitehead database) and further practical evidence suggested it to be a feasible candidate gene for DHRD. Therefore the analysis of this gene was undertaken, which involved characterisation of this gene to establish the exon-intron structure of the gene followed by mutation screening in families linked to the 2p16 region (chapter 5).

CHAPTER 2

METHODS AND MATERIALS

2.1 DNA Extractions

2.1.1 Human DNA extractions from blood samples

Venous blood samples were collected in 10 ml tubes and EDTA was added prior to freezing samples at −80 °C until DNA extraction. A Nucleon DNA extraction kit (Scotlab, Scotland) was used to carry out all extractions. Blood samples were thawed to room temperature and transferred to a 50 ml Falcon tube prior to adding Reagent A (10 mM Tris-HCl pH 8.0, 320 mM sucrose, 5 mM $MgCl_2$, 1% Triton X-100) and mixed by inverting tubes, followed by centrifugation at 4000 g for 10 min. The supernatant was discarded and the pellet was resuspended in 2 ml of Reagent B (400 mM Tris-HCl pH 8.0, 60 mM EDTA, 150 mM NaCl and 1 % SDS). The pellet was broken using a clean plastic Pasteur pipette and the suspension was transferred to a 5 ml tube. Then 500 μl of 5 M sodium perchlorate was added prior to rotary mixing for 15 min at room temperature followed by 25 min at 65 °C in an oven. The suspensions were cooled on ice prior to adding 2 ml of chloroform and 300 μl of Nucleon Silica suspension. These suspensions were rotary mixed for 5 min and then pelleted in a centrifuge for 6 min at 1400 g. The top aqueous layer containing the DNA was aspirated to a universal tube and 2 volumes of ethanol was added. Precipitated DNA became visible which could be removed using a sterile needle, placed in a 1.5 ml Eppendorf tube then washed with 70% ethanol before leaving to air dry. Subsequent DNA pellets were resuspended in volumes of 400 μl-1000 μl of sterile distilled water (depending on the size). Stocks of DNA samples were stored at −80 °C and 1/10 dilutions of the stock DNA were routinely used for analytical purposes.

2.1.2 Isolation of YAC DNA in solution

This protocol yields DNA fragments in the range 50-200 kb, sufficient for PCR analysis. YAC clones were received as stabs in agar, they were streaked out on YEPD agar plates supplemented with ampicillin (50 μg/ml) and incubated at 30 °C for 48 h. Single colonies were used to inoculate 10 ml YEPD broth supplemented with ampicillin

and incubated at 30 °C overnight with agitation. This culture was used to seed 100 ml YEPD broth containing ampicillin for a further 36 h (until an OD_{600} of 1.5-2.0 corresponding to a 3.3×10^6 cells/ml was reached) at 30 °C with agitation. Cultures were pelleted by centrifugation at 3000 g for 10 min at 4 °C and the supernatant was discarded. Pellets were resuspended in 5 ml of 0.9 M sorbitol, 20 mM EDTA, 14 mM 2-β,mercaptoethanol, 20 µl of 10 mg/ml lyticase in distilled water and then cells were incubated for 1 h at 37 °C with agitation. Cells were pelleted gently at 1000 g for 10 min and the supernatant was discarded. Pellets were resuspended in 5 ml of guanidinium chloride solution (4.5 M GuHCl, 0.1 M EDTA, 0.15 M NaCl, 0.05 % sarkosyl, pH 8.0). This suspension was heated at 65 °C for 10 min and then allowed to cool at room temperature prior to the addition of an equal volume of ethanol. Nucleic acids were pelleted at 2000 g for 10 min. Pellets were resuspended in 1 X TE and RNAse was added followed by incubation at 37 °C for 30 min. Proteinase K (200 µg/ml final concentration) was added and the mixture was incubated for 1 h at 65 °C. This was followed by cooling the suspensions to room temperature prior to a phenol:chloroform:isoamyl alcohol (25:24:1) extraction followed by 100 % ethanol precipitation. Precipitated DNA was removed using a sterile needle and washed in 70 % ethanol, before leaving to air-dry at room temperature followed by resuspension in 250 µl of sterile distilled water. 1/50 dilution of the stock YAC DNA was routinely used for PCR amplifications e.g. STS content mapping.

2.1.3 Small scale preparation of plasmids, PAC, cosmids and Fosmid DNA

The alkaline lysis mini-prep method (modification of Birnboim & Doly, 1979) yielded sufficient quantities of DNA for PCR amplifications and restriction digestions. Colonies from a bacterial stab or a glycerol stock were streaked out on a Liquid Broth (LB) agar plate supplemented with the appropriate antibiotic and grown overnight at 37 °C. Single colonies were chosen from these plates and used to inoculate 10 ml of LB supplemented with the same antibiotic and grown overnight at 37 °C with agitation. Plasmids were grown in the presence of ampicillin (50 µg/ml) and cosmids in the presence of kanomycin (25 µg/ml). Glycerol stocks were routinely prepared at this stage

(0.5 ml culture + 0.5 ml 40 % sterile glycerol) and stored at -80 °C for further experiments. Cultures were centrifuged at 3000 g for 10 min and the supernatant was discarded prior to resuspending pellets in 200 µl of cell resuspension buffer (50 mM Tris-HCl, pH 7.5, 10 mM EDTA, 100 µl/ml RNAse) and transferred to a 1.5 ml Eppendorf tube. 200 µl cell lysis buffer (0.2 M NaOH, 1 % SDS) was added and mixed by inverting until the lysate had a clear appearance. This was followed by the addition of 200 µl of neutralisation buffer (1.32 M KoAC, pH 4.8) to precipitate the bacterial chromosomal DNA prior to centrifugation at 13, 000 rpm for 10 min. The clear supernatant was aspirated to a clean Eppendorf tube and 1 ml of DNA purification resin (6 M GuHCl, 50 mM Tris-HCl, 20 mM EDTA, Celite analytical filter aid (BDH, U.K.)) added. The DNA-resin mixture was applied to the top of a 3 ml open syringe attached to a mini column and vacuum pump. The DNA resin mixture was by the suction of the vacuum pump into the mini column. The DNA was eluted by washing the column with volumes of 40-50 µl of sterile distilled water at 80 °C and centrifuged at 13, 000 rpm for 2 min.

2.2 Purification of DNA

2.2.1 Phenol/Chloroform extraction

For smaller volumes of DNA (such as digests) the extraction volume was increased to 200 µl by addition of sterile 1 X TE. Larger volumes were directly extracted. An equal volume of phenol chloroform isoamyl (25:24:1) was added to each DNA solution and mixed by inversion prior to centrifugation at 6000 rpm for 3 min. The top aqueous layer was removed to a clean eppendorf tube and an equal volume of chloroform was added, mixed by inverting and re-centrifuged (the phenol extraction can be repeated a few times depending on the protein content in the sample). The aqueous supernatant containing the DNA was removed to a clean Eppendorf tube for ethanol precipitation.

2.2.2 Ethanol precipitation

Two volumes of absolute ethanol and a 1/10th of the total volume of 3 M sodium acetate was added, mixed thoroughly and placed at -80 °C for 30 min to allow precipitation of DNA. The precipitate was centrifuged at 13, 000 rpm for 15 min to pellet

the DNA. The pellet was rinsed in 70 % ethanol prior to air-drying and resuspended in sterile distilled water.

2.2.3 Purifying PCR products using Sephacryl® HR columns (S200/400)

These columns (Pharmacia, U.K.) provide a convenient method for desalting, buffer exchange, removal of primers and labelled and unlabelled nucleotides from DNA solutions. They can be used for purification of plasmid minipreps prior to sequencing and for purification of PCR products. The Sephacryl® HR resin (sephacryl equilibrated in TE buffer, pH 7.6) is initially resuspended in the column by gentle vortexing. The screw cap was loosened and the base snapped off before placing in an open-topped Eppendorf tube and pelleting at 3000 rpm for 1 min to compact the column. The column was removed into a clean Eppendorf tube and 20-25 µl of DNA sample was applied to the top centre of the compacted bed being careful not to disturb the matrix. Centrifugation for 1 min allowed DNA to elute into the Eppendorf tube below. S200 columns were routinely used for purification of labelled probes prior to hybridisation. These columns also facilitated buffer exchange and desalting for purification of probes before hybridisation. S400 columns were used for removal of excess primers and 'primer dimers' from PCR products prior to sequencing. Both gel matrices removed unincorporated dNTPs provided the DNA fragment was greater than 100 bp in length.

2.2.4 Centricon 100 spin columns (Centricon, USA)

These were routinely used for the purification of PCR products prior to ABI sequencing. Columns were assembled according to manufacturer's guidelines and 5-10 µl of PCR product in 2 ml of sterile distilled water was added to the upper reservoir of each column. These were centrifuged at 1000 g for 15 min (allowing the product DNA to remain on the membrane while all unincorporated primers and dNTPs pass through). The column was then inverted and centrifuged for 5 min at 3000 g allowing the DNA eluate to be collected. The purified products were directly used for cycle sequencing.

2.3 Sizing DNA

2.3.1 Restriction digests

All digests were carried out in total volumes of 20 μl. On average 10 μg of human DNA was used for digestion whereas 3 μg of plasmid DNA was used in a 1 X buffer as supplied by the manufacturer. Sometimes Bovine serum albumin (BSA) at 1 X concentration was added to enhance the enzyme activity. Appropriate enzyme units for digestions were worked out according to the manufacturer's enzyme concentrations. Enzymes were obtained from a range of manufacturers: Pharmacia (U.K.), New England Biolabs (U.K.), Promega (U.K.) and GIBCO, BRL (U.K.). Most enzymes are supplied in concentrated forms. Thus, 1 μl of enzyme is sufficient to digest 10 μg of DNA in 1 h. As a standard, one unit of enzyme is usually defined as the amount of enzyme required to digest 1 μg of DNA to completion in 1 h in recommended buffers at required temperatures in 20 μl reactions. All enzymes were supplied in 50 % glycerol and can be stored at –20 °C for further use. When preparing for a restriction digest, all reagents were mixed on ice and the enzyme was mixed at the final stage.

Example of a restriction digest with EcoR1 (Pharmacia, U.K.):

DNA (e.g. 10 μg of human DNA)	10 μl
10 X OPA$^+$ buffer	2 μl
EcoR1	1 μl
H_2O	7 μl
Total volume	20 μl

Digest was left to incubate at 37 °C for 1 h.

To analyse the digest, 5 μl of gel loading buffer was added to the total digest and only a 1/10th of the total volume of the digest was loaded on an agarose gel to view the digested products and UV photographed.

2.3.2 Agarose gel electrophoresis

Commercially available agarose (Biorad, U.K.) was used to prepare gels used in routine PCR analysis, restriction digests and in estimation of concentration of DNA. Gels were melted in 1 X TAE buffer, until clear and poured into the desired molds with the appropriate combs and allowed to polymerise at room temperature. Once ploymerised, the comb was removed and the DNA samples were mixed with loading buffer and loaded in wells. Commercially available markers supplied by companies were also used to estimate the size and concentration of DNA. A low percentage (0.8 %) agarose was used to separate relatively large molecules of DNA (PCR products of ~900 bp) and a high percentage gel (2 – 3%) was used to separate small fragments (PCR products of ~150 bp). Gels were subjected to an electric field and the negatively charged DNA migrated from the cathode to the positive anode in 1 X TAE buffer. At low voltages, rate of migration of linear DNA is proportional to the voltage applied. Gels were stained with Ethidium bromide (0.5 μg/ml) which is a fluorescent intercalating dye and reduces the mobility of DNA by 15 %. The dye intercalates between stacked base pairs of DNA, extending the length of linear and nicked circular DNA and makes them more rigid. Gels were viewed under UV light and photographed.

The agarose concentrations and the range of resolution achieved are as follows:

Agarose {%(w/v)}	Range of resolution of linear DNA (Kb)
0.3	5.0 – 6.0
0.6	1.0 – 20
1.0	0.5 – 10
1.5	0.2 – 6.0
2.0	0.1 – 2.0
3.0	- < 0.1

2.4 PCR amplifications

2.4.1 Standard PCR

The conditions provided in this protocol are standards and relevant alterations are stated where essential. A typical PCR was carried out in a 25 μl reaction volume

consisting of 1 X PCR buffer (10 X NH₄ buffer, Bioline, U.K.), 200 µM each dNTP (Promega, U.K.), 7.5 pmoles each primer, 0.3 units of Taq DNA polymerase (Bioline, U.K) and ~100 ng of the template DNA. The temperature cycling profile consisted of an initial denaturation at 94 °C for 4 min followed by 30 cycles of denaturation at 94 °C for 30 seconds (annealing temperature being primer dependent for 30 seconds) and extension at 72 °C for 30 seconds. The final step is extension at 72 °C for 2 min. Annealing temperature for PCR is determined by the melting temperatures ™ of the two primers. Tm can be calculated by the nucleotide sequence of the primer using the following equation:

Tm = 4(G+C) + 2(A+T). A Hybaid Omnigene thermal cycler or a Perkin-Elmer Cetus system 2400 or a 9600 thermal cycler was routinely used for all PCR analyses.

2.4.2 *Alu* –vector arm PCR

This protocol is a modification of Nelson *et al*, 1989. Standard PCR protocols were carried out in total volumes of 50 µl reactions containing ~1 µg each of YAC DNA in solution, with the following combinations of primers. Ale 1 and Ale 3 represent human specific Alu primer sequences while RA and LA represent PCR primers corresponding to the relevant pYAC 4 vector arms.

Ale 1 + RA (5'-ata tag gcg cca gca acc gca cct gtg gc-3')

Ale 1 + LA (5'- cac ccg ttc tcg gag cac tgt ccg acc gc-3')

Ale3 + RA

Ale3 + LA

Ale1 only (5'-gcc tcc caa agt gct ggg att aca-3')

Ale3 only (5'- cca t/ctg cac tcc agc ctg gg-3')

The temperature profile consisted of 35 amplification cycles at 94 °C for 1 min, 60 °C for 1 min and 72 °C for 2 min. Products were visualised by agarose gel electrophoresis and unique products present within the Ale-vector arm samples which represented YAC insert termini were directly sequenced using internal pYAC4 vector arm primers.

PYAC4 internal LA primer sequence: (5'-ggt ggt tta cgc aag-3')

pYAC4 internal RA primer sequence: (5'-gtc gaa cgc ccg atc tca a-3')

2.4.3 Heteroduplex analysis

The PCR products of normal and mutant alleles can be separated from each other using non-denaturing gel electrophoresis. Resolution is based upon conformational differences that occur in the DNA molecule as a result of insertions, deletions or single base pair changes mismatches. Heteroduplex DNA was generated by standard PCR amplification. Amplification occurs between homologous DNA segments as well as across the segment containing the mutant allele. By denaturing these samples and allowing the temperature of the PCRs to drop down to room temperature, double stranded DNA forms between the identical complementary strands (homoduplexes) and also between strands of the 2 different amplified segments (heteroduplexes). These heteroduplexes migrate at a slower rate through the polyacrylamide gel matrix than the homoduplexes.

MDE gels (Flowgen, U.K.) were routinely used for the detection of heteroduplexes. The size range of PCR products analysed in this study ranged from 100 bp-300 bp in size (this is within the optimum range for resolution). The electrophoresis apparatus (using 40 cm X 20 cm) was vertically assembled according to the manufacturer's instruction (J.T. Baker, U.S.A.) and clamped within the casting tray. A 100 ml gel solution was prepared by the addition of 50 ml MDE gel solution, 6ml 10 X TBE, 44 ml sterile distilled water, 400 μl 10% Ammonium per sulphate (APS) and 40 μl TEMED. Prior to addition of APS and TEMED, 2 ml was removed, to which 30 μl APS and TEMED was added and gently poured between the plates and left to set forming a plug at the base of the gel. The remaining gel was poured and a comb was inserted before leaving to polymerise for 1 h after which the comb was removed and 0.6 X TBE was added to the upper and lower buffer reservoirs. Wells were thoroughly rinsed using a syringe filled with the buffer. 10 μl of samples containing 100-200 ng PCR product in 2 μl loading buffer containing xylene cyanol and bromophenol blue was loaded in each well. Electrophoresis was carried out for an average of 16 h at 180 volts where the

xylene cyanol and bromophenol blue were indicators of resolution. The gels were stained with ethidium bromide (final concentration of 0.5 µg/ml) and UV photographed.

2.4.4 YAC screening methods

YAC clones were obtained by screening the ICI (Anand *et al*, 1990) and ICRF YAC (Larin *et al* 1991) genomic library with Sequence Tagged Sites (STSs) and microsatellite markers. The ICI library consisted of 40 primary pools and 9 secondary and 20 tertiary pools. The ICRF library consisted of 27 primary pools, 8 secondary pools and 20 tertiary pools. All YAC library pools were received as agarose plugs from the Human Genome Mapping Project (HGMP) resource centre (Hinxton, U.K.) in 5 mM EDTA and were rinsed several times in sterile 1 X TE and distilled water prior to use. Plugs were melted at 65 °C for 10 min and 2-3 µl was used per PCR reaction. These pools were screened with a variety of polymorhic markers, STSs and EST markers following the standard PCR protocol. A single positive in the secondary pools and two positives in the tertiary pools were expected from each positive primary pool, although a single positive in a primary pool can sometimes yield more than one positive in the secondary pools. In the tertiary pools, one positive was expected in pools 1-8 which represented an array of rows while the other in pools 9-20 which represented a series of columns. The row and column along with primary and secondary pool identities represented the co-ordinates for identification of the specific YAC. CEPH library primary pool screening results were sent to the CEPH / Genethon database where secondary and tertiary pool screenings were carried out. All identified YACs were ordered from the Human Genome Mapping Project resource centre.

2.4.5 PAC library screenings

All PAC clones were supplied routinely by the Human Genome Mapping Project resource centre. Peter de Jong and his group at the Roswell Park Cancer Institute, Buffalo, constructed the PAC library RPC11. The library was constructed in the vector, pCYPAC2N (Ioannou P.A and de Jong P.J, 1996). The source was a normal male blood donor, and the insert size was approximately 110kb. 25 % of the clones lack insert. The library consisted of approximately 120, 000 clones in 315 384-well micro-titre plates.

The plates were numbered from 1 to 321 (where plates 174-176, 284, 285 and 311 do not exist).

The primary pools were coded from A to U (21 vials of 100 µl each) and consisted of 15 plates each. For each positive primary pool identified, the secondary plates were requested. These consisted of 15 individual plate pools (20 µl in a 96-well micro-titre plate), from the plates that comprised that primary pool. A concise table was provided to allow the identification of a positive plate. Once the positive plate was identified, these were received as complete plates to eventually organise a pooling system of our own which were pooled into rows or columns.

The pools were received as live cultures in dry ice and it was recommended that as the cells were thawed for screening, the remaining material was divided into aliquots for further experiments to avoid unnecessary freeze thawing to prevent damage to cells. When handling the 384-well plates, care was taken to avoid pressing the lid to prevent cross contamination between wells. All media contained 7.5 % glycerol and LB broth supplemented with the antibiotic kanamycin (final concentration of 25 µg/ml) and could be stored at –70 °C. PCR assays were performed to confirm a known sequence that could be amplified from the relevant clones, plate pools and primary pools.

2.4.6 STS content mapping

To detect overlaps between adjacent YACs for chromosome walking and to determine any chimerism present, YACs were tested with all STSs, ESTs and microsatellite markers in the region by standard PCR amplification with specific primers. STS content mapping was carried out using YAC solution DNA. However, due to the instability of YACs, YAC colonies were mixed in 20 µl of 1 X TE, cells were lysed at 95 °C for 10 min, cell debris was spun down by pulse spinning in a micro-centrifuge and 1 µl of the lysate was used in a PCR reaction. If proven positive these colonies were further grown and DNA isolated.

2.4.7 Single primer extension PCR

This is a modification of the Screaton *et al*, 1993 method that relies on the linear amplification of a target sequence using a single primer of pYAC4 vector. Based on the

standard PCR protocol, these reactions were carried in 50 µl volumes of 2.5 mM MgCl$_2$, 400 nM single pYAC4 vector arm primer, 100 ng template DNA and 1.5 units Taq polymerase. The cycling parameters consisted of one cycle of 95 °C for 5 min, 60 °C for 30 seconds and 72 °C for 2 min. Parallel reactions were performed with annealing temperatures of 45 °C, 55 °C. An altered temperature cycling protocol was also often used consisting of three cycling stages. An initial 99 cycles of 94 °C for 10 seconds, 65 °C for 15 seconds and 72 °C for 30 seconds followed by 5 cycles of 94 °C for 10 seconds, 40 °C for 15 seconds and 72 °C for 45 seconds. The initial cycling profile was then repeated for a final 35 cycles. All products were visualised by agarose gel electrophoresis and sequenced using pYAC4 vector arm primers lying internal to the primers used in PCR.

2.4.8 Reverse Transcriptase (RT) PCR

First strand cDNA synthesis was performed by mixing on ice the following reagents:

5x reverse transcriptase buffer (50 mM Tris-HCl pH 7.6, 60 mM KCL, 10 mM MgCl$_2$, (BRL, UK)), 3.5 µl dithiolthreitol ((DTT),BRL,UK), 2 µl of 20 mM dNTP (Pharmacia,UK), 1 µl RNAase inhibitor (human placental, BRL,UK), 50 pmoles reverse (antisense) oligonucleotide primer (or 1000 pmoles random primers) 5 µg total RNA, and the final volume was made up to 33 µl with DEPC (diethyl pyrocarborate) treated water (100 µl DEPC in 1 litre of distilled water overnight at 37 °C prior to autoclaving).

The mixture was heated at 65 °C for 10 min, placed on ice before adding 2 µl of reverse transcriptase (BRL, UK) and incubated at 42 °C for 90 min. The first strand cDNA could be stored at –20 °C or used immediately for PCR analysis. This procedure produced enough DNA template for 7 PCRs.

2.4.9 Radioactive PCRs

This procedure involved the γ ^{32}P labelling of a 5' end (either a forward or a reverse primer) of an oligonucleotide (see section 2.5.1) followed by it's addition to a preprepared mixture of a regular PCR mixture (see section 2.4.1) one which lacked the

primer that was being labelled. Radioactive PCRs were carried out in total volumes of 10 µl which were aliquotted into the individual samples of DNA and a layer of mineral oil was added before programming the PCR block.

2.5 Radioisotopic labelling

2.5.1 5' endlabelling of primers

Microsatellite markers were chosen from a range of genome maps (Weissenbach *et al*, 1992; Gyapay *et al*, 1994) and associated primers obtained commercially (Cruachem, HGMP Resource Centre, Bioline, Genosys, U.K.). To optimise conditions, all microsatellite markers were initially tested on genomic DNA by standard PCR analysis in 10 µl volumes containing 20 pmoles of each primer.

For 5' endlabelling, 20 pmol (100ng) of forward or reverse primer for each marker was end labelled prior to addition to PCR mix. Endlabelling was carried out in 1X reaction buffer (One-Phor-All *plus*, Pharmacia), 10µCi [γ^{32}P] ATP (6000 Ci/mmole, Amersham) and 5units of T4 polynucleotide kinase (Pharmacia) in a total reaction volume of 20 µl. The reaction was incubated at 37 °C for 40-50 minutes and used immediately afterwards or stored at -20 °C (for no more than a few hours) until required.

The incorporation method of labelling involved the incorporation of [α^{32}]-dATP or [α^{32}]-dCTP directly into the PCR reaction. The protocol was essentially the same as for endlabelling except the dNTP concentration used i.e. 1/10th less unlabelled dCTP or dATP was used depending on the radioactive isotope. 4 µl of formamide loading dye was added to each synthesised product prior to heat denaturing and electrophoresis through a 6 % denaturing polyacrylamide gel for resolution of the allele systems.

2.5.2 Random prime method

Approximately 50-100 ng of Cot-1-DNA (Sigma, UK) was routinely labelled by using an α–dCTP labelling kit (Pharmacia, U.K.). The total volume of DNA was increased to 34 µl with 1 X TE, denatured at 94 °C and placed on ice for 5 min. To this 10 µl of Reagent mix (buffered aqueous solution containing dATP, dGTP, dTTP and random hexadeoxy-ribonucleotides) was added, 1 µl of Klenow fragment of DNA polymerase I, 50 µCi [α^{32}P] CTP and sterile distilled water to a total volume of 49 µl.

90

The mixture was incubated at 37 °C for 30 min to label. Incorporation was checked by setting up a Geiger counter places between a clamp, facing downwards. A filter paper was placed on a flat surface facing the Geiger. In the centre of the filter paper, 1 µl of the labelled mixture was dotted and the position of the Geiger was adjusted to read approximately 100 counts. The label was washed off the filter paper with 5 % Tricholroacetic acid (TCA) and the new count level was calculated as the percentage labelled. A good incorporation is between 80-90 %. The mixture was eluted through a S200 column at low speed to remove unincorporated dNTPs. The clear label was denatured at 95 °C for 3 min and used as a probe for hybridisations at 65 °C.

2.6 Southern blotting

2.6.1 Transfer of DNA to nylon membrane

Identification of individual fragments from complex DNA was routinely accomplished by resolving DNA by gel electrophoresis. This method was first described by Southern in 1975. It was routinely used to identify specific DNA sequences through hybridisations with a homologous DNA probe. This method was used to analyse YAC, human and plasmid DNA. Electrophoresis of DNA was carried out until required resolution was achieved. The complex nature of YAC and cosmid DNA gel was treated through a successive stages of depurination in 0.25 M HCl solution for 15 min, rinsing in distilled water, denaturing for 15 min and then neutralizing for 15 min. The treated gel was placed with DNA side upon a 3 MM Whatmann paper assembled as a wick over a reservoir of 10 X SSC solution (standard Southern blotting method). A sheet of Hybond N+ (Amersham) membrane was placed on top of the gel, and 2 sheets of Whatmann paper soaked in 10 X SSC were placed on the membrane, taking care not to introduce any bubbles. All sheets were cut to the size of the gel. Paper towels and a small weight was placed above the Whatmann paper to maximize capillary action. To allow maximum transfer of DNA onto the membrane, blotting was carried out overnight. The following day, the membrane was baked at 80 °C for 10 minutes and UV cross-linked (70, 000 $\mu J/cm^2$). The membrane was then used for hybridisations.

2.6.2 Hybridizations

Human genomic DNA was hybridised in 25 ml Denhardt's solution (5 X SSC, 5 X Denhardt's solution (2 % BSA, 2 % Ficoll^{TM} and 2 % polyvinylpyrrolidone) and 0.5 % SDS, 0.5 ml (1mg/ml) of denatured sonicated non-homologous DNA was added to the prehybrisation solution for greater sensitvity. All other DNA was hybridised in 20 ml of pH 7.2 Church's buffer (7 % SDS, 0.125 M NaPPi (68.4 Na$_2$HPO$_4$ and 31.6 ml NaH$_2$PO$_4$ per 100ml solution), 1mM EDTA). Filters were prehybridised for 2-3 hours before leaving for overnight hybridisations at 58 °C in an oven.

2.6.3 Post hybridisation washes

Filters were washed to remove non-specific hybridisation with decreasing concentration of SSC and SDS and increasing temperature. Initially, a low stringency wash for 10 min at room temperature in 2 X SSC and 0.1 % SDS was carried out. If background counts were still high on monitoring, the stringency of wash was increased by gradually decreasing SSC concentration to a maximum of 0.1 % SSC with 0.1 % SDS and raising the temperature to 65 °C. Washed filters were exposed to Kodak or Fuji X-ray film between two intensifying screens.

2.7 YAC experiments

2.7.1 Preparation of YAC DNA in agarose plugs

This is a modification of the Vollrath and Davies method 1987 used to isolate intact yeast chromosome DNA and is recommended for the sizing of YACs by Pulse Field Gel Electrophoresis (PFGE).

Individual YACs were streaked out on YEPD plates supplemented with ampicillin and incubated at 30 °C for 2 days. When required, colony PCRs were performed on half a colony to confirm the presence of an STS that the YAC should have been positive for (according to the database information). If the colony was positive then the colony of interest was chosen for inoculation using a sterile toothpick under sterile conditions. One colony was used for inoculation of 10 ml of YEPD broth supplemented with ampicillin and incubated for 24 h at 30 °C with agitation in a 50 ml tube. The 10 ml

inocullum was used to seed 100 ml of YEPD broth supplemented with ampicillin for 36-48 h at 30 °C with agitation.

Once the cells were grown (OD_{600} of 1.5-2.0 corresponding to a 3.3 X 10^6 cells/ml was reached) the culture was used to prepare YAC plugs. In parallel, glycerol stocks of these cultures were made (500 μl of culture and 500 μl of 50 % glycerol) and frozen at –80 °C for further experiments.

Cultures were split into two equal volumes of 50 ml each and pelleted at 4000g for 10 min. The supernatant was discarded and the pellets were resuspended in 15 ml of SCE (1 M sorbitol, 0.1 M sodium citrate, 10 mM EDTA) media using sterile loops. Solution was pelleted in 0.8 ml SCEM (SCE media containing β-mercaptoethanol suspension) media (since pellet has volume, volume increased to 1ml) to approximately a cell density of 2.9 X 10^9 cells. Individual YAC solutions were pooled and 120 μg/ml of lyticase was added and left to incubate for 1 h at 30 °C without agitation. In the meantime, 1 % low melting agarose in 1M Sorbitol was prepared and incubated at 55 °C (melting temperature of agarose). Equal volumes of 0.5 ml of cells were mixed with 0.5 ml of agarose and aliquotted into pre-cooled molds and set on ice for 30 min. Once the plugs set, they were removed using sterile loops into 15ml proteinase-K / sarcosyl solution (0.5 M EDTA, 1% N-lauryl sarcosine and 2 mg/ml proteinase-K) and incubated for 48 h at 30 °C followed by extensive rinsing in 1 X TE buffer for 3 X 20 min. Plugs were stored at 4 °C until required for Pulse Field Gel Electrophoresis analysis where a quarter of the plug was electrophoresed.

2.7.2 Pulse Field Gel Electrophoresis (PFGE) of YAC plugs

PFGE resolves DNA fragments up to 10 Mb in size by periodically changing the electric field between two spatially distinct pairs of electrodes. Yeast chromosomes are easily separated by this technique. Alternating angle electrophoresis used in this study for the sizing of YACs is based on the CHEF (clamped homogeneous electric field) technique (Carle and Olsen, 1984) utilising the CHEF-DR II apparatus (Biorad). A 1 % agarose gel (molecular biology certified, Biorad) in 0.5 X TBE buffer was prepared in a 100 ml volume, poured into a gel casting tray containing a comb and allowed to polymerize for 1 h. A quarter of a YAC plug was loaded into each well and sealed by

pouring 1 % low melting agarose (Sigma, U.K.) dissolved in 0.5 X TBE. Initially, the electrophoresis chamber was rinsed with 1 litre of distilled water after which 2 litres of 0.5 X TBE were poured in and circulated using a circulatory pump at 4 °C. The gel was removed from its casting tray, placed inside the tank on a metal plate and subjected to electrophoresis. For separation of fragments between 100 kb and 2000 kb the following parameters were implemented: an initial time of 60 seconds, a final time of 90 seconds, start ratio of 1.0 and a run time of approximately 20 h.

2.8 Sequencing by the dideoxy chain termination method (Sanger *et. al.*, 1977):
2.8.1 Direct sequencing of PCR products

All reagents used for sequencing were obtained from Pharmacia, U.K.

(a) PCR products were purified through S400 spin columns. If a single product was not present alternative methods were adopted to purify the required product. These included the use of NA45-DEAE paper or electrophoresis of 10-20 μl of the PCR product on a low percentage agarose gel and excising the required band into 50 μl of sterile water, in which it was left to elute overnight. 10 pmoles of sequencing primer was endlabelled in a 10 μl reaction using 10 μCi [γ^{32}P]-ATP and 2 μl of this was added to 10 μl volume of purified DNA (~100 ng). Following denaturation at 95 °C for 5-10 min, the contents were snap frozen on ice, briefly centrifuged and replaced on ice for 2 min. Then, 2 μl of annealing buffer, 2 μl of labelling mix A and 2 μl T7 DNA polymerase (diluted 1:4 in enzyme dilution buffer) were added to the annealed template and mixed by gentle pipetting. Samples were transferred immediately into the chain termination mixes.

(b)2.5 μl of each dideoxy chain termination mix (A,C,G,T) were aliquotted into separate tubes and pre-warmed at 37 °C for 1-2 min. 4 μl of the pre-prepared sequencing mix from section (a) was added to each of the 4 tubes, gently mixed and incubated at 37 °C for 10 min. Sequencing reactions were terminated by adding 4 μl of formamide dye. Reactions were analysed by electrophoresis on 6 % denaturing polyacrylamide gels.

2.8 Sequencing of cloned DNA

Plasmid DNA was extracted using the alkaline lysis mini prep method (section **2.1.3**). The concentration of the DNA for sequencing was adjusted so ~1-2 μg was present in a 32 μl volume (10 μl of mini prep DNA was usually added to 22 μl of sterile water). 8 μl of relatively fresh (no more than 6 months old) 2 M NaOH was added, briefly vortexed and centrifuged prior to incubating at room temperature (22 °C) for 10 min. DNA precipitation was performed (section **2.2.2**) with 11 μl of 2 M NaOAc (pH 4.8) and 120 μl of 100 % ethanol. The purified DNA pellet was resuspended in 10 μl of sterile distilled water followed by the addition of 2 μl sequencing primer (5 pmol/μl) and 2 μl annealing buffer. The contents were briefly vortexed, centrifuged and incubated at 65 °C for 5 min, followed by their immediate transfer to 37 °C for 10 min before leaving at room temperature for a further 5 min. To the annealed template 3 μl of labelling mix, 1 μl of $[\alpha^{35}S]$-dATP (6000 μCi/μl) and 2 μl of T7 DNA polymerase (diluted 1: 4 in enzyme dilution buffer) were added, mixed by gentle pipetting and left at room temperature for 5 min. The remaining protocol is as described for direct sequencing of PCR products. The use of ^{35}S in sequencing produced sharper bands than with ^{32}P as there was less scattering of the weaker particles produced during decay.

2.8.3 Automated sequencing

An ABI 373a DNA sequencer (Perkin Elmer, USA) was used based on a laser detection system of fluorescently tagged nucleotides. The detected fluorescence is presented as a graphical image from which the quality of the sequence can be deciphered. Two types of kits were made available, one which used fluorescently tagged dideoxy terminators with any sequence specific primer and another which used fluorescently labelled specific primers. For all YAC and plasmid sequencing the fluorescently tagged dideoxy terminator kit was used.

Single PCR products of (5-10 μl) or multiple bands with a specific target could be used to purify through Centrikon 100 spin columns. Mini prep DNA (2 μl) was used directly.

Cycle sequencing was performed on a Perkin-Elmer Cetus 2400 or 9600 PCR machine. Cycle sequencing reactions were of 20 μl volume containing 8 μl reaction mix

(ABI PRISM™ dye terminator cycle kit with Amplitaq® DNA polymerase FS), 3.2 M sequencing primer and approximately 1 µg purified DNA. The temperature cycling profiles consisted of 25 cycles of denaturation at 96 °C for 10 seconds, annealing at 50 °C for 30 seconds and extension at 60 °C for 4 min. The resultant products were transferred to a sterile 0.5 µl Eppendorf and purified to remove unincorporated fluorescence by a standard ethanol precipitation using 80 µl of 95% ethanol and 3 µl of 2 M sodium acetate (pH 4.5) and vacuum dried. The dried samples were immediately used or stored at −20 °C for a maximum period of a week prior to loading on a gel.

Gel plates were cleaned with detergent, wiped with distilled water and then ethanol wiped before assembling. 50ml of gel solution (40 ml Sequagel 1-6 and 10 ml Sequagel-complete, National Diagnostics) was mixed with 400 µl of 10 % ammonium per sulphate and poured between the gel plates with the aid of a syringe, to form a 6 % gel. A comb was inserted and the gel was left to polymerise for 1 h. Once the gel polymerised, the comb was removed. The plates were cleaned with tap water and then distilled water prior to placing them within the electrophoresis tank. The gel was pre-run for 15 min. Samples for loading were prepared during this time by adding 5-6 µl of loading dye containing formamide/EDTA to the DNA pellets, vortexed and briefly centrifuged, denatured at 94 °C for 3 min and snap frozen until loaded on the gel for analysis. Running conditions were as follows: 1 X TBE buffer was used for a 13 h at 25 volts. Data analysis was carried out using an Apple Macintosh computer software linked to the ABI sequencer. The output consisted of two types of files, a text only file containing the read sequence and an analysis file containing the raw data, analysed data and detailed sequenced information. Quality of sequence was judged by viewing the electrophoregram or a sequence scan presented within the file.

Geneworks™ version 4.45 was used for aligning sequences obtained from the different plasmid clones to identify overlapping regions and to identify any restriction sites. **BLAST/BLASTN/FASTA programs** (Pearson and Lipman 1988; Altschul *et al*, 1990) run through HGMP, were consistently used to compare sequences with entries within the database for sequence identities/similarities. This was of great importance while designing primers from cloned plasmid vectors or YAC vectors to avoid repetitive elements e.g. *ALU* regions.

2.9   Linkage

2.9.1   Denaturing polyacrylamide gel electrophoresis

This method was used for the resolution of DNA fragments and microsatellite analysis in linkage studies. The gel plates were washed with detergent, ethanol wiped and assembled with spacers according to the manufacturers instructions (Biorad, U.K.) and placed within a gel casting tray. The back plate that contained the buffer was silanised prior to assembly (Sigmacote, Sigma). 6 % gels were routinely used where a 200 ml gel solution was prepared consisting 132 ml diluent (Sequagel diluent, National Diagnostics), 20 ml 10 X TBE and 88 ml of concentrate (Sequagel concentrate, National Diagnostics). This recipe was sufficient for a 48 cm X 68 cm apparatus. 50 ml of this solution was removed to make a plug for the gel. To this aliquot, 300 µl of ammonium per sulphate (APS) and 100 µl of TEMED (Sigma) was added. To the remaining 150 ml of gel, 600 µl of APS and 60 µl of TEMED was added and poured between the plates once the plug was set, avoiding the formation of bubbles. The plates were rested at an angle and a comb was inserted and clamped in place. The gel was allowed to polymerise for approximately 45 min after which the gel was removed from the casting tray and placed in a buffer tank. The buffer tank reservoirs were filled with 1 X TBE and the gels were pre warmed to 55 °C. Prior to use, the comb was removed and the wells were thoroughly rinsed with a syringe filled with buffer and then the samples were loaded into the wells. Electrophoresis was carried out at 100 volts where the length of time depended on the product size. The loading dye was made up of Bromophenol blue which migrates at ~26 bp on a 6 % gel and xylene cyanol at 110 bp, both acted as indicators of resolution. On completion of a run, the plates were carefully separated so that the gel remained intact on the unsilanised glass plate. The gel was fixed in 10 % methanol/10 % acetic acid solution for 5-10 min. The gel was removed by lowering a Whatmann paper on top of the gel, wrapped in cling film and dried under a vacuum at 80 °C for 1h. The dried gels were exposed to Fuji X-ray film. The length of exposure was dependent on the strength of the radioactive signal. For a weak ^{32}P signal the gels were autoradiographed at −80 °C with intensifying screens to enhance the signal.

2.9.2 LINKAGE packages

Linkage was performed using the LINKSYS (Attwood and Byrant, 1988) and LINKAGE packages (Lathrop and Lalouel, 1984). The LINKSYS package facilitates the management of genetic data to be used in conjunction with the analytical packages of LINKAGE and LIPED. The LS4 data management package of LINKSYS, organises and processes genotypic data, allele frequencies of markers and pedigree information. The LINKAGE package includes programs MLINK, ILINK and LINKMAP. Two-point analysis was carried out using MLINK that tabulates two-point lod scores. The ILINK program enabled recombination fractions between markers to be calculated while LINKMAP was used for multipoint analysis.

FASTMAP (Curtis and Gurling, 1992) was often used enabling rapid estimation of disease position in relation to surrounding markers. It provides an approximation of distances between markers and disease. Multipoint and FASTMAP analysis was performed through the computing facilities at HGMP Resource Centre.

2.10 RNA work and treatment of equipment to prevent RNAse activity

Diethyl pyrocarborate (DEPC) treated water (100 µl in 1 litre of distilled water) was routinely used for all solutions. DEPC was added to the distilled water and left to incubate overnight (a minimum time of 12 h is recommended) at 37 °C to allow DEPC to breakdown into CO_2 and H_2O prior to autoclaving.

Plastic equipment was chloroform treated and left in the fumehood overnight. All gel apparatus including combs, gel casting tray, and tank were washed with 2 X SSC overnight on a shaker and then rinsed with DEPC treated water prior to use.

Sensible precautions were taken to avoid contamination of materials contaminated with DNA e.g. frequent change of rubber gloves was made, where possible separate materials were kept for RNA work and an ideal situation was to have a separate area for this work.

2.10.1 Hybridising Northern blots

Hybridisations were carried out in bottles overnight (18-24 h) at 42 °C in an oven. The Hybridisation buffer consisted of 5 X SSPE (a stock of 20 X SSPE 3 M NaCl, 0.2 M

$NaH_2PO_4.H_2O$, 0.02 M Na_2EDTA, pH adjusted to 7.4 with 10 N NaOH and stored at room temperature), 10 X Denhardt's solution (50 X Denhardt's solution consisted of Ficoll® 400 (Pharmacia, U.K.), Polyvinylpyrrolidone (Sigma, U.K.) and acetylated Bovine Serum Albumin (BSA) (Molecular Biology Grade; Sigma, U.K.) stock stored at –20 °C, sheared salmon sperm DNA (100 µg/ml), 2.0 % SDS and 50 % deionised formamide. Salmon sperm DNA was denatured for 5 min at 95 °C before adding to the other ingredients or could be stored at 4 °C for a fortnight or for long-term storage at –20 °C. As a control 100 ng of 2.0 kb human ß-actin cDNA probe in 20 µl of TE buffer (pH 7.5, sufficient for 2-4 labelling experiments) was used to hybridise the blot.

Hybridisation buffer was heated at 50 °C to dissolve the SDS and filters were prehybridised in 6 ml of at 42 °C for 3-6 h while agitated continuously. The labelled probe was added at a concentration of 1-2 X 10^6 cpm/ml to at least 6 ml of fresh hybridisation solution and mixed thoroughly. The prehybridisation solution was replaced with the fresh hybridisation solution/probe ensuring there were no air bubbles and evenly distributing over the blot.

2.10.2 Post hybridisation washes

Filters were washed at 50 °C for 40 min with 0.1 X SSC, 0.1 % SDS with one change of fresh wash solution. Filters were kept moist and sealed in polythene bags and exposed to Kodak or Fuji X-ray film using two intensifying screens at either –80 °C or at room temperature depending on the strength of radioactivity.

2.10.3 Removing radio-labelled probes from blots

A solution of H_2O/0.5 % SDS solution was prepared to boiling and incubated with the blot for 10 min, shaking frequently. The blot was then placed in 2 X SSC solution and incubated for 5 min at room temperature. The excess solution was shaken off and the blot was covered in plastic wrap and stored at 4 °C until next use.

2.11 General solutions and media

LB-broth (1 litre)	TE buffer
10 g NaCl	10mM Tris-HCl (required pH)
10 g Bactotryptone	1mM EDTA (pH 8.0)
5g Yeast Extract	
LB-agar	**Depurinating solution**
LB-broth with 15 g/L Bactoagar	0.25 M HCl
YEPD broth	**Neutralising solution**
2% glucose	3M NaCl
2% Bactotryptone	0.5 M Tris
2 % Yeast extract	

Table 2.1:

The common solutions regularly used in this study.
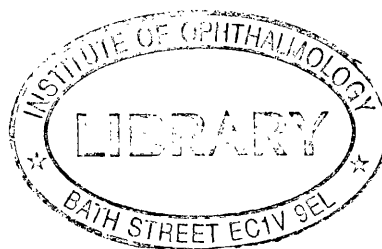
CHAPTER 3

Linkage of autosomal dominant Doyne Honeycomb retinal dystrophy (DHRD) to chromosome 2p16 and further refinement of the critical region.

3.1   Historical background of DHRD

In 1899, DHRD was first observed in four sisters by Robert W. Doyne. The observation was made ophthalmoscopically describing closely grouped lesions of white spots involving the disc-macular area in a "Honeycomb" pattern. The lesions were believed to be exudations of the choroid and thus in 1910, Doyne named this condition, honeycomb choroiditis. In 1913, Treacher Collins concluded that the white spots were nodular thickenings of the Bruch's membrane and that the choroid was normal. The nodules were termed as "Drusen", described as hyaline substances found in histological sections and staining reactions. The hyaline substance was found to be continuous layer and supposed to be a product of the retinal epithelium. Doyne concluded from his study that the lesion was inherited and he drew up a pedigree of three families. In 1937, Tree and Franceschetti followed up Doyne's families and Frances and Babel continued their follow up in 1963. The condition was found to exist in other parts of Britain (Foster, 1932) and in the rest of the world (Alper and Alfano, 1953).

In 1968, Pearce carried out a genetic survey of the condition in areas where Doyne drew his cases and described various aspects of this survey and outlined the main genetic findings and the number of affected individuals, their fundus appearances and the degree of visual disturbance. Conclusions were made that 76 patients from 6 kindreds with Doyne honeycomb retinal degeneration were shown to have this condition due to a dominantly inherited gene. Other people who had made similar conclusions based on these clinical observations in other retinal diseases were Alper *et al.* 1953; Fuchs *et al.*, 1956.

3.2   Clinical characteristics of DHRD

DHRD is a late onset, fully penetrant, progressive macular dystrophy of variable phenotype and severity leading to the bilateral loss of central vision with minor abnormalities in central and colour vision. Although the disease is localised to the macular region, phenotypic variability exists within and between different families.

Affected individuals become symptomatic by the 2nd to 6th decade of life. Although the age of onset and disease severity indicates some association with age, this is not a consistent observation. Visual loss usually develops later than the ophthalmic manifestations and visual acuity can range between 20/30 and 20/100. Typical DHRD features are drusen deposits in the macular region and around the optic disc with associated atrophy.

The condition first appeared in individuals of 20-30 years of age, where white spots appeared to be in peripapillary areas and the macular area; this was called the first stage. In the second stage from 35-60 years, the white spots multiplied and in the late stages the white spots became confluent to produce a white atrophic area. Thus, the condition was concluded to be progressive with age (Pearce,1968). The appearance of the white colloid bodies on the nasal side of the disc was regarded as phenotypically characteristic of DHRD.

A recent clinical study based on haplotype data quantifies the disease severity into 3 types with the mildest form exhibiting minimal fundal abnormalities with few drusen deposits and normal visual acuity while the most severe form exhibit profound visual acuity loss associated with prominent macular drusen, atrophy and sub-retinal neovascularisation. (Evans *et al.*, 1997).

3.3   Drusen

Drusen represents accumulations of yellowish hyaline bodies in the sub-retinal region which can be observed histopathologically in the young. However, drusen deposits observed clinically with an ophthalmoscope at an early age indicates the manifestation of a disease process. Fluorescence angiography reveals that some drusen deposits might fluoresce while others may not, implying a variation in the chemical composition of these deposits (Pauleikhoff, *et al.*, 1992). Clinical demonstration of these deposits were carried out in 1855 (Donders, 1855) and concluded that they resulted from a degenerative process; their appearance occurred with age as observed with age-related macular degeneration (Friedman *et al.* 1963; Gas 1963) or inherited with a dominant pattern (dominant drusen). The dominant drusen pattern to date has been observed in several retinal disorders like Malattia leventinese (Klainguti, 1932), DHRD (Doyne, 1899), Hutchinson-Tay
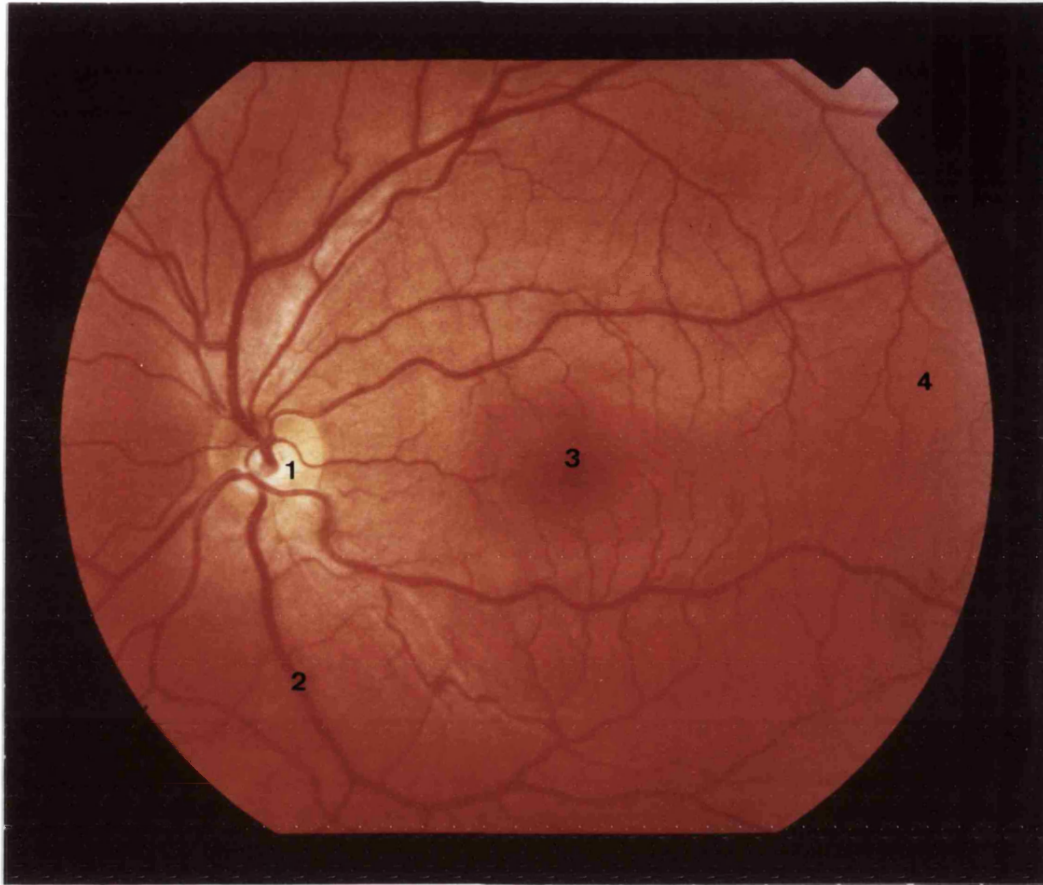
Fig. 3.0a :
A fundus image of a normal retina.

Key:-
1. Optic nerve demarcating the site of entry of the retinal blood vessels and the site of departure of the optic nerve.
2. Major retinal vessels.
3. The macular region.
4. Peripheral region..
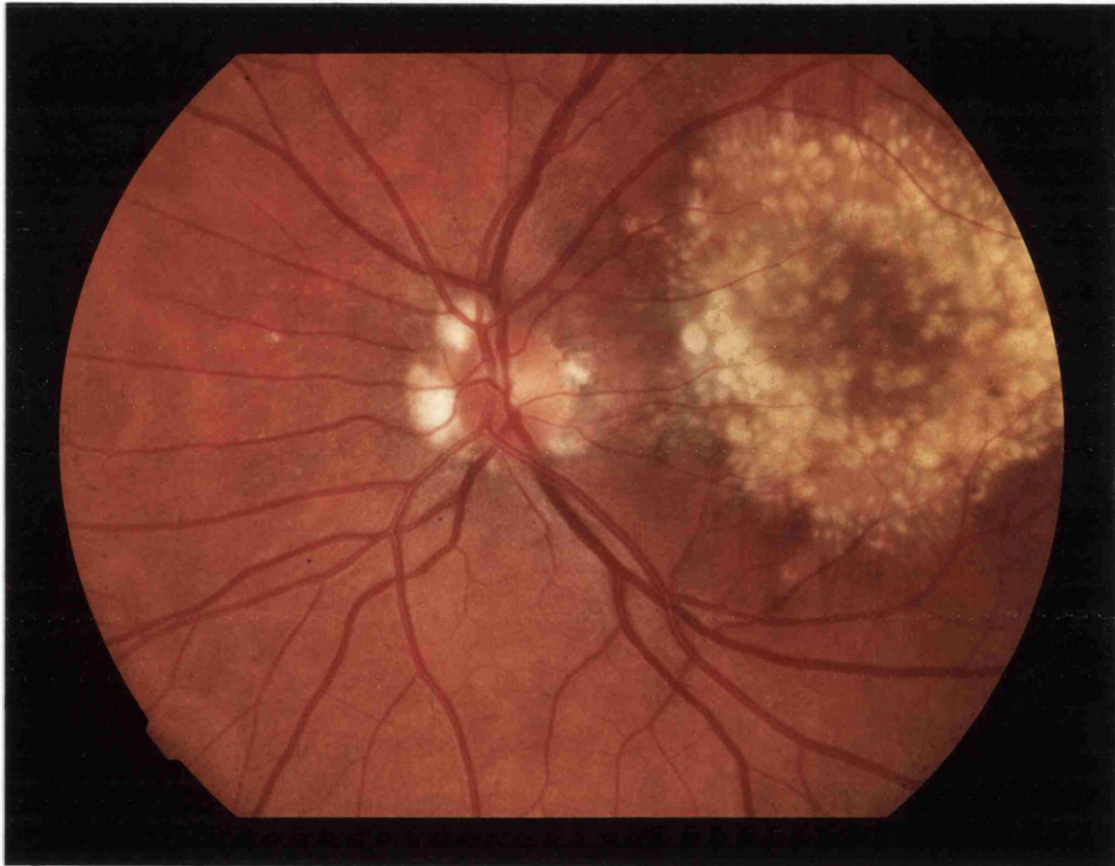
Fig. **3.0b:**

A fundus photograph of a 37 year old patient showing drusen deposits around the optic nerve head and across the entire macula region forming a honeycomb pattern typical of DHRD. Some radial deposits can be observed around the peripheral macula region.

choroidoitis (Hutchinson and Tay, 1875), Holthouse-Batten superficial choroiditis (Holthouse and Batten, 1897) and crystalline retinal degeneration (Evans, 1950). The common observation of dominant inheritance of these diseases has been termed 'dominant drusen' constituting a single inherited condition (Franschetti *et al.*, 1963, Deutman and Jan, 1970, Gass *et al.*, 1973). The molecular mechanism underlying the formation of drusen deposits is unknown but they have been clinically re-evaluated (Piguet, 1995) and it has been concluded that the dominant drusen phenotype is a term commonly used for several unknown genetically separate entities.

3.4   Malattia leventinese

Malattia leventinese is a phenotypically similar autosomal disease that is also inherited dominantly. It originated from the Leventine valley of the Tricino canton of southern Switzerland and was first described by Vogt, in 1952. Several discrete deposits are found in the peripheral macula displaying a radial pattern which is a consistent ophthalmic finding and characteristic of this disease. Histopathologically, these drusen termed basal laminar drusen are found to be continuous with or internal to the basement membrane of the retinal pigment epithelium (RPE) (Dusek *et al.*, 1982). Drusen of a radial pattern is an infrequent finding of DHRD but it seems to lie external to the basement membrane of the RPE pervading the entire thickness of the Bruch's membrane (Collins, 1913). Waadenburg and co-workers in 1948 and Forni and Babel in 1962 considered DHRD and Malattia leventinese to be clinically indistinguishable but the recent detailed finding of Piguet and his group in 1995 indicated that Malattia leventinese and DHRD clearly represented dominant drusen phenotypes differentiated by their clinical and ultra-structure features thus distinguishable clinically as two distinct diseases. Based on these findings, it has also been proposed that DHRD has more resemblance to age-related macular degeneration (AMD) than Malattia leventinese, therefore it can be said that DHRD is the best candidate model for AMD.

AMD accounts for 50 % of registered blindness in England and Wales (Evans, J. 1995). The high prevalence is likely to exist in all economically developed Caucasian communities (Leibowitz, *et al.*, 1993-75; Rosenberg and Klien 1996; Newland *et al.*, 1996). Evidence indicates that AMD is genetically predisposed (Piguet *et al.*, 1993; Heiba *et al.*, 1994; Silvestri *et al.*, 1994 and Klein *et al.*, 1994) and that it manifests in the presence of environmental influences. It is possible that more than one gene is involved

but the number may be small (Heiba *et al.* 1994). Thus AMD is similar to other polygenic diseases like diabetes and glaucoma.

AMD is divided into two subtypes: 80 % of patients have 'dry' AMD, which include one or more of the presence of cellular debris (drusen) in or under the RPE, irregularities in pigmentation of RPE or geographic atrophy. 20 % of the patients have the 'wet' AMD characterised by the detachment of RPE or choroidal neovascularisation or both. Visual loss results from either choroidal neovascularizaton, detachment of RPE or geographic atrophy (Gass, 1967). It is believed that this results as a response to accumulation of debris in Bruch's membrane (Hogan 1972, Sarks 1976, Green and Key 1977; Burns 1980 and Burns 1985) which is recognised clinically as drusen and pigmentory changes referred to as age-related maculopathy (ARM). It is believed that the debris derives from the RPE that discharges cytoplasmic material throughout life into the inner portion of Bruch's membrane to achieve cytoplasmic renewal (Ishibashi *et al.*, 1986; Marshall 1987). It is likely that the material is cleared through the choriocapillaris. Disorders like Malattia leventinese and DHRD also have phenotypic similarity to ARM and their disease causative genes might shed light on the age-related pathogenesis of AMD.

3.5 Aim of study

To perform linkage analysis on a large British DHRD pedigree with the objective to mapping the disease to a specific chromosomal region as a preliminary step towards the search for a disease causative gene playing a significant role in the pathogenesis of other macular degenerations like AMD.

This study was undertaken at a stage where the total genome search of approximately 15-20 cM intervals and exclusion of candidate gene loci had previously been completed by a former colleague in the group but significant linkage had not been localised to any specific chromosomal region.

3.6 Methods and Materials

3.6.1 Geneology of the DHRD pedigree

The original family described by Doyne currently resides in Buckinghamshire, United Kingdom. The living descendants were contacted and consent obtained prior to any clinical evaluation and family history studies. Genealogical techniques were used (Jay, 1995) to establish 4 of the original DHRD families (see pedigrees A1, A2, C and D,

Pearce 1968). An extended pedigree consisting of over 400 individuals was constructed based on this information and that of living descendants and family histories of unsampled generations (fig. 3.1)

3.6.2 Clinical evaluation and DNA sampling for Linkage study

107 members in the last four generations of the main pedigree were examined at Moorfields Eye Hospital, London. Diagnosis was based on ophthalmological examinations, fluorescein angiography, electrodiagnostic tests, psycohophysical tests and autofluorescent fundus imaging. Detailed results of these evaluations are presented in Evans *et al.* 1997. The main diagnostic criterion for allocation of disease status was the presence of soft drusen deposits seen ophthalmoscopically in the macular region around nasal side of the optic disc. Blood samples were collected from all living members and DNA extracted as described in section 2.1.1.

3.6.3 History of the Linkage study

An autosomal dominant mode of inheritance with complete penetrance was clearly observed in the DHRD family. As the disease was of late onset, subjects over 45 years with no 'typical' fundus features were assigned as 'unaffected'. Thus many individuals who failed to satisfy this criterion were excluded and only 39 members (from branches A1 and A2) were recruited to constitute the preliminary linkage panel of 20 affected individuals, 17 unaffected individuals, and 2 spouses. During the course of the study several individuals were re-evaluated with more stringent diagnostic criteria for the classification of affected individuals and 3 consanguinities were noted (see fig. 3.1). Thus, the original linkage panel (fig. 3.2) was modified. For simplification alterations have not been shown but fig. 3.3a is the panel of individuals used in the genome search and candidate gene exclusions. Subsequently, an additional branch C was incorporated and the new panel of individuals consisted of 63 members (see fig. 3.3a) including 35 affected individuals, 20 unaffected individuals and 8 spouses. This panel of individuals was used for subsequent re-calculation of putative lodscores that resulted from the genome   search   and   candidate   gene   exclusions.
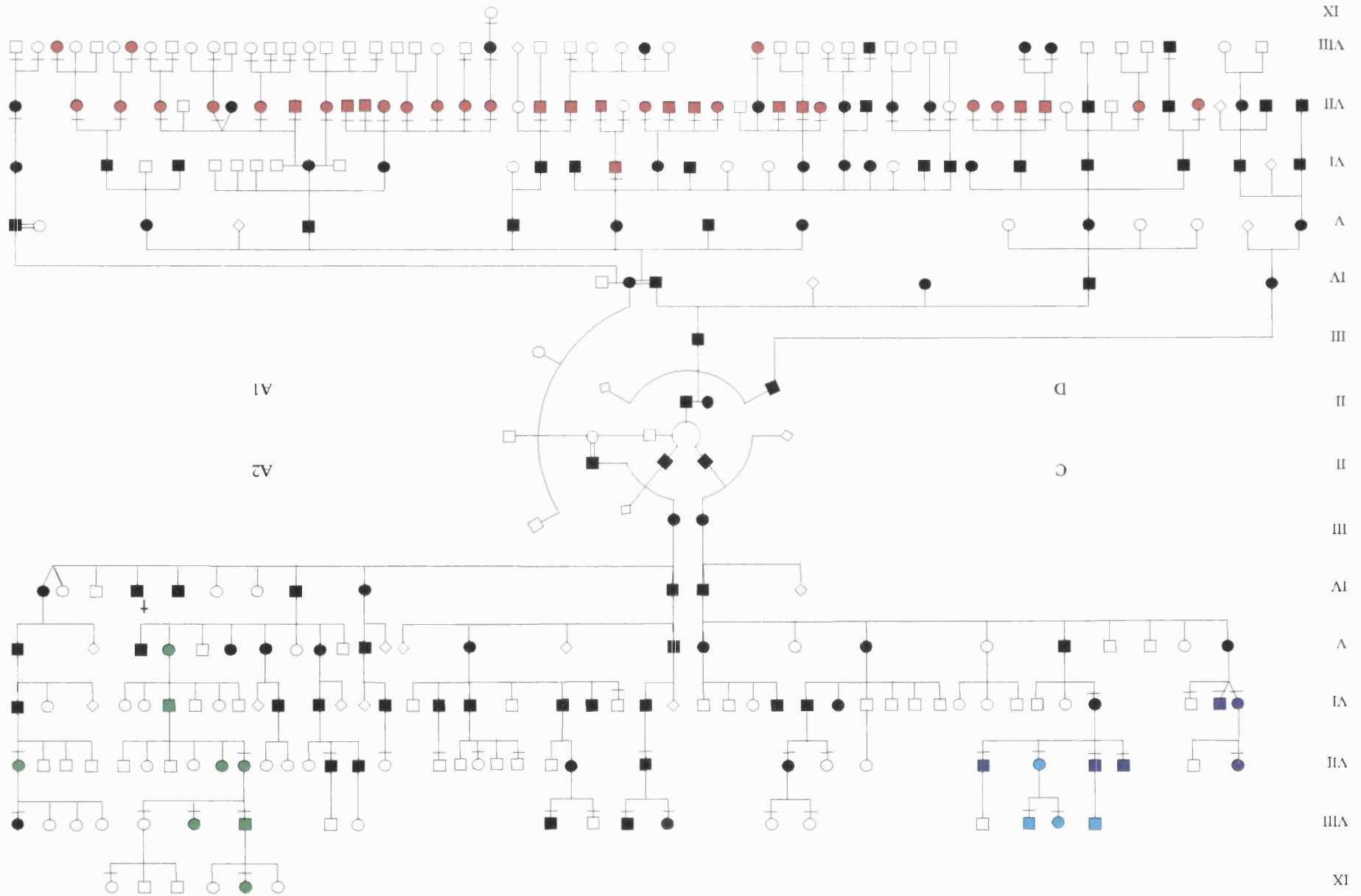
Fig 3.1 depicts the entire DHRD pedigree. DIfferent coloured individuals indicate the 4 separate branches incorporated as one family in our study. Branches A1, A2, C and D are shown separately for simplification from Fig. 3.1a-3.1d respectively.

108

A1
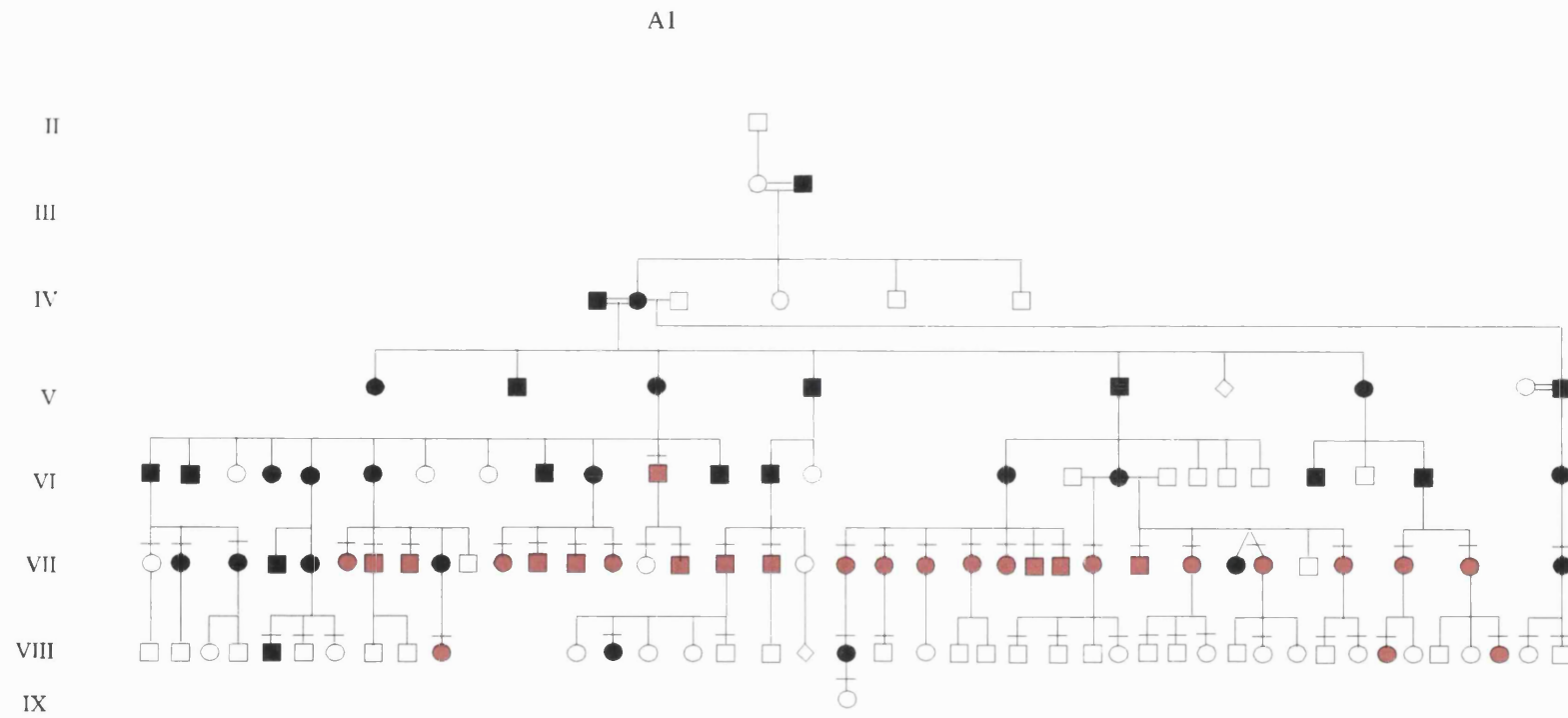
Fig. 3.1a depicts one of the 4 branches of the large DHRD pedigree.

A2
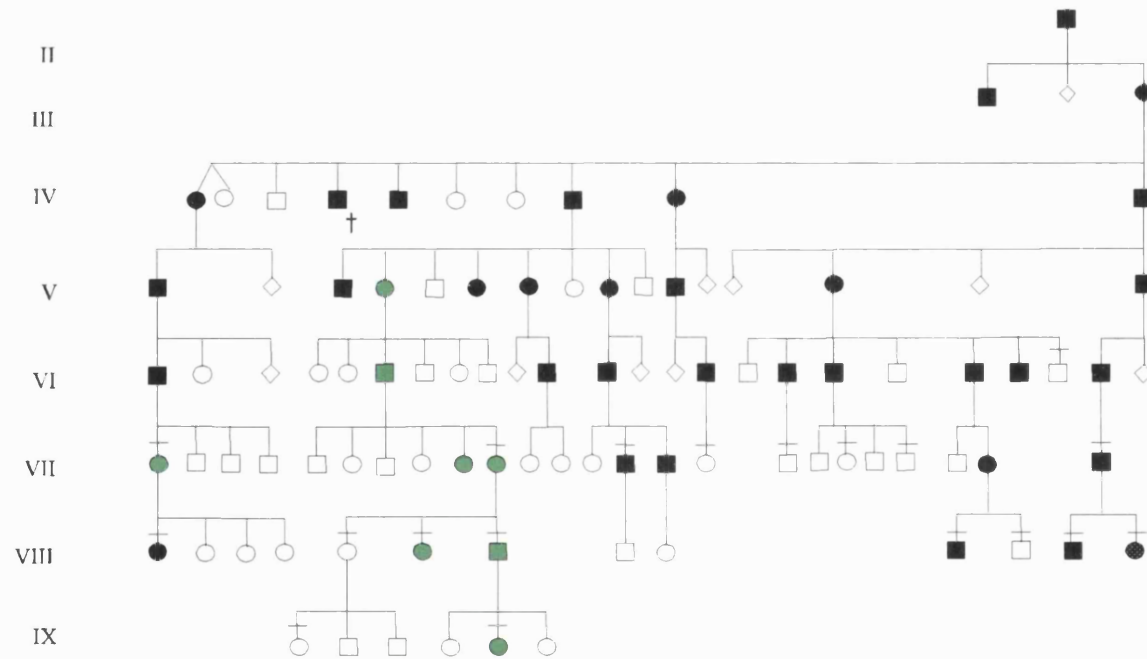
Fig 3.1b depicts one of the 4 branches of the large DHRD pedigree.

C
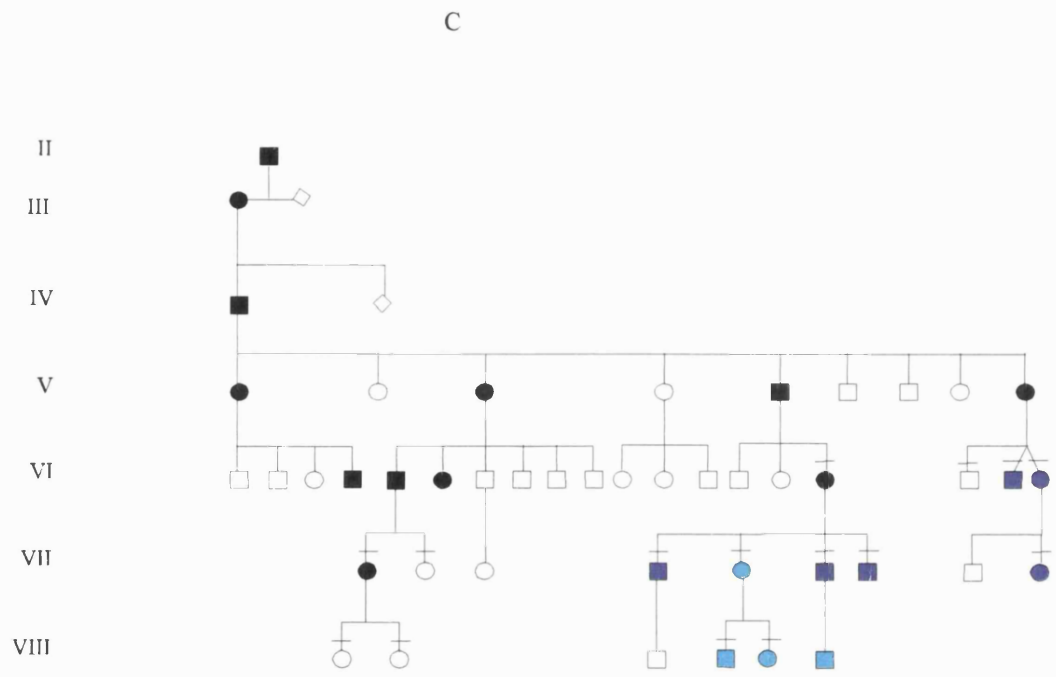
Fig 3.1c depicts one of the 4 branches of the large DHRD pedigree.
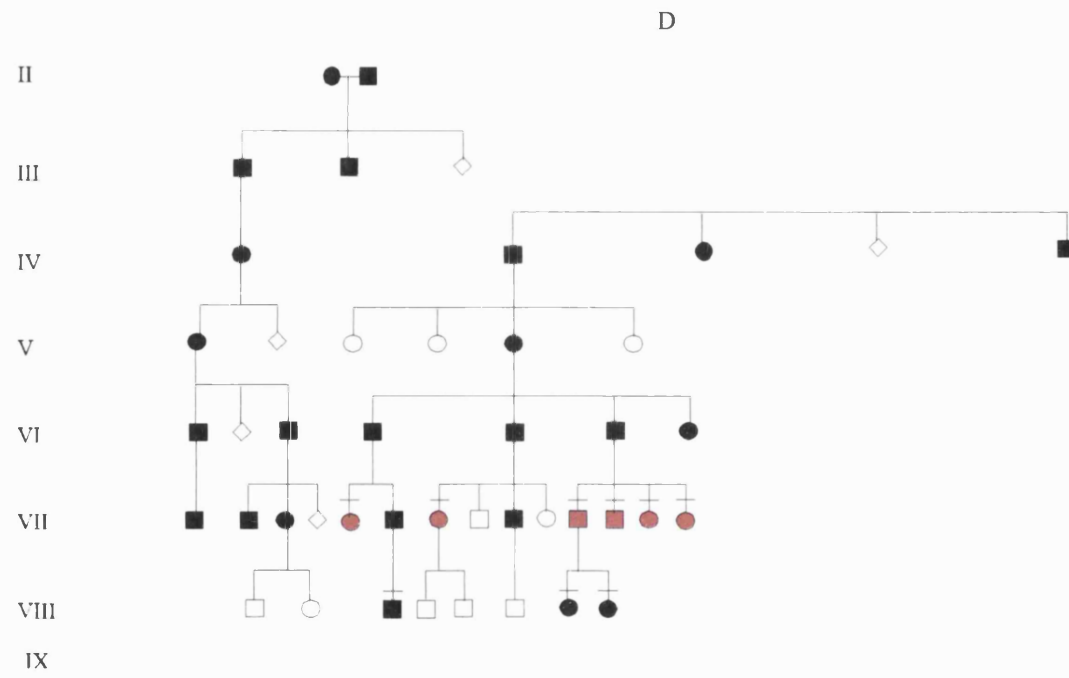
Fig 3.1d depicts one of the 4 branches of the large DHRD pedigree.
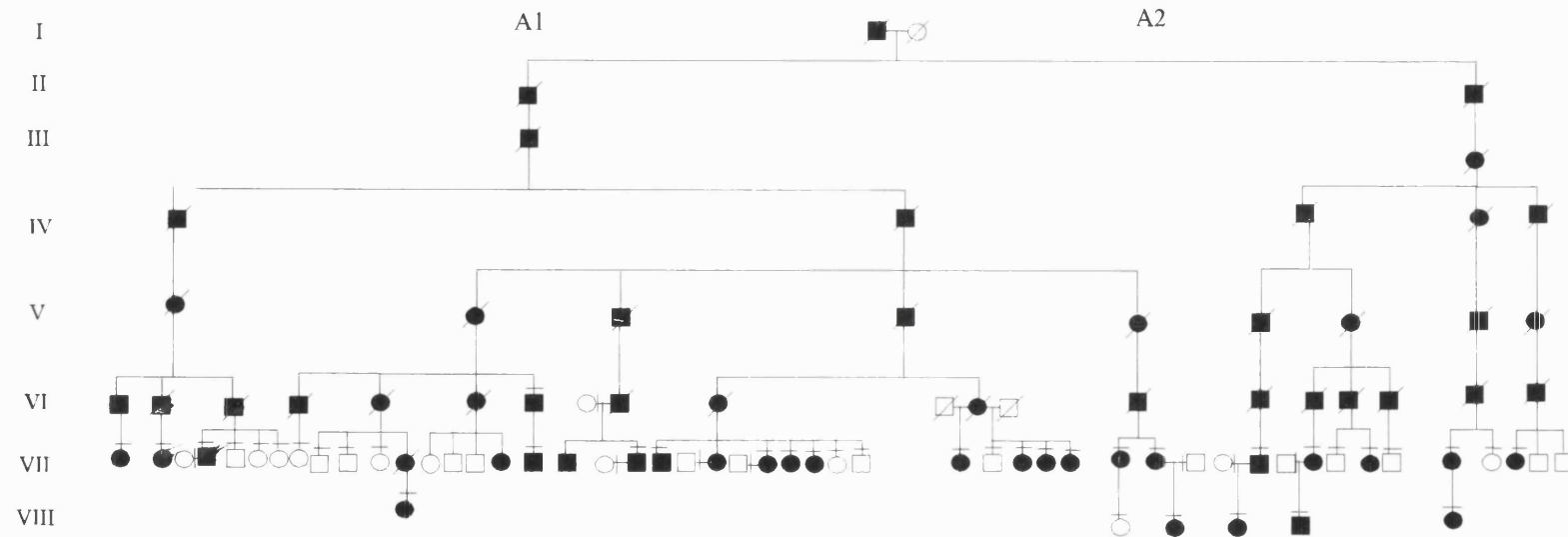
Fig. 3.2 depicts individuals that constituted the original linkage panel used for genome search and candidate gene exclusions.

3.6.4 Selection of microsatellite markers

Most of the markers used in this study were of (CA)n type made available by CEPH Généthon marker maps (Weissenbach *et al.*, 1992; Gyapay *et al.*, 1994) or tetranucleotide markers from the Cooperative Human Linkage Centre (CHLC) (Sheffield *et al.*, 1995). Where possible, markers with heterozygosity values greater than 0.7 were used.

3.6.5 Analysis of microsatellite markers and recording genotypes

All markers were amplified using PCR and radioactive labelling methods as described in section 2.5.1. Allele systems were resolved on 6 % polyacrylamide gels and visualised by autoradiography (see section 2.9.1). Genotypic data was scored independent of the family pedigree information. On transfer of the data to the family, if discrepancies occurred they were re-analysed for mis-scoring and those results were repeated. In several circumstances, the amplification of a long tandem repeat exceeded the capacity of the Taq polymerase used for this purpose and resulted in the visualisation of a ladder of bands unique to each allele. This is termed 'slippage'. It is possible to distinguish the true alleles amongst the background ladder of bands by their relative intensities or by their Mendelian pattern of segragation in the family. If this failed the markers were re-tested increasing the annealing temperatures of the markers reducing the ladder of bands and making the allele system clearer to read.

3.6.6 Statistical analysis

All family data, allele frequencies of markers and genotypic data processed through LS4 data management package of the LINKSYS program (Attwood and Bryant, 1988) in the form of locuslib, phenolib, and family files. Output data files were compatible with the analytical program of LINKAGE version 5.1 (Lathrop and Lalouel, 1984). Output files of LINKSYS were used as input files for the calculation of twopoint lodscores (pairwise linkage analysis) utilising the MLINK program of LINKAGE. For these calculations, autosomal dominant mode of inheritance was specified and a penetrance value of 0.98 was applied. Initially to begin with the allele frequencies used were based on the published allele frequencies for the CEPH families, obtained from the HGMP Resource Centre, UK. As the allele numbers and frequencies deviated from the those of CEPH with extra unpublished alleles, more unrelated spouses were recruited into the study and for subsequent pedigrees allele frequencies were calculated using these

individuals providing a more realistic value for allele frequency based on the gene pool from which the family originated.

3.7   Results

3.7.1   Tentative linkage assignments

Macular disease loci and choroidoretinal disorders were the initial candidates for the study. Several candidate genes such as TIMPs, Cathepsins and ring chromosomes had also been taken into consideration due to their functional features for mapping the disease locus. All putative candidate genes were excluded at lodscore values corresponding to θ = -2. Major macula disease loci were also excluded in a similar manner. A total of 230 microsatellite markers had previously been genotyped before branch C was incorporated into the study.

This study was continued by taking into consideration the numerous positive lodscores below the threshold value of 3.0, but above 1.0 at θ = 0.05 to 0.4 obtained in scattered regions of the genome. A lodscore of 3.0 shows significant linkage thus any initial positive lodscore of 1.0 or above was taken into account for further refining the initial 'blips' on different chromosomal regions. These tentative positive lodscores were present on chromosome 2, 7, 8,14 and two regions on chromosome 1. These regions were further investigated with greater density of markers placed at 1-2 cM intervals in order of preference with those displaying the highest lodscores being investigated first. An additional branch C was added to the original panel and regions of positive lodscores were re-analysed.

3.7.2   Linkage of Malattia Leventinese to the 2p21-2p16 locus

Markers from chromosomal regions of 1, 7 and 14 were being genotyped across the latest panel of individuals with greater densities in the hope of mapping DHRD to one of these chromosomes. In the meantime, Héon and his colleagues mapped Malattia leventinese to chromosomal region 2p16-21 across a 14 cM genetic interval. Although chromosome 2 was a region where positive lodscores of less than 3 and greater than 1 had been obtained, the values were relatively smaller than those obtained for chromosomes 1, 7, 8 and 14. With the new mapping information of Malattia leventinese and keeping in mind that both diseases were dominant drusen phenotypes, this region was

subsequently given priority. Subsequently, markers that had been typed for the linkage of Malattia leventinese, were genotyped across the DHRD affected panel.

3.7.3 Linkage of DHRD to the 2p21-16 locus

Malattia leventinese was localised to a 14 cM genetic interval on chromosome 2p21-16, between the northern flanking marker D2S1761 and southern flanking marker D2S444 (Héon *et al.,* 1996). Nine markers that mapped within this region were either uninformative or showed no recombination with the disease phenotype in the DHRD affected panel. Linkage of DHRD to this region was observed when marker D2S119 was genotyped across the linkage panel (see fig 3.3b). Genotyping further markers of this region and the one used by Héon and his colleagues provided significant linkage data for this interval between markers D2S2316 and D2S378 (fig 3.3a). Two point lodscore analysis indicated significant linkage to 9 of the markers tested with Zmax ranging from 3.67 – 9.49 (table 3.1). The highest lodscore obtained was with marker D2S378 of 9.49 at θ = 0.06. Maximum two point lodscores of 6.56, 7.29 and 4.14 with no recombinants were observed with the CHLC tetranucleotide marker D2S2739 and markers D2S2251 and D2S2251, respectively. Marker D2S147 which lies 3 cM distally from D2S370 did not show linkage to the disease providing exclusion of 4 cM based on the lodscore value obtained at θ =-2.0 (table 3.1).

Haplotypes constructed from recombinant individuals localised the disease within a 5 cM interval encompassed within the Malattia leventinese region, between marker D2S2316 proximally for which 3 recombinant individuals existed and marker D2S378, distal for which 5 recombinant individuals were present, one of which was an unaffected individual (VII-10) carrying the disease haplotype distal to marker D2S378 (Fig. 3.4). D2S2316 was uninformative in 4 of 8 individuals in the recombinant panel (VII-31, VII-33, VII-34 and VII-35) while D2S378 was fully informative across the panel the non recombinant markers D2S2739 and D2S2352 were relatively uninformative in the panel being uninformative 3 out of 8 and 5 out of 8 recombinant individuals respectively while D2S2251 was only uninformative for a single individual. Close analysis of recombinants alongside pedigree information identified three individuals recombinant at locus D2S2316 (VII-42, VII-44, VI-49) to possess the same recombinant allele and to be descendants of one branch of the pedigree (branch A2), implying that a single ancestral recombinational event in individual III-3. Recombination events in individuals VII-31,

VII-33, VII34, VII-35 with marker D2S378 were observed implying that a single recombination event in individual VI-11 had taken place. Thus, DHRD was proximally flanked by a single recombination event with marker D2S2316 and distally by two recombination events with D2S378 placing the disease in a 5 cM interval in 2p16 region. No double recombination events were observed in this region.

Recombination fraction (θ)

Locus	0.0	0.01	0.05	0.1	0.2	0.3	0.4	Zmax	θmax
D2S119	-∞	-0.86	4.49	5.96	5.99	4.64	2.55	6.24	0.15
D2S391	-∞	5.62	8.73	9.12	7.89	5.64	2.84	9.12	0.10
D2S2227	-∞	0.34	2.92	3.63	3.39	2.33	1.00	3.67	0.09
D2S2316	-∞	8.23	8.25	7.62	5.29	3.99	1.91	8.38	0.03
D2S2739	6.56	6.45	5.97	5.29	3.78	2.18	0.74	6.65	0.00
D2S2251	7.29	7.04	6.32	5.13	3.27	2.21	1.13	7.29	0.00
D2S2352	4.14	3.98	3.37	2.16	1.09	0.41	0.09	4.14	0.00
D2S378	-∞	7.64	9.43	9.32	7.71	5.37	2.63	9.49	0.06
D2S370	-∞	2.58	3.92	3.86	2.80	1.51	0.46	3.98	0.08
D2S147	-∞	-6.45	-1.85	-0.96	0.81	0.94	0.46	-2.0	0.04

Table 3.1

Two point lodscores between chromosome 2p21-16 markers and the DHRD disease phenotype. Maximum lodscore values are in bold. Markers are presented in order of occurrence along the chromosome from D2S119 proximally to D2S147 distally. Marker locus D2S147 is not linked to the locus providing a 4 cM exclusion based on the lodscore value obtained at θ = -2.0.
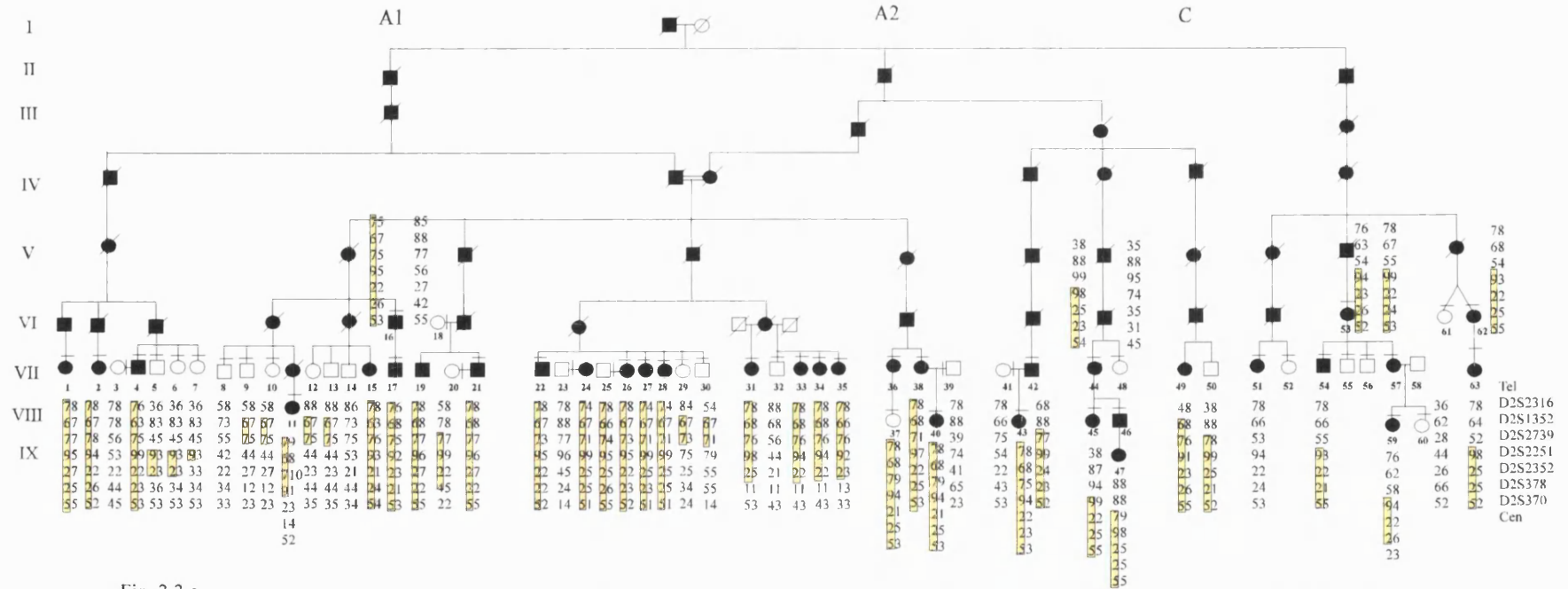
Fig. 3.3 a
DHRD pedigree showing the incorporation of an ancestral branch C used in the linkage study. Haplotype analysis of 2p16 markers in the DHRD panel is depicted by a disease haplotype in a yellow box. Filled symbols represent affected individuals and open symbols represent unaffected individuals. Order of markers tested in each family is denoted.
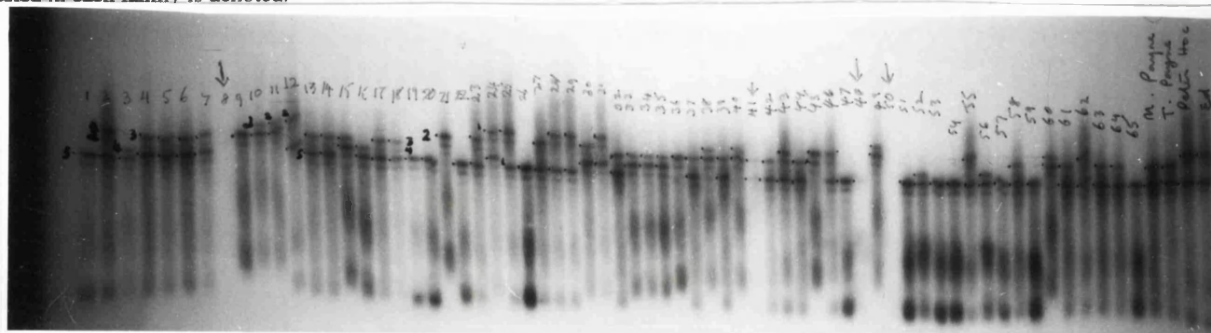
Fig. 3.3 b
Autoradiograph image of linked marker D2S119 in DHRD pedigree. Allele 5 is seen to cosegragate with the disease phenoype. Lane numbers are indicated above each individual in the gel image. Lane numbers 1-63 correspond to 1-63 in the above panel. Lanes 64 onwards are further individuals of the DHRD family.

118
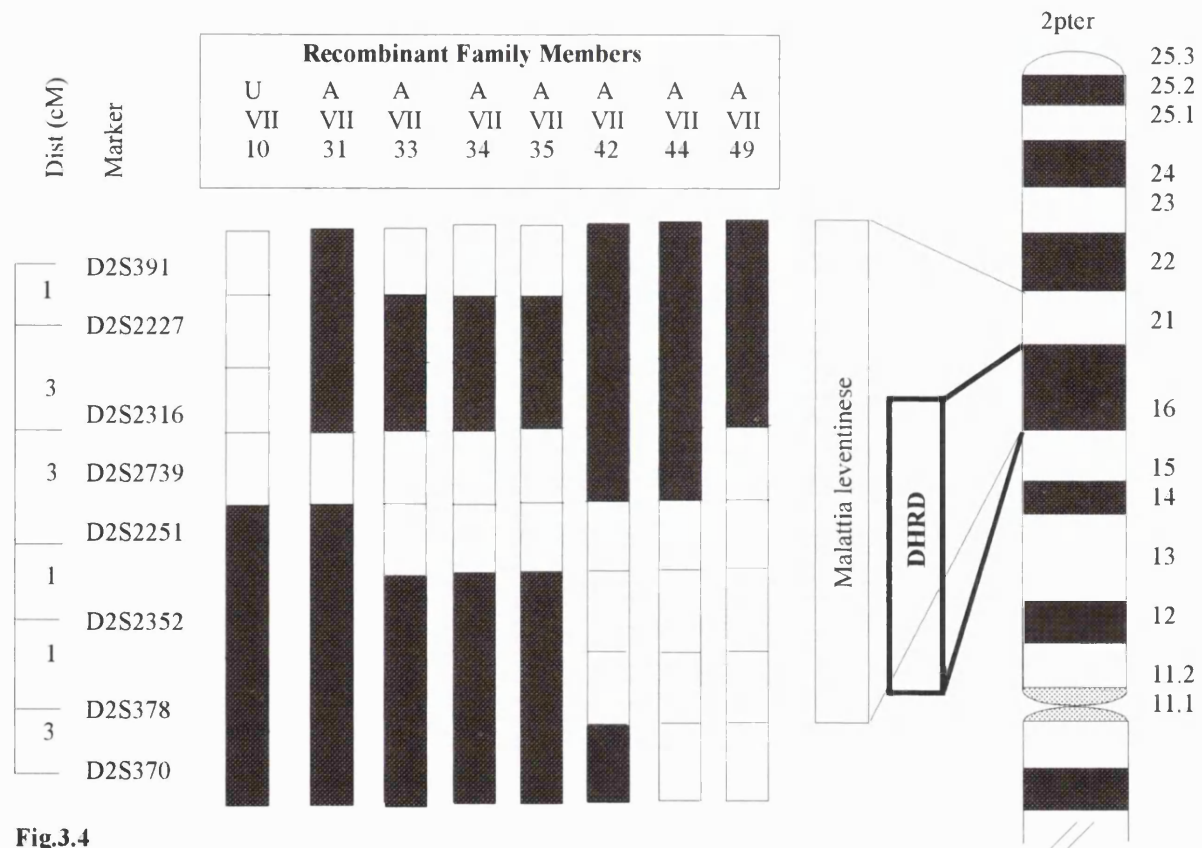
Fig.3.4
Recombination events as observed between disease and chromosome 2p markers in family members from DHRD pedigree.

3.7.4 Refinement and haplotype data analysis

Since the preliminary mapping of DHRD individuals using the affected panel, further individuals were haplotyped with the linked markers of the region in the hope of finding new recombination events refining the disease locus and to further analyse whether there was any significant genotype/phenotype correlation. These individuals were initially not included in the affected panel due to insufficient clinical data. The refinement was achieved with marker D2S2739. The highest lodscore was obtained with marker D2S378. Fifty individuals who carried the disease haplotype between marker D2S2739 and D2S378 were allocated as affected. A further 30 individuals were found not to carry the disease haplotype and were assigned as unaffected. Further twenty seven individuals carried part of the disease-associated haplotype between the disease-flanking loci. None of these patients had fundus abnormalities suggestive of the disease phenotype therefore they were assigned as unaffected and were not included in the reassessment of the DHRD phenotype.

Haplotype study quantified the disease severity into 3 types: mild moderate and severe, with the mildest form exhibiting minimal fundal abnormalities with few drusen deposits and normal visual acuity while the severe form exhibiting profound visual acuity loss associated with prominent macular drusen, atrophy and sub-retinal neovascularisation (Evans *et al.*, 1997). Overall evaluation of the 50 affected individuals confirmed the previously described features of the disease suggesting that the disease is localised to the macular region only and is fully penetrant with variation in severity. Although haplotype data suggested that disease severity was to some extent associated with age, with the mildest form seen between ages 22-43 years; moderate disease between 31-78; and severe disease, 49-90 years, this was not a consistent finding as notable exceptions were observed. New clinical features that came to light were that the previously thought of earliest features like large soft drusen found around the nasal optic disc were not actually identified until the 4th decade of life and that the severest maculopathy reported was one in childhood with little progression in adult life, thus suggesting that DHRD can potentially cause childhood onset visual loss (Evans *et al.*, 1997). Radial drusen were also observed in some of the affected individuals, a feature which is common to patients with Malattia leventinese. The only feature differentiating between the two diseases are the constancy and quantity of radial drusen, as in DHRD

they are infrequent and a minor feature whereas in Malattia leventinese they are an abundant feature and invariable.

3.7.5 Mapping of two dominant drusen families to the DHRD locus and further refinement with new members of the DHRD pedigree

Two dominant drusen pedigrees of British descent analysed in this study are shown in Fig. 3.5 (family A) and Fig. 3.6 (family B). Both families exhibited characteristic features of drusen deposits. Loci implicated in previous studies on autosomal dominant macular dystrophy or cone dystrophy, namely STGD1, RDS, GUCA1A, STGD3, NCMD/PBCRA, CYMD, VMD2, STGD2, RCD2, CACD, RETGC1, CORD6, CORD2 AND SFD (RetNet 1998), were excluded in these families. Linkage to 2p16 in these families was established by genotyping 6 marker loci previously linked to DHRD. In family A, marker D2S2352 gave a maximum lodscore of 2.58 without recombination (see table 3.2). In family B, marker D2S2352 gave a maximum lodscore of 2.11 without recombination (see table 3.2).

A lodscore of 2 is accepted as sufficient (although not significant) evidence for linkage of a disease to a previously known locus of similar phenotype (Terwilliger and Ott, 1994) and is supported by exclusion of other disease loci by linkage analysis in these families. The haplotypes that define the chromosomal interval containing the disease-causing gene is indicated in table 3.3. In family A (Fig 3.5) affected individual III-3 and unaffected individual IV-1 are recombinant for D2S1352. In addition, individual III-3 is also recombinant for D2S2379 placing the disease locus centromeric to D2S2379, confirming our previous telomeric flanking marker (Evans *et. al.* 1997). In family B (Fig 3.6), affected individuals II-4 is a recombinant for D2S1352 as well as the centromeric marker D2S2379, placing the disease gene centromeric to D2S2379 and reconfirming the published flanking marker. Thus, neither of these families further refined the DHRD disease locus. However, the different haplotypes in each of the three families indicated that three independent mutational events had occurred (table 3.3).

Current genetic and clinical analysis of a new branch of the DHRD pedigree highlighted two recombinational events (table 3.3). Affected individual I is recombinant for D2S1352, D2S2379 and D2S2352 placing the disease centromeric to D2S2352. Affected individual II is recombinant for D2S2251, D2S378 and D2S370 placing the disease telomeric to D2S2251. Thus, the disease gene resides in a genetic interval of 1 cM (Dib *et al.* 1996) flanked by markers D2S2352 and D2S2251.

Family A

I

II

6 8
2 6
5 7
9 6
6 6

III

7 8
4 6
3 7
6 6
6 6

IV

6 8
1 4
2 3
8 6
7 6

6 7
1 4
2 3
8 6
7 6

6 7
1 4
2 3
8 6
7 6

Tel
D2S1352
D2S2739
D2S2352
D2S2251
D2S378
Cen
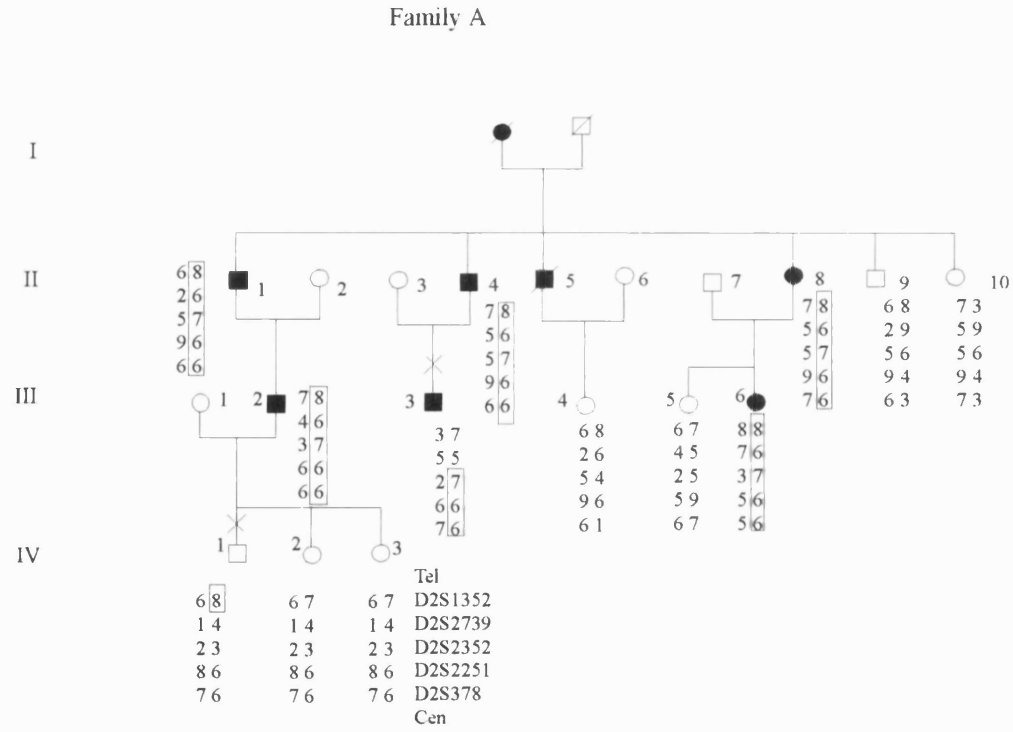
Fig. 3.5

Haplotype analysis of 2p16 markers in dominant drusen family A.
Filled symbols represent affected indiviudals, open symbols represent
unaffected individuals. A cross indicates a recombinant individual.
The disease haplotypes are boxed. Order of markers tested in each family
is denoted.

122
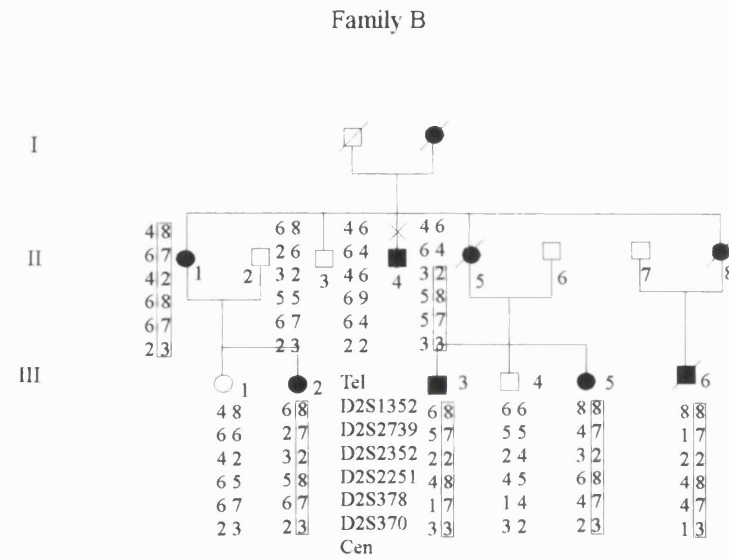
Family B

Fig. 3.6

Haplotype analysis of 2p16 markers in dominant drusen family B.
Filled symbols represent affected indiviudals, open symbols represent
unaffected individuals. A cross indicates a recombinant individual.
The disease haplotypes are boxed. Order of markers tested in each family
is denoted..

Recombination fraction (θ)

Marker	0.0	0.05	0.1	0.2	0.3	0.4
Family A:						
D2S2379	-∞	-1.14	-0.63	-0.20	-0.03	0.03
D2S2352	2.58	2.37	2.14	1.62	1.02	0.40
D2S2251	1.24	1.14	1.12	1.01	0.74	0.35
D2S378	1.03	0.93	0.83	0.39	.22	0.07
Family B:						
D2S2379	-∞	1.42	1.20	0.98	0.66	0.48
D2S2352	2.11	1.88	1.65	1.15	0.61	0.16
D2S378	1.21	0.98	0.91	0.86	0.59	0.26
D2S370	0.87	0.78	0.70	0.52	0.35	0.17

Table 3.2 :

Two-point lodscores between the DHRD locus

and 2p16 markers of dominant drusen family A and B.

Family or Individual	Marker loci and DHRD locus haplotypes					
	Tel D2S1352	D2S2379	D2S2352	D2S2251	D2S378	Cen D2S370
Family A	8	6	7	6	6	2
Family B	8	7	2	8	7	3
DHRD family	6	7	**4**	**9**	**2**	**5**
Affected I	6	4	2	**9**	**2**	**5**
Affected II	6	7	**4**	8	1	**5**

Table 3.3:

Disease haplotypes of different families with dominant drusen mapping to 2p16. Bold numerics of recombinant affected individuals I and II denotes haplotype in comparison to the main DHRD family disease haplotype. This disease lies between D2S2352 and D2S2251. Families A and B show disease haplotypes which are different to the original DHRD haplotype.

3.8   Discussion

3.8.1   Linkage and haplotype analysis

Following a genome wide search and candidate gene exclusions, pairwise linkage analysis localised DHRD to the 2p16 genetic region. Haplotype analysis of recombinant individuals enabled the disease to be localised to a 5 cM region, between markers D2S2316 and D2S378, encompassed within the Malattia leventinese disease region. Three markers in the linked region obtained significant positive lodscores greater than 3.0 and the most informative marker was a tetranucleotide marker (D2S2739) known to map within this interval. The exact genetic distance of this marker in relation to other Généthon markers in the region is not known as it was isolated by the Cooperative Human Linkage Consortium (CHLC) (http://www.chlc.org/ChlcMaps.html). No double crossovers were observed across the 55 meiotic events.

3.8.2   Genotype/Phenotype correlation

The most striking feature observed in the family was the variability in the phenotype and the presence of deposits differed in appearance from one another. The variability in drusen deposits is a common feature to most dominantly inherited macular disorders and is thought to be a result of the modifying effects of other genetic attributes. Age-related macular studies indicate that there is good evidence of genetic influence on metabolic function on the retina (Piguet *et al.* 1993, Heiba *et al.* 1994, Silvestri *et al.* 1994, Klein *et al.* 1994). As age-related degeneration is a major cause of blindness in the West, it would seem that genetic abnormalities in the genes involved are common to this community suggesting that different genetic backgrounds in individuals may modify the effects of the mutations of interest. Environmental factors may play a modifying role in the disease phenotype as shown in several age-related degeneration studies (Tsang *et al.* 1992, Seddon *et al.* 1994, Mares-Perlman *et al.* 1995). Within the UK there may be very little environmental differences and this argument may not be strong enough to support the variation within the DHRD family but can be used to explain the difference between the clinical features of the DHRD family and the Malattia leventinese family which belongs to the Leventine Valley of Switzerland.

3.8.3 DHRD and Malattia Leventinese could be allelic

The clinical similarities between the two diseases coupled with their mapping to the same region of chromosome 2p is indicative that the two diseases could be allelic, thus two mutations lie within one gene giving rise to the two different clinical phenotypes. This is a common phenomenon, as observed in mutations in the outer segment protein, peripherin/RDS manifesting a range of phenotypes from typical retinitis pigmentosa (RP) to typical macular dystrophy (Wells *et al.*, 1993). A cysteine deletion at codon 118/119 was associated with retinitis pigmentosa in one family. Three of the families with a similar macular dystrophy had mutations at codon 172, arginine being substituted by tryptophan in two and by glutamine in one. A stop sequence at codon 258 existed in a family with adult vitelliform macular dystrophy. These results demonstrated that both retinitis pigmentosa and macular dystrophies were caused by mutations in RDS and that the functional significance of certain amino-acids in peripherin-RDS may be different in cones and rods. A similar example could be observed for the allelic nature of DHRD and Malattia leventinese.

This phenomenom becomes possible if a protein has several cellular functions. A common observation is that alterations in structural proteins results in dominantly inherited diseases while those in functional proteins i.e. enzymes lead to recessive disorders. Exceptions to these rules do exist like in Rhodopsin. Mutations in Rhodopsin can cause either recessive or dominant RP (Rosenfield *et al.*1992, Al Maghtheh *et al.* 1993). Certain mutations may alter the structure, resulting in altered protein folding leading to structural instability of the cell and eventually cell death whereas a complete lack can cause a recessive phenotype.

3.8.4 Implications of consanguinity

In general a consanguineous marriage of two affected individuals like in generation VI (branch A1 and A2) gives the possibility of 'double dominant' individuals carrying two affected genes in their offspring. This could give rise to two different haplotypes segregating with disease in the family; a feature beyond the capability of the LINKAGE program used to calculate the lodscores. However, haplotype data analysis on the linked pedigree has confirmed the presence of a single disease associated haplotype.

3.8.5 Further refinement of the DHRD locus with a new branch and implication of different haplotypes

Many retinal diseases are clinically and genetically heterogeneous, which reflects the limited repertoire of responses of the eye to a variety of genetic lesions. In addition, allelic heterogeneity is an emerging concept in retinal dystrophies in which different mutations in the same gene can cause clinically distinct ocular phenotypes (Wells *et al.* 1993; Cremers *et al.* 1998). The dominant drusen phenotype (including a number of similar diseases) is thought to represent an unknown number of genetically distinct entities based on specific clinical differences. However, the genetic analysis of two dominant drusen families in this study has established their linkage to the same chromosomal region as DHRD, which with the drusen phenotype Malattia leventinese, makes at least three phenotypes mapping to the same region. This implies that either different mutations in the same gene or microheterogeneity in the region due to the presence of another gene(s) causes a variation in the phenotype. This will become evident once the disease gene is cloned for one of these phenotypes. Moreover, haplotype analysis from the two dominant drusen families and from the Doyne family eliminates the possibility of a founder effect, which has been observed in other retinal dystrophies (TIMP-3 mutation in Sorsby's fundus dystrophy, Gregory *et al.* 1996, Small *et al.* 1997). Furthermore, we have been able to refine the genetic region where the gene must lie by analysis of further members of the DHRD pedigree, thus placing the gene between markers D2S2352 and D2S2251.

3.8.6 Further analysis of the disease region

Since the initial mapping of the disease, positional cloning efforts using YAC clones were initiated to facilitate the search for the disease gene causing DHRD and related phenotypes (as discussed above) as well as providing candidates for other diseases mapping to the region. This work has been further discussed in Chapter 4.

CHAPTER 4

Construction of a YAC and a partial PAC contig across the DHRD critical region

4.0 Introduction

A physical mapping approach is applied to a study; once the disease has been linked by genetic linkage analysis to a relatively small genetic interval, to which further cloning strategies can be applied. To prevent gross time consumption in construction of large contigs, the advisable maximum genetic distance across which a construction of a contig is suitable is approximately 1 centi Morgan (cM), which in molecular distance approximates to 1 mega-base (Mb). Unfortunately, narrow refinements of a cM do not always occur and the constructions of YAC contigs are initiated across intervals greater than a mega base.

Initially, Doyne honeycomb retinal dystrophy (DHRD) was genetically reduced by linkage analysis to chromosome 2p16-21, in the genetic interval D2S2316 and D2S378 of approximately 5 cM (Gregory *et al.*, 1996). This locus was later refined to a 4 cM interval between the microsatellite markers D2S2739 and D2S378 (Evans *et al*, 1997). Since this interval could not be genetically refined further at that point in time, due to lack of availability of microsatellite markers in the region, a physical map using YACs was initiated across the DHRD locus. Recently, recombination events found within individuals from an additional branch of the Doyne's family have further refined the DHRD locus between markers D2S2352 and D2S2251 (Kermani *et al.*, 1999), an estimated physical distance of approximately 3 Mb.

4.1 Physical mapping

Physical mapping involves the assembly of overlapping clones known as a contig that would faithfully represent the genomic region of interest in a linear order. Physical mapping of a disease should allow direct access to the genomic segment that would include the disease gene. Following the construction of a complete contig, the genomic region can be characterised in detail for the identification of the disease gene. Incidentally, the disease region can be used to map pre-characterised genes to the locus or used in the isolation of novel transcripts using various techniques like exon trapping/exon amplification (Duyk *et al.*, 1990; Buckler *et al.*, 1991). An alternative method is to use cDNA selection (Parimoo *et al.*, 1991) to isolate genes in the critical region. This strategy

has been called the positional cloning approach as it allows the isolation of a disease gene based on its map position.

Physical maps arrayed with yeast artificial chromosomes (YACs) provide long range-continuous coverage which are aligned by microsatellite markers, sequence tagged sites (STS) and expressed sequence tags (EST) at appropriate distances.

4.1.1 Yeast Artificial Chromosomes (YACs)

The development of YACs has increased the genomic cloning capacity by 5-10 fold over cosmids, which contain inserts of approximately 40 kb compared to YACs which contain inserts of up to 1 Mb (Burke *et al.*, 1987; Anand *et al.* 1989, Albertson *et al.* 1990, Larin *et al.* 1991). In general, large fragments of the human genome are cleaved by restriction enzymes and then ligated between two vector arms, each of which ends in telomere sequences and contain centromeres (CEN), replication origin (ARS) and selectable markers to stabilise the YACs in the yeast host. The original vectors contained a suppressor tRNA (which, because it was split allowed the recognition of YAC colonies) and pBR322 sequences to facilitate mapping and recovery of one end of the insert as a plasmid in *E. coli*. The vector sequences total approximately 10 kb and the inserts are usually 300 to 500 kb. Owing to their large size, contigs of up to several megabases can be assembled, facilitating the construction of overlapping clone/STS maps over large regions of chromosomes.

The development of Pulse Field Gel Electrophoresis (PFGE) allows a modified electrophoretic apparatus to separate DNA molecules as large as 10 Mb enabling intact yeast chromosomes to be separated and thus inserts can be sized (Schwartz and Cantor, 1984). YACs introduced into mammalian cells have the ability to encode normal enzymatic products (D'Urso *et al.*, 1990, Huxley *et al.*, 1991). Therefore, YACs can be important tools for research in gene expression and regulation with potential clinical applications as well as useful for the construction of YAC contigs.

The main disadvantage of YACs (Kouprina *et al.* 1994; Monaco & Larin 1994) is that it can often contain chimeric inserts which implies that the insert is composed of two or more fragments that were derived from noncontiguous regions of the genome. Chimerism can be verified by FISH analysis. Approximately 10-60 % of YAC clones in existing libraries can represent chimeric DNA sequences. Chimeric clones may result from a co-ligation of two different restriction fragments prior to transformation. Unstable clones that have a tendency to delete internal regions from their inserts are also an

important drawback in construction of a contig. Deletions vary in size from 20 to 260 kb which can be generated both during the transformation process and mitotic growth transformants (Kouprina *et al.*, 1993). Loss of entire YACs can also occur during mitotic growth. Use of recombination deficient strain can reduce frequency of deletion. Co-cloning events are also a common drawback, where two or more YACs are cloned into the same yeast cell. Difficulties in purifying YAC inserts from the yeast background and poor insert DNA yields are other limitations with YACs. However, the easy availability of YAC libraries and their large insert size capacity is helpful for providing long range continuous coverage of disease regions and for this region YACs were our initial choice for the construction of a contig across the DHRD interval.

4.1.2   Sequence-Tagged Site (STS) content mapping

Primary construction of a contig entails the identification of relevant clones followed by verification of STSs in the hope of finding a degree of overlap between neighbouring clones which contain random end points. Fingerprinting is a method used frequently to determine overlaps between YAC clones. This method involves the restriction digest of clones followed by their Southern blot analysis using a repetitive sequence (e.g. Alu repeat or L1 repeat) which allows neighbouring clones to be identified by the presence of common bands (Bellane-Chatelote *et al.* 1992). Fingerprinting for inter-Alu PCR products is also used to determine overlap between YACs (Nelson *et al.* 1989). The most common and reliable method used is through the advent of PCR, STS content mapping which was routinely utilised in this study in the construction of the YAC contig spanning the DHRD interval. STS content mapping relies on the availability of short DNA sequences, a PCR assay can be developed for that particular sequence by designing oligonucleotide primers flanking the sequence. The region from which the original sequence is derived from the genome is then thought of as tagged by the ability to be PCR assayed for that sequence and is known as a sequence-tagged site (STS). In general, most STSs are non polymorphic, however, the main advantage that their specific chromosomal location can be found conveniently by PCR, by typing either a somatic hybrid panel or a radiation hybrid panel. Microsatellite markers are highly polymorphic STSs that are assigned specific chromosomal locations on the basis of a mapping panel, as well as on the basis of linkage analysis. Thus, STSs can bridge the gap between genetic and physical maps. In simple terms, if two or more clones contain the same STS

then they must overlap and the overlap must include the region containing the STS (see section 2.4.6).

4.1.3   Chromosome walking

Chromosome walking is utilised in regions of insufficient number of STSs and it relies on the establishment of clones from fixed starting points. DNA fragments can be isolated from ends or near ends of relevant clones which can subsequently be used for STS (or probe) to screen the library and identify more clones if necessary creating an overlap in the region. Screening libraries with such STSs identifies neighbours with a bare minimum overlap and can lead to a lengthier but a more efficient walking procedure. Failure of a walking step with an end-clone is a quick indication of a gap in the collection of clones being screened. Various methods are used to isolate YAC ends, which include techniques of vectorette PCR (Riley *et al.* 1990), inverse PCR (Silverman *et al.* 1989), single primer extension PCR (Screaton *et al.*, 1993) and vector-Alu PCR (Nelson *et al.*, 1989, 1991). The latter method was utilised in this study and is described in section 4.4.3.

4.1.4   YAC libraries

YACs used in the study were obtained through various screenings of YAC libraries provided by the UK HGMP Resource Centre from where relevant three human libraries were routinely obtained (see table 4.1). The sequence of primers for microsatellite markers and STSs were obtained from the genetic and physical maps available on the Whitehead database (http://carbon.wi.mit.edu:8000/cgi-bin/contig/phys_map). STS content mapping was performed on YACs to construct a continuous overlapping framework of clones across the disease interval (see section 2.6.4).

YAC library	Derivative Human cell line	Average insert size (kb)	No of clones	Reference
ICI	Lymphoblastoid 48XXXX-cell line	350	34,500	Anand *et al.*, 1990
ICRF[1] 164 plates (labelled 4X1-4X164)	Lymphoblastoid 48XXXX-cell line	600		Larin *et al.*, 1991
ICRF[2] 24 plates (labelled 4Y1-4Y24)	Male lymphoblastoid 49 XYYYY-cell line	400-500		Larin *et al.*, 1991
ICRF[3] 26 plates (labelled HD1-HD26)	Lymphoblastoid, Huntingdon's disease 46XX-cell line	600	20,500	Larin *et al.*, 1991
CEPH		920	35,600	Chumakov *et al.*, 1992

Table 4.1:

Human YAC libraries available from HGMP resource centre.

4.2 The genomic region of 2p21-16

The human chromosome 2, at 255 Mb (Morton *et. al.*, 1991) constitutes approximately 8 % of the human genome. A preliminary physical map was published in 1993 by Cohen and coworkers who estimated that approximately 84 to 99 % of chromosome 2 was represented in the contig. The map was constructed using sequence specific tags (STSs) from the dinucleotide markers produced at Généthon (http://gopher.genethon.fr/genethon_en.html). Thus each YAC was isolated with a genetic marker located on chromosome 2 initially integrating CEPH YACs into a physical map.

Several genes have been mapped to the 2p21-2p16 region. Malattia leventinese, another autosomal dominant retinal dystrophy was initially mapped to this region (Héon *et. al.* 1996, Héon *et. al.*, 1996a, Edwards *et. al.* 1998). The phenotypic similarity and genetic mapping data was used to evaluate that the two diseases may share an allelic relationship.

Other disease genes and expressed genes localised to the 2p16 region are Carney-complex (CNC; Stratakis *et al.* 1996), homologous gene to drosophila sine oculis (*SIX3*; Rodriguez de Cordoba *et al.*, 1998), fibrillin like (*FBNL*; Ikegawa *et al.*, 1996), G/T mismatch-binding protein (GTBP, *MSH6*; Papadopoulos *et al.*, 1995), malate dehydrogenase, soluble form (*MDH1*; Tanaka *et al.*, 1996) and exportin-1; required for chromosome region maintenance (*XPO1, CRM1*; Fornerod *et al.*, 1997). Solute carrier family 3 genes (*SLC3A1, ATR1, D2H, NBAT*; Calonge *et al.*, 1995) have also been localised to the 2p16.3 cytogenetic band. Genes that have been broadly localised to 2p16 and adjacent cytogenetic (e.g. p16-15 or p21-16 or p22-16) bands are Spectrin, beta-nonerythrocytic-1 form (*SPTBN1*; Chang *et al.*, 1993), Follicle stimulating hormone receptor (*FSHR, ODG1*; Rousseau-Merck *et al*, 1993), phosphatidylinositol glycan; class F (*PIGF*; Ohishi *et al.*, 1995), vaccinia-related kinase (*VRK2*; Nezu *et al.*, 1997), Calcineurin B (*PPP3R1;* Wang *et al.*, 1996), Human T-cell leukaemia virus enhancer factor (*HTLF;* Lee *et al.*, 1992) and Calmodulin 2 is localised to 2p21.3-21.1 (*CALM2;* Berchtold *et al.*, 1993).

4.2.1 Physical maps of chromosome 2

Physical maps of chromosome 2 have been constructed by the Whitehead Institute/MIT Centre for Genome research [Hudson *et al.*, 1995, (http://carbon.wi.mit.edu:8000/cgi-bin/contig/phys_map)]. The Whitehead map of chromosome 2 is composed entirely of YAC clones derived from the CEPH mega-YAC library. These mega-YACs were isolated by PCR based screening with STSs, which include Généthon microsatellite markers from the genetic map of chromosome 2 (Dib *et al.*, 1996) and STSs mapped and ordered by radiation hybrid (RH) mapping. Chromosomal region 2p16 which corresponds to the genetic interval flanked by D2S119 and D2S378, covers a genetic distance of approximately 16 cM (see fig.4.1). This region is underrepresented in the maps of chromosome 2 and is mainly due to large gaps of unknown physical distance within the Yeast Artificial Chromosome map. The Whitehead map as yet does not provide complete coverage of chromosome 2 and is composed of several isolated, non-overlapping contigs distributed along the length of the chromosome. Singly linked contig WC2.4 and WC-1583 are Whitehead YAC contigs relevant to the 2p21-16 region harbouring all mega-YACs for this region.

The University of Washington is currently sequencing chromosome 2 and their target is to sequence the entire chromosome

Human chromosome 2p
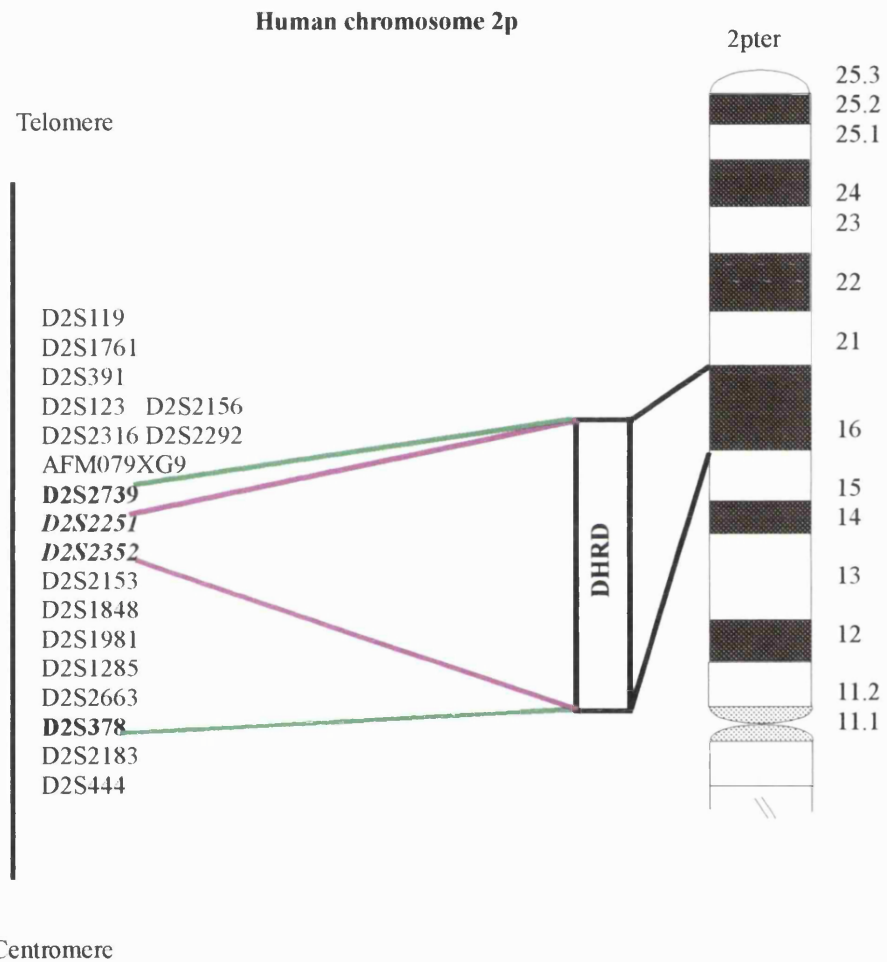
Fig **4.1**

Integrating the human chromosome 2 Whitehead and Genethon maps across the DHRD region. Polymorphic marker D2S2739 is a marker from Cooperative Human linkage Center (CHLC; http://www.chlc.org/) . Green lines depict the previously refined DHRD locus anad pink lines depict the current refined locus.

http://genome.wustl.edu/gsc/human/chrom2.shtml. Around 950 probes have been used to isolate approximately 10,000 Bacterial Artificial chromosome (BACs) clones. Construction of a contig through restriction pattern fingerprint analysis is underway; more than 250 contigs are already present. Only selected clones are currently being sequenced whose regional localisation will soon be made available to the public on the database.

Human chromosome region 2p16 is syntenic with mouse chromosome 11 which can be observed with the genes Malate dehydrogenase (Mor2) and Reticuloendotheliosis oncogene (Rel) (Mouse Genome Database, 1995). Updated versions of human and mouse homology maps can be observed on the database (http://www.ncbi.nlm.nih.gov/Homology/).

4.3   Aim of study

Following the initial linkage assignment of DHRD to the 2p16 region, the next step was to embark on the construction of a YAC contig across the disease interval. The aim was to physically characterise this region in the hope of identifying or isolating retinally expressed transcripts localised within the disease region that would eventually lead to the identification of the disease gene.

Although a YAC contig exists on the Whitehead database (http://carbon.wi.mit.edu:8000/cgi-bin/contig/phys_map) for the DHRD region, it was essential to verify the nature of these CEPH mega –YAC clones (see fig 4.2) which provide long range coverage of chromosome 2 regions. While utilising these mega-YACs in this study, it was kept in mind that chimeric clones could be identified through the Whitehead database (as reported by other labs) prior to use in the laboratory. Subsequently this could be verified by FISH analysis of clones of interest. Part of the effort was to obtain all mega-YACs that mapped to the DHRD region so as to create a preliminary framework to allow contig building. Secondly work was undertaken to isolate novel ICI and ICRF YACs from their respective libraries creating a reliable representation of the original genomic interval in an effort to create a deeper contig of the region than that already present on the database. Where possible, non-chimeric YACs would be isolated for future mapping of genes and isolation of STSs to bridge gaps in the contig. If satisfactory coverage was not achieved by YAC clones, then PACs would be isolated to consolidate the YAC contig, and bridge gaps that could not be closed by chromosome walking with

YACs with the added advantage of providing non-chimeric clones to map genes within the disease region.

4.4   Materials and methods

4.4.1   YAC libraries

All YACs were obtained by screening any of the three YAC libraries (ICI, ICRF and CEPH) provided by the UK HGMP Resource Centre (see table 4.1). In this study, the ICI and ICRF libraries were screened and CEPH YACs were obtained by using database information.

4.5   Results

4.5.1   Verification of the integrity of mega-YACs obtained from pre-existing contigs.

The construction of the YAC contig was initiated subsequent to the linkage assignment of DHRD where the critical region extended between D2S2316 and D2S378 (Gregory, *et al.*, 1996). CEPH YACs that contained microsatellite markers and STSs within this region were selected from the Whitehead WC2.4 contig as an initial starting point for the DHRD physical map. These YACs were obtained from the HGMP Resource Centre, UK.

Table 4.2 shows the panel of YACs across the DHRD region and fig. 4.2 depicts STS content mapping of the mega-YACs using 14 STSs localised to the DHRD region, which included microsatellite markers D2S123, D2S2316, D2S2292, AFM076XG9, D2S2739, DS2352, D2S2251, D2S2153 and D2S378, an STS of exon 14 of gene *SPTBN1*, ESTs D2S1848E and D2S1981E and nonpolymorphic STSs D2S1285 and D2S2663. In addition markers telomeric to the DHRD region, overlapping with the Malattia leventinese region were also tested on the YACs to further determine their STS content. Linkage analysis mapped Malattia leventinese (Héon *et. al.*, 1995) between polymorphic markers D2S1761 (not shown in the DHRD YAC contig, lies between D2S119 and D2S391 on Whitehead map) and marker D2S444 (also not shown in the DHRD contig but is placed below marker D2S2183 on Whitehead map).

Inconsistencies were found in the STS content of a number of the mega-YACs and some chimerism was found to be consistent with previous findings for the YAC library (Todd *et al.*, 1995). Thus, the mega-YAC contig was assembled from a total of seventeen STSs in 17 mega-YAC clones. Most YAC clones were shown to contain more

than one STS and several clones did not contain the expected STS. In addition, the STS content of three YACs, telomeric to the DHRD locus encompassing the Malattia leventinese locus were determined.

YAC data resolved the order of polymorphic markers (Généthon map order was Tel-D2S2251-D2S2352- D2S2153-Cen) based on STS content mapping data and meiotic data to be Tel-D2S2739-D2S2352-D2S2251-D2S2153-D2S378-Cen. The order of D2S2156/D2S123 or D2S2316/D2S2292 could not be resolved with this or the meiotic data. In addition, an STS for the ß-fodrin gene was placed between markers D2S2153 and D2S1848E and an STS WI-3027 between D2S123 and D2S2316. STS D2S2674 was present in three YACs (675-E-2, 847-D-2, 899-F-10) thus broadly localised between D2S391 and WI-3027. Another STS WI-4077 was not present in any of the YACs, thus the most likely position is in the gap between WI-3027 and D2S2316. A gap exists between markers WI-3027 and D2S2316/D2S2292. It seemed reasonable to screen the ICI and ICRF libraries for new YACs in this region. However, YACs were not available in this gap that lies outside the DHRD region.

Within the DHRD region gaps observed were between markers D2S1981 and D2S1285, D2S2352 and D2S2251, and between D2S2251 and D2S2153. Although YAC clone 806-C-12 broadly covers the gap between D2S2352 and D2S2153, it is deleted for

CEPH Mega YACs

944A6 753H1 743G4 758E5 919A6 806C12 709F10 713A11 901H5 929F5 929A8 919F6 726E11 890G10 847D2 899F10 675E5

D2S119
D2S391
D2S2156
D2S2674
WI-3027
D2S123
D2S2316
D2S2292
AFM076XG9
D2S2739
D2S2352
D2S2251
D2S2153
SPTBN1
D2S1848E
DS21981E
758E5RA
D2S1285S
D2S2663S
D2S378
D2S2183
D2S370

Refined DHRD locus
DHRD Linked locus
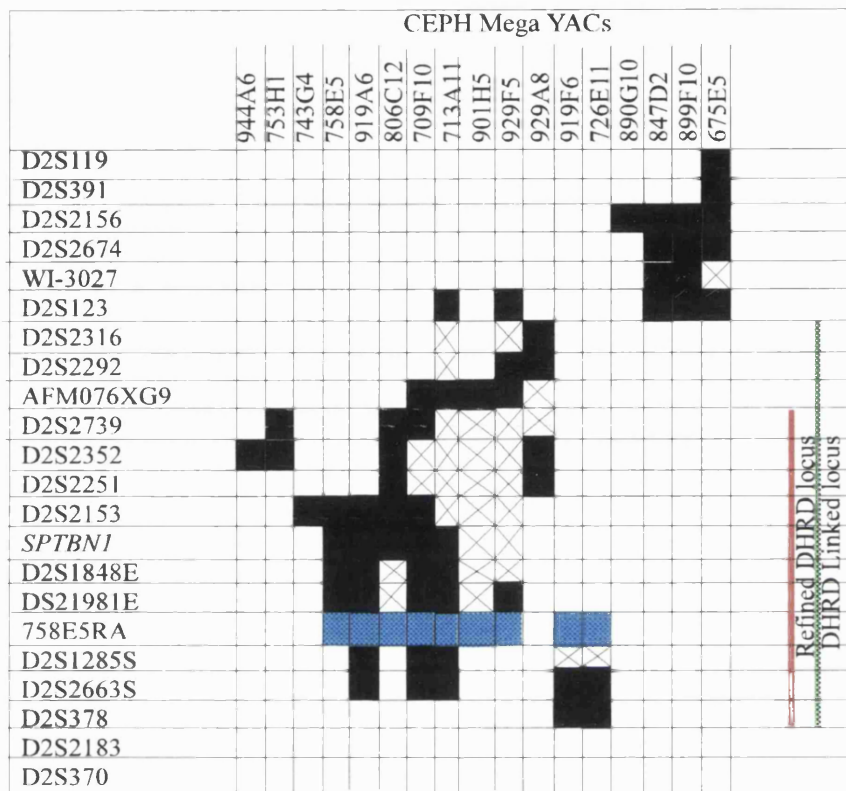
Fig4.2

The STS content map of CEPH Mega YACs across the DHRD region. Black and blue solid boxes indicate the presence of an STS by PCR analysis. Blue colour represents an STS created by *ALU*-PCR. STSs from genes are shown in italics. The letter S denotes STS and the letter E denotes EST.

the distal markers and is a published chimeric YAC (Bray-Ward *et. al.*, 1996) and thus should be used with caution. YAC data showed that 4 mega-YACs and 1 ICI YAC clone also showed deletions for this critical region indicating that this was a difficult region to clone.

| YAC id | YAC size kb | | FISH data | STS hits in | No of bands |
	Expected	Observed		chromosomes	in PFGE
675-E-2	290	630	-	**2**	1
709-F-10	900,1060	650	-	**2,6,5**,12	1
713-A-11	1330	1500	-	**2**,4,10,14,1,15,10, 2	1
726-E-11	390	420	-	**2,13**,1,18	1
743-G-4	1580	720	-	**2,20**,1,3,4,12, 21	1
753-H-1	-	360	-	**2**,1,4,21	1
758-E-5	1350	380	NC	**2,18**,4,22	1
806-C-12	-	1500	-	**2,3,12**,1,7,13	1
847-D-2	730	650	-	**2**	1
890-G-10	1520	470	-	**2,5**,1,15	1
899-F-10	1380	1100	-	**2,10**	1
901-H-5	380	460	-	**2,6,13**,1,22,10	1
919-A-6	1720	2000	-	**2**	1
919-F-6	1130	1000	-	**2**,1,20,9,3,X, 10,15	1
929-A-8	670	1130	NC	**2,17**,10,15,17	1
929-F-5	760	800	-	**2,6**,10,13,11,5	2
944-A-6	1320	1120	-	**2,18**	1

Table 4.2:

Verification of CEPH mega-YACs obtained from the Whitehead map. Unambiguous hits are in bold, ambiguous hits are not highlighted. NC depicts non chimeric clones.

4.5.2 Isolation of novel YACs using YAC libraries

Initially, the ICI library was screened with microsatellite markers D2S2739 and D2S378 as at that point in time these were the flanking markers of the critical region. Two YACs were obtained with the polymorphic marker D2S378 and one YAC was obtained with the tetranucleotide repeat CHLC marker D2S2739 (see table 4.3).

Subsequent screenings of the ICRF library were carried out with all five microsatellite markers (D2S2251, D2S2153, D2S2352, D2S2739 and D2S378) within the region. In addition, two STSs (D2S1285 and D2S2663) and three ESTs (D2S1981E, D2S1848E and *SPTBN1*) were also used to screen the ICRF library, using PCR amplification of YAC solution DNA. A total of 12 novel YAC clones were identified from screening both the ICI and ICRF library which were subsequently obtained from the HGMP Resource Centre. STS content mapping of YACs revealed that most of them contained more than one STS and only a few contained only one STS. STS content analysis also revealed that YAC 37AE3 was deleted for polymorphic marker D2S2251 and that gaps still existed between markers D2S2352 and D2S2153 and D2S1981 and D2S1285 (see Fig. 4.3) which were now required to be covered by end cloning methods or by isolating other clone lines consisting of PACs or BACs or cosmids.

Lab ID	YAC	Origin	Size (kb)	Chimerism
GATA ICI	37AE3	ICI	400	NC
GATA ICRF1	4X118-F10	ICRF	840	-
GATA ICRF2	4X112-H7	ICRF	780	-
378 ICI	8CD4	ICI	500	NC
1285 ICRF	4X15C4	ICRF	500	-
1285 ICI	11AC3	ICI	290	-
1981 ICRF	4X34F5	ICRF	300	-
2663 ICRF	4X109E9	ICRF	390	-
Fodrin 1	4X135-A8	ICRF	*	-
Fodrin 2	4X133-A8	ICRF	<225	-
Fodrin 3	4X133-E8	ICRF	670	-
Fodrin 4	4X135-A5	ICRF	*	-
758-E-5	758-E-5	CEPH	380	NC
929-A-8	929-A-8	CEPH	1130	NC
753-H-1	753-H-1	CEPH	360	-
743-G-4	743-G-4	CEPH	720	-
919-F-6	919-F-6	CEPH	1000	-
726-E-11	726-E-11	CEPH	420	-
919-A-6	919-A-6	CEPH	2000	-
944-A-6	944-A-6	CEPH	1120	-
806-C-12	806-C-12	CEPH	1500	-
713-A-11	713-A-11	CEPH	1500	-
709-F-10	709-F-10	CEPH	650	-
901-H-5	901-H-5	CEPH	460	-
929-F-5	919-F-5	CEPH	*	-
890-G-10	890-G-10	CEPH	470	-
847-D-2	847-D-2	CEPH	650	-
899-F-10	899-F-10	CEPH	1100	-
675-E-2	675-E-2	CEPH	630	-

Table 4.3:

YACs across the DHRD interval indicating Origin, Size, and

Chimerism NC depicts non chimeric clones.

4.5.3 Investigation of chimerism of critical YACs spanning the DHRD interval by FISH analysis

This technique allows the DNA probe to be labelled by incorporation of modified nucleotides, obtained by covalent binding of a reporter molecule (e.g. biotin or digoxygenin which can be detected by specific binding to another molecule). The standard protocol followed can be seen in section 2.7.3. Once the DNA has been hybridised, the probe is washed off and the chromosome preparation is incubated in a solution containing a fluorescently labelled affinity molecule that binds to the reporter on the hybridised probe. The intensity of the hybridisation signal is increased by using large DNA inserts e.g. cosmid clones that contain inserts of 40 kb are routinely used. As large sequences contain repetitive elements, the probe is mixed with an excess of unlabelled genomic DNA and denatured, and then allowed to reanneal thus saturating the repetitive elements in the probe, to prevent masking of the signal generated by the unique sequence. Advantage of FISH is that rapid results are generated which can be easily scored by eye under a fluorescence microscope. In metaphase spreads, positive signals are seen as double spots corresponding to the hybridised probe to both sister chromatids.

ICI YACs (8CD4 and 37AE3) obtained by the previously flanking markers D2S2739 and D2S378 were FISH mapped (courtesy of M. Fox, Galton lab, University College London) to verify whether the clones isolated contained any chimeric portions prior to end sequence isolation to 'walk' across and isolate more YAC clones. Results indicated that these clones mapped specifically to the 2p16 region.

Mega-YACs 758-E-5 and 929-A-8 was also FISH mapped to detect possible chimerism prior to end sequence isolation (see Fig. 4.4). All four YACs proved to contain sequences exclusively from chromosome 2p16. These YACs were thought to be ideal for isolating end sequences to bridge gaps in the DHRD interval.

ICI and ICRF YACs

	4XI12-H7	4X118-F10	37AE3	4X135-A8	4X133-A8	4X133-E8	4X135-A5	4X34F5	4X15C4	11AC3	4X109E9	8CD4	Refined DHRD locus	DHRD Linked locus
D2S119														
D2S391														
D2S2156														
D2S2674														
WI-3027														
D2S123														
D2S2316														
D2S2292														
AFM076XG9		■	■											
D2S2739	■		■											
D2S2352			■											
D2S2251			⊠											
D2S2153			■	■	■	■								
SPTBN1				■	■	■	■							
D2S1848E								■						
DS21981E								■						
758E5RA														
D2S1285S									■					
D2S2663S									■	■	■			
D2S378											■			
D2S2183														
D2S370														
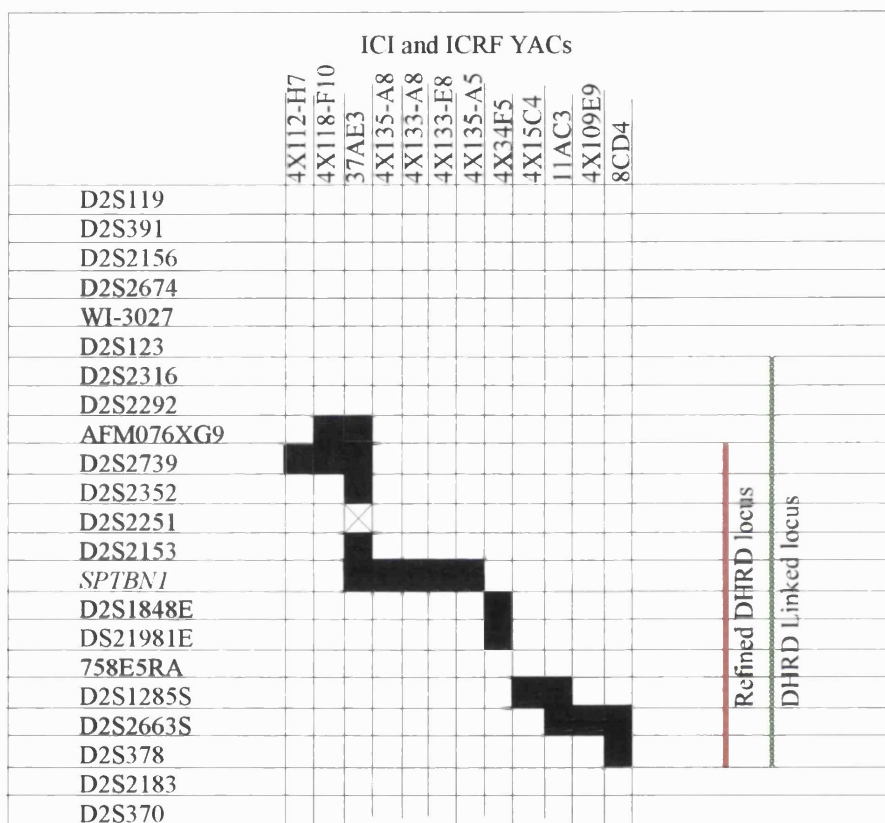
Fig4.3

STS content mapping of the ICI and ICRF YACs across the DHRD region. Black solid boxes indicate the presence of an STS by PCR analysis. STSs from genes are shown in italics.The letter S denotes STS and the letter E denotes EST.

4.5.4 Sizing YACs by Pulse Field Gel Electrophoresis (PFGE)

All YACs were sized by PFGE (see table 4.3). Fig. 4.5a is an example of an autoradiograph of a PFGE gel. Fig. 4.5b shows the hybridisation result with Cot-1 (of the former result) verifying the presence of human insert within the yeast chromosomal background. Incidentally, two YAC clones showed two bands per YAC lane on PFGE gel analysis i.e. YACs 4X135-A5 and 4X135-A8 (see table 4.3). This could be due to a mixture of two strains or the presence of two YACs within the same cell. In a pure clone, the presence of more than one species are an indication of a structurally unstable YAC. To check the stability of a clone, several independent colonies need to be analysed by PFGE to see if this is a recurring problem. In the current context, this would be unnecessary as these YACs were being tested for their STS content across the DHRD interval. Most of the mega clones were either bigger or smaller than the expected size. The most likely explanation is that these YACs originally contained unstable sequences, which were either lost or rearranged during growth in yeast, producing a stable derivative.

4.5.5 Closure of gaps by chromosome walking

STSs were developed from YAC insert termini sequences by pYAC4-*ALU* PCR (Tagle and Collins, 1992). The unique PCR products were obtained and sequenced with relevant primers (see section 4.4.3). Sequences obtained by *ALU*-PCR, were analysed for homology to known DNA sequences in Genbank using BLAST/BLASTN programs (Altschul *et. al.,* 1990) prior to designing STSs. Chromosomal origins of STSs can be tested on a panel of clones to identify the STS content and overlapping YACs in the region (in this case the panel of DHRD YAC clones). Alternatively, they can be tested using a Genbridge4 radiation hybrid mapping panel (Gypay *et al.* 1996).

Initially, YACs that were used to isolate the ends were 37AE3 (fig. 4.9), 4X118F10, 4X112-H7 and 8CD4, but failed to show unique PCR products with Ale 1 and outer LA/RA pYAC4 vector or Ale 3 and outer LA/RA vector.

One of the terminal sequence of YAC 758E5, was determined by *ALU*-PCR and a 73 bp end fragment (758-E-5RA, Accession No. AF039310) was PCR amplified on the YAC panel and found to be present in YAC 758-E-5 and in 8 mega-YACs (919-A-6, 806-C-12, 709-F-10, 713-A-11, 901-H-5, 929-F-5, 929-A-8, 919-F-6 and 726-E-11, fig. 4.6) in the region, confirming its chromosomal position. A human positive control and a

145

negative control were also used for PCR analysis. Fig. 4.6c shows the sequence obtained from mega-YAC 758-E-5.

The sequence of this STS (forward primer 5'-ACACAGTACAAAAACATAGAGTAA-3', reverse primer 5'-TTTCTTAATAGTTGGCAAGACCA-3') was compared with sequences in EMBL/Genbank and failed to reveal significant homology to any known sequence on the database. In addition, mega-YACs 753-H1 (fig. 4.6d) and 919-A-6 (data not shown) were also used for *ALU*-PCR and unique products were observed but, unfortunately the sequences obtained from these products were short and contained highly human repetitive regions when compared with sequences on the database.

Fig. 4.4:

YAC fluorescent *in situ* hybridisation (FISH) results to metaphase chromosomes (from normal male 46, XY male). The above FISH result depicts that of non-chimeric YAC 37AE3 showing signal on chromosome 2p16 only.
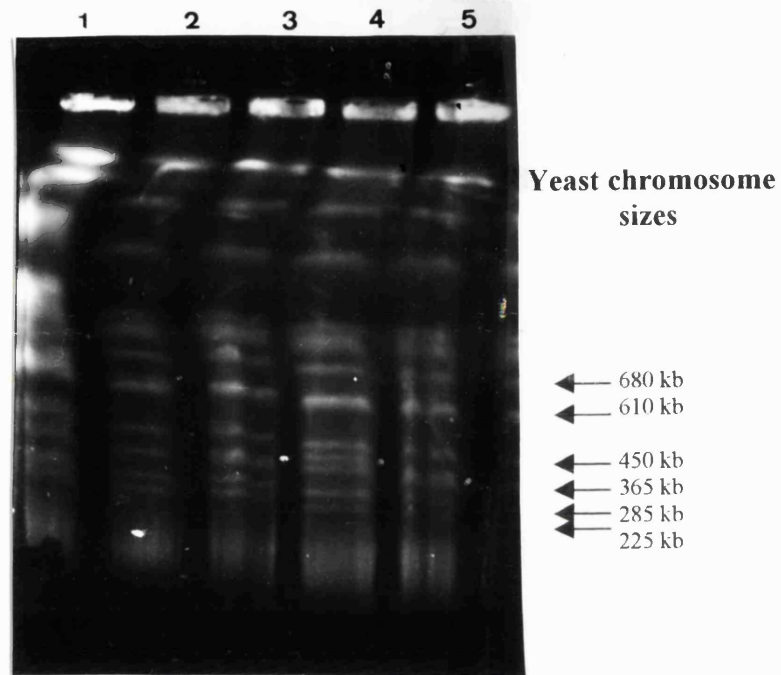
Fig. 4.5a:

Ethidium bromide stained 1% agarose gel depicting YACs subjected to PFGE analysis. Lanes 1-5 (L-R) correspond to mega-YACs 919F6, 743G4, 758E5, 726E11 and 753H1 respectively. YAC inserts of 758E5 and 726E11 are clearly visible between yeast chromosomal bands 365 kb and 450 kb marked by white dots on right side of each lane. Mega-YAC insert of 753H1 is observed just below the 365 kb yeast chromosomal band.
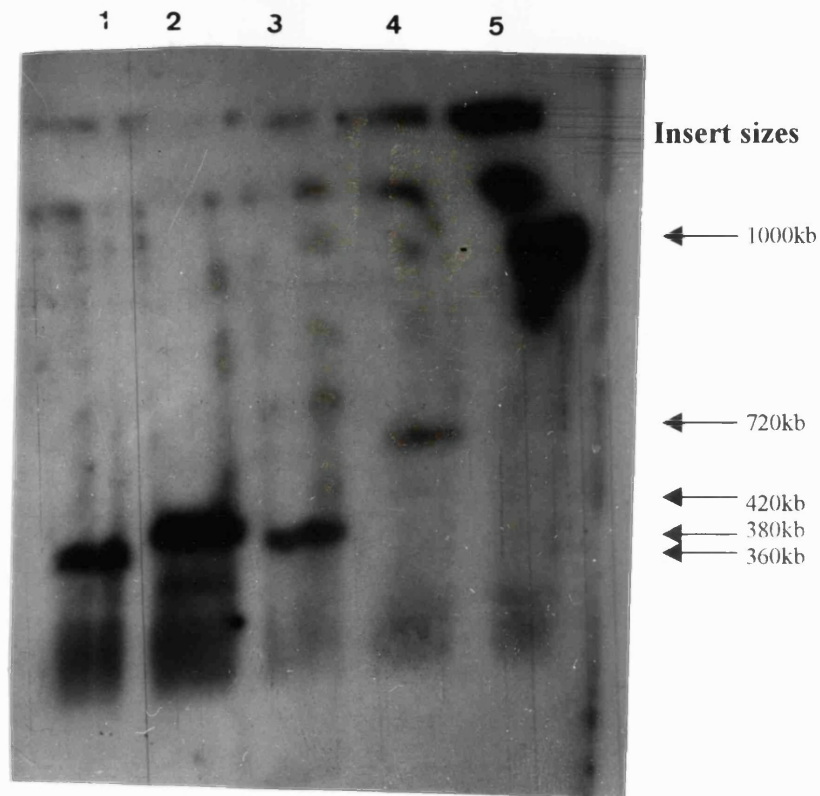
Fig. 4.5b:

An autoradiograph of the PFGE gel presented in figure 4.5a, following a Southern blotting and hybridisation result with human Cot-1 DNA. Although the yeast chromosomal background appears it is not as clear as the human inserts of the selected mega-YACs. Lanes 1-5 correspond to mega-YACs 753H1 (360 kb), 726E11 (420 kb), 758E5 (380 kb), 743G4 (720 kb) and 919F6 (1000 kb) respectively. Note:-This picture has been developed back to front in comparison to the previous picture (fig. 4.5a).
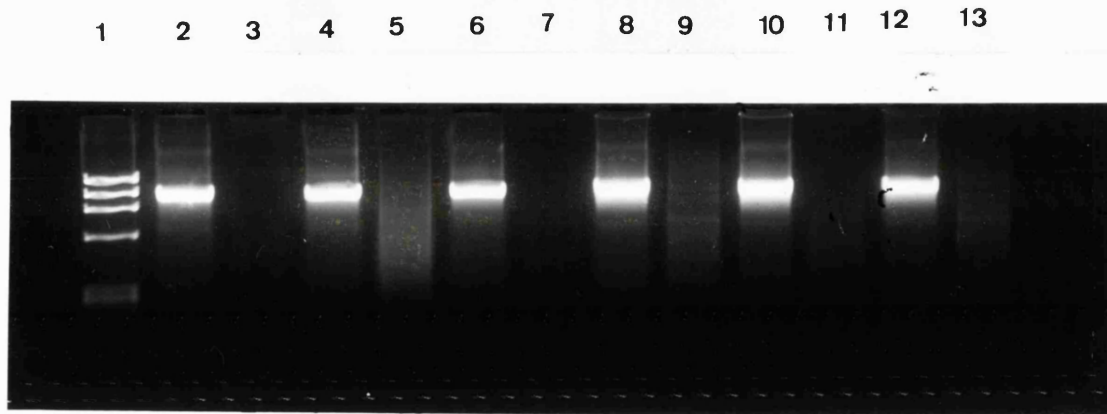
Fig. 4.6:

A photograph of a 1% agarose gel stained in ethidium bromide of YAC clone 37AE3 showing the absence of unique *ALU*-PCR product. Lane 1 corresponds to marker ØX174/HaeIII and lanes 2 to 13 correspond to LA+A1, negative control of LA+A1, A1, negative control of A1, RA+A1, negative control of RA+A1, LA+A3, negative control of LA+A3, A3, negative control of A3, RA+A3 and negative control of RA+A3 respectively.
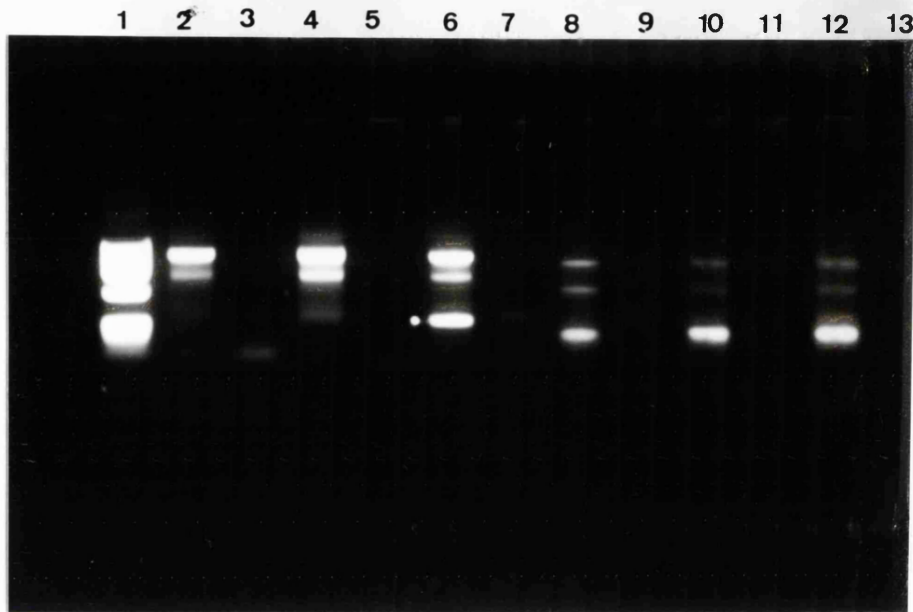
Fig. 4.6a:

A photograph of an ethidium bromide stained 1% agarose gel showing a unique YAC *ALU*-PCR product (~300bp, indicated by a white dot) of mega-YAC 758-E-5 (lane 6). Marker X174/HaeIII is present in lane 1. Lanes 2 to 13 correspond to LA+A1, negative control of LA+A1, A1, negative control of A1, RA+A1, negative control of RA+A1, LA+A3, negative control of LA+A3, A3, negative control of A3, RA+A3 and negative control of RA+A3 respectively.
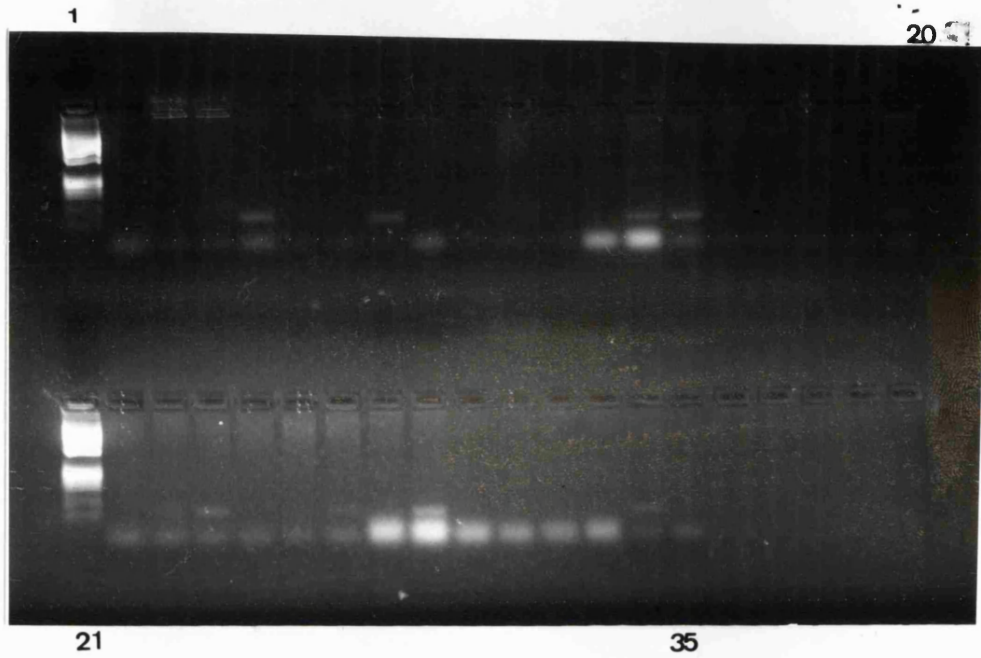
Fig. 4.6b:

A photograph of a 3% agarose gel stained in ethidium bromide showing the STS content of 758E5RA across the YAC panel. Lane 1 and 21 corresponds to marker ØX174/HaeIII Lanes 5, 8, 13,14,20, 23, 24, 27 and 29 correspond to YACs 919-A-6, 806-C-12, 709-F-10, 713-A-11, 901-H-5, 929-F-5, 929-A-8, 919-F-6 and 726-E-11 respectively indicating a PCR product of ~70 bp. Lane 34 corresponds to a positive genomic control and lane 35 corresponds to a negative control.

*TCCCGGGG*GCGAGTCGAACGCCCGATCTCAAGATTACG*GAATTC*
ACACAGTACAAAAACATAGAGTAATTCCATACTACTTTAGTCCTA
TATTTTGGTCTTGCCAACTATTAAGAAAAAGAAGTCAGCCAGGTG
TTGTGGCTCACACCTGTAATCCCAGCACTTTGG

Fig **4.6c.**

YAC end sequence generated by Alu-vector PCR method from YAC 758-E-5 showing the forward primer
enclosed in a red box and the reverse primer enclosed in a green box. The pYAC4 vector sequence is shown
in blue, letters in blue italics are enzyme restriction sites.

*TCCCGGGG*GCGAGTCGAACGCCCGATCTCAAGATTACG*GAATTC*
ATTTTCTGTCTCCGGTCCATTGCTTCAAACTCACTTTATTCTTTCT
TTTTTTTTTTTGAAAAAGATTTCCCCCCCCCGCCCGGGGGGGGAT
TG

Fig **4.6d**

YAC end sequence generated by Alu-vector PCR method from YAC 919-A-6 showing the sequence generated
with the pYAC4 right arm inner primer. The pYAC4 vector sequence is shown in blue, letters in blue italics
are enzyme restriction sites.

153

4.5.6   Isolating PACs from a total genomic PAC library to bridge gaps in the contig.

Similar to YAC libraries, the PAC library has been constructed in the vector, pCYPAC2N and has been organised in hierarchical pool system with primary, secondary and tertiary pools for PCR screening (Ioannou P.A and de Jong P. J., 1996). The STS content mapping of PACs was performed to create a deeper contig of the critical region (see section 2.4.6).

In total 16 PACs were isolated in order to bridge the gap between the recent flanking markers D2S2352 and D2S2153. Six PAC clones were isolated using microsatellite marker D2S2352 and ten PACs were isolated with microsatellite marker D2S2251. The gap between markers D2S2352 and D2S2251 in the critical DHRD region seemed to be bridged by the PAC clone 130-13-O. Although when PAC libraries were used to isolate additional PAC clones with marker D2S2251, PAC clone 130-13-O was not obtained neither were any additional clones. Thus, it seemed that PAC clones could not be obtained with this polymorphic marker by screening the PAC pools. Nevertheless, any YAC or PAC clone isolated with markers D2S2352 and D2S2251 could be used to preliminarily map genes in this region.   PAC clones that were isolated for marker D2S2153 only contained that marker and failed to be positive for either of the adjacent markers. Ideally any PAC clone isolated with marker D2S2352 and D2S2153 could be in future used to isolate end sequences to re-enforce the continuity of these genomic segments in the region lying between D2S2352 and D2S2153 which appears to be a difficult region to clone.

Future work would entail, linear extension PCR that can be used to isolate end sequences from PAC clone 130-13-O which could be verified in the remaining 15 PAC clones or could be further utilised to isolate novel PAC clones in order to 'walk' across the region flanked by markers D2S2352 and D2S2251. Once an overlapping tiling path of PAC clones has been produced, the resulting clones can then be sized by PFGE.

4.5.7   Genes and ESTs located in the DHRD region

A partially pre-characterised gene *SPTBN1* and 2 ESTs D2S1848 and D2S1981 were initially mapped within the previous DHRD refined region (D2S2739 and D2S378). In an effort to place more genes within the DHRD interval and thereby facilitate the identification of the DHRD gene, information on partial cDNA sequences or Expressed

Sequences Tags (ESTs) of genes that were placed on 2p16 by the gene map consortium (Schuler *et al.,* 1996) was accessed through the electronic database at http://www.ncbi.nih.nlm.gov/SCIENCE96/. The EST database revealed that at least 44 cDNA markers have been mapped to this region. However, the localisation of these ESTs is not precise and needs further to be tested on a physical contig for further accuracy of localisation. While the contig was incomplete, this exercise was essentially preliminary. However, since the DHRD region was genetically refined to 1 cM and a preliminary PAC contig was present, this exercise gained more importance. Some of the ESTs that have been mapped to 2p16 region are shown in table 4.4. ESTs that showed retinal or brain expression were given preference. ESTs derived from brain cDNA libraries are also given preference, as retina is part of the central nervous system and derived from the neural ectoderm. Of the ESTs that have been mapped, ESTs D2S1848 and D2S1981 and gene *SPTBN1* have been excluded due to their position in the contig which lie outside the current refinement.

Some of the cDNA markers other than D2S1848 and D2S1981 mapping to the 2p16 region were WI-6704, Z38593, AA018184, AA058672 and AA176619 (see table 4.4). Expression profiles on the database showed ubiquitous expression for most of these genes except WI-31133.

Among the cDNA markers that have been mapped to the contig, an EST (WI-31133) from eye has been mapped to some of the PAC clones (301-14-O, 301-1-P, 301-13-N, 301-13-L and 293-14-O, see fig, 4.8b) and YACs (37AE3 and 758-E-5, see fig. 4.8a) thus broadly localising the EST between the polymorphic marker D2S2352 and D2S2251. Based on database information and consequent information resulting from the YAC contig, this EST is a good candidate for the DHRD gene. Confirmation of its expression profile and the genomic organisation for subsequent mutation analysis constitutes chapter 5 and is the current ongoing work of this study.

Fig4.7

STS content mapping of CEPH mega-YACs, ICI, ICRF YACs and PACs across the DHRD region. Black and blue solid boxes indicate the presence of an STS by PCR analysis. Blue colour represents an STS created by *ALU*-PCR. STSs from genes are shown in italics. The letter S denotes STS and the letter E denotes EST.

EST clone ID	cDNA library	Primer sequences 5'-3'	Tm (°C)	Size (bp)	Expression information on database
WI-6704	Infant brain	F-TTTGAAAATAAATTCATGCACCA R-CAGAGTGATAACCATGTCTGCC	55	270	Fetal brain, fetal heart, germinal centre B cell
Z38593	Infant brain	F-TAGCTCCACCATCTCTGCAA R-GTCTTGACTGCCATGTGTTCA	56	174	Infant brain, fetal spleen, melanocyte, brain, retina, neuroepithilium, (N2RAM1), liver, fetal liver/spleen
AA018184	Whole embryo	F-TCCACCATCTCTGCAACTTGCC R-CAAAGCTGAATGAAAACGCCC	55	500	Fetal cochlea, fetal lung, fetal spleen, fetal liver/spleen, retina, muscle, fetal retina, endothelial, melanocyte
AA058672	Brain, retina, liver	F-AAGATGCGGCAAGACTATCTGC R-CCTTGACGTTGCAGTGCAGTTTC	60	250	Fetal spleen, infant brain, melanocyte, brain, retina, neuroepithilium (NT2RAM) liver, fetal liver/spleen
AA176619	Lung, Spleen, Retina, Muscle	F-GCTCCACCATCTCTGCAACTTG R-GTCAGGGAAGAACGAACCTTGAC	60	280	Fetal cochlea, fetal lung, fetal spleen, fetal liver/spleen, retina, muscle, fetal retina, endothelial, melanocyte
WI-31133	eye	F-CACATCAAATCTTAAGATGTCAACA R-CTAACTTGAGATCAGTGGCGG	50	135	retina

Table 4.4:

Characteristics of some of the ESTs that have been mapped within the 2p16 region. EST that has been mapped within the DHRD contig is shown in bold type.
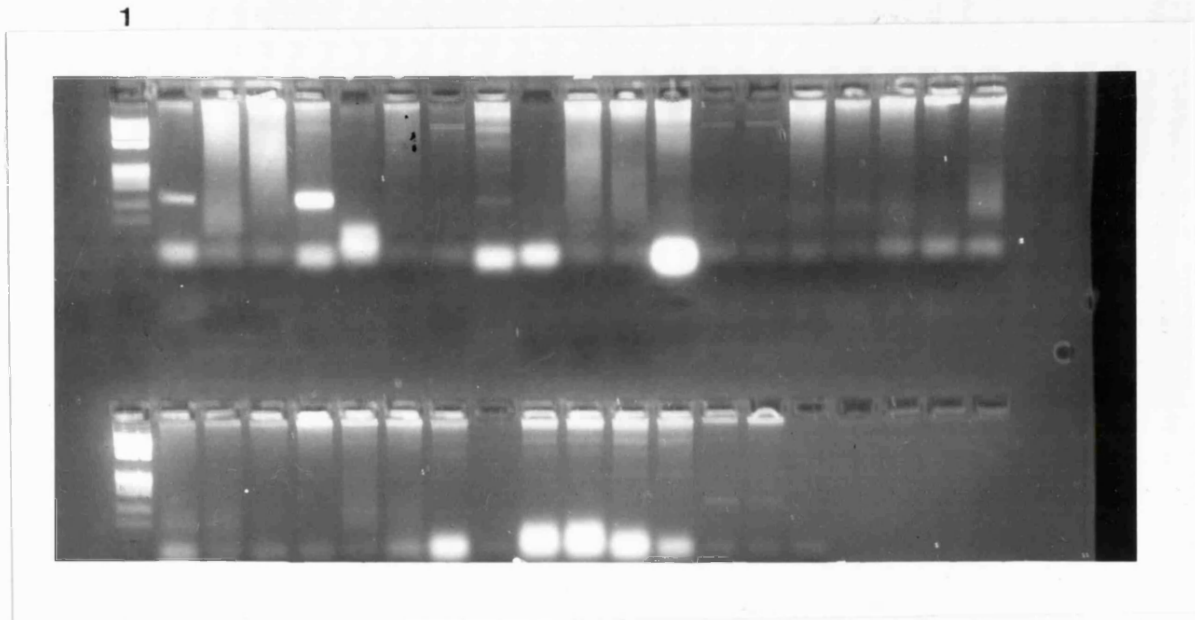
Fig 4.8a:

A photograph of an ethidium bromide stained, 3% agarose gel showing amplification of EST WI-31133 across the DHRD YAC panel. A PCR product of 135 bp is seen in lane 2 (YAC 37AE3) and lane 5 (YAC 806-C-12) (from L to R). Marker ØX174/HaeIII is present in lane 1 and 21. Lanes 34 and 35 correspond to the positive genomic controls and lane 36 corresponds to the negative control.
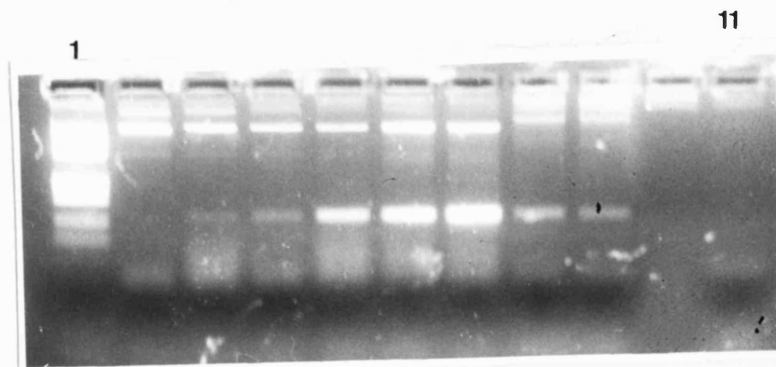
Fig. 4.8b:

A photograph of an ethidium bromide stained 3% agarose gel. A PCR product of 135 bp of EST WI-31133 is in PAC clones 301-13-L, 301-13-N, 301-13-O, 301-13-P and 301-14-O (lanes 3 to 7 from L to R). Lane 2 corresponds to PAC clone 293-14-O which does not contain this EST. Lanes 8 and 9 correspond to the positive genomic controls, and lane 11 is the negative control.

4.6   Discussion

4.6.1   Current status of the contig

The identification of a mutant gene involved in a specific human disease usually includes the establishment of a physical map of the chromosomal region where the disease initially maps to, especially when candidate genes are not obvious. This strategy was applied to the 2p16 region where DHRD had been mapped. The physical map consisted of 29 YAC clones of which 12 of them (from the ICI/ICRF library) have not been previously reported. Later, this physical map consisted of 16 PAC clones for the current refined region. The genetic interval between markers D2S2352 and D2S2251 seemed to lie on a single PAC clone (130-13-O). As previously observed from the YAC clones, marker D2S2251 is deleted in most of them, indicating that this must be a difficult region to clone. Ideally, this PAC can be sized by PFGE analysis and the integrity of its DNA should be verified by using the flanking markers as oligonucleotide probes. Alternatively, any end sequence obtained by linear extension PCR of PAC 130-13-O can be used to design primers and test the STS content of all the YACs and PACs in the region. If necessary, further PAC clones can then be isolated from the PAC library by screening the PAC pools. Currently, the DHRD interval is spanned by markers D2S2251 and D2S2352 of a genetic distance of 1 cM encompassing a tiling path of YAC clones approximating 3 Mb.

4.6.2   YAC Chimerism

YAC clones can often have chimeric inserts which means that the insert is composed of two or more fragments derived from non-contiguous regions of the genome. Chimerism can be verified by FISH analysis. Chimeric clones may result from a co-ligation of two different restriction fragments due to the co-transformation in clones with large inserts.

4.6.3   Difficulties in YAC endcloning

ALU-PCR was used to isolate ends of YAC clones. Major problems faced were that repetitive sequences were obtained from which STSs could not be designed or the

sequence yielded was too short to design STSs or that YACs of interest like 37AE3 (isolated with the former flanking marker) failed provide a unique *ALU*-PCR products.

4.6.4 YAC versus PAC data

An ideal cloning system would be one that produced clones containing a perfect representation of the genomic region that contained the disease gene. YAC clones from the DHRD region revealed that most of them were associated with the common problems encountered using them. The mega-YACs were mostly deleted or chimeric, some deletions were also observed in the YACs from ICI or ICRF libraries. Unfortunately, these YACs were the critical YACs that spanned the disease region. The HGMP Resource Centre provided PAC clones that were isolated by screening PAC libraries. PAC clones were initially chosen to reinforce the original tiling path of existing YACs in the current refinement and to aid the construction of a deeper contig of the DHRD critical region. Several PAC clones for markers D2S2352 and D2S2251 have been isolated and these clones can be used to map ESTs from the database in the process of finding the DHRD gene.

Bacterial artificial clones (BACs) and P1-derived artificial chromosomes (PACs) have been developed as alternative vectors to YACs (Shizuya *et. al*, 1992; Ioannou *et. al*, 1994). Both BAC and PAC possess features from the bacteriophage P1, which has a capacity for DNA fragments as large as 100 kb with an ability to produce a high copy number of clones with reduced Chimerism (Sternberg 1990; Pierce *et. al*, 1992). The PAC vector can have insert sizes of approximately 100-300 kb and no chimerisms or clone instabilities. These advantageous properties of PACs make them more reliable cloning vectors than YACs. 16 PACs have been isolated to consolidate the contig spanning the current DHRD interval and have been analysed by STS content mapping. Isolating PAC end sequences can further reinforce this PAC contig.

4.6.5 Isolation of novel polymorphic markers

Prior to the current refinement, cosmid clones from a chromosome 2 specific library could have been isolated by probing with non-polymorphic STSs. Alternatively, non-chimeric YACs within the critical region could have been digested and subcloned into cosmids in the effort of isolating novel $(CA)_n$ repeat sequences in STS deficient regions within the previously published DHRD region. This strategy has a dual

advantage, if the endeavour was not successful not only would it increase the STS density and facilitate the isolation of other YACs but also to obtain novel polymorphic microsatellite markers which may provide new informative cross-overs within the family, for further locus refinement.

4.6.6 Future of the DHRD contig

DNA can be easily purified from PAC clones and they can be used for molecular analysis. The next logical step is to map genes to the PAC of interest in the DHRD interval. With the current progress of the human genome sequencing project as well as due to the efforts of the rest of the human genetics community, the database is inundated with numerous uncharacterised ESTs mapping to the 2p16-21 region. Once these ESTs are mapped to the YACs and PAC of interest, they automatically become potential positional candidate genes of DHRD. Based on their expression data the partial clones of these ESTs can be sequenced and their entire transcript can be obtained from chromosome or tissue specific libraries that can then be used for mutation analysis.

In the event of the EST resource failing to identify the DHRD gene, it may be necessary to identify retinal specific transcripts or genes highly expressed in the retina. This can be executed through the application of direct selection method utilising the smaller non-chimeric YAC clones or PAC 130-13-O on a retinal cDNA library subtracted for housekeeping genes (Monaco 1994). It is not worthwhile searching for genes in a gene rich region (according to the gene map) using techniques like exon trapping (Buckler *et al.,* 1991), detection of CpG islands associated with genes (Bird, 1987), island rescue PCR (Valdes *et al.,* 1994) or other non-specific transcript isolation methods that are likely to isolate house keeping genes. Instead, selective methods like cDNA selection (Lovett *et. al.,* 1991; Parimoo *et. al.,* 1991) or direct selection on a retinal cDNA library are more likely to result in a good candidate gene for DHRD.

CHAPTER 5

Analysis of a candidate gene:
WI-31133

5.1   Introduction

Analysing candidate genes, located within a genetically defined interval for an inherited disease is described as a **positional candidate** approach. Unlike positional cloning, this method does not involve the laborious task of isolating new genes but involves a survey of the disease interval to find the most suitable candidate gene for the disease. The screening of such a candidate could either lead to the identification of a disease causing mutation or its exclusion from disease causation. The positional candidate gene approach has been successfully used to identify many disease genes, particularly for the discovery of retinal genes such as rhodopsin and peripherin. With the increasingly dense, high-resolution human transcript map, the positional candidate gene approach will soon become the predominant method of disease gene discovery.

5.2   Positional candidates for DHRD

Previously two known diseases (namely Malattia leventinese and Carney complex (CNC)) had been mapped to the 2p21-2p16 locus. As discussed earlier (see chapter 3), Malattia leventinese has been of particular interest due to phenotypic similarity to DHRD, thus sharing the same genetic interval lead to the hypothesis that the two diseases could be allelic. CNC has recently been genetically refined between markers D2S378 and CA-2 (Taymans *et. al.*, 1999). Initially a non-erythroid form of beta-spectrin known as fodrin (*SPTBN1*) and Calmodulin-2 (*CALM2*) were candidates with the previous localisation of DHRD (D2S2316 and D2S378). Following partial refinement (D2S2739 and D2S378), these genes still mapped within the 'critical' interval. Subsequently, these genes were excluded through further genetic refinement (D2S2352 and D2S2251), refining DHRD to a 1 cM genetic interval (Kermani *et al.*, 1999).

5.2.1 *SPTBN1*, *CALM2* and ESTs in the DHRD region

Screening a DNA library with a synthetic oligonucleotide probe corresponding to human erythroid beta-spectrin, a genomic clone for nonerythroid beta-spectrin (*SPTBN1*, β-fodrin) was obtained (Watkins *et al.*, 1988). The erythrocytic form of β-spectrin had previously been mapped to human chromosome 14. *SPTBN1* was mapped by hybridisation to DNA of a panel of somatic hybrid cell lines and later localised to human chromosome 2p21 by isotopic *in situ* hybridisation. Genomic organisation of *SPTBN1* contains regions that show a high degree of identity, a similar intron/exon organisation and 76% homology to erythroid β-spectrin (Chang *et al.*, 1993). The genomic clone of *SPTBN1* was utilised in mapping the gene to human chromosome 2 using somatic cell hybrids. Studies demonstrate (Nelson and Veshnock, 1990) a high affinity interaction between Na, K-ATPase and ankyrin, which is linked to fodrin. Gunderson and his group (1991) demonstrated that Na, K-ATPase, ankyrin and fodrin form an entire membrane-cytoskeleton complex along the apical surface of RPE cells of rat. As pathological processes induce a breakdown of junctional complexes (between cell-cell contacts), the Na, K-ATPase activity becomes redistributed from the apical surface to lateral and basal regions of RPE cells.

Calmodulin (CaM) is a highly conserved ubiquitous Ca^{2+} binding protein which is involved in regulation of several Ca^{2+}-dependant processes (Klee *et al.* 1982, Wylie Vanaman 1988). The CaM protein (Nojima *et al.*, 1989, Koller *et al.* 1989) gene family consists of three bona fide members (*CALM1*, *CALM2* and *CALM3*). The high degree of conservation between the *CALM* genes indicates their close ancestral relationship. Human *CALM1* and *CALM3* genes have been assigned to chromosomes 14 and 19, respectively (McPherson *et al.* 1991). The gene of interest to this study was *CALM2* that was mapped by *in situ* hybridisation to chromosome 2 region 2p21.1-21.3 (Berchtold *et al* 1993). Incidentally, Calmodulin is found in abundance in the central nervous system, including the retina of six vertebrate species (Pochet *et al.* 1991). As described in section 1.8.6, Ca^{2+} binding proteins are involved in the phototransduction pathway, thus studies indicated *CALM2* as a plausible candidate for the DHRD gene.

SPTBN1 and *CALM2* have been shown to be expressed in the RPE and localise to human chromosome 2p21. Following the initial linkage assignment of DHRD, these genes were considered valid candidates for the disease.

In addition to these genes, there were 44 ESTs (between D2S2352 and D2S2251) whose STSs existed as cDNA markers on the database (**http://www.ncbi.nlm.nih.gov/cgi-bin/SCIENCE98/**). Towards the end of chapter 4, some of these ESTs (see table 4.8) have been mapped into the DHRD contig in the hope of finding the DHRD gene. The preceding sections will deal with the potential candidate gene exclusion and inclusion of those ESTs as a candidate for the DHRD gene.

5.3 Aim of study

The analysis of a candidate gene (in the 'critical' region) was to be performed prior to mutation analysis in the DHRD family.

5.4 Methods and materials

For general preparation of RNA work see section 2.10

5.4.1 RNA extraction from tissues

Total RNA was extracted from human tissues to create a tissue expression profile for subsequent gene expression studies and for size verification of mRNA by Northern blot analysis. Reagent RNAzol^{TM} B (Biognesis, U.K.) promotes the formation of complexes of RNA with guanidinium and water molecules and abolishes hydrophilic interactions of DNA and proteins which can be removed from the aqueous phase while RNA remains. A volume of 2 ml of RNAzol^{TM} / 100 mg of tissue was required for the homogenisation step. (Note:-All tissues were homogenised on ice in separate glass homogenisers). Tissue samples frozen at −80 °C were promptly weighed prior to flash freezing them in liquid nitrogen. Frozen tissue samples were wrapped in foil prior to placing between tissue papers and shattered with the aid of a mallet. Calculated amount of RNAzol^{TM} was added to the tissue and homogenised with a few strokes of the glass rod of the homogeniser. For minimum degradation the protocol required tissue homogenisation to be less than 20 min. A 1/10th volume of chloroform was added to the homogenate and shaken vigorously for 15 seconds prior to being placed on ice for 5 min.

The suspension was centrifuged for 15 min at 12, 000 g (4 ° C). The homogenate formed two phases: a lower blue phenol-chloroform phase and a colourless upper aqueous phase. The DNA and proteins were contained in the interphase and organic phase. A volume of the aqueous phase is approximately 50 % of the initial volume of RNAzol^{TM} plus a volume of the tissue used for the homogenisation. RNA was precipitated by transferring the aqueous phase to a fresh Eppendorf tube prior to adding an equal volume of isopropanol and stored for 15 min at 4 °C. Samples were centrifuged for 15 min at 12 000 g (4 °C). The supernatant was removed and the pellet was washed with 75 % ethanol (~0.8 ml) by vortexing and subsequent centrifugation for 8 min at 7500 g (4 °C). The pellet was briefly (~10-15 min) dried under vacuum ensuring that it was not overdried to facilitate solubility in DEPC water.

5.4.2 Quantifying yields of RNA

An UV mass spectrophotometer was used to quantify yields of RNA obtained from different tissues. Samples were analysed by diluting 2 µl of the RNA sample in 500 µl of DEPC water (a dilution factor of X 250). These solutions were analysed by the UV mass spectrophotometer (initially DEPC treated water was used as a blank, optical density (OD$_{260}$) would equal ~0.00). Absorbance (A) readings at OD$_{260}$ and OD$_{280}$ were taken for tissue samples. A solution for which OD$_{260}$ = 1, contains approximately 40 µg of RNA per ml. The amount of RNA was calculated using the formula: **the dilution factor X 40 X OD$_{260}$** providing the yield in µg/ml.

5.4.3 Preparation for a Northern blot

100 ml of 1 % agarose gel (Biorad, U.K.) was prepared (85 ml DEPC water and 10 ml of 10 X MOPS buffer). 5 ml of formaldehyde was added to the cooled gel in a fumehood (to prevent inhalation of toxic fumes) and left to polymerise. 15-20 µg of RNA from each tissue was used for Northern blot analysis. 5 µl of sterile loading buffer (0.75 ml formamide, 0.24 ml formaldehyde, 0.1 ml DEPC water, 0.1 ml glycerol, 0.08 ml of 10 % bromophenol blue, 0.15 ml of 10 X MOPS) and ethidium bromide to a final concentration of 0.5 µg/ ml was added to the RNA samples prior to loading the gel for electrophoresis. Greater concentrations than 0.5 µg/ ml of ethidium bromide prevent

maximum RNA transfer to the membrane. A stock of 10 X MOPS buffer [0.2 M MOPS (3-(N-morpholino) propanesulfonic acid), 50 mM of sodium acetate, 10 mM EDTA in 800 ml DEPC treated water]. The pH of the buffer was adjusted to 7.0 with concentrated NaOH solution. The total volume of the 10 X stock buffer was made up to 1 litre and filter sterilised through a 0.2-micron Millipore filter prior to storing at room temperature following protection from light (by wrapping foil around the bottle). A buffer concentration of 1 X was used for routine gel electrophoresis. Gel was subjected to electrophoresis at 85 volts for 3 h before visualising by UV light.

5.4.4 Northern blot analysis

Formaldehyde gels were washed several times in DEPC water for 10 min to remove formaldehyde in the gel prior to RNA transfer to a nylon membrane. The RNA transfer was allowed to occur overnight in 20 X SSC buffer as the procedure outlined in section 2.6.1. The following day the filter was washed in 2 X SSC buffer prior to baking the filter for 2 h at 80 °C. The filters were hybridised in hybrisidation solution and probed with a 1.3 kb PCR product (using primers SK2F and SK5R). For hybridisation of Northern blots see section 2.10.1

5.4.5 First-strand cDNA synthesis

A 3' RACE (Rapid amplification of cDNA ends) kit (Boehringer Mannheim, UK) was used for the purpose of synthesising first-strand cDNA. The starting material required for this process was total RNA (or poly $(A)^+$ can be used to reduce background or to enrich very rare messages). For a control reaction, control RNA and a neo 1/rev primer has been supplied. The cDNA synthesis buffer (5X concentration) contains 100 μl of 250 mM Tris-HCl, 40 mM $MgCl_2$, 150 mM KCl, 5 mM dithiotreitol and pH adjusted to 8.5. The deoxynucleotide mixture contains 50 μl of dATP, dCTP, dGTP, dTTP, 10 mM each, in tris-HCl and pH adjusted to 7.5. The following were assayed in a sterile microcentrifuge tube on ice in a reaction volume of 20 μl:

component	Amount (μl)
cDNA synthesis buffer	4
deoxynucleotide mixture	2

cDNA synthesis primer SP1 (12.5 µM)   1

Total RNA   0.2-2 µg

AMV reverse transcriptase   1

Redistilled water to make upto the final volume of 20 µl

The above reaction was mixed on ice and briefly spun prior to incubation at 55 °C for an hour. In addition the mixture was incubated at 65 °C for 10 min. For PCR amplification, 1 µl was utilised.

5.5   Results

5.5.1   Exclusion of genes

In order to find the DHRD gene, ESTs and genes that mapped within the initial DHRD genetic interval (D2S2316 and D2S378) were all potential candidates for the DHRD gene. STS content mapping of all the YACs with an STS for the *CALM2* gene revealed that this gene was absent from the YAC clones in the DHRD physical map. Thus as previously designated (by *in situ* hybridisation), *CALM2* is most probably localised to the 2p21 region but lies telomeric to the DHRD physical map.

STS content mapping of the YAC clones in the DHRD critical region revealed that *SPTBN1* mapped within the previously refined region, between marker D2S2739 and D2S378. Partial characterisation of this gene had been reported by Chang and his group (1993) who showed its high similarity with the beta spectrin gene (Hu *et al.*, 1992). The partial clone of the *SPTBN1* gene contained sequence for exons 9-14. These published exons were preliminarily screened for mutations in the DHRD family. Two affected individuals and two unaffected individuals from the DHRD family were PCR amplified for exons 9-14 (see table 5.1). Mutation screening of *SPTBN1* was performed by direct sequencing of PCR products and heteroduplex analysis. Neither single base pair mutations nor any polymorphisms existed that were associated with the DHRD phenotype for this portion of the *SPTBN1* gene.

Significant similarity existed between the erythroid and non-erythroid forms of β-Spectrin which has been shown by Chang and his group (1993). For exons 9-14, a 3 bp difference existed between the two forms (Hu et al., 1992). Thus, it was proposed that *SPTBN1* could also contain the remaining 26 exons as that of the erythroid form. Amin

168

and his group (1993) have performed complete genomic characterisation of this form. An STS of exon 14 was PCR amplified with the DNA of YAC 758-E-5 in the hope of retrieving genomic clones containing the remainder of the *SPTBN1* gene. The resulting PCR product (871 bp) was used to hybridise to a chromosome 2 specific library. YAC 758-E-5 (was one of the few YAC clones that contained this gene) had previously been tested positive for *SPTBN1* exons 9-14 placing the gene within the initial DHRD interval (D2S2316 and D2S378).

A chromosome 2 specific library constructed at Lawrence Livermore National Laboratories Genome Centre was obtained from the HGMP Resource Centre (Cambridge, Hinxton, UK). This library consisted of 6 different gridded filters composed of cosmid, fosmid and PAC clones. Hybridisation results provided 22 clones of which 11 were cosmids, 8 were fosmids and 3 were PAC clones (see table 5.2). Fig. 5.1 shows hybridisation result of the cosmid filter (AE1) with PCR product of exon 14. The resulting clones were obtained from HGMP resource centre (Hinxton, Cambridge, UK). Characterisation for the presence of *SPTBN1* exons was the ensuing step. However, this work was made redundant due to the current genetic refinement (Kermani *et al.*, 1999) of DHRD that excluded *SPTBN1* from the latest 'critical' region (D2S2352 and D2S2251). Similarly, ESTs D2S1848 and D2S1981 were also genetically excluded from the current DHRD region.

Following the subsequent genetic exclusion of genes/ESTs from the refined genetic region, the pursuing approach in the search for the DHRD gene, was mapping of various transcripts from the database. The Science map of 1996 (Schuler *et al.*, 1996) had placed 44 ESTs within the DHRD region. Some of these ESTs were tested within the YAC contig by PCR. ESTs that were retinally expressed were then characterised and screened for mutations.

Exon	Primers	PCR product (bp)	T_m (°C)
9	F-ttgttgccaggtgcttgac R-accacccaagtaagatgca	188	47
10	F-ctgtgtttagatttactga R-atcaacaaggtaaagtgga	118	47
11	F-atttttgtaggcctgggaa R-gtgtctcaggttctcctct	159	47
12	F-ttctctgtaggacaacttt R-gaaatgaaggtaaaacctt	303	47
13	F-ttgtgcacaggtgctagta R-acggggaaggtaaggatgg	154	55
14	F-tgttaaacaggttacaagc R-ccagcacaggtgagcgggg	871	55

Table 5.1:

Working conditions of *SPTBN1* primers (exons 9-14*)*
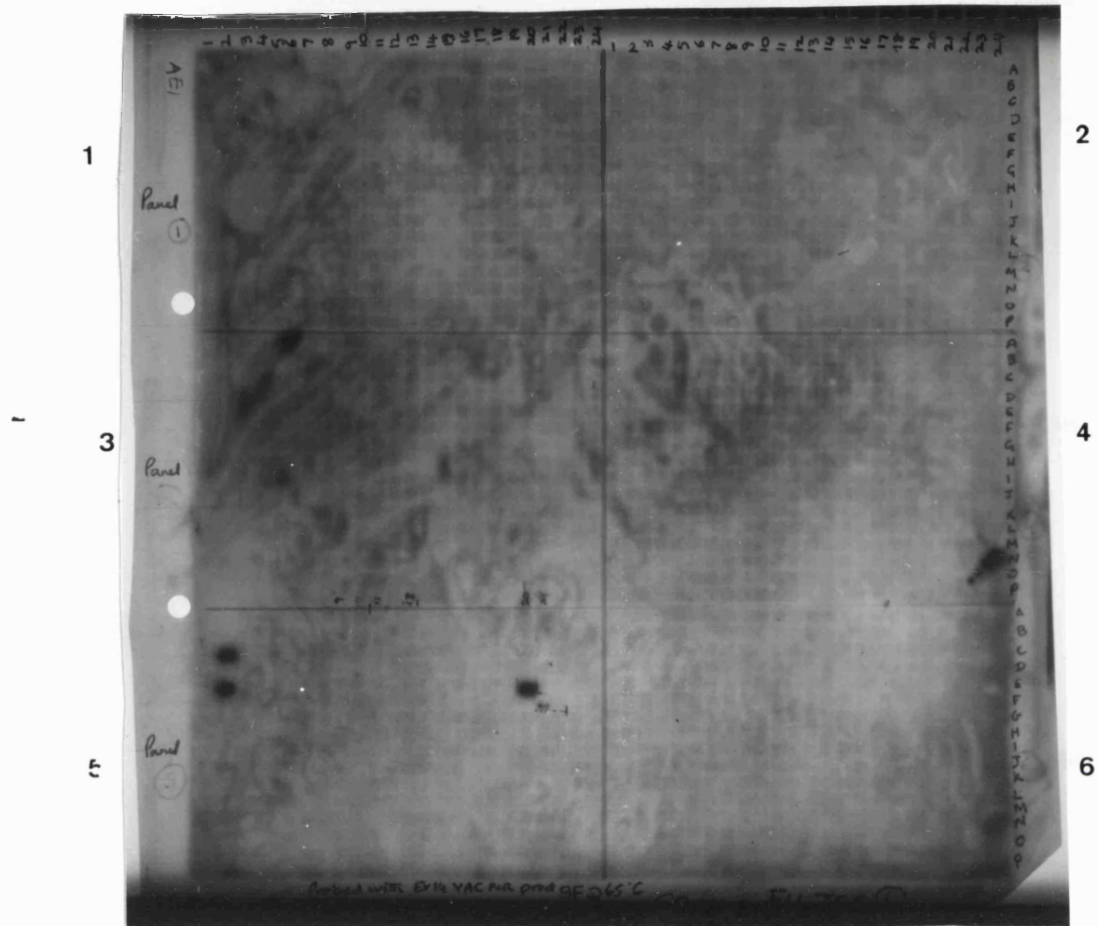
Fig. 5.1:

An autoradiograph of filter AE1 (one of the chromosome 2 genomic filter) hybridised with a PCR product of exon 14 of *SPTBN1* displaying some of the genomic clones in Panel 3, 4 and 5. The first nine clones in table 5.2 correspond to these clones.

Clone ID	HGMP ID
AE1,22-A	86-A3
AE1,33-E20	130-C10
AE1,33-F21	131-C11
AE1,33-C2	130-B1
AE1,33-E2	130-C1
AE1,33-C3	129-B2
AE1,33-E3	129-C2
AE1,30-O22	118-H11
AE1,30-N23	119-G12
AE2, 39-O7	153-H4
AE2, 46-N10	184-G5
AG1,20-I6	78-E3
AG1,33-L4	132-F2
AG1,42-L4	168-F2
AG1,43-5G	169-D3
AG2,8-F7	31-C4
AG2,8-J7	31-E4
AG2,17-N14	68-G7
AG2,14-I18	54-E9
AI,2-J4	8-E2
AI,2-J8	8-E4
AI,2-N12	8-G6

Table 5.2:

Various clones isolated from the hybridisation result of chromosome 2 specific library with exon 14 of *SPTBN1*. AE1, AE2 and AE3 consisted of cosmid clones, AG1 and AG2 consisted of fosmid clones and AI consisted of PAC clones.

5.5.2 Mapping of EST WI-31133 to the current critical region

PCR amplification of an STS (GenBank accession number:G22580) across the DHRD YAC panel, placed this EST within two YAC clones (37AE3 and 806-C-12) and six PAC clones (293-14-O, 301-13-L, 301-13-N, 301-13-O, 301-13-P and 301-14-O) as shown in fig. 4.8a and 4.8b. Mapping information on this EST and clone availability is provided by the Unigene database (http://www.ncbi.nlm.nih.gov/UniGene/) suggesting that this EST mapped between markers D2S123 and D2S378, near marker D2S350. This EST originated from the retina of a 55 year old, Caucasian human male. Three overlapping cDNA clones existed (see table 5.3). Information from the Unigene database suggested that this particular gene mapped to chromosome 2 (elucidated by the radiation hybrid mapping panel data.) Mapping data of this EST was further reinforced by FISH analysis of the three cDNA clones (222124, 363848, 363252) and the PAC clone 130-13-O. Results indicated that this gene mapped to the 2p16 region. Previously this technique had been used to verify chimaerism of YAC clones (see chapter 4). Clones 222124 and 363848 had both 3' and 5' end sequences available on the database but clone 363252 only had 3' sequence available. Following this data, all three clones were obtained for sequence analysis and genomic characterisation (see fig. 4.8).

Partial sequence from the 3' and 5' end of the gene was present for the three clones (see table 5.3) As the cDNA clone 222124 was the largest and contained the STS used to map within the contig, it was chosen for subsequent sequence analysis. Database information revealed that the cDNA had been cloned in a pt7T3D (Pharmacia, UK) vector (with a modified polylinker) between EcoR1 and Not1 sites. The first strand cDNA was primed with Not1-oligo(dT) primer (5'-TGTTACCAATCTGAAGTGGGAGCGGCCGCGCTTTTTTTTTTTTTTTTTT 3'), double strand cDNA was selected, ligated to EcoR1 adapters (Pharmacia, UK), digested with Not1 and cloned onto the Not1 and EcoR1 sites of the modified pT7T3 vector (Pharmacia, UK). The retinas were obtained and total cellular poly(A)+ RNA was extracted 6 hours after removal. The vector arms harboured the M13 annealing sites, thus forward and reverse primers were used in the sequence analysis to determine the authenticity of the clones. The initial sequence obtained with these primers was verified

with that present on the database and subsequent task involved designing primers bidirectionally to sequence the entire cDNA insert.

GenBank Acc. No.	IMAGE id	5' or 3' read	Clone size (kb)
H85783	222124	5'	2.5
H84878	222124	3'	2.5
AA021025	363848	5'	2.2
AA020972	363848	3'	2.2
AA0191917	363252	3'	-

Table 5.3:

Various cDNA clones of WI-31133 present on the database.

5.5.3 Expression information on EST WI-31133

Total RNA from post mortem whole human retina and RPE was prepared using an RNA extraction kit (see section 5.4.1). Fig. 5.2 shows a picture of the quality of RNA yield from the total RNA preparations of human retina and RPE. This gel was eventually blotted for Northern blot analysis and hybridised with a 1.3 kb PCR product of the EST clone (222124). Unfortunately, a signal was not observed on this blot. On the contrary, a commercially available (CLONTECH, UK) Northern blot (containing poly A^+ RNA of all parts of the human brain) was hybridised with the same probe and a 7 kb transcript was observed (see fig. 5.2b).

In order to test the expression of this gene in retina, first strand cDNA was synthesised from RNA of retina and RPE using a 3' RACE kit (see section 5.4.5). PCR amplification of this EST on the cDNA of retina and RPE revealed expression in the retina and in the RPE (see fig. 5.3). In order to assess the exact tissue location of

Ribosomal

units

28 S

18 S
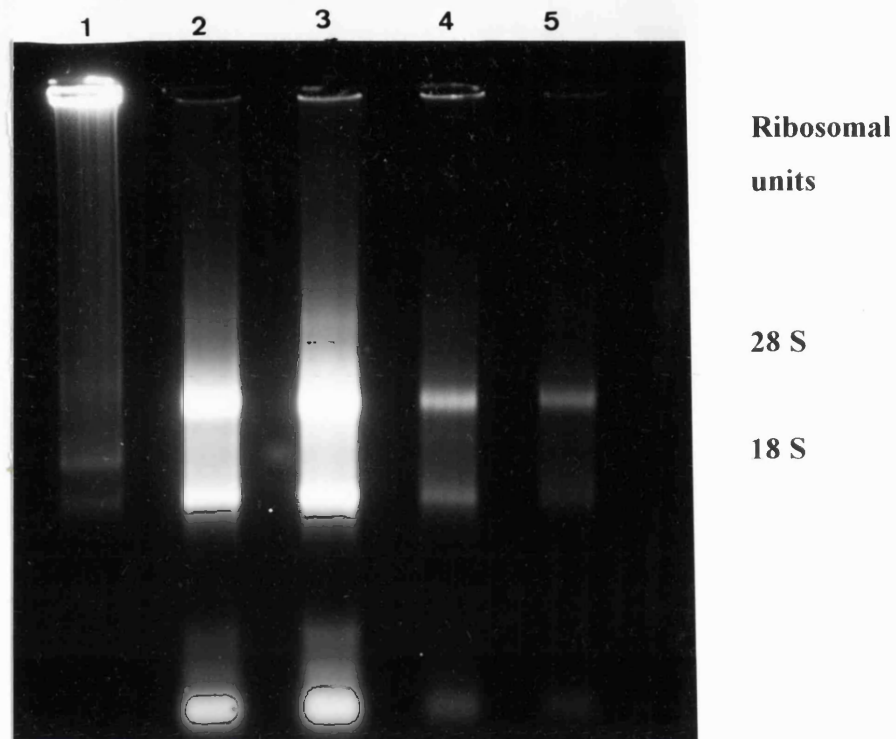
Fig. 5.2a:

A 1% agarose gel with formamide showing the quality of total RNA yielded from human retina (lanes 2 and 3) and RPE (lanes 4 and 5). A commercially available RNA ladder is present in lane 1.
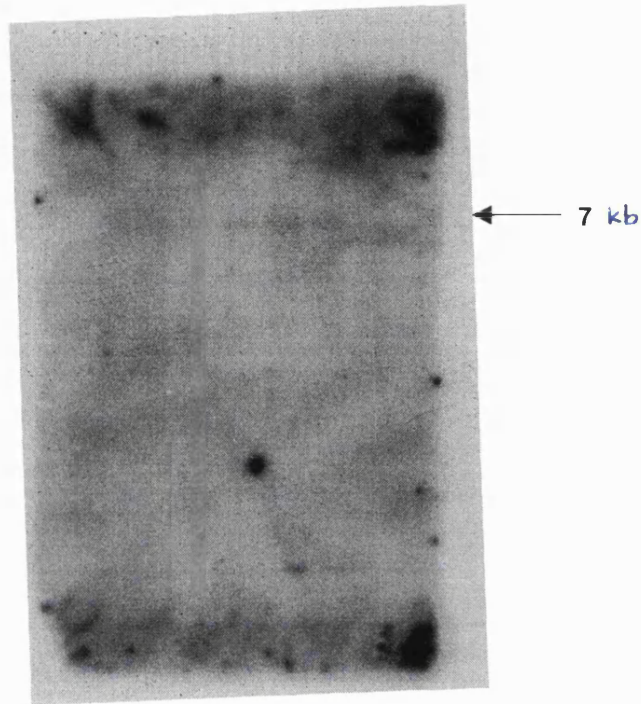
Fig. 5.2b:

Hybridisation result of a commercially available Northern blot of human brain (CLONTECH, UK). Lanes 1-7 correspond to amygdala, caudate nucleus, corpus callosum, hippocampus, whole brain, substantia nigra and thalamus respectively. A 7 kb transcript (depicted by the black arrow) is observed in lanes 1-6, with highest expression in the 5th lane (whole brain). The pen marks on the left-hand side of the autorad indicate the size markers (from top to bottom, 9.5 kb, 7.5kb, 4.4 kb, 2.4 kb and 1.35kb).

| Marker | 2 | 3 | 4 | 5 | 6 | 7 | 8 |
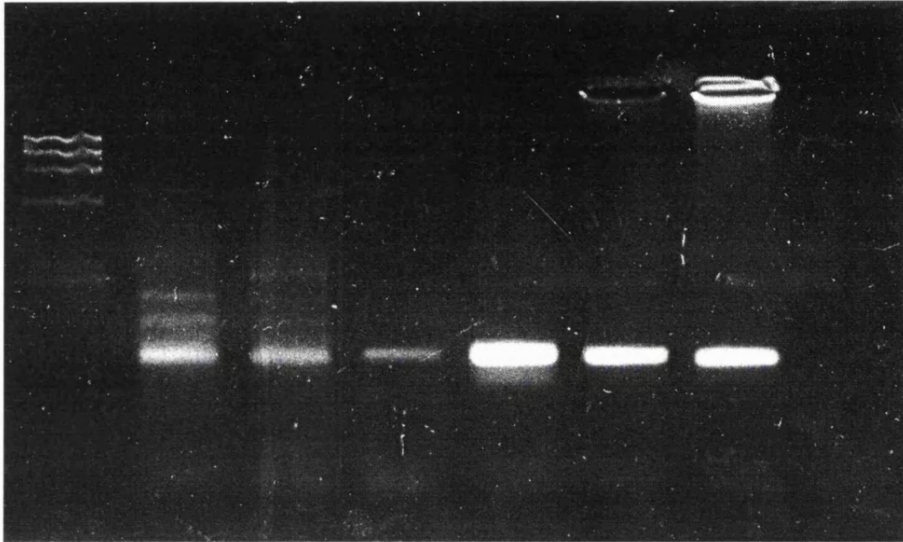
Fig. 5.3:

A photograph of a 3% agarose gel depicting the presence of WI-31133 in human retinal cDNA (lane 2), human RPE cDNA (lane 3), PAC 301-13-O (lane 4), cDNA clone 222124 (lane 5), genomic control 1 (lane 6), genomic control 2 (lane 7) and negative control (lane 8). Lane 1 corresponds to ØX174/HaeIII marker. The size of the PCR product is approximately 135 bp using the original STS of the gene (GenBank number: G22580).

this gene in the retina, *in situ* hybridisations of human eye sections should be performed.

5.5.4 Genomic organisation of the WI-31133 gene

Primarily, M13 forward and reverse primers were used to sequence either ends of clone 222124. The sequence obtained was verified with that present on the database and the first bp of the cDNA sequence corresponds to that of the cDNA insert in the clone and must not be mistaken as the first bp of the genomic sequence of the gene. Primers were designed in bidirectionally to obtain further sequence of the insert (see fig. 5.4 and table 5.4). Incidentally, these primers were later used for mutation analysis in the DHRD family. Direct sequence analysis of the clone revealed a 2054 bp insert with a 1623 bp open reading frame (ORF) (see fig. 5.4). The initiation /start (ATG) codon is present at 211 bp. The ORF finder at the NCBI database (http://www.ncbi.nlm.nih.gov/gorf/gorf.html) predicted this. Apart from the ORF prediction program there were no other sequence motifs that lead to the conviction of this ATG being the plausible start site.

The entire nucleotide sequence was analysed by the NIX program at the HGMP database. Scrutiny of the nucleotide sequence revealed that a splice site motif (AG-exon-GC) were present in the 5' sequence of the cDNA clone at 101 bp (Breathnach *et al.*, 1978). Such sequences were verified while mutation screening the DHRD individuals and PAC 130-13-O (CGAATTCCTTTCTGTTTCTACATTAATCCCTTTCTGTTTCTGGGTGTGCATTTT TGTGTGTAG). The 5' UTR that is present in this sequence is incomplete and PAC 130-13-O can be used to obtain the remainder of this gene which can be screened for further mutation analysis in the DHRD family.

5.5.5 Putative protein prediction

PCR reactions (whose primers were designed from cDNA) amplified from genomic DNA showed that the gene really must have only one exon (in the coding region, at least). Although this is unusual yet not completely unlikely. If this gene had one or more introns (found commonly with vertebrate genes) then one or more of the PCR products would have been either larger than expected or absent (where the intron

would have been too large to amplify, or the primer itself spanned an intron). An alternate possibility might be that by chance cDNA was amplified in the genomic PCR reactions, but negative controls were found to be clean (see Fig. 5.4a).

Analysis of the cDNA sequence by the NIX program at HGMP database revealed the longest ORF from 211 bp to 1833bp predicting a single exon of 540 amino acids with a molecular weight of 59.4 kDa. The intended ATG start codon is present although in a weak context; AAAatgA as opposed to RNNatgG (Kozak *et al.*, 1996). It must be noted that by analysing cDNA sequence with NIX the result will usually come up with a single exon because the continuity of the ORF will heavily bias the algorithm. Thus without obtaining genomic sequence (GenBank AF101472 (Tartellin *et al.*, 1999) from the database, which has been deposited in the last few months) or by sequencing PAC 130-13-O (which also contains this gene) and then comparing it with the cDNA (routinely running NIX on it), the exact exon/intron structure cannot be established. At the time of writing this thesis, the gene structure was not known.

From the difference in size between the result of the Northern and from that of the cDNA clone, one would expect most of the 3' UTR to be where most of the uncomplete sequence lies (as 3' UTRs are often several kbs while 5' UTRs are much smaller). Amino acid sequence analysis (http://www.ncbi.nlm.nih.gov/gci-bin/BLAST/) revealed 38 % homology to a NPY Y1 receptor gene product *C. elegans* (Genbank accession number:U41028) and 31% homology to dopaminergic receptor D3 of *Rattus norvegicus* (Genbank accession number:AF031522). A prediction program (http://www.expasy.ch/cgi-bin/get-produc-entry?PDOC00210) used to predict the secondary structure of the protein revealed that these receptors all have the seven-hydrophobic regions, each of which spans the membrane. The N-terminus is located in the extracellular side of the membrane and is often glycosylated. Three extracellular loops alternate with three intracellular loops to link the seven transmembrane regions. Most of these receptors lack a signal peptide. The conserved part of these proteins are transmembrane regions and the first two cytoplasmic loops (Attwood *et al.*, 1991). A conserved acidic–Arg-aromatic triplet is present in the N-terminal extremity of the second cytoplasmic loop and could be implicated the interaction with G proteins. A majority of receptors belong to this class of proteins. Thus it could be hypothesised that a

179

mutation in this gene (similar in structure to rhodopsin) may be the underlying cause of DHRD.

5.5.6 Mutation analysis in DHRD families

The full length coding sequence of EST WI-31133 was screened for mutations in the DHRD family (see Fig. 5.7 a,b,c,d) and the two dominant families that mapped to the locus. Mutational analysis was carried out by sequencing PCR products (see Fig. 5.4a) with the different overlapping fragments of the single exon (see table 5.5). Sequence analysis was performed using the ABI sequencer. Neither single base pair mutations nor polymorphisms were observed in any of the individuals. Thus this gene was potentially excluded (for the coding regions) as the disease-causing gene for DHRD. For complete exclusion, it is of importance to characterise the 5' UTR region and eventually screen for mutations in the DHRD family.

Primer name	Primer sequence (5'-3')	Tm (°C)
ER	CATTTTCGGAGAGAAATGTCTC	62
SK1F	GGTCATCTTCTTGCCTGGG	60
SKR	CCCAGGCAAGAAGATGACC	60
SK2F	GCACCGGCTCCGGATGGTG	66
SK2R	CACCATCCGGAGCCGGTGC	66
SK3F	CAGACCACAGCCTTTCATGG	62
SK3R	CCATGAAAGGCTGTGGTCTG	62
SK4F	CCTGGTGTGCTGTCTTCC	58
SK4AR	GGAAGACAGCACACCAGG	58
SK5F	AGGGAACCTCGAAGTCAACAG	64
SK5AR	CTGTTGACTTCGAGGTTCCCT	64
SK5R	CAGGGTAAAAAATCTAAAACTTTC	72
SK6F	GCTATAGGATCTTATGTAAACAG	62

Table 5.4:

Primers (and their relative Tm values) designed across cDNA clone 222124 for sequence analysis that were eventually used for mutation analysis.

Fragment number	Primer combination	Fragment size (bp)	Annealing temperatures (°C)
1	SF+ER	278	55
2	SK1F+SK2R	292	55
3	SK2F+SK3R	387	55
4	SK3F+SK4AR	267	55
5	SK4F+SK5AR	267	55
6	SK5F+SK6R	421	55
7	SK6F+SK5R	211	55

Table 5.5:

Fragments of the single exon used for mutation analysis in the DHRD family. This table correlates to Fig. 5.6.
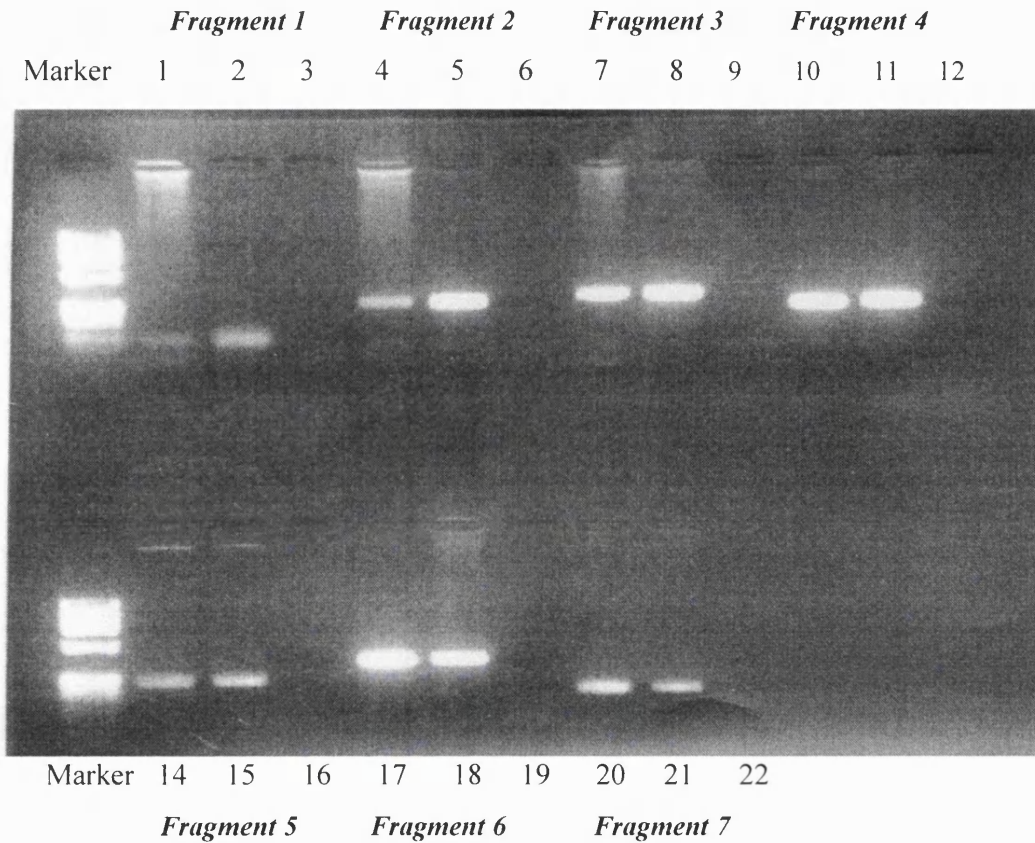
Fig. 5.4a:

A photograph of a 2% agarose gel depicting the seven fragments of WI-31133. Lanes 1,4,7,10,14,17,20 correspond to in human DNA, lanes 2,5,8,11,15,18,21 correspond to cDNA clone 222124 and lanes 3,6,9,12,16,19,22 correspond to negative control. Lane 1 and 13 corresponds to ØX174/HaeIII marker. The sizes of the PCR products can be verified with table 5.5.

GCGATGGCGA	TGATGCCTCT	AGTCCTGCAT	CATCCAGAGC	GGCAGGCGAG	50
CTGGGGTCCG	GACTGCGAGA	TGGAGGAGGG	GCGCGCTGCG	GCACCCGGCA	100
GGCTTATCTG	TCTTGGGCCT	CTTTTGTCAC	ATATTGCTCA	TCTGTGAGCT	150
GAGGCCCTGA	CTCACTGAGT	ATTTTTGGGG	AGCAGAAGAA	GGAGACATTT	200
CTCTCCGAAA	*AT*GAACTCAA	CAGGCCACCT	TCAGGATGCC	CCCAATGCCA	250
CCTCGCTCCA	TGTGCCTCAC	TCACAGGAAG	GAAACAGCAC	CTCTCTCCAG	300
GAGGGTCTTC	AGGATCTCAT	CCACACAGCC	ACCTTGGTGA	CCTGTACTTT	350
TCTACTGGCG	GTCATCTTCT	GCCTGGGTTC	CTATGGCAAC	TTCATTGTCT	400
TCTTGTCCTT	CTTCGATCCA	GCCTTCAGGA	AATTCAGAAC	CAACTTTGAT	450
TTCATGATCC	TGAACCTGTC	CTTCTGTGAC	CTCTTCATTT	GTGGAGTGAC	500
AGCCCCCATG	TTCACCTTTG	TGTTATTCTT	CAGCTCAGCC	AGTAGTATCC	550
CGGATGCTTT	CTGCTTCACT	TTCCATCTCA	CCAGTTCAGG	CTTCATCATC	600
ATGTCTCTGA	AGACAGTGGC	AGTGATCGCC	CTGCACCGGC	TCCGGATGGT	650
GTTGGGGAAA	CAGCCTAATC	GCACGGCCTC	CTTTCCCTGC	ACCGTACTCC	700
TCACCCTGCT	TCTCTGGGCC	ACCAGTTTCA	CCCTTGCCAC	CTTGGCTACC	750
TTGAAAACCA	GCAAGTCCCA	CCTCTGTCTT	CCCATGTCCA	GTCTGATTGC	800
TGGAAAAGGG	AAAGCCATTT	TGTCTCTCTA	TGTGGTCGAC	TTCACCTTCT	850
GTGTTGCTGT	GGTCTCTGTC	TCTTACATCA	TGATTGCTCA	GACCCTGCGG	900
AAGAACGCTC	AAGTCAGAAA	GTGCCCCCCT	GTAATCACAG	TCGATGCTTC	950
CAGACCACAG	CCTTTCATGG	GGGTCCCTGT	GCAGGGAGGT	GGAGATCCCA	1000
TCCAGTGTGC	CATGCCGGCT	CTGTATAGGA	ACCAGAATTA	CAACAAACTG	1050
CAGCACGTTC	AGACCCGTGG	ATATACCAAG	AGTCCCAACC	AACTGGTCAC	1100
CCCTGCAGCA	AGCCGACTCC	AGCTCGTATC	AGCCATCAAC	CTCTCCACTG	1150
CCAAGGATTC	CAAAGCCGTG	GTCACCTGTG	TGATCATTGT	GCTGTCAGTC	1200
CTGGTGTGCT	GTCTTCCACT	GGGGATTTCC	TTGGTACAGG	TGGTTCTCTC	1250
CAGCAATGGG	AGCTTCATTC	TTTACCAGTT	TGAATTGTTT	GGATTTACTC	1300
TTATATTTTT	CAAGTCAGGA	TTAAACCCTT	TTATATATTC	TCGGAACAGT	1350
GCAGGGCTGA	GAAGGAAAGT	GCTCTGGTGC	CTCCAATACA	TAGGCCTGGG	1400
TTTTTTCTGC	TGCAAACAAA	AGACTCGACT	TCGAGCCATG	GGAAAAGGGA	1450
A CCTCGAAGT	CAACAGAAAC	AAATCCTCCC	ATCATGAAAC	AAACTCTGCC	1500

184

TACATGTTAT	CTCCAAAGCC	ACAGAAGAAA	TTTGTGGACC	AGGCTTGTGG	1550
CCCAAGTCAT	TCAAAAGAAA	GTATGGTGAG	TCCCAAGATC	TCTGCTGGAC	1600
ATCAACACTG	TGGTCAGAGC	AGCTCGACCC	CCATCAACAC	TCGGATTGAA	1650
CCTTACTACA	GCATCTATAA	CAGCAGCCCT	TCCCAGGAGG	AGAGCAGCCC	1700
ATGTAACTTA	CAGCCAGTAA	ACTCTTTTGG	ATTTGCCAAT	TCATATATTG	1750
C CATGCATTA	TCACACCACT	AATGACTTAG	TGCAGGAATA	TGACAGCACT	1800
TCAGCCAAGC	AGATTCCAGT	CCCCTCCGTT	TAAAGTCATG	GAGGCTATAG	1850
GATCTTATGT	AAACAGTTTT	TGTTTCTGAT	AGTAATGGAC	TTTATTCTAA	1900
CTTGAGATCA	GTGGCGGATC	AAAACCTACA	AGATTCAACT	GAAAAGTTGG	1950
CAGTTATGGT	TTTCTTTCAT	CTGATGTGTC	AGTATCTGTT	GATTTGCTTT	2000
GTAGTTTGTT	GACATCTTAA	GATTTGATGT	GAAAGTTTTA	GATTTTTTAC	2050
C CTG					2054

Fig. 5.4:

Sequence yielded from cDNA clone 222124.

Primers are depicted in red and the black arrows show direction. For simplification, only the forward arrows are shown. Reverse primers that were used are as in table 5.4.

GCGATGGCGA   TGATGCCTCT   AGTCCTGCAT   CATCCAGAGC   GGCAGGCGAG   50

CTGGGGTCCG   GACTGCGAGA   TGGAGGAGGG   GCGCGCTGCG   GCACCCGGCA   100

GGCTTATCTG   TCTTGGGCCT   CTTTTGTCAC   ATATTGCTCA   TCTGTGAGCT   150

GAGGCCCTGA   CTCACTGAGT   ATTTTTGGGG   AGCAGAAGAA   GGAGACATTT   200

CTCTCCGAAA   ATGAACTCAA   CAGGCCACCT   TCAGGATGCC   CCCAATGCCA   250
              M   N   S   T   G   H   L   Q   D   A   P   N   A

CCTCGCTCCA   TGTGCCTCAC   TCACAGGAAG   GAAACAGCAC   CTCTCTCCAG   300
 T   S   L   H   V   P   H   S   Q   E   G   N   S   T   S   L   Q

GAGGGTCTTC   AGGATCTCAT   CCACACAGCC   ACCTTGGTGA   CCTGTACTTT   350
 F   G   L   Q   D   L   I   H   T   A   T   L   V   T   C   T

TCTACTGGCG   GTCATCTTCT   GCCTGGGTTC   CTATGGCAAC   TTCATTGTCT   400
 F   L   L   A   V   I   F   C   L   G   S   Y   G   N   F   I   V

TCTTGTCCTT   CTTCGATCCA   GCCTTCAGGA   AATTCAGAAC   CAACTTTGAT   450
 F   L   S   F   F   D   P   A   F   R   K   F   R   T   N   F   D

TTCATGATCC   TGAACCTGTC   CTTCTGTGAC   CTCTTCATTT   GTGGAGTGAC   500
 F   M   I   L   N   L   S   F   C   D   L   F   I   C   G   V

AGCCCCCATG   TTCACCTTTG   TGTTATTCTT   CAGCTCAGCC   AGTAGTATCC   550
 A   A   P   M   F   T   F   V   L   F   F   S   S   A   S   S   I

CGGATGCTTT   CTGCTTCACT   TTCCATCTCA   CCAGTTCAGG   CTTCATCATC   600
 P   D   A   F   C   F   T   F   H   L   T   S   S   G   F   I   I

ATGTCTCTGA   AGACAGTGGC   AGTGATCGCC   CTGCACCGGC   TCCGGATGGT   650
 M   S   L   K   T   V   A   V   I   A   L   H   R   L   R   M   V

GTTGGGGAAA   CAGCCTAATC   GCACGGCCTC   CTTTCCCTGC   ACCGTACTCC   700
 L   G   K   Q   P   N   R   T   A   S   F   P   C   T   V   L

TCACCCTGCT   TCTCTGGGCC   ACCAGTTTCA   CCCTTGCCAC   CTTGGCTACC   750
 L   T   L   L   L   W   A   T   S   F   T   L   A   T   L   A   T

TTGAAAACCA   GCAAGTCCCA   CCTCTGTCTT   CCCATGTCCA   GTCTGATTGC   800
 L   K   T   S   K   S   H   L   C   L   P   M   S   S   L   I   A

TGGAAAAGGG   AAAGCCATTT   TGTCTCTCTA   TGTGGTCGAC   TTCACCTTCT   850
 G   K   G   K   A   I   L   S   L   Y   V   V   C   F   T   F

GTGTTGCTGT   GGTCTCTGTC   TCTTACATCA   TGATTGCTCA   GACCCTGCGG   900
 C   V   A   V   V   S   V   S   Y   I   M   I   A   Q   T   L   R

AAGAACGCTC   AAGTCAGAAA   GTGCCCCCCT   GTAATCACAG   TCGATGCTTC   950
 K   N   A   Q   V   R   K   C   P   P   V   I   T   V   D   A   S

CAGACCACAG   CCTTTCATGG   GGGTCCCTGT   GCAGGGAGGT   GGAGATCCCA   1000
 R   P   Q   P   F   M   G   V   P   V   Q   G   G   G   D   P

TCCAGTGTGC   CATGCCGGCT   CTGTATAGGA   ACCAGAATTA   CAACAAACTG   1050
 I   Q   C   A   M   P   A   L   Y   R   N   Q   N   Y   N   K   L

CAGCACGTTC   AGACCCGTGG   ATATACCAAG   AGTCCCAACC   AACTGGTCAC   1100
 Q   H   V   Q   T   R   G   Y   T   K   S   P   N   Q   L   V   T

CCCTGCAGCA	AGCCGACTCC	AGCTCGTATC	AGCCATCAAC	CTCTCCACTG	1150
P A A	S R I	Q L V S	A I N	L S T	
CCAAGGATTC	CAAAGCCGTG	GTCACCTGTG	TGATCATTGT	GCTGTCAGTC	1200
A K D S	K A V	V T C	V I I V	L S V	
CTGGTGTGCT	GTCTTCCACT	GGGGATTTCC	TTGGTACAGG	TGGTTCTCTC	1250
L V C	C L P L	G I S	L V Q	V V L S	
CAGCAATGGG	AGCTTCATTC	TTTACCAGTT	TGAATTGTTTG	GATTTACTCT	1300
S N G	S F I	L Y Q F	E L F	G F T L	
TATATTTTT	CAAGTCAGGA	TTAAACCCTT	TTATATATTC	TCGGAACAGT	1350
I F F	K S S	L N P F	I Y S	R N S	
GCAGGGCTGA	GAAGGAAAGT	GCTCTGGTGC	CTCCAATACA	TAGGCCTGGG	1400
A G L R	R K V	L W C	L Q Y I	G L G	
TTTTTTCTGC	TGCAAACAAA	AGACTCGACT	TCGAGCCATG	GGAAAAGGGA	1450
F F C	C K Q K	T R L	R A M	G K GN	
ACCTCGAAGT	CAACAGAAAC	AAATCCTCCC	ATCATGAAAC	AAACTCTGCC	1500
I F V	N R N	K S S H	H F T	N S A	
TACATGTTAT	CTCCAAAGCC	ACAGAAGAAA	TTTGTGGACC	AGGCTTGTGG	1550
Y M L S	P K P	Q K K	F V D Q	A C G	
CCCAAGTCAT	TCAAAAGAAA	GTATGGTGAG	TCCCAAGATC	TCTGCTGGAC	1600
P S H	S K F S	M V S	P K I	S A G H	
ATCAACACTG	TGGTCAGAGC	AGCTCGACCC	CCATCAACAC	TCGGATTGAA	1650
Q H C	G Q S	S S T P	I N T	R I F	
CCTTACTACA	GCATCTATAA	CAGCAGCCCT	TCCCAGGAGG	AGAGCAGCCC	1700
P Y Y S	I Y N	S S P	S Q F F	S S P	
ATGTAACTTA	CAGCCAGTAA	ACTCTTTTGG	ATTTGCCAAT	TCATATATTG	1750
C N L	Q P V N	S F G	F A N	S Y I A	
CCATGCATTA	TCACACCACT	AATGACTTAG	TGCAGGAATA	TGACAGCACT	1800
M H Y	H T T	N D L V	Q F Y	D S T	
TCAGCCAAGC	AGATTCCAGT	CCCCTCCGTT	TAAAGTCATG	GAGGCTATAG	1850
S A K Q	I P V	P S V		
GATCTTATGT	AAACAGTTTT	TGTTTCTGAT	AGTAATGGAC	TTTATTCTAA	1900
CTTGAGATCA	GTGGCGGATC	AAAACCTACA	AGATTCAACT	GAAAAGTTGG	1950
CAGTTATGGT	TTTCTTTCAT	CTGATGTGTC	AGTATCTGTT	GATTTGCTTT	2000
GTAGTTTGTT	GACATCTTAA	GATTTGATGT	G AAAGTTTTA	GATTTTTTAC	2050
CCTG					2054

Fig. 5.5: Sequence yielded from cDNA clone 222124. Start codon is indicated in red and the stop codon is indicated in blue. Green lettering within boxes is amino acid abbreviations of the protein sequence.

GCGATGGCGA   TGATGCCTCT   AGTCCTGCAT   CATCCAGAGC   GGCAGGCGAG   50

CTGGGGTCCG   GACTGCGAGA   TGGAGGAGGG   GCGCGCTGCG   GCACCCGGCA   100

                              [SF →]

GGCTTATCTG   TCTTGGGCCT   CTTTTGTCAC   ATATTGCTCA   TCTGTGAGC T   150

GAGGCCCTGA   CTCACTGAGT   ATTTTTGGGG   AGCAGAAGAA   GGAGACATTT   200

CTCTCCGAAA   *ATG*AACTCAA   CAGGCCACCT   TCAGGATGCC   CCCAATGCCA   250

CCTCGCTCCA   TGTGCCTCAC   TCACAGGAAG   GAAACAGCAC   CTCTCTCCAG   300

GAGGGTCTTC   AG[← ER]CCACACAGCC   ACCTTGGTGA   CCTGTACTTT   350

TCTACTGGC G   GTCAGCTTCT   GCCTGGG TTC   CTATGGCAAC   TTCATTGTCT   400

            [SK1F →]

TCTTGTCCTT   CT[GCCTTCAGGA   AATTCAGAAC   CAACTTTGAT   450

TTCATGATCC   TGAACCTGTC   CTTCTGTGAC   CTCTTCATTT   GTGGAGTGAC   500

AGCCCCCATG   TTCACCTTTG   TGTTATTCTT   CAGCTCAGCC   AGTAGTATCC   550

CGGATGCTTT   CTGCTTCACT   TTCCATCTCA   [SK2F →]   CTTCATCATC   600

ATGTCTCTGA   AGACAGTGGC   AGTGATCGCC   CT GCACCGGC   TCCGGATGGT   650

                                   [SK2R ←]

G TTGGGGAAA   CAGCCTAATC   GCACGGCCTC   CTTTCCCTGC   700

TCACCCTGCT   TCTCTGGGCC   ACCAGTTTCA   CCCTTGCCAC   CTTGGCTACC   750

TTGAAAACCA   GCAAGTCCCA   CCTCTGTCTT   CCCATGTCCA   GTCTGATTGC   800

TGGAAAAGGG   AAAGCCATTT   TGTCTCTCTA   TGTGGTCGAC   TTCACCTTCT   850

GTGTTGCTGT   GGTCTCTGTC   TCTTACATCA   TGATTGCTCA   GACCCTGCGG   900

AAGAA[SK3F →]TCAGAAA   GTGCCCCCCT   GTAATCACAG   TCGATGCTTC   950

CAGACCACAG   CCTTTCATGG   GGGTCCCTGT   GCAGGGAGGT   GGAGATCCCA   1000

     [SK3R ←]

TCCAGT[CCGGCT   CTGTATAGGA   ACCAGAATTA   CAACAAACTG   1050

CAGCACGTTC   AGACCCGTGG   ATATACCAAG   AGTCCCAACC   AACTGGTCAC   1100

CCCTGCAGCA   AGCCGACTCC   AGCTCGTATC   AGCCATCAAC   CTCTCCACTG   1150

CCAAC[SK4F →]AGCCGTG   GTCACCTGTG   TGATCATTGT   GCTGTCAGT C   1200

CTGGTGTGCT   GTCTTCCACT   GGGGATTTCC   TTGGTACAGG   TGGTTCTCTC   1250

CAGCAA[SK4AR ←]ATTC   TTTACCAGTT   TGAATTGTTT   GGATTTACTC   1300

TTATATTTTT   CAAGTCAGGA   TTAAACCCTT   TTATATATTC   TCGGAACAGT   1350

GCAGGGCTGA   GAAGGAAAGT   GCTCTGGTGC   CTCCAATACA   T[SK5F →]   1400

TTTTTTCTGC   TGCAAACAAA   AGACTCGACT   TCGAGCCATG   GGAAAAGGGA   1450

A CCTCGAAGT   CAACAGAAAC   AAATCCTCCC   ATCATGAAAC   AAACTCTGCC   1500

TACAT[SK5AR ←]AAGCC   ACAGAAGAAA   TTTGTGGACC   AGGCTTGTGG   1550
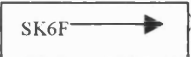
CCCAAGTCAT	TCAAAAGAAA	GTATGGTGAG	TCCCAAGATC	TCTGCTGGAC	1600
ATCAACACTG	TGGTCAGAGC	AGCTCGACCC	CCATCAACAC	TCGGATTGAA	1650
CCTTACTACA	GCATCTATAA	CAGCAGCCCT	TCCCAGGAGG	AGAGCAGCCC	1700
ATGTAACTTA	CAGCCAGTAA	ACTCTTTTGG	ATTTGCCAAT	TCATATATTG	1750
C CATGCATTA	TCACACCACT	AATGACTTAG	TGCAGGAATA	TGACAGCACT	1800
TCAGCCA SK6F➝ CCAGT		CCCCTCCGTT	TAAAGTCATG	GAGGCTATAG	1850
GATCTTATGT	AAACAGTTTT	TGTTTCTGAT	AGTAATGGAC	TTTATTCTAA	1900
CTTGAGA SK6R⬅ GATC		AAAACCTACA	AGATTCAACT	GAAAAGTTGG	1950
CAGTTATGGT	TTTCTTTCAT	CTGATGTGTC	AGTATCTGTT	GATTTGCTTT	2000
GTAGTTTGTT	GACATCTTAA	GATTTGATGT	GAAAGTTTTA	GATTTTTTAC	2050
C CTG				SK5R⬅	2054

Fig. 5.6:

Sequence demonstrating the fragments used for mutation analysis in the DHRD family. Primers are coloured in turquoise and depicted by the black arrows (➝) indicating the forward or reverse direction.

Model 373   45•A1   Signal G:184 A:460 T:502 C:313   Page 1 of 3
Version 3.0   DT6%Ac{A Set-AnyPrimer}   Tue, Aug 4, 1998 12:01 pm
ABI50   A1   1290 Matrix File   Mon, Aug 3, 1998 4:01 pm
Version 3.0   Lane 45   Points 843 to 7340   Base 1: 843   Spacing: 10.09{10.09}

ABI PRISM

GGG G GGG CCT TNATGTG G G A G C CT CT AAT CG CACG GC CNC CT T T CCCT G CACC G T A CT CCT CA CC CTG CT T CT
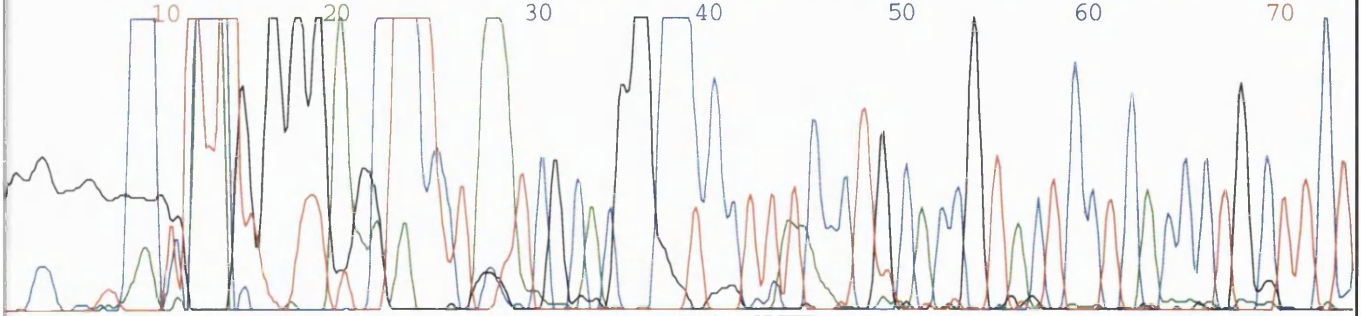
T GG G CCACCAG T T TCACC CT TG C CACC T TGG CTA CC T TG A AAA C CAG CA AG T CC CA CC TCTG T CT T C
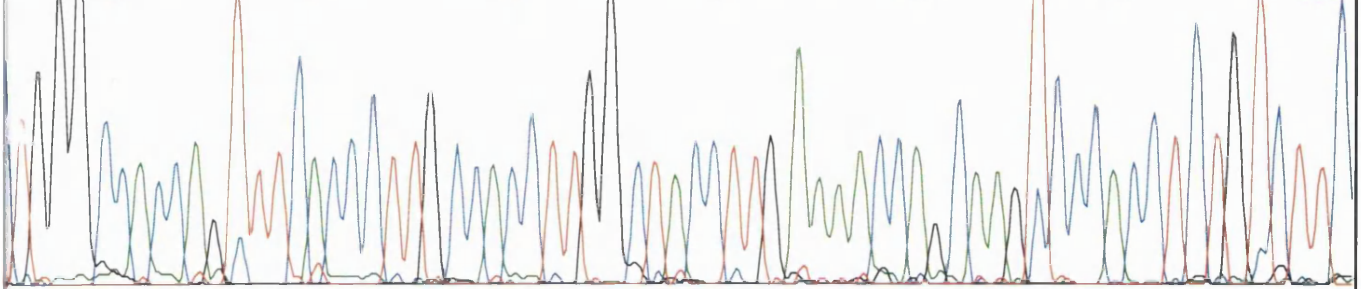
CA TG TC CAG T CTG AT TG C TGG AAA AG GG AAA GC CAT T T TG T CTCTC TA TG TG C TCG ACT T CACC T
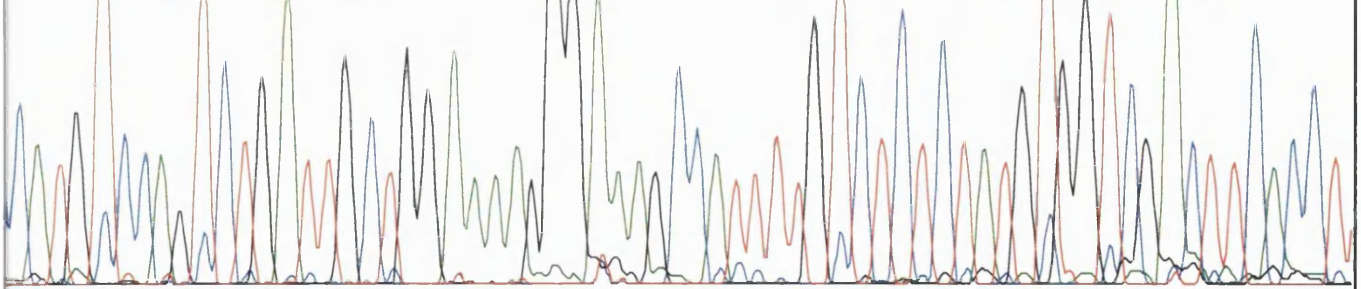
C TG TG T TG C TG TG G TCTCTG T CTC T T A CATCA TG ATTG CTCAG ACC CTG CG G A AG A ACG CT CA AC
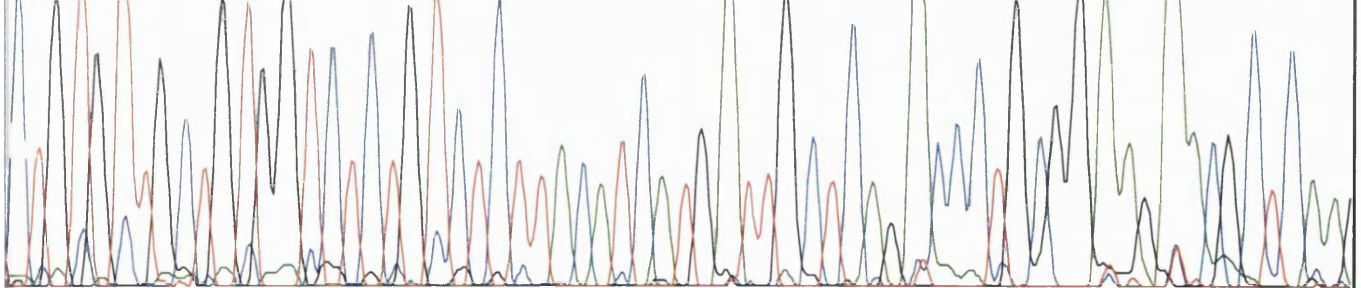
T CAGA AAG TG CCCCC CTG TA AT CA CAG T CG A TG CT TC CAGA CCA CAGCCTTC G GGGGG NGGGG NNN NN

ABI PRISM™
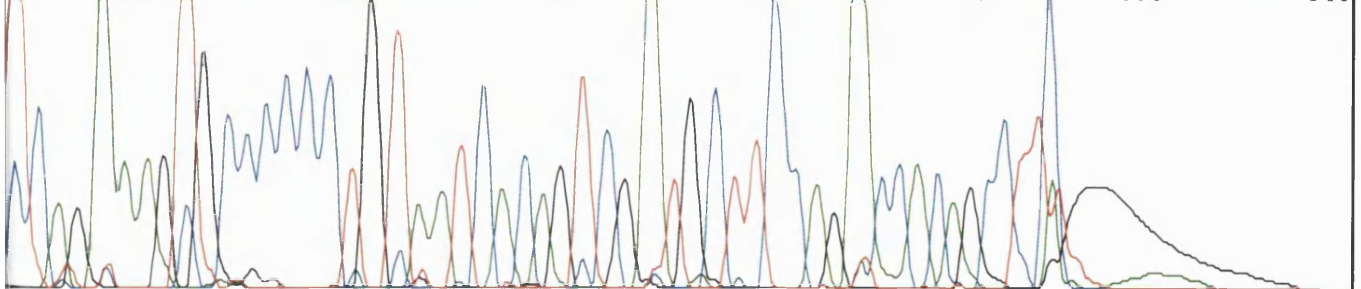
Model 373	47·A3	
Version 3.0		
ABI50	A3	
Version 3.0	Lane 47	

Signal G:157 A:492 T:562 C:342　　　　　Page 1 of 3
DT6%Ac{A Set-AnyPrimer}　　Tue, Aug 4, 1998　12:01 pm
1290 Matrix File　　　　　Mon, Aug 3, 1998　4:01 pm
Points 832 to 7340　Base 1: 832　Spacing: 10.12{10.12}

GNG NCNN NNCGT TATCCGTAA AAGC TTA TCTT CGCAAGGGCTC GTC TCCCTG CACCG TA CTCCT CACC CTG CTTC
10　　20　　30　　40　　50　　60　　70
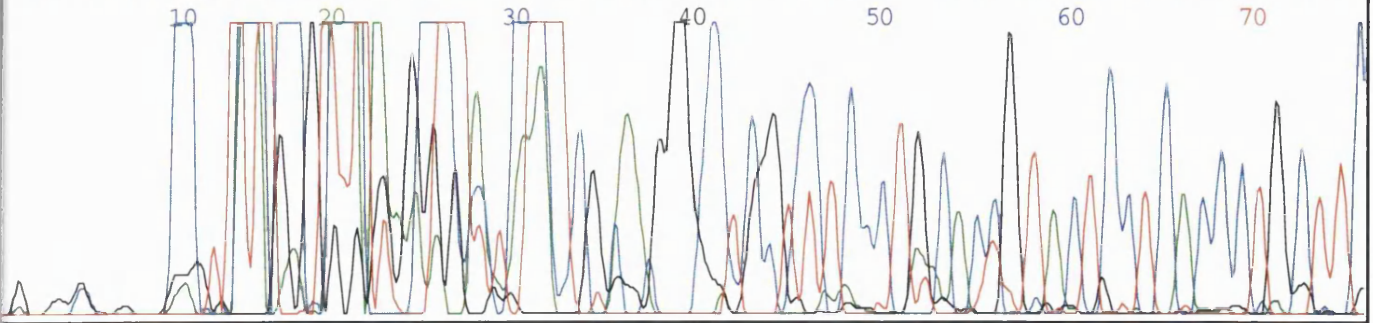
CTCTG GG CCACCAG TTTCACCCTTG CCACCTTGG CTACCTTG A AAACCAG CAAGTCCCACC TCTG TCTT
80　　90　　100　　110　　120　　130　　140

CCCA TG T CCAGTCTGATTG CTG G AAAAG GG AAAGCCATTTTG TCTCTCTATG TGG T CGA CT TCACCT
150　　160　　170　　180　　190　　200　　21

TCTG TGTTG CTG TGG TCTCTG TCTCTTA CATCATG ATTG CTCAGACC CTG CGG AAG AACGCTCAA
220　　230　　240　　250　　260　　270

GTCAGA AAGTGCCCCCCTG TA ATCACAGT CGATG CTTCCAGACCACAGCCTCGGGGGGGGGGGNNNN
280　　290　　300　　310　　320　　330　　340

ABI PRISM™
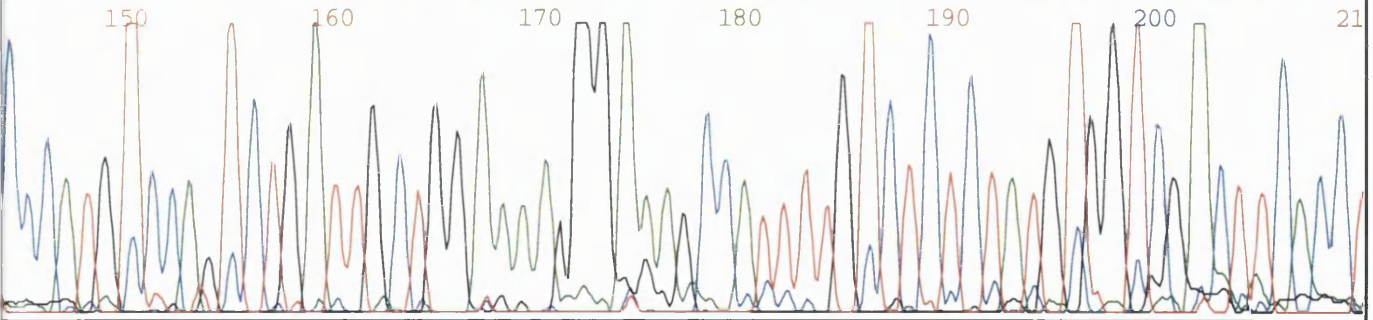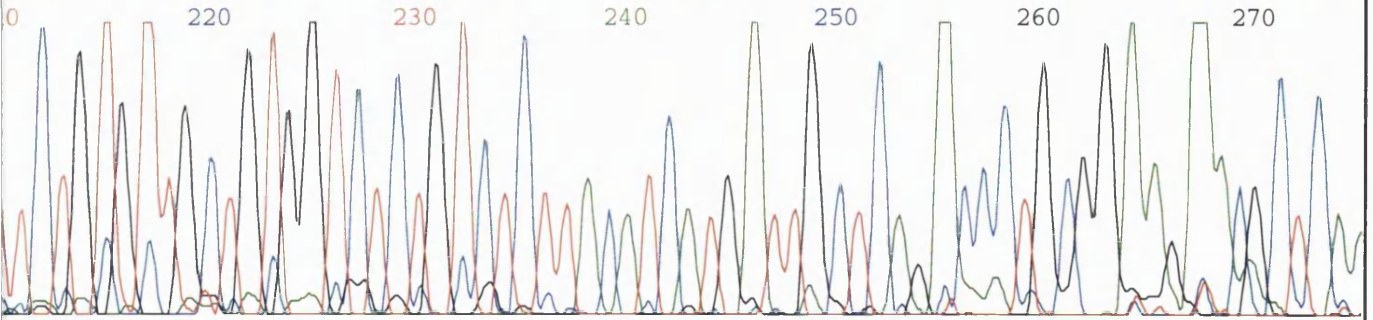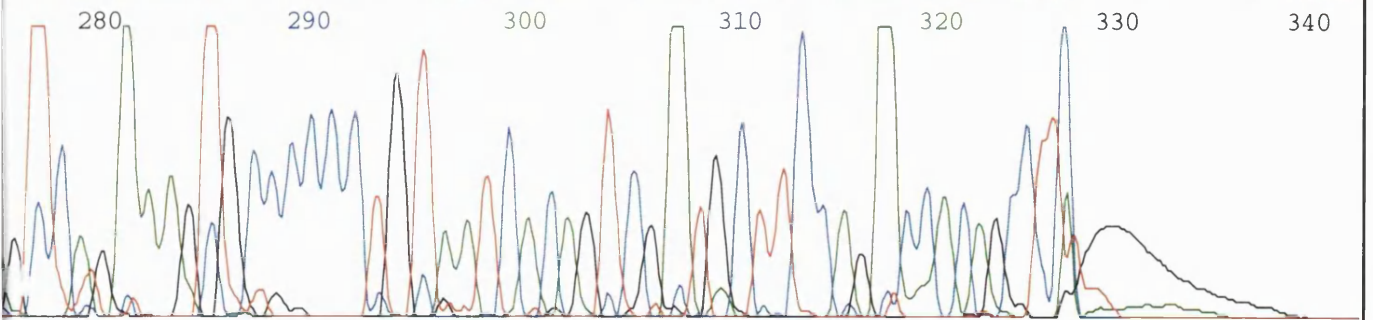
Model 373
Version 3.0
ABI50
Version 3.0

49•A5

A5
Lane 49

Signal G:180 A:409 T:580 C:280
DT6%Ac{A Set-AnyPrimer}
1290 Matrix File
Points 834 to 7340   Base 1: 834

Tue, Aug 4, 1998 12:01 pm
Mon, Aug 3, 1998 4:01 pm
Spacing: 10.10{10.10}

GGGGGGGGGGGTCGTTNTNCTTGCTTTACAGGGGGGGNCTTTCTGACTTGAGCGTTCTTCCGCAGGGT
10   20   30   40   50   60

CTGAGCAATCATGATGTNAGAGACAGAGACCACAGCAACACAGAAGGTGAANTCGACCACATAGAGAGA
70   80   90   100   110   120   130

ACAAAATGGCTTTCCCTTTTCCAGCAATCAGACTGGACATGGGAAGACAGAGGTGGGACTTGCTGGT
140   150   160   170   180   190   200

TTTCAAGGTANCCAAGGTGGCAAGGGTGAAACTGGTGGCCCANANAAACAGGGTGAGGANTACGG
210   220   230   240   250   260

TGCAGGGAAAGGAGGCCGTGCGATTAGGCTGTTTCCCCAACACCATCCGACGGGGANNANANNNN
270   280   290   300   310   320   330

Model 373   51·A7   Signal G:206 A:471 T:740 C:335   Page 1 of 3
Version 3.0   DT6%Ac{A Set-AnyPrimer}   Tue, Aug 4, 1998 12:01 pm
ABI50   A7   1290 Matrix File   Mon, Aug 3, 1998 4:01 pm
Version 3.0   Lane 51   Points 782 to 7340   Base 1: 782   Spacing: 10.01{10.01}

ABI PRISM

G G G G GG GGGG GG GG G G NT GGT NNTC C T TG T TATTAC G GGGG G NACT T TCTG ACT TG AG CG T TCT TC CC

      10   20   30   40   50   60
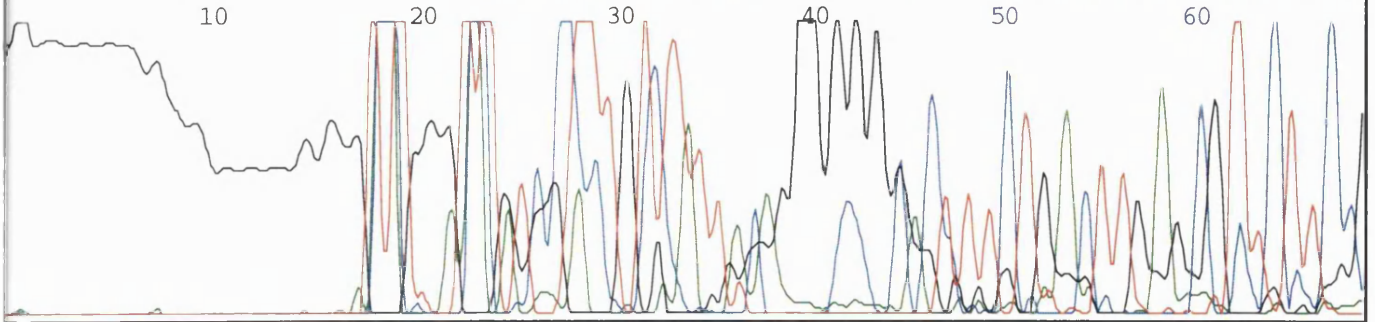
G CNGGG TCTG AG CAATCATGA TG TAAG AG ACAG AG ACCA CAG C AACACAG A AGG TG AATT CGACCA CAT

  70   80   90   100   110   120   130
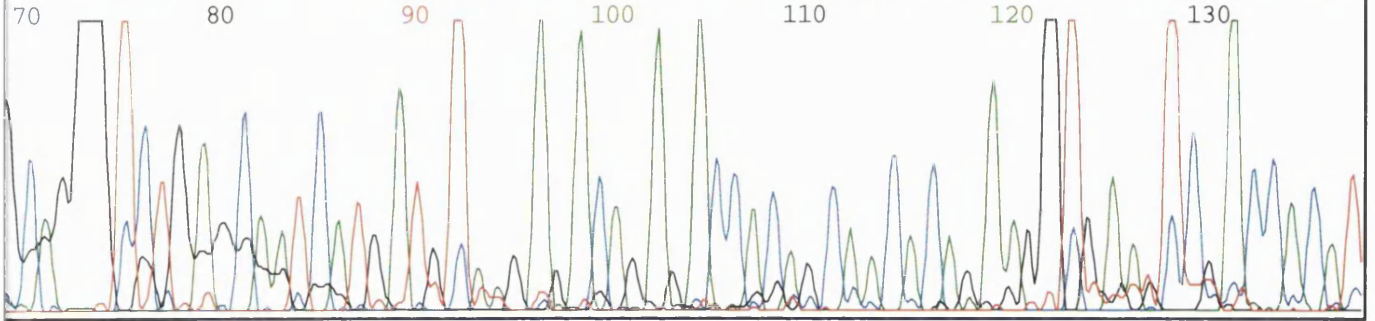
AG AGAG ACAAAATG G CTTTCCCT TTTCCAG CAATCAG ACTG G ACATGGG AAG ACAGAGG TGGG ACT

   140   150   160   170   180   190   200
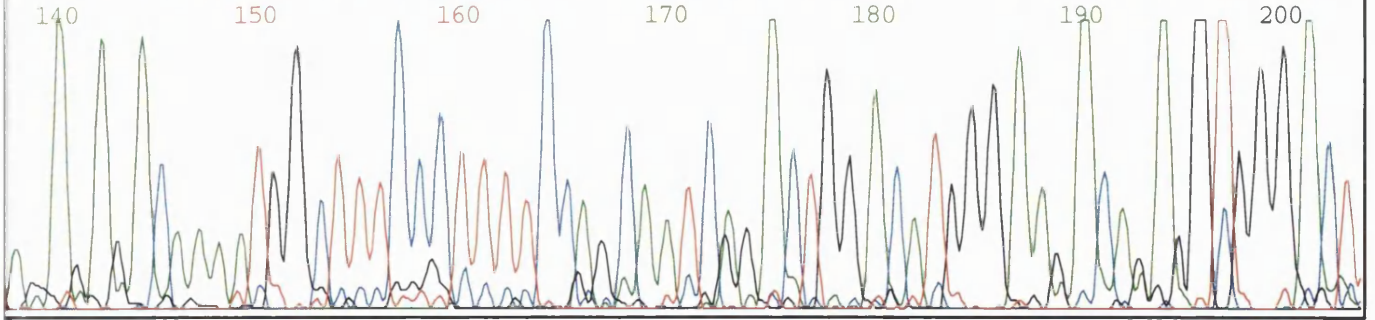
TG CTGG TTT TCAAG G TAGCCAAG G TGG CA AGG GT GAA ACTG G TGG CCC ANANA AG CAG GG T GAGG

   210   220   230   240   250   260
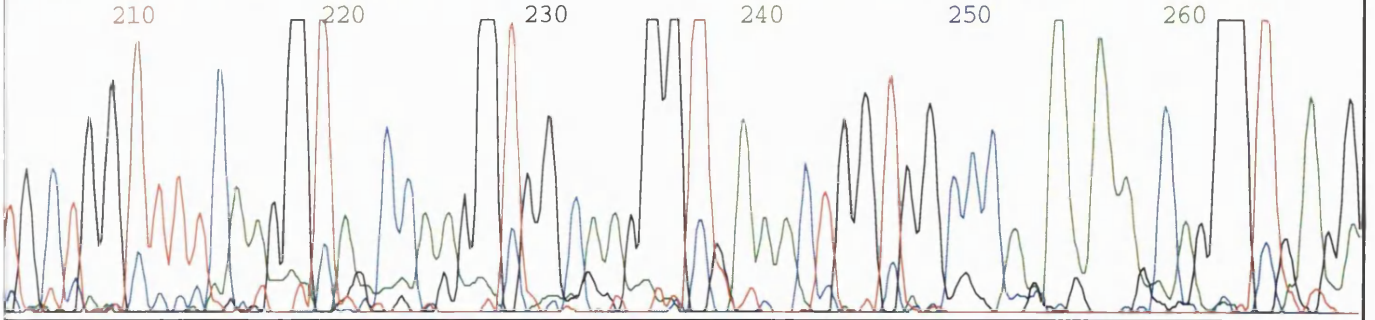
AN TACGGT G CAGGG AA ANGAAG C CG TG C NA T TAGGCTG T TTCCC CAACACCATCC A NGGGNGN A

   270   280   290   300   310   320   330
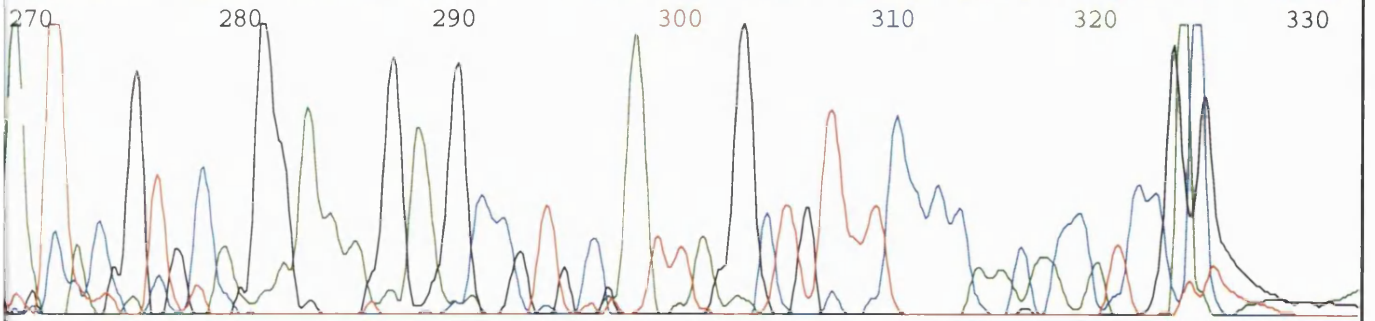
Fig. 5.7 a,b,c,d:

Sequence data depicting mutation screening of fragment 3 (SK2F+SK3R) with an affected individual (a) and a normal individual (b) with primer SK2F and with an affected individual (c) and a normal individual (d) with primer SK3R.

5.6   Discussion

5.6.1   A novel gene that encodes for a G-coupled receptor protein

Following the recent genetic refinement of the critical region between polymorphic markers D2S2352 and D2S2251 (Kermani *et. al.*, 1999), a retinal EST (WI-31133) that mapped within this genetic interval was identified from the Whitehead database (http://www-genome.wi.mit.edu/). This EST originated from a retinal cDNA library and was made available as an IMAGE clone (222124). PCR amplification of this EST across the DHRD physical contig, localised it between the current flanking markers of DHRD within six PAC clones (including PAC clone 130-13-O) and two YAC clones. The expression of WI-31133 (in human retina and RPE layer) was observed by PCR amplification in the respective cDNAs. The full length coding sequence of this gene was obtained from the original cDNA clone revealing a 2054 bp insert containing a 1623 bp open reading frame (ORF). Prediction of the initiation/start (ATG) codon was at 211 bp and the ORF frame extended from 211 bp to 1833 bp predicting a single exon of 540 amino acids with a molecular weight of 59.4 kDa. Although the start codon was at 211 bp, no other sequence motifs were present prior to this ATG site (Kozak, 1996). Amino acid sequence revealed homologies to several G-coupled proteins that contain a 7 transmembrane motif (Dryja *et al.*, 1990). Subsequent to this work, the total RNA blot of the human retina and RPE was to be utilised to obtain the transcript size. Nevertheless, this blot did not show any signal when hybridised but instead the commercial Northern blot (of different brain tissues) containing mRNA showed a 7 kb transcript. Unfortunately, this novel work was published by a former colleague (Tartellin *et. al.*, 1999) who has also been involved in the search for the DHRD gene. The full length coding region of this gene has potentially been screened for mutations in the DHRD family. Our study and that of Tartellin and colleagues indicates that this gene is not associated with the disease causing phenotype of DHRD.

5.6.2   Pattern of expression

In addition to our data, Tartellin and co-workers identified specific sites of expression of this gene in the retina using *in situ* hybridisation to adult human eye

sections. Expression was observed only in the perivascular cells surrounding the retinal arterioles, in the ganglion cell/nerve fibre layer. Transcripts were not detected in the neurosensory layer of the retina or RPE. In contrast, mouse sections staining was found in the inner segments of the photoreceptors and in the outer plexiform layer, thus a difference in expression was revealed between human and mouse. The difference in pattern of distribution could have been due to the design of the probe (which had been designed for the 3' end of the human sequence) and this sequence probably differed in mouse. Our Northern blot data revealed a 7 kb transcript in most areas of the human brain (see fig. 5.2b). This result was later verified by Tartellin and co-workers. In addition their data revealed expression in spinal cord and RPE tissue. It was proposed that the heavy pigmentation of the RPE layer could have interfered with expression of the transcript thus not being visible in the *in situ* sections. However, in this study, expression was observed in the RPE layer when PCR amplifcation was performed on the RPE cDNA. Nevertheless, it must be added that this technique is not representative for this layer, as during dissection other layers also are torn away with it.

5.6.3 A single mutation in the Epidermal Growth Factor (EGF)-containing fibulin-like extracellular matrix protein 1 (*EFEMP1*) gene causes mutation in DHRD and Malattia leventinese.

Whilst mutation analysis for the coding sequence of WI-31133 excluded it as the disease causing gene for DHRD, Stone and his co-workers (1999) found a single non-conservative mutation (Arg345Trp) in the *EFEMP1* gene in 39 families with Malattia leventinese or DHRD. This particular change was absent from 477 controls and in 494 age-related individuals. Although this particular change had been observed in families obtained for the US study, this mutation has also been verified in this study. All affected individuals in the British DHRD family displayed the Arg345Trp change which remained absent from the unaffected individuals of the same family, thus reinforcing Stone and his workers' latest data. However, the *EFEMP1* gene lies external to the recent DHRD refinement. This phenomenon shall be discussed in detail in the proceeding chapter.

In addition to the Arg345Trp variant, three other coding sequence variants (Thr181Thr, ACG-ACA; Ile220Phe, ATC-TTC; Ser456, TCA-TCG) were also reported (Stone *et. al.,* 1999) in a control individual. Furthermore, four intragenic two-allele polymorphisms were indentified (from intronic sequence) and all families (with DHRD or Malattia leventinese) carried the most common allele of each in phase with the Arg345Trp variant (Stone *et. al.,* 1999).

5.6.4 *EFEMP1*

Fibrillin is a major component of extracellular microfibrils and is ubiquitously expressed in both elastic and nonelastic connective tissue. *EFEMP1* is a "fibrillin like" gene that had originally been isolated as cDNA sequence (originally known as S1-5) that was over-expressed in human fibroblasts obtained from a patient with Werner Syndrome (McKusick *et al.,* 1962) a genetic disease characterised by accelerated aging. Thus, *EFEMP1* was originally designated the name of *FBNL EFEMP1* was originally designated the name of *FBNL*. *EFEMP1* had previously been mapped to chromosome 2p16 region by Ikegawa and his group (1996) using *in situ* hybridisation. They characterised the genomic organisation of this gene and found it highly homologous to fibrillin. Thus, *EFEMP1* was originally designated the name of *FBNL*.

The *EFEMP1* cDNA probe detected two transcripts of 2.2 and 3.0 kb in mRNA from multiple tissues. Expression data revealed that *EFEMP1* was expressed in several tissues except in brain and lymphocytes. The amino acid sequence of the *EFEMP1* gene is 36.3% identical to human fibrillin gene (*FBN1,* Magenis *et al.,* 1991) which was found mutated in individuals with Marfan syndrome and 35.4% identical to a second fibrillin gene (*FBN2,* Lee *et. al.,* 1991*)* that was found mutated in patients with congenital contractural arachnodactyly (CCA).

Both *FBN1* and *FBN2* contain repeated calcium-binding epidermal growth factor-like (CBEGF) domains, a cardinal motif of *FBN* genes. The *EFEMP1* gene spans approximately 18 kb of genomic DNA and contains 12 exons. The Arg345Trp mutation alters the last EGF domain of the gene product which is similar to the many mutations of *FBN1* for Marfan syndrome.

197

Northern blot analysis of *EFEMP1* demonstrated high levels of expression in adult mice eye and lung tissue and moderate expression was observed in tissues such as brain, heart, spleen and kidney. RT-PCR of RNA extracted from retinal pigmented epithelium (RPE) and choroid and isolated neurosensory retina of the human eye revealed expression in all these tissues (Stone *et al.,* 1999).

5.6.5 Is DHRD allelic with Malattia leventinese?

Initially the two diseases were clinically assessed as distinct, owing to the difference in distribution of the drusen deposits; concentric deposits were observed for DHRD individuals and radial deposits for Malattia leventinese patients. This question had been formerly addressed in section 3.8.3. following the genetic mapping of DHRD to the same interval as Malattia leventinese. Malattia leventinese had been mapped between polymorphic markers D2S1761 and D2S444 (Héon *et. al.,* 1996) which flanked the DHRD interval (between markers D2S2316 and D2S378, Gregory *et. al.* 1996). Thus, it was hypothesised that as the two diseases mapped within the same genetic interval, the mutations would be different but lying in the same gene, showing an allelic relationship between the two diseases. This has not been the case as demonstrated by Stone (1999) since both the diseases have been shown to be caused by the same mutation in the *EFEMP1* gene. This work has been confirmed in our laboratory and further work is being performed to assess this data (this shall be discussed in detail in Chapter 6).

CHAPTER 6

GENERAL DISCUSSION AND FUTURE PROSPECTS

6.1   Overview of the work presented

The DHRD locus on chromosome 2p16 was found by a genome wide linkage analysis on a large British pedigree in our laboratory and since its discovery, progress has been made toward the identification of the disease-causing gene. At the start of the project DHRD locus was confined between markers D2S316 and D2S378 to a genetic interval of 5 cM. During the course of time, this region was refined between markers D2S2739 and D2S378. Subsequent research identified two dominant drusen families that were also mapped to this locus but did not provide refinement of the previous genetic interval but instead reinforced the existing data. An additional branch of the Doyne's family further refined the disease region between markers D2S2352 and D2S2251 to a genetic distance of 1 cM.

Simultaneous to the genetic endeavours, physical mapping was undertaken to provide a preliminary YAC contig. Construction of the contig was not limited to the DHRD region but was extended to provide partial telomeric coverage of the Malattia leventinese locus. The Malattia locus was linked between telomeric marker D2S1761 and centromeric marker D2S444, a genetic distance of approximately 14 cM, thus the telomeric extension in the DHRD contig lies between markers D2S2316 (cen) and D2S119 (tel). The contig was assembled from three different YAC libraries. Interestingly, STS content mapping revealed deletions in several YAC clones that were meant to provide coverage of the disease region. Therefore, PAC clones replaced YACs as the cloning vector of choice and subsequent work of the project involved the construction of a complete PAC contig across the DHRD region but this work has been made redundant due to the discovery of the *EFEMP1* gene. As yet, complete coverage has not been achieved of the previously refined region but instead preliminary PAC isolations and STS content mapping covers the current genetic refinement of 1 cM region onto a single PAC.

The EST WI-31133 is localised to several PAC clones including the PAC (130-13-O) which may contain both the refined polymorphic markers D2S2352 and D2S2251.

This retinally expressed gene was considered a potential candidate gene worthy of a thorough investigation. The full length coding sequence has been determined and subsequent characterisation revealed that this was a single exon gene. However, mutation screening of this gene in the DHRD family failed to show any single base pair mutations or any polymorphisms. Future work regarding this gene entails sequencing a genomic clone (PAC 130-13-O) to obtain the complete 5' UTR DNA sequence for completion of its genomic characterisation.

Therefore, at the end of this research the DHRD disease interval has been refined to ~1 cM genetic distance and ~3 Mb of physical distance which is traversed by a YAC/PAC contig. The full-length coding sequence of WI-31133 has been screened and potentially excluded from DHRD family. Immediate work concerns further genomic characterisation of the gene. Since this gene is retinally expressed, it could be a suitable candidate for any other retinal disease that maps to the 2p16 region, thus in future this gene should be screened in any other dominant drusen family that maps to this region.

6.2 Is *EFEMP1* the gene for DHRD?

As discussed in the previous chapter that a single variant (Arg345Trp) has been demonstrated as the disease-causing gene for DHRD and Malattia (Stone *et al.* 1999), following this discovery we are currently awaiting blood samples from a Japanese family that are affected with DHRD. It is of interest to screen their DNA with exon 10 of the *EFEMP1* gene to demonstrate whether they possess the disease-causing (Arg345Trp) variant. If the affected individuals do not demonstrate this change, then the entire coding region of the *EFEMP1* gene would be screened to identify the disease causative mutation. If such a mutation is identified it would provide further evidence for *EFEMP1* being the DHRD gene.

A single non-conservative mutation (Arg345Trp) in the *EFEMP1* gene has been identified in families with DHRD and Malattia leventinese (Stone *et al.* 1999). Although, this data has been confirmed in this study, there are several interesting issues that must be addressed.

Firstly, the *EFEMP1* gene maps within the refined Swiss Haplotypic interval between markers 133018CA and 322A4AAAT (Stone *et al.* 1999). These two

polymorphic markers lie between the Généthon markers tel D2S2153 and D2S378 cen. Thus this gene lies external to our recent genetic refinement which is localised between markers D2S2352 and D2S2251. Incidentally, Stone and his group have not addressed our refinement. Two possible scenarios could explain this result, in the first instance the individual that provided the telomeric crossover for marker D2S2251 (Individual I, table 3.3) could have been misdiagnosed and may not be affected by DHRD, alternatively this individual may represent a phenocopy (that a mutation in another gene can result in a similar phenotype). It is also possible that, the individual could have been an AMD patient that exhibited drusen deposits like that of DHRD. This explanation is plausible as the age of the patient is such that AMD can be suspected. However recent, personal communication with Gregory-Evans, K. (St. Mary's College, London) who originally clinically diagnosed this individual for DHRD, has confirmed that this individual has drusen deposits in the macula, especially around the nasal side of the optic nerve head, characteristic of DHRD. Therefore, it must be stressed that accurate clinical diagnosis is critical prior to any genetic study.

However, it cannot be ruled out that there could have been other errors in blood/DNA tube labelling which could have given rise to a false genetic refinement. Therefore, the individual in question must be primarily clinically re-assessed and fresh blood must be drawn for re-haplotypic analysis in order to address this controversy. Currently, this data is being repeated by Gregory-Evans, C.Y. (Imperial College, London) who is also associated with this project.

Secondly, if our data is true i.e. the genetic refinement of DHRD is localised between D2S2352 and D2S2251, then the *EFEMP1* gene that shows the non-conservative change (Arg345Trp) could be due linkage disequilibrium; a possibility which has not been ruled out by Stone (1999). In spite of the extensive patient resources available to them, they were unable to demonstrate that the ancestrally shared interval is entirely contained within the *EFEMP1* gene, thus it cannot be excluded that a disease causing mutation could be present in an adjacent gene. This implies that the hunt for the DHRD gene should not be ceased.

A similar case has been observed in our lab for the Retinitis Pigmentosa locus on chromosome 19q13.4 (Vithana *et al.* 1998) with the protein kinase gamma gene

(PRKCG). Following its characterisation, a mutation (non-conservative replacement of Arginine to Serine at codon 659) was found in two autosomal dominant RP families and two sporadic cases. Haplotypic analysis in these families subsequently revealed that they were all derived from one common ancestor. Screening of *PRKCG* in six other families linked to the locus failed to reveal any other changes in *PRKCG* thus leading to the exclusion of this gene as the disease-causing gene for adRP. This is parallel to DHRD and *EFEMP1* can be drawn here since similar to Arg659Ser mutation in *PRKCG*, only one mutation has been identified in *EFEMP1* which could just be a polymorphism found in linkage disequilibrium with the actual disease causative mutation lying in a nearby gene!

In order to answer the question whether *EFEMP1* is the gene for DHRD, an animal model that manifests the Arg345Trp mutation must be created. If the Arg345Trp mutant model mimics DHRD i.e. has the same pathology then it would prove to be the gene for this disease. To prove it further there should be structural and functional rescue in the mutant photoreceptors by the *EFEMP1* transgene. In a similar study McNally and colleagues (1999) achieved complete rescue of photoreceptors harbouring a rhodopsin mutation.

If *EFEMP1* is the DHRD gene then the next logical step would be to instigate a series of detailed and comprehensive biochemical analysis of both the wild type and the mutated protein following their expression in an appropriate expression system, in order to understand the functional abnormality and the underlying pathogenic mechanism of the mutation. This would address many fundamental problems associated with retinal degeneration such as whether it is a lack of protein function that leads to degeneration or the loss of protein structure.

Interestingly, *EFEMP1* was originally named as "fibrillin like" *(FBNL)* which was originally isolated during screening of a subtractive enriched cDNA library derived from fibroblasts established from an individual with Werner syndrome, a genetic disorder of premature aging. This gene is overexpressed in cells from the patient and in growth-arrested normal human fibroblasts that are either in the senescent or the quiescent stage. The expression of this gene is inversely related to the replication condition of cells; mRNA level is low in young vigorously proliferating cells and in serum concentrations

that promote the cellular proliferation but is rapidly elevated after serum depletion. The gene was originally isolated to study the function and regulation in human tissues and in an effort to determine human disorders. Eventually the gene was excluded for Werner syndrome as *in situ* data mapped it to the chromosomal 2p16 region (Ikegawa *et al.*, 1996).

The mRNA of *EFEMP1* was found to contain 5 or 6 epidermal growth factor (EGF)-like domains depending on the translation site (Lecka-Czernick *et al.*, 1995). Computer scanning of the databases showed that similar type of EGF-like domains were present in some members of the large EGF-like protein family, where the homology is restricted to these domains and shows a strong conservation in amino acid specificity and their positions. In addition to the conservation of cysteine residues in these domains, which promote protein folding into a β-sheet structure other well-conserved amino acids are also present among them are aspartic acid and tyrosine which are involved in Calcium binding. The evidence of EGF-like domains in this gene implies that these domains are required for interactions with other proteins and for functional activity such as in cell signalling pathways (Lecka-Czernick *et al.*, 1995).

Other EGF domain mutations are present in the Fibrillin (*FBN1*) gene which is mutated in patients of Marfan syndrome, an autosomal dominant disorder of connective tissue characterised by pleiotropic manifestation s involving primarily the occular, skeletal and cardiovascular systems. *FBN1* is a major component of the 10-12 nm microfibrils which play a role in tropoelastin deposition and elastic fibre formation in addition to possessing an anchoring function in some tissues (Robinson *et al.*, 2000).

The *FBN2* gene is found to be highly homologous to the *FBN1* gene and shown to be cause a phenotypically related disorder called congenital contractural arachnodactylly. Mutations in the fibrillin genes are likely to affect the global function of the microfibrils, the term microfibrillopathy is the most appropriate to use. The understanding of the function of these genes is as yet incomplete and correspondingly no comprehensive theory has emerged for Marfan syndrome and congenital contractural arachnodactylly (Robinson *et al.*, 2000).

6.3 Macular genes and AMD

To date several macular genes have been found such as *RDS, TIMP-3, ABCR, CRX,* and *VMD-2* that are all implicated in the formation of drusen. To this date no disease causing mutations for AMD have been reported in *TIMP-3* and other retina specific genes like Rhodopsin (*RHO*) and peripherin (*RDS*).

Recently, Shastry and Trese (1999) studied two unrelated families having familial-type AMD, with the assumption that mutations in the peripherin/retinal degeneration slow (*RDS*) gene could contribute to the disease phenotype. They identified two silent mutations (84D and 106V) in one family in the same allele of exon 1, which segregated in 3 patients with AMD. However, the fourth affected individual in the same family, as well as 40 normal controls, did not contain this mutation. Further analysis of exon 2 and exon 3 in both families did not show any other sequence alterations. Since one of these silent mutations (106V) has been reported to exist in certain populations and the other mutation (84D) failed to segregate completely in the family, it is unlikely that these mutations are pathogenic. Their results suggested that the peripherin/RDS gene is not a major factor responsible for AMD.

As previously discussed, drusen formation is also characteristic of AMD (see section 1.9.6 and 3.4) and as discovered by Stone, *EFEMP1* coding sequence mutations do not cause typical AMD, but the Arg345Trp mutation can be utilised in the creation of an animal model to study the potential of drusen formation and for future prevention. *EFEMP1* genes show homology with other genes that code for extracellular matrix proteins, thus, this group of genes can also prove to be good candidates for AMD.

In 1997 Allikmets and his group found mutations in the photoreceptor-specific gene *ABCR* which is also mutated in Stargardt disease (see section 1.9.6). Allikmets found a total of 13 different AMD-associated alterations, both deletions and amino-acid substitutions, in heterozygous state suggesting that these alterations will lead to presymptomatic testing of high-risk individuals and early diagnosis of AMD and new strategies for prevention and therapy. Recently, two specific alterations of *ABCR* (G1961E and D2177N) have been associated with AMD (Allikmets and the International *ABCR* Consortium, 1999). The statistical significance of this data has been calculated by Fishers exact test suggesting that they were detected in 2.5% of AMD patients. This data

confirms that atleast these two *ABCR* variants are found more frequently in AMD patients when analysed in large patient/control populations and account for 5% of all *ABCR* variants with AMD. Furthermore, our laboratory represents the UK study of the International *ABCR* Consortium. 1/90 AMD individuals show the G1961E variant and similarly 1/90 AMD individuals show the D2177N variant (*in press*) and this data correlate with that found by Allikmets.

Recently, in order to identify the gene associated with age-related macular degeneration (AMD) at the ARMD1 locus at 1q25-31. The *phosducin* and *RGS16* genes were screened for mutations and have been excluded as candidates for *ARMD1*. Additional candidate genes, including *PLA2G4*, are being screened for mutations (Schultz *et al.*, 1999).

6.4 Gene therapy for macular diseases

The Human Genome Project will identify, map and sequence all 50,000-100,000 human genes and will provide the tools to determine the genetic basis of both common and rare diseases. The ultimate goal of understanding the cause of disease is to provide treatment that can either cure the disease or retard the degenerative process. It must be appreciated that over the past few years' great progress has been achieved in the molecular cause of macular diseases but as yet no advances have been made beyond identifying pre-symptomatic individuals and providing genetic counseling.

Understanding the genetic basis of human disease will allow for the development of highly specific drugs and for replacement of the mutated gene through gene therapy. Gene therapy may also be used to introduce a new function into cells with resulting therapeutic benefit. Genes may be delivered into cells in vitro or in vivo utilizing viral or nonviral vectors. Viral vectors, which have been used, include retroviruses, adenoviruses, adeno-associated viruses and herpes viruses.

Ocular disorders with the greatest potential for benefit of gene therapy at the current time include hereditary ocular diseases, including Retinitis Pigmentosa, tumors such as retinoblastoma or melanoma, and acquired proliferative and neovascular retinal disorders. In the future, gene therapy has the potential for the replacement of defective gene products or introduction of new gene products into ocular cells. The selection of

appropriate target genes and cells will be critical, as will the development of a methodology for safe, targeted gene transfer.

Therapies of non-genetic nature, usage of growth-factors, cytokines and neurotrophins that inhabit the microenvironment of the photoreceptor cells have been promoted for therapeutic use. A great deal of study has been focussed on the basic fibroblast growth factor (BFGF) which has shown to delay photoreceptor degeneration in Royal College of Surgeons (RCS) rats and also to protect photoreceptor cells from damaging effects of constant light (Faktorovich *et al.* 1990)

The inherited retinal dystrophy observed in RCS rats is a widely used model for the study of the photoreceptor degeneration that occurs in Retinitis Pigmentosa and macular degeneration. The RPE fails to phagocytose shed outer segments and subsequently photoreceptors die. The visual cell degeneration is accompanied by an abnormal accumulation of microglial cells in the retina of RCS rats presenting the dystrophy. Recently, it has been shown that combined stimulation of RCS dystrophic retinal Muller glial (RMG) cells with interferon-gamma (IFN-gamma) and lipopolysaccharide (LPS) induced the release in culture supernatants of significantly higher amounts of tumor necrosis factor (TNF) and nitric oxide (NO) compared to nondystrophic congenic controls. The retinal dystrophy observed in RCS dystrophic rats could result from an abnormal reactivity of RMG and microglial cells to release TNF and NO in response to stimulants. The immunomodulatory cytokine TGF-beta and inhibitors of NOS could be negative regulators in the cytokine network and nitrite synthesis thus interfering with the development of photoreceptor cell death (de Kozak *et al.* 1997). Recently, a gene coding the receptor for Tyrosine kinase Mertk has been found deleted in RCS DNA samples. The deletion includes the splice acceptor site upstream of the second coding exon of Mertk and results in a shortened transcript lacking this exon. This aberrant transcript joins the first and third exon resulting in a frameshift and a translation termination 20 codons after the AUG thus indicating that this gene is responsible for the RCS defective phenotype (D'Cruz. *et al.*, 2000).

The eye is an attractive model for gene therapy due to ease of accessibility and well-defined anatomy. The ideal end stage of therapy would be the ability for the transgene to be functional within its specific cellular environment, in this case within the

photoreceptors, while being regulated by cell specific promoters and regulatory systems. Successful surgical access to the subretinal space is critical for achieving adenovirus-mediated gene transfer to the retinal pigment epithelial (RPE) cells or photoreceptor cells. An example of a surgical approach allowing an efficient delivery of recombinant replication-deficient adenoviral vectors into the subretinal space of newborn rats has been achieved by Ribeaudeau and colleagues in 1997 suggesting that this method may be useful for infecting reproducibly large areas of the RPE cell layer of normal newborn rats and should be applicable to RCS pups. Their group has also shown the feasibility of infecting ex vivo RPE cells in culture using the same recombinant adenoviral vector.

For the rescue of recessive mutations, the transfer of a normal copy of the gene should theoretically be sufficient to ease the condition. Nevertheless, for this method to be successful the gene has to be targeted to the correct cells and preferably integrate into the host genome to ensure long-lasting expression driven by the natural promoter and enhancer elements within the cell thus avoiding the need for repeated delivery of the transgene. On the contrary, for dominant disease the case is more complex, especially if the gene mutation has a dominant negative effect and the disease is due to haploinsufficiency. For such cases, it has been suggested that a similar mutant gene to be transferred in its reverse orientation into the affected cells to allow RNA-RNA hybrid arrest to occur, thus removing the mutant protein from expression (anti-sense RNA therapy) (Pepose and Leib, 1994). For genetically heterogeneous diseases like RP, the task is harder and in order to overcome such difficulties Millington-Ward and his group (1997) designed, and evaluated in vitro, three strategies which avoided a requirement to target individual mutations for genetic suppression. In the first, normal and mutant alleles were suppressed by targeting sequences in transcribed but untranslated regions of transcript (UTRs), enabling introduction of a replacement gene with the correct coding sequence but altered UTRs to prevent suppression. A second approach involved suppression in coding sequence and concurrent introduction of a replacement gene by exploiting the degeneracy of the genetic code. A third strategy utilised intragenic polymorphism to suppress the disease allele specifically, the advantage being that a proportion of patients with different disease mutations had the same polymorphism. These approaches provided a wider choice of target sequence than those directed to

207

single disease mutations and were appropriate for many mutations within a given gene. General methods for suppression may be directed towards the primary defect or a secondary effect associated with the disease process, such as apoptosis. Three general methods targeting the primary defect which circumvent problems of allelic genetic heterogeneity were explored *in vitro* using hammerhead ribozymes designed to target transcripts from the rhodopsin, peripherin and collagen 1A1 and 1A2 genes, extensive genetic heterogeneity being a feature of associated disease pathologies.

Ocular gene therapy is occupied with the testing of various viral derived vector systems for their ability to transfer the therapeutic gene into photoreceptor cells and various means of delivering the vector to the tissue in animal models. The viral vectors being tested are the adenovirus (AV), adeno associated virus (AAV) and herpes simplex (HSV1) based vectors. So far none of these vectors have managed to transduce sufficient numbers of photoreceptor cells or produce stable long lasting expression. It has been suggested that modified retroviral vectors which have low immunogenicity and the potential for integration into non dividing neural cells would be more effective as a vector (Wright, 1997b). Non-viral methods (i.e. liposomes and receptor-mediated endocytosis) for introducing genes into the retina are also being tested. These approaches are attractive as they circumvent some of the safety concerns raised by viral vectors and the risk of an immune response to the introduced vector proteins. As yet, only a few genes responsible for causing retinal degeneration have as yet had the research input to partake in gene therapy. These include Rhodospsin (RHO), peripherin/RDS and cGMP phosphodiesterase (PDEB) genes for which there are several mutations with known functional consequences and animal models for testing the feasibility of somatic gene therapy. Therefore, even though greatly promising as a therapeutic alternative to retinal degeneration, retinal gene therapy is still far from reaching its clinical trial stage and requires more basic research to ensure its safety and efficacy. Also, given the large number of mutations present for a disease, strategies of gene therapy aimed at correcting each individual mutation may be overwhelming and impractical.

Finally, therapeutic solutions may lie in that irrespective of the primary genetic lesion photoreceptor cell death is finally mediated by apoptosis. Strategies aimed at introducing a gene that would interfere with the cells' ability to carry out apoptosis is a

more practical approach since it could be applicable to multiple mutations. Over expression of *bcl*-2, which prevent apoptosis, in mice with retinal degeneration due to 3 different molecular causes have already been shown to result in increased photoreceptor survival (Chen *et al.* 1996).

However, the therapeutic utility of blocking cell death remains unclear as the question remains whether cells rescued from apoptosis can function. In an effort to answer this question, Davidson and Stellar (1998) expressed the baculoviral cell survival protein (which antagonises cell death by blocking cysteine proteases known as caspases) in *Drosophila* carrying retinal degeneration mutations in either *ninaE* (encoding for rhodopsin 1) and *rdgC* (encoding for a putative rhodopsin phosphatase). In both cases the retinal degeneration was prevented and behavioural tests on the ninaE mutant flies showed hat visual function was also preserved. By the time gene therapy is ready and applicable to humans as a therapeutic alternative on a more global scale hopefully it would be used in a strict and moral context.

References

Adams, M.D., Kelley, J.M., Gocayne, J.D., Dubnick, M., Polymeropoulos, M.H., Xiao, H., Merril, C.R., Wu, A., Olde, B. and Moreno R.F. (1991) Complementary DNA sequencing: expressed sequence tags and human genome project. *Science* **252**, 1651-1656.

Albertsen, H.M., Abderrahim, H., Cann, H.M., Dausset, J., LePaslier, D and Cohen. (1990) Construction and characterisation of a yeast artificial chromosome library containing haploid genome equivalents. *Proct. Natl. Acad. Sci. USA* **87** 4256-4260.

Allikmets, R., Shroyer, N.F., Singh, N., Seddon, J.M, Lewis, R.A., Bernstein, P.S., Peiffer, A., Zabriskie, N.A., Li, Y., Hutchinson, A., Dean, M., Lupski, J.R., Leppert, M. (1997a) Mutation of the Stargardt disease gene (ABCR) in age-related macular degeneration. *Sci.* **277**:1805-1807.

Allikmets, R., Singh, N., Sun, H., Shroyer, N.F., Hutchinson, A., Chidambaram, A., Gerrard, B., Baird, L., Stauffer, D., Peiffer, A., Rattner, A., Smallwood, P., Li, Y., Anderson, K.L., Lewis, A., Nathans, J., Leppert, M., Dean, M., Lupski, J.R. (1997b) A photoreceptor cell-specific ATP-binding transporter gene (ABCR) is mutated in recessive Stargardt macular dystrophy. *Nat. Genet.* **15**:236-246

Al-Maghtheh, A., Gregory, C., Inglehearn, C., Hardcastle, A., and Bhattacharya, S.S. (1993) Rhodopsin mutations in autosomal dominant retinitis pigmentosa. *Hum. Mutat.*, **2**, 249-255.

Altschul, S.F., Gish, W., Miller, W., Myers, E.W. and Lipman, D.J. (1990) Basic local alignment search tool. *J. Mol. Biol.* **215**, 403-410.

Amin, K.M., Scarpa, A.L., Winkelmann, J.C., Curtis, P.J. and Forget, B.G. (1993) The exon-intron organisation of the human erythroid beta-spectrin gene. *Genomics* **18**:118-25.

Anand, R., Riley, J.H., Butler, R., Smith, J.C. and Markham, A.F. (1990) A 3.5 genome equivalent multi-access YAC library: construction, characterisation, screening and storage. *Nucleic Acids Research* **18**, 1951-1956.

Anand, R., Villasante A and Tyler-Smith C. Construction of yeast artificial chromosome libraries with large inserts using pulse field gel electrophoresis. (1989) **17**(9):3425-33.

Anderson, D.H. and Fisher, S.K. (1976) The photoreceptor of diurnal squirrels: outer segment disc shedding and protein renewal. *J. Ultrastruct. Res.* **55**, 119.

Anderson, K.L, Baird, L., Lewis, R.A., Otterud, B., Lupski, J.R., Leppert, M. (1994). Genetic and physical location for Stargardt's disease and further evidence for genetic heterogeneity. *Am. J. Hum. Genet.* **55**:1477.

Apfelstedt-Sylla, E., Theischen, M. Ruther, K., Wedemann, H., Gal, A. and Zrenner, E. (1995) Extensive intrafamilial and interfamilial phenotypic variation among patients with autosomal dominant retinal dystrophy and mutations in the human peripherin/RDS gene. *Br. J. Ophthalmol.*, **79**, 28-34.

Arikawa, K., Molday, L.L., Molday, R.S., Williams, D. (1992). Localization of peripherin/rds in the disk membranes of cone and rod photoreceptors: relationship to disk membrane morphogenesis and retinal degeneration. *J. Cell Bio.* **116**:659-667.

Attwood, J., and Bryant, S. (1988) A computer programme to make analysis with LIPED and LINKAGE easier to perform and less prone to input errors. *Ann. Hum. Genet.*, **52**, 259.

Baehr, W., Devlin, M.J., Applebury, M.L. (1979). Isolation and characterization of cGMP phosphodiesterase from bovine rod outer segments. *J Biol Chem* 25;254(22):11699-77

Baehr, W., Morita, E.A., Swanson, R. J. and Applebury, M.L. (1982) Characterisation of bovine rod outer segment G-protein. *J. Biol. Chem.* **257**, 6452-6460.

Balciuniene, J., Johanssen, K., Sandgren, O., Wachmeister, L., Holmgren, G. and Forsman, G. (1995) A gene for autosomal dominant progressive cone dystrophy (CORD5) maps to chromosome 17p12-p13. *Genomics* **30**, 281-286.

Ballabio, A. (1993) The rise and fall of positional cloning. *Nat. Genet.* **3**, 277-279.

Banfi, S., Borsani, G., Ross, E., Bernard, L., Guffanti, A., Rubboli, F., Marchitiello, A., Giglio, S., Coluccia, E., Zollo, M., Zuffardi, O. and Ballabio, A. (1996) Identification of human cDNAs homologous to *Drosophila* mutant genes through EST database searching. *Nat. Genet.* **13**, 167-174.

Bassett, D.E., Boguski, M.S., Spence, F., Reeves, R., Kim, S., Weaver, T. and Hieter, P. (1997) Genome cross-referencing and XREFdb: Implications for the identification and analysis of genes mutated in human disease. *Nat. Genet.* **15**, 339-344.

Bauer, P.H., Muller, S., Puzicha, M., Pippig, S., Obermaier, B., Helmreich, E.J. and Lohse, M.J. (1992) Phosducin is a protein kinase A-regulated G-protein regulator. *Nature* **358**, 73-76.

Baylor, D. (1996) How photons start vision. *Proc. Natl. Acad. Sci. U.S.A.* **93**, 560-565.

Beckmann, J.S. and Weber, J.L. (1992) Survey of human and rat microsatellites. *Genomics* **12**, 627-631.

Bellanné-Chantelot, C. and 21 others (1992) Mapping the whole human genome by fingerprinting yeast artificial chromosomes. *Cell* **70**, 1059-1068.

Bellingham, J., Wilkie, S.E, Morris, A.G., Bowmaker, J.K., Hunt, D.M. (1997). Characterisation of the ultraviolet-sensitive opsin gene in the honeybee, Apis mellifera. *Eur J Biochem* 1997 Feb 1;**243**(3):775-81

Bender, W., Sperer, P. and Hogness, D.S. (1983) Chromosome walking and jumping to isolate DNA from the Ace and rosy loci and the bithorax complex in *Drosophila melanogaster. J. Mol. Biol.* **168**, 17-33.

Berchold, M.W., Egli, R., Rhyner, J.A., Hemeister, H., Strehler, E.E. (1993) Localisation of the human bona fida calmodulin genes CALM1, CALM2 and CALM3 to chromosome s 14q24-31, 2p21.1-p21.3 and 19q13.2-q13.3. *Genomics* **16** :461-465.

Bergen, A.A.B., van Schooneveld M.J., Orth U (1993a). Multipoint linkage analysis in X-linked juvenile retinoschisis. *Clin. Genet.* **43**:113-116.

Bergen, A.A.B., Pinckers, A.J.L.G (1997). Localization of a novel X-linked progressive cone dystrophy gene to Xq27: evidence for genetic heterogeneity. *Am. J. Hum. Genet.* **60**:1468-1473.

Bird, A.P. (1987), CpG islands as gene markers in the vertebrate nucleus. *Trend Genet* **3**(12): 342-347.

Birnboim, H.C. and Doly, J. (1979) A rapid alkaline extraction procedure for screening recombinant plasmid DNA. *Nuc. Acids. Res.* **7**, 1513-1523.

Bither, P.P., Berns, L.A. Dominant inheritance of Stargardt's disease. *J AM Optom Assoc.* 1988,**59**:112

Blattner, F.R., Plunkett, G., Bloch, C.A., Perna, N.T., Burlandm, V., Rileym M, Collado-Vides, J., Glasner, J.D., Rode, C.K., Mayhew, G.F., Gregor, J., Davis, N.W., Kirkpatrick, H.A., Goeden, M.A., Rose, D.J., Mau, B., Shao, Y. (1997). The complete genome sequence of Escherichia coli K-12. *Science* 5;**277**(5331):1453-74.

Boehnke, M., Lange, K. and Cox, D.R. (1991). Statistical methods for multipoint radiation hybrid mapping. *Am. J. Hum. Genet.* **49**: 1174-1188.

Boguski, M.S. and Schuler, G.D. (1995) ESTablishing the human transcript map.

Bok, D. (1985). Retinal photoreceptor-pigment epithelium interactions. *Invest. Ophthamol. Vis. Sci.* **26**, 1659-1694.

Botstein, D., White, R.L., Skolnick, M. and Davies, R.W. (1980) Construction of a genetic linkage map in man using restriction fragment length polymorphisms. *Am. J. Hum. Genet.* **32**: 314-331

Bourne, H.R., Sanders, D.A. and McCormic, F. (1990) The GTPase superfamily: a conserved switch for diverse cell function. *Nature* **348**, 125-132.

Bowes, C., Li, T., Danciger, M., Baxter, L.C., Applebury, M.L. and Farber D.B. (1990) Retinal degeneration in the *rd* mouse is caused by a defect in the beta subunit of rod cGMP-phosphodiesterase. *Nature* **347**, 677-680.

Bressler, N.M., Bressler, S.B. and Fine, S.L. (1988) Age-related macular degeneration. Surv. Ophthalmol., **32**, 375-413.

Buckler, A.J., Chang, D.D., Graw, S.L., Brook, D., Haber, D.A., Sharp, P.A. and Houseman, D.E. (1991) Exon amplification: a strategy to isolate mammalian genes based on RNA splicing. *Proc. Natl. Acad. Sci. USA* **88**, 4005-4009.

Buetow, K.H., Weber, J.L., Ludwigsen, S., Scherpbier-Heddema, T., Duyk, G.M., Sheffield, V.C., Wang, Z. and Murray, J.C. (1994) Integrated human genome-wide maps constructed using the CEPH reference panel. *Nat. Genetics* **6**, 391-393.

212

Bukall, B., Marknell T., Ingvast S., Koisti MJ., Sandgren O., Li W., Bergen AA., Andreasson S., Rosenberg T., Petrukhin K., Wadelius C. (1999) The mutation spectrum of the bestrophin protein-functional implications. *Hum Genet* **104**(5):383-9.

Burke, D.T., Carle, G.F. and Olson, M.V. (1987) Cloning of large segments of exogenous DNA into yeast by means of artificial chromosome vectors. *Science* **236**, 806-813.

Burmeister, M., Monaco, A.P., Gillard, E.F., Van Ommen, G.B., Affara, N.A., Ferguson-Smith, M.A., Kunkel, L.M. and Lehrach, H. (1988) A 10-megabase physical map of human Xp21, including the Duchenne muscular dystrophy gene. *Genomics* **2**, 189-202.

Calogne, M.J, Ndal, M., Calvano, S., Testar, X., Zelante, L., Zorano, A., Estivill, X., Gasparini, P., Palacin, M., and Nunes, V. (1995). Assignment of the gene responsible for cystinuria (rBAT) and of markers D2S119 and D2S177 to 2p16 by fluorescence in situ hybridisation. *Hum Genet.* 1995 (6):633-6.

Capon, M.R.C., Marshall, J., Krafft, J. I., Alexander, R. A., Hiscott, P.S. and Bird, A.C. (1988). Sorsbys fundus dystrophy: a light and electron microscopic study: *Ophthalmology* **96**: 1769-1777.

Carle, G.F. and Olson, M.V. (1984) Separation of chromosomal DNA molecules from yeast by orthogonal-field-alteration gel electrophoresis. *Nuc. Acids. Res.* **12**, 5647-5664.

Carmi, R., Rokhlina, T., Kwitek-Black, A., Elbedour, K., Nishimura, D., Stone, E.M. and Sheffield, V.C (1995) Use of a DNA pooling strategy to identify a human obesity syndrome locus on chromosome 15. *Hum Mol. Genet.* **4**, 9-13.

Chang, G.Q., Hao, Y. and Wong, F. (1993) Apoptosis: final common pathway of photoreceptor death in *rd, rds* and rhodopsin mutant mice. *Neuron* **11**, 595-605.

Chang, J.G., Scarpa, A., Eddy, R, L., Byers, M.G., Harris, A. S, Morrow, J. S., Watkins, P., Shows, T. B., and Forget, B.G. (1993) Cloning a portion of the chromosomal gene and cDNA for human ß-fodrin, the non-erythroid form of ß-spectrin . *Genomics*, **17**, 287-293.

Chen, C.K., Inglese, J., Lefkowitz, R.J. and Hurley, J.B. (1995a) Ca (2+)-dependent interaction of recoverin with rhodopsin kinase. *J. Biol. Chem.* **270**, 18060-18066.

Chen, J., Flannery, J.G., LaVail, M.M., Steinberg, R.H., Xu, J. and Simon, M.I. (1996) bcl-2 overexpression reduces apoptotic photoreceptor cell death in three different retinal degenerations. *Proc. Natl. Acad. Sci. U.S.A.* **93**, 7042-7047.

Chen, T. Y., Peng, Y. W., Dhallan, R. S., Ahamed, B., Reed, R.R. and Yau, K.W. (1993) A new subunit of the cyclic nucleotide-gated cation channel in retinal rods. *Nature* **362**, 764-767.

Chumakov, I. and 35 others. (1992) Continuum of overlapping clones spanning the entire human chromosome 21q. *Nature* **359**, 380-387.

Chumakov, I. M., Rigault, P., Le Gall, I., Bellanne-Chantelot, C., Billault, A., Gillou, S., Soularue, P., Guasconi, G., Poullier, E., Gros, I.,Belova, M., Sambucy, J.-L., Susini, L., Gervy, P., gilbert, F., Beaufils, S., Bui, H., Massart, C., De Tand, M. -F., Dukasz, F., Lecoulant, S., Ougen, P., Perrot, V., Saumier, M., Soravit, C., Bahouayila, R., Cohen-Akenine, A., Barillot, E.,

Bertrand, S., Codani, J.-J., Caterina, D., Georges, I., Lacroix, B., Lucotte, G., Sahbatou, M., Schmit, C., Sangouard, M., Tubacher, E., Dib, C., FaureS., Fizames, C., Gyapay, G., Millasseau, P., Nguyen, S., Muselet, D., Vignal, A., Morissette, J., Menninger, J., Lieman, J., Desai, T., Banks, A., Bray-Ward, P., Ward, D., Hudson, T., Gerety, S., Foote, S., Stein, L., Page, D. C., Lander, E. S., Weissenbach, J., Paslier, D., and Cohen, D. (1995) A YAC contig map of the human genome. *Nature,* **377**(suppl.), 175-297.

Cibis, G.W., Morey, M., Harris, D.J. Dominantly inherited macular dystrophy with flecks (Stargardt). *Arch Ophthalmol.* **198**: 1785-1789.

Coffey, A.J., Roberts, R.G., Green, E.D., Cole, C.G., Butler, R., Anand, R., Giannelli, F. and Bently, D.R. (1992) Construction of a 2.6 Mb contig in yeast artificial chromosomes spanning the human dystrophin gene using an STS-based approach. *Genomics* **12**, 474-484.

Cohen, A.I. (1983) Some cytological and initial biochemical observations on photoreceptors in retina of *rds* mice. *Invest. Ophthal. Vis. Sci.* **24**, 9677-9688.

Collins, F.S. (1995) Positional cloning moves from perditional to traditional. *Nat. Genet.* **4**, 347-350.

Collins, R.J., Harmon, B.V., Gobe, G.C. and Kerr, J.F. (1992) Internucleosomal DNA cleavage should not be the sole criterion for identifying apoptosis. *Int. J. Radiat. Biol.* **61**, 451-453.

Collins, T. (1913) A pathological report on a case of Doyne's chorodoitis ('honeycomb' or 'family chorodoitis'). *Ophthalmoscope,* **11**, 537-538.

Connell, G.J., Bascom R, Molday L, Reid D, McInnes RR, Molday RS (1991). Photoreceptor peripherin is the normal product of the gene responsible for retinal degeneration in the rds mouse. *Proc. Natl. Acad. Sci.* USA **38**:723-726.

Cook, N.J., Molday, L.L., Reid, D., Kaupp, U.B. and Molday, R.S. (1989) The cGMP-gated channel of bovine rod photoreceptors is localised exclusively in the plasma membrane. *J. Biol. Chem.* **264**, 6996-6999.

Coulson, A., Sulston, J., Brenner, S. and Karn, L. (1986) Toward a physical map of the genome of nematode *Caenorhabditis elegans. Proc. Natl.Acad. Sci. USA* **83**, 7821-7825.

Cox, D.R., Burmeister, M., Price, E.R., Kim, S. and Myers, R.M. (1990) Radiation hybrid mapping: a somatic cell genetics method for constructing high resolution maps of mammalian chromosomes. *Science* **250**, 245-250.

Cox, S., Bryant, S.P., Collins, A., Weissenbach, J., Donnis-Keller, H., Koelman, B.P.C., Steinkasserer, A., and Spurr, N.K. (1995) Integrated map of human chromosome 2. *Ann. Hum. Genet.,* **59**, 413-434.

Craig, J.M. and Bickmore, W.A. (1994) The distribution of CpG islands in mammalian chromosomes. *Nat. Genet.* **7**, 376-381.

Curtis, D., Robertson, M.M and Gurling, H.M (1992) Autosomal dominant gene transmission in a large kindred with Gilles de la Tourette syndrome. Br. J. Psychiatry. **160**:845-9.

Daiger, S.P., McGuire, R.E., Sullivan, L.S., Sohocki, M.M., Blanton, S.H., Humphries P., Green, Mintz-Hittner, H., Heckenlively, J.R. (1997). Progress in positional cloning of RP10 (7q31.3), RP1 (8q11-q21) and VMD1 (8q24). In 'Degenerative Retinal Diseases', LaVail, et al. eds, *Plenum Press*.

Dacey, D.M. and Lee, B.B. (1994) The 'blue-on' opponent pathway in primate retina originates from a distinct bistratified ganglion cell type. *Nature* **367**, 731-735.

Dash-Modi, A., Seymour, A.B., Stefko, T., Mah, T., Shaffer-Gordon, M., Ferrell Re, Gorin, M.B. (1996). Localization of X-linked cone-rod dystrophy (DOD-1) to a limited region of Xp11.4-p11.3 that encompasses the RP2 locus. *Invest. Ophthalmol. Vis. Sci.* **37**:998.

Davidson, F.F. and Stellar, H. (1998) Blocking apoptosis prevents blindness in Drosophila retinal degeneration mutants. *Nature* **391**, 587-591.

D'Cruz, P.M, Yasumura, D., Weir, J., Matthes, M.T., Abderrahim, H., LaVail, M.M, Vollrath, D. (2000). Mutation of the receptor tyrosine kinase gene Mertk in the retinal dystrophic RCS rat. *Hum Mol Genet* 1;9(4):645-651.

de Kozak Y, Cotinet, A., Goureau, O., Hicks, D. and Thillaye-Goldenberg, B.(1997) Tumor necrosis factor and nitric oxide production by resident retinal glial cells from rats presenting hereditary retinal degeneration. *Ocul Immunol Inflamm* Jun;5(2):85-94.

De La Paz, M.A., Lewis, R.A., Patrinely, J.R., Merin, L., Greenberg, F. (1991). A sibship with unusual anomalies of the eye and skeleton (Michels' syndrome) *Am J Ophthalmol* 112(5):572-80.

De la Paz, M.A., Itoh, Y., Toth, C.A. and Nagase, H. (1998) Matrix metalloproteinases and their inhibitors in human vitreous. *IOVS* 39(7):1256-1260.

Deterre, P., Bigay, J., Forquet, F., Robert, M. and Chabre, M. (1988) cGMP phosphodiesterase of retinal rods is regulated by two inhibitory subunits. *Proc. Natl. Acad. Sci. USA* **85**, 2424-2428.

Dib, C., Faure, S., Fizames, C., Samson, D., Drouot, N., Vignal, A., Millasseau, P., Marc, S., Hazan, J., Seboun, E., Lathrop, M., Gyapay, G., Morissette, J. and Weissenbach, J. (1996) A comprehensive genetic map of the human genome based on 5,264 microsatellites. *Nature* **380**, 152-154.

Dizhoor, A.M., Ray, S., Kumar, S., Niemi, G., Spencer, M., Brolley, D., Walsh, K.A., Philipov, P.P., Hurley, J.B. and Stryer, L. (1991) Recoverin: a calcium sensitive activator of retinal rod guanylyl cyclase. *Science* **251**, 915-918.

Dizhoor, A.M., Lowe, D.G., Olshevskaya, E.V., Laura, R.P., Hurley, J.B. (1994). The human photoreceptor membrane guanylyl cyclase, RetGC, is present in outer segments and is regulated by calcium and a soluble activator. *Neuron.* Jun;12(6):1345-52.

Dizhoor, A.M., Olshevskaya, E.V., Henzel, W.J., Wong, S.C., Stults, J.T. Ankoudinova, I., Hurley, J.B. (1995). Cloning, sequencing, and expression of a 24-kDa Ca(2+)-binding protein activating photoreceptor guanylyl cyclase. J Biol Chem Oct 20;**270**(42):25200-6.

215

Dodt, G., Braveman, N., Valle, D. and Gould, S.J. (1996) From expressed sequence tags to peroxisome biogenesis disorder genes. *Proc. NY. Acad. Sci.* **804**, 516-523.

Donis-Keller, H. and 32 others (1987) A genetic linkage map of the human genome. *Cell* **51**, 319-337.

Dowdy, S.F., Scanlon, D.J., Fasching, C.L., Casey, G. and Stanbridge, E.J. (1990) Irradiation microcell-mediated chromosome transfer (XMMCT): the generation of specific chromosomal arm deletions. *Genes Chromosome Cancer* **2**, 318-327.

Dowling, J.E. (1960) Chemistry of visual adaptation in the rat. *Exp. Eye Res.* **3**, 348-356.
Downing, J.P. and Zimmerman, A.L. (1995) *J. Physiol.* **486**, 533-546.

Doyne, R.W., (1910) A note on fanily chorodoitis. *Trans. Ophthalmol. Soc. UK.*, **30**, 93-95.

Dryja, T.P., Hahn, L.B., Kajiwara, K., Berson, E.L. (1997). Dominant and digenic mutations in the peripherin/RDS and ROM1 genes in retinitis pigmentosa. *Invest. Ophthalmol. Vis. Sci.* **18**:1972-1982.

D'Urso, M., Zucchi, I., Ciccodicola, A., Palmieri, G., Abidi, F.E. and Schlessinger, D. (1990) Human glucose 6-phosphate dehydrogenase gene carried on a yeast artificial chromosome encodes active enzyme in monkey cells. *Genomics* **7**, 531-534.

Duyk, G.M., Kim, S.W., Myers, R.M. and Cox, D.R. (1990) Exon trapping: a genetic screen to identify candidate transcribed sequences in cloned mammalian genomic DNA. *Proc. Natl. Acad. Sci. U.S.A* **87**, 8995-8999.

Edwards, A.O., Klein, M.L., Berselli, B., Hejtmancik, J.F., Rust, K., Wirtz, M. K., Weleber, R.G., and Acott, T.S. (1998) Malattia leventinese: refinement of the genetic locus and phenotypic variabilty in autosomal dominant macular drusen. *Am.J. Ophthalmol.* **126**(3): 417-24.

Evans, G.A. and Lewis, K.A. (1989) Physical mapping of complex genomes by cosmid multiplex analysis. *Proc. Natl .Acad. Sci. USA* **86**, 5030-5034.

Evans, J. and Wormald, R. (1996) Is the incidence of registrable age-related macular degeneration increasing? *Br. J. Ophthalmol.*, **80**, 9-14.

Evans, K., Fryer A., Ingleheam, C., Duvall-Young, J., Whittaker, J. L., Gregory, C. Y., Butler, R., Ebenezer, N., Hunt, D. M. and Bhattacharya S. (1994) Genetic linkage of Cone-rod retinal dystrophy to chromosome 19q and evidence for segragation distortion. *Nature Genet.*, **6**, 210-213.

Evans K, Duvall-Young J, Fitzke FW, Arden GB, Bhattacharya SS, Bird AC (1995). Chromosome 19q cone-rod retinal dystrophy.Ocular phenotype. *Arch. Ophthalmol.* **113**:195-201

Evans, K., Gregory, C.Y., Wijesuriya, S.D., Kermani, S., Jay, M.R., Plant, C., Bird, A.C. Assessment of the phenotypic range seen in Doyne honeycomb retinal dystrophy. *Archives of Ophthalmology.* 1997, Vol. **115**, 904-910.

Faktorovich, E.G., Steinberg, R.H., Yasumura, D., Matthes, M.T. and LaVail, M.M. (1992) Basic fibroblast growth factor and local injury protect photoreceptors from light damage in the rat. *J Neurosci* **12**(9):3554-67.

Farber, D.B. (1995). From mice to men: the cyclic GMP phosphodiesterase gene in vision and disease. *Invest. Ophthal. Vis., Sci.* **36**, 263-275.

Farrar, G.J., Kenna P, Jordan SA, Kumar-Singh R, Humphries P (1991). A sequence polymorphism in the human peripherin/RDS gene. *Nucleic Acids Res* **25**;19(24):6982

Fastman, K.H., Cuticchia, A, J., and Kinsbury, D.T., (1994) The GDB ™ human genome. *Nucleic Acids Res.* **22**, 3462-3469.

Felbor, U., Stohr, H., Amann, T., Schonherr, U., and Weber, B.H. (1995) A novel Ser156Cys mutation in the tissue inhibitor of metalloproteinase-3 (TIMP) in Sorsby's fundus with unusual clinical features . *Hum. Mol. Genet.*, **4**, 2415-2416.

Felbor, U., Suvanto, E.A., Forsius, H.R., Eriksson, A.W., Weber, B.H.F. (1997). Autosomal recessive Sorsby fundus dystrophy revisited: molecular evidence for dominant inheritance. *Am. J. Hum. Genet.* **60**:57-62.

Felbor, U., Schilling, H., Weber, B.H.F. (1997a). Adult vitelliform macular dystrophy is frequently associated with mutations in the peripherin/RDS gene. *Hum. Mutat.* **10**:301-309.

Ferrell, R.E., Hittner, H.M., and Antoszyk, J.H. 1983, *Am. J. Hum.* Genet. **35**,78-84.

Fesenko, E.E., Kolesnikov, S.S. and Lyubarsky, A.L. (1985) Induction by cGMP of cationic conductance in plasma membrane of retinal rod outer segments. *Nature* **313**, 310-313.

Fornerod, M., Baal, S., Valentine, V., Shapiro, D.N., and Grosveld, G. (1997) Chromosomal localisation of genes encoding CAN/Nup214-Interacting proteins-human CRM1 localises to 2p16, whereas Nup88 localises to 17p13 and is physically linked to SF2p32. *Genomics* **42**:538-540.

Forsman, K., Graff, C., Nordstrom, S., Johansson, K., Westermark, E., Lundgren, E., Gustavson, K.H., Wadelius, C., Holmgren, G. (1992). The gene for Best's macular dystrophy is located at 11q13 in a Swedish family. *Clin. Genet.* **42**:156-159.

Freund, C.L., and 16 others (1997) Cone-rod dystrophy due to mutations in a novel photoreceptor-specific homeobox gene (*CRX*) essential for maintenance of the photoreceptor. *Cell* **91**, 543-553.

Freund, C.L., Wang, Q-L., Chen, S., Muskat, B.L., Wiles, C.D., Sheffield, V.C., Jacobson, S.G., McInnes, R.R., Zack, D.J and Stone, E.M. (1998) De novo mutations in the CRX homeobox gene associated with Leber congenital amaurosis. *Nat. Genet.* **18**, 311-312.

Fulton, T.R., Bowcock, A.M., Smith, D.R., Daneshvar, L., Green, P., Cavalli-Sforza, L.L. and Donis-Keller, H. (1989) A 12 megabase restriction map at the cystic fibrosis locus. *Nucleic Acids Res.* **17**, 271-284.

Fung, B.K., Navon, S.E. (1987). Mapping the binding sites of transducin by sequence homology, chemical modification, and by using monoclonal antibodies. *Biochem Soc Trans* Feb;15(1):39-42.

Fung, B.K, Young, J.F., Yamane, H.K. and Griswol-Prenner, I. (1990) Subunit stoichiometry of retinal rod cGMP phosphodiesterase. *Biochemistry* 29, 2657-2664.

Furukawa, T., Morrow, E.M. and Cepko, C. L. (1997) *Crx*, a novel *otx*-like homeobox gene, shows photoreceptor-specific expression and regulates photoreceptor differentiation. *Cell* 91, 531-541.

Gerber, S., Rozet, J.M., Bonneau, D., Souied, E., Camuzat, A., Dufier, J.L., Amalric, P., Weissenbach, J., Munnich, A., Kaplan, J. (1995). A gene for late-onset fundus flavimaculatus with macular dystrophy maps to chromosome 1p13. *Am. J. Hum. Genet.* 56:396-399.

Gerber, S., Rozet, J.M., van de Pol, T.J.R., Hoyng, C.B., Marker, C.B., Munnich, A. Blankenagel, Kaplan. J., Cremers. F.P.M. (1998). Complete exon-intron structure of the retina-specific ATP binding transporter gene (ABCR) allows the identification of novel mutations underlying Stargardt disease. *Genomics* 48:139-142.

Gessler, M., Poustka, A., Cavenee, W., Neve, R.L., Orkin, S.H. and Bruns, G.A.P. (1990) Homozygous deletion in Wilms tumours of a zinc finger gene identified by chromosome jumping. *Nature* 343, 774-778.

Gillett, G.T., McConville, C.M., Byrd, P.J., Stankovic, T., Taylor, A.M., Hunt, D.M., West, L.F., Fox, M.F., Povey, S. and Benham, F.J. (1993) Irradiation hybrids for human chromosome 11: characterisation and use for generating region specific markers in 11q14-q23. *Genomics* 15, 332-341.

Goffeau, A., Barrel, B.G., Bussey, R.W., Davies, W., Dujon, B., Feldmann, H., Gailbert, F., Hoheisel, J.D., Jacq, C., Johnston, M., Louis, E.J., Mewes, H.W., Murakami, Y., Philippsen, P., Tettelin, H. and Oliver, S.G. (1996) Life with 6000 genes. *Science* 274, 546-567.

Goldberg, H. Goldberg's genetic and metabolic eye diseases, 2nd Ed, William Andrew Renee, USA, pp81-99 (1986)

Gorczyca, W.A., Polans, A.S., Surgucheva, I.G., Subbaraya, I., Baehr, W., Palczewski, K. Guanylyl cyclase activating protein (1995). A calcium-sensitive regulator of phototransduction. *J Biol Chem* 15;270(37):22029-36.

Gorodovikova, E.N., and Philippov, P.P. (1993) the presence of a calcium-sensitive p26-containing complex in bovine retina rod cells. *FEBS Lett.* 335, 277-279.

Gorodovikova, E.N., Gimelbrandt, A.A., Senin, I.I. and Philippov, P.P. (1994) Recoverin mediates the calcium effect upon rhodopsin phosphorylation and cGMP hydrolysis in bovine retina rod cells. *FEBS Lett.* 349, 187-190.

Goss, S.J. and Harris, H. (1975) New method for mapping genes in human chromosomes. *Nature* 255, 680-684.

Graff, C., Forsman, K., Larsson, C., Nordström, S., Lind, L., Johansson, K., Sandgren, O., Weissenbach, J., Holmgren. G., Gustavson, K.H., Wadelius, C. (1994). Fine mapping of Best's

218

macular dystrophy localizes the gene in close proximity to but distinct from the D11S480/ROM1 loci. *Genomics* **24**:425-434.

Graff, C., Eriksson, A., Forsman, K., Sandgren, O., Holmgren, G., and Wadelius, C. (1997). Refined genetic localisation of the Best disease gene in 11q13 and physical mapping of linked markers on radiation hybrids. *Hum Genet.* **101**: 263-270.

Gray-Keller, M.P., Polans, A.S., Palczewski, K. and Detweiler, P.B. (1993) The effect of recoverin-like calcium binding proteins on the photoresponse of retinal rods. *Neuron* **10**, 523-531.

Green, E.D. and Olson, M.V. (1990) Chromosomal region of the cystic fibrosis gene in yeast artificial chromosomes: a model for human genome mapping. *Science* **250**, 94-98.

Green, R.C., Narod, S. A., Morasse, J., Young, T-L., Cox, J., Fitzgerald, G. W. N., Tonin, P., Ginsburg, O., Miller, S., Jothy, S., Poitras, P., Laframboise, R., Routhier, G., Plante, M., Morissette, J., Weissenbach, J., Khandjian, E.W. and Rousseau, F. (1994) Hereditary nonpolyposis colon cancer: analysis of linkage to 2p15-16 places the COCA1 locus telomeric to D2S123 and reveals genetic heterogeneity in seven Canadian families. *Am. J. Hum. Genet.* **54**, 1067-1077.

Gregory, C.Y., Evans, E.,Wijesuriya, S.D., Kermani, S., Jay, M.J., Plant, C., Cox, N., Bird, S.C., and Bhattacharya, S. The gene responsible for autosomal dominant Doyne's honeycomb retinal dystrophy (DHRD) maps to chromosome 2p16. *Hum. Mol. Genet.* 1996, Vol. 5, No. 7, 1055-1059.

Gregory, C.Y., Evans, K., Whittaker, J.L., Fryer, A., Weissenbach, J. and Bhattacharya, S.S. (1994) Refinement of the cone-rod retinal dystrophy locus on chromosome 19q. *Am. J. Hum. Genet.* **55**, 1061-1063.

Gregory-Evans, K., and Bhattacharya S.S. (1998) Genetic blindness: current concepts in the pathogenesis of human outer retinal dystrophies. *Trends Genet.* **14** (3):103-8.

Griesinger, I.B., Sieving, P.A., Ayyagari, R. (2000). Autosomal dominant macular atrophy at 6q14 excludes CORD7 and MCDR1/PBCRA loci. *Invest. Ophthalmol. Vis. Sci.* **41**:248-255.

Gu, S., Thompson, D.A., Srikumari, S., Lorenz, B., Finckh, U., Nicoletti, A., Murthy, K.R., Rathmann, M., Kumaramanickavel, G., Denton. M.J. and Gal, A. (1997) Mutations in RPE65 cause autosomal recessive childhood onset severe retinal dystrophy. *Nat. Genet.*. **17**, 194-197.

Gunderson, D., Orlowski, J., and Rodriguez-Boulan, E., (1991) Apical polarity of Na K-AtPase in retinal pigment is linked to a reversal of the ankyrin fodrin submembrane cytoskeleton. *J. Cell Biology* **112** (5): 863-872.

Gyapay, G., Morissette, J., Vignal , A., Dib, C., Fizames C., Millasseau P., Marc, S., Bernardi, G., Lathrop, M. and Weissenbach, J. (1994) The 1993-94 Généthon human genetc linkage map. *Nat. Genet.,* **7**, 246-249.

Gyapay, G., Morissette, J., Vignal, A., Dib, C., Fizames, C., Millasseau, P., Marc, S., Bernardi, G., Lathrop, M., and Weissenbach, J. (1996) The Généthon human genetic linkage map. *Nat. Genet.,* **7**, 246-335.

Hargrave, P.A., Fong, S-L., McDowell, J.H., Mas, M.T., Curtis, D.R., Wang, J.K., Juszczak, E. and Smith, D.P. (1980) The partial primary structure of bovine rhodopsin and its topography in the retinal rod cell disc membrane. *Neurochem. Int.* 1, 231-244.

Hargrave, P.A., McDowell, J.H., Feldmann, R.J., Atkinson, P.H., Rao, J.K., Argos, P. (1984). Rhodopsin's protein and carbohydrate structure: selected aspects. *Vision Res*;24(11):1487-99.

Hargrave, P.A. Methods in Neurosciences : Photoreceptor Cells (1996-book).

Heiba, I.M., Elston, R.C., Klein, B.E.K. and Klein, R. (1994) Sibling correlations and segragation analysis of age-related maculopathy: The Beaver Dam Eye Study. *Gen.Epidemiol.*, 11, 51-67.

Heon, E., Piguet, B., Munier, F., Sneed, S. R., Morgan, C. M., Forni, S., Pescia, G., Schorderet, D., Taylor, C. M., Streb, L. M., Wiles, C. D., Nishimura, D. Y., Sheffield, V. C. and Stone, E. M. (1996) Linkage of autosomal dominant radial drusen (malattia leventinese) to chromosome 2p16-21. *Arch. Ophthalmol.*, 114, 193-198.

Héon E, Piguet B, Munier F, Sneed SR, Morgan CM, Forni S, Schorderet D, Polk TD, Taylor CM, Streb LM, Wiles CD, Nishimura DY, Sheffield VC, Stone EM. Clinical and haplotypic characterization of 14 families affected with radial drusen (malattia leventinese). *Invest. Ophthalmol. Vis. Sci.* 37:1124 (1996a).

Herrmann, B.G., Labeit, S., Poustka, A., King, T.R. and Lehrach, H. (1990) Cloning of the T gene required in mesoderm formation in the mouse. *Nature* 343, 617-622.

Hieter, P., Bassett, D.E. and Valle, D. (1996) The yeast genome- a common currency. *Nat. Genet.* 13, 253-255.

Hogan, M.J., Wood, I. and Steinberg, R.H. (1974) Phagocytosis by pigment epithelium of human retinal cones. *Nature* 252, 305.

Hoheisel, J.D., Maier, E., Mott, E., McCarthy, L., Grigoriev, A.V., Schalkwyk, L.C., Nizetic, D., Francis, F. and Lehrach, H. (1993) High resolution cosmid and P1 maps spanning the 14 Mb genome of fission yeast *S. pombe*. *Cell* 73, 109-120.

Holthouse, E. H. and Batten, R. D. (1897) A case of superficial chorioretinitis of peculiar form and doubtful causation. *Trans. Ophthalmol. Soc. UK*, 17, 62-63.

Holz, F. G., Wolfensberger, T.J., Piguet, B., Gross-Jendroska, M., Wells, J.A., Minassian, D.C., Chisholm, I.H. and Bird, A.C. (1994) Bilateral macular drusen in age-related macular degeneration. *Ophthalmology*, 101, 1522-1528.

Hou, Y., Richards, J.E., Bingham, E., Pawar, H., Scott, K., Lunetta, K. L., Boehnke, M., and Sieving, P. (1996). Linkage study of Best vitelliform macular dystrophy (VMD2) in a large North American family. *Hum Hered.* 46: 211-220.

Hoyng, C. B., Heutink, P., Deutman, A. F., and Oostra, B. A. (1995) A mutation in codon 142 in central areolar choroidal dystrophy. *Invest. Ophthalmol. Vis. Sci.*, 36 (Suppl), 3817.

Hu, R., Watanabe, M., amd bennet, V. (1992) Characterisation of human brain cDNA encoding the general isoform of β-Spectrin. *J.Bio. Chem.* **267**(15):18715-18722.

Humphries, M.M., Rancourt, D., Farrar, D., GJ., Kenna, P., Hazel, M., Bush, RA., Seiving, P., Sheils, DM., McNally, N., Creighton, P., Erven, A., Boros, A., Gulya, K., Capecchi, MR. And Humphries, P. (1997) Retinopathy induced in mice by targeted disruption of the rhodopsin gene. *Nat.Genet.***15**,216-219.

Huopaniemi L., Rantala, A., Tahvanainen, E., de la Chapelle, A., Alitalo, T. (1997). Linkage disequilibrium and physical mapping of X-linked juvenile retinoschesis. *Am. J. Hum. Genet.* **60**:1139-1149.

Hsu, Y-T. and Molday, R. S., (1993) Modulation of the cGMP-gated channel of rod photoreceptor cells by calmodulin. *Nature*, **361**, 76-79.

Huang, P.C., Gaitan, A.E., Hao, Y., Petters, R.M. and Wong, F. (1993) Cellular interactions implicated in the mechanism of photoreceptor degeneration in transgenic mice expressing a mutant rhodopsin gene. *Proc. Natl. Acad. Sci. U.S.A.* **90**, 8484-8488.

Hudson, T. and 50 others. (1995) An STS-based map of the Human Genome. *Science* **270**, 1945-1954.

Hurley, J.B., Dizhoor, A.M., Ray, S. and Stryer, L. (1993) Recoverin's role: conclusion withdrawn. *Science* **260**, 740.

Hutchinson, J. and Tay, W. (1875) Symmetrical central chorioretinal disease occurring in senile persons. *R. London Ophthalmol. Hosp. Rep.*, **8**, 231-244.

Huxley, C., Hagino, Y., Schlessinger, D. and Olson, M.V. (1991) The human HPRT gene on a yeast artificial chromosome is functional when transferred to mouse cells by cell fusion. *Genomics* **9**, 742-750.

Igekawa, S., Toda, T., Okui, K. and Nakamura, Y. (1996) Structure and chromosomal assignment of the human S1-5 gene (*FBNL*) that is highly homologous to Fibrillin. *Genomics* **35**: 590-592

Illing, M., Colville CA., William AJ., and Molday RS (1994) Sequencing cloning and characterisation of a third subunit of the cyclic nucleotide gated channel complex of rod outer segments. *Invest. Ophthal. Vis. Sci.* **35**, 1474 (no 1022).

Ioannou, P.A. and de Jong, P.J. (1996) Construction of Bacterial Artificial chromosome Libraries using the modified P1 (PAC) System. In Current Protocols in Human Genetics. (eds. Dracolpoli *et al.*), Unit 5.15. John Wiley and Sons, NY.

Ioannou, P.A., Amemiya, C.T., Garnes, J., Kroisel, P.M., Shizuya, H., Chen, C., Batzer, M.A. and de Jong, P.J. (1994) A new bacteriophage P1-derived vector for the propagation of large human DNA fragments. *Nat. Genetics* **6**, 84-89.

Jacobson, S.G., Cideciyan, A.V., Regunath, G., Rodriguez, F.J., Vandenburgh, K., Sheffield, V.C., Stone, E.M. (1995). Night blindness in Sorsby's funds dystrophy reversed by vitamin A. *Nat. Genet.* **11**:27-32.

Jordan, S.A., Farrar, G.J., Kumar-Singh, R., Kenna, P., Huphries, M.M., Allamand, V., Sharp, E.M., Humphries, P. (1992a). Autosomal dominant retinitis pigmentosa (adRP; RP6): cosegregation of RP6 and the peripherin-RDS locus in a late-onset family of Irish origin. *Am. J. Hum. Genet.* **50**:634-639.

Jay, M. (1995) Ophthalmic genetics: a genealogical guide to sources in England and Wales, *J. Med. Genet.*, **32**, 946-950.

Jeffreys, A.J., Wilson, V. and Thein, S.L. (1985) Hypervariable 'minisatellite' regions in human DNA. *Nature*. **314**, 67-73.

Kajiwara, K., Hahn, L.B., Mukai, S., Travis, G.H., Berson, E.L., Dryja, T.P. (1991). Mutations in the human retinal degeneration slow gene in autosomal dominant retinitis pigmentosa. *Naure.* **354**:480-483.

Kaplan, J., Gerber, S., Larget-Piet, D., *et al.* (1993). A Gene for Stargardt's disease (fundus flavimaculatu) maps to the short arm of chromosome 1. *Nature Genet.* **5**:308-311.

Kaplan, J., Gerber, S., Roset, J.M., Souied, E., Bonneau, D., Dufier, J.L., Munnich, A. (1994). Late-onset Stargardt-like macular dystrophy maps to chromosome 1p13. *Am. J. Hum. Genet.* **55**:190.

Kawamura, S. and Murakami, M. (1991) Calcium-dependent regulation of cyclic GMP phosphodiesterase by a protein from frog retinal rods. *Nature* **349**, 420-423.

Kawamura, S., Hisatomi, O., Kayada, S., Tokunaga, F. and Kuo, C.H. (1993) Recoverin has S-modulin activity in frog rods. *J. Biol. Chem.* **268**, 14579-14582.

Keen, T. J., et al. A YAC contig spanning the dominant retinitis pigmentosa locus (RP9) on chromosome 7p. Genomics 1995 Aug 10;28(3):383-8.

Keen, T. J., Inglehearn, C. F., Kim, R.,Bird, A. C., and Bhattacharya, S. (1994) Retinal pattern dystrophy associated with a 4bp insertion at codon 140 in the RDS-peripherin gene. *Hum. Mol. Genet.*, **3**, 367-368.

Kelsell, R.E., Godley, B.F., Evans, K., Tiffin, P.A.C., Gregory, C.Y., Plant, C., Moore, A.T., Bird, A.C., Hunt, D.M. (1995). Localization of the gene for progressive bifocal chorioretinal atrophy (PBCRA) to chromosome 6q. *Hum. Mol. Genet.* **4**:1653-1656.

Kelsell, R.E., Evans, K., Gregory, C.Y., Moore, A.T., Bird, A.C. and Hunt, D.M. (1997) Localisation of a gene for dominant cone-rod dystrophy (CORD6) to chromosome 17p. *Hum Mol. Genet.* **6**, 597-600.

Kelsell, R.E., Gregory-Evans, K., Payne, A.M., Perrault, I., Kaplan, J., Yang, R.B., Garbers, D.L., Bird, A. C. Moore, A.T. and Hunt, D.M. (1998) Mutations in the retinal guanylate cyclase (RETGC-1) gene in dominant cone-rod dystrophy. *Hum Mol. Genet.* **7**, 1179-1184.

Kermani, S., Gregory-Evans, K., Tarttelin, E.E., Bellingham, J., Plant, C., Bird, A.C., Fox, M., Bhattacharya, S.S., Gregory-Evans, C.Y. (1999) Refined genetic and physical positioning of the gene for Doyne honeycomb retinal dystrophy (DHRD). *Hum Genet.*; **104**(1): 77-82

Khan, A.S., Wilcox, A.S., Polymeropoulos, M.H., Hopkins, J.A., Stevens, T.J., Robinson, M., Orpana, A.K. and Sikela, J.M. (1992) Single pass sequencing and physical and genetic mapping of human brain cDNAs. *Nat. Genet.* **2**, 180-185.

Kim, R.Y., Dollfus, H., Keen, T.J. Fitke, F.W., Arden G.B., Bhattacharya, S.S and Bird, A.C. (1995) Autosomal dominant pattern dystrophy of the retina associated with a 4 bp insertion at codon 140 in the RDS / peripherin gene. *Arch. Ophthalmol.*, **113**, 451-455.

Klainguti, R. (1932) Die tapeto-retinal degeneration im Kanton Tessin. *Klin. Monatsbl. Augenheilkd.*, **107**, 361-372.

Klee, C.B., and Vanaman, T.C. (1982) Calmodulin Adv Protein Chem. **35**:213-321.

Klein ML, Schultz DW, Edwards A, Matise TC, Rust K, Berselli CB, Trzupek K, Weleber RG, Ott J, Wirtz MK, Acott TS (1998). Age-related macular degeneration. Clinical features in a large family and linkage to chromosome 1q. *Arch. Ophthalmol.* **116**:1082-1088.

Klenchin, V.A., Calvert, P.D. and Bownds, M.D. (1995) Inhibition of rhodopsin kinase by recoverin. Further evidence for a negative feedback system in phototransduction. *J. Biol. Chem.* **270**, 16147-16152.

Klystra, J.A. and Aylsworth, A.S. (1993) Cone-rod retinal dystrophy in a patient with neurofibromatosis type 1. *Can. J. Ophthalmol.* **28**, 79-80.

Kniazeva M, Chiang, Morgan B, Anduze AL, Zack DJ, Han M, Zhang K (1999). A new locus for autosomal dominant Stargardt-like disease maps to chromosome 4. *Am. J. Hum. Genet.* **64**:1394-1399.

Kniazeva MF, Chiang MF, Cutting GR, Zack DJ, Han M, Zhang K (1999a). Clinical and genetic studies of an autosomal dominant cone-rod dystrophy with features of Stargardt disease. *Ophthalmic Genet.* **20**:71-81.

Koch, K.W. Stryer, L. (1988) Highly co-operative feedback control of retinal rod guanylate cyclase by calcium ions. *Nature* **334**, 64-66.

Koller, M., Schnyder, B., and Strehler, E.E. (1990) Structural organisation of the human CaMIII calmodulin gene. *Biochim, Biophys. Acta.* **1087**:180-189.

Kohara, Y., Akiyama, K. and Isono, K. (1987) The physical map of the whole E. coli chromosome: application of a new strategy for rapid analysis and sorting of a large genomic library. *Cell* **50**, 495-508.

Kouprina, N., Eldarov, M., Moyzis, R., Resnick, M. and Larionov, V. (1994) A model system to assess the integrity of mammalian YACs during transformation and propogation in yeast. *Genomics* **21** (1), 7-17.

Koutalos, Y. and Yau, K.W. (1996) Regulation of sensitivity in vertebrate rod photoreceptors by calcium. *Trends Neurosci.* **19**, 73-81.

Kozak, M. (1996) Interpreting cDNA sequences: some insights from studies on translation.*Mamm. Genome* 7: 563-574.

Kremer, H., Pinckers, A., Helm, B., Deutman, A.F., Ropers, H. and Stone, C.M.M. Localisation of the gene for dominant cystoid macular dystrophy on 7p. 1994; *Hum Mol Genet, Vol.* 3, No2, 299-302.

Krill, A.E., Deutman, A.F. and Fishman, M. (1973) The cone degenerations. *Doc. Ophthalmol.* 35, 1-80.

Kruglyak, L. (1997) The use of genetic map of biallelic markers in linkage studies. *Nat. Genet..* 17, 21-24.

Kwitek-Black, A., Carmi, R., Duyk, G.M., Buetow, K.H., Elbedour,K., Parvari, R., Yandava, C.N., Stone, E.M. and Sheffield, V.C (1993) Linkage of Bardet-Biedl syndrome to chromosome 16q and evidence for non-allelic heterogeneity. *Nat. Genet..* 5, 392-396.

Lambrecht, H.G. and Koch, K.W. (1991) A 26 kd calcium binding protein from bovine rod outer segments as modulator of photoreceptor guanylate cyclase. *EMBO J.* 10, 793-798.

Lander, E.S. (1996) The new genomics: Global views of biology. *Science* 274, 536-539.

Lander, E.S. and Botstein, D. (1987) Homozygosity mapping: A way to map human recessive traits with the DNA of inbred children. *Science* 236, 1567-1570.

Lander, E.S. and Green, P. (1987) Construction of multilocus genetic linkage maps in humans. *Proc. Natl. Acd. Sci. U.S.A* 84, 2363.

Larin Z., Monaco, A.P. and Lehrach, H. (1991) Yeast artificial chromosome libraries containing large inserts from mouse and human DNA. *Proc. Natl .Acad. Sci. USA* 88, 4123-4127.

Lathrop, G.M., Lalouel, J.M., Julier, C. and Ott, J. (1984) Strategies for multipoint linkage analysis in humans. *Proc. Natl. Acad. Sci. USA*, 81, 3443-3446.

Leach, R.J, Banga, S.S., Ben-Othame, K., Chughtai, S., Clarke, R., Daiger, S.P., Sohocki, MM, et al. Report of the Third International Workshop on Human Chromosome 8 Mapping 1996. *Cytogenet. Cell Genet.* 75:71-84.

Lee, R.H., Lieberman, B. and Lolley, R.N. (1990) Retinal accumulation of phosducin/T beta, gamma and transducin complexes in developing normal mice and in mice and dogs with inherited retinal degeneration. *Exp. Eye Res.* 51, 325-333.

Lee, B., Godfrey, M., Vitale, E., Hori, H., Mattei, M.G., Sarfarazi, M., Tsipouras, P., Ramirez, F., Hollister, D.W. (1991) Linkage of Marfan syndrome and a phenotypically related disorder to two different fibrillin genes. 352:330-334.

Legouis, R. and 14 others (1991) The candidate gene for the X-linked Kallman syndrome encodes a protein related to adhesion molecules. *Cell* 67, 423-435.

224

Leibowitz, H.M., Krueger, D. E., Maunder, L.R., Milton, R.C., Kini, M.M.,Kahn, H. A., Nickerson, R. J., Pool,J., Cotton,T.L., Ganley, J.P., Loewenstein, J., and Dawber, T.R. (1980) The Framingham eye study monograph. *Surv. Ophthalmol.*, **24**(Suppl.), 335-610.

Leppert, M., Baird, L., Anderson, K.L., Otterud, B., Lupske, J.R. and Lewis, R.A. (1994) Bardet-Biedl syndrome is linked to markers on chromosome 11q and is genetically heterogeneous. *Nat. Genet.*. **7**,108-112.

Lewis RA, Shroyer NF, Singh N, Allikmets R, Hutchinson A, Li Y, Lupski JR, Leppert M, Dean M (1999). Genotype/phenotype analysis of a photoreceptor-specific ATP-binding cassette transporter gene, ABCR, in Stargardt disease. *Am. J. Hum. Genet.* **64**:422-434.

Li, T., Snyder, WK., Olsson, JE and Dryja, TP (1996) Transgenic mice carrying the dominant rhodopsin mutation P347S: evidence for defective vectorial transport of rhodopsin to the outer segments. *Proc. Natl. Acad. Sci. USA*. **93**,14176-14181.

Li X., Chen, S., Wang, Q., Zack, D.J., Snyder, S.H., Borjigin, J. (1998). A pineal regulatory element (PIRE) mediates transactivation by the pineal/retina-specific transcription factor CRX. *Proc. Natl. Acad Sci.* USA **95**:1876-1881.

Li Y., Fuhrmann C., Schwinger, E., Gal, A., Laqua, H. (1992). The gene for autosomal dominant familial execudative vitreoretinopahy (Criswick-Schepens) on the long arm of chromosome 11. *Am. J. Ophthalmol.* **113**:712-713.

Li, Y., Müller, B., Fuhrmann, C., van Nouhuys, C.E., Laqua, H., Humphries, P., Schwinger, E., Gal, A. (1992a) The autosomal dominant familial exudative vitreoretinopathy locus maps on 11q and is closely linked to D11S533. *Am. J. Hum. Genet.* **51**:749-754.

Ling, L.L., Ma, N. S.F., Smith, D.R., Miller, D.D. and Moir, D.T. (1993) Reduced occurrence of chimeric YACs in recombination deficient hosts.

Litt, M. and Luty, J.A. (1989) A hypervariable microsatellite revealed by *in vitro* amplification of a dinucleotide repeat within the cardiac muscle actin gene. *Am. J. Hum. Genet.* **44**, 397- 401.

Liu, X., Seno, K., Nishizuka, Y., Hayashi, F., Yamazaki, A., Matsumoto, H., Wakabayashi, T. and Usukura, J.(1994) Ultrastructural localisation of the retinal guanylate cyclase in human and monkey retinas. *Exp. Eye. Res.* **59**,761-768.

Lolley, R. N., Craft, C.M. and Lee, R.H. (1992) Photoreceptors of the retina and pinealocytes of the pineal gland share common components of signal transduction. *Neurochem. Res.* **17**, 81-89.

Lotery AJ, Ennis KT, Silvestri G, Nicholl S, McGibbon D, Collins AD, Hughes AE (1996). Localization of a gene for central areolar choroidal dystrophy to chromosome 17p. *Hum. Mol. Genet.* **5**:705-708.

Lovett, M. (1994) Fishing for complements: finding genes by direct selection. *Trends in Genetics* **10**, 352-357.

Lovett, M., Kere, J. and Hinton, L.M. (1991) Direct selection: a method for the isolation of cDNAs encoded by large genomic regions. *Proc. Natl .Acad. Sci. USA* **88**, 9628-9633.

Lowe, D.G., Dizhoor, A.M., Liu, K., Gu, Q., Spencer, M., Laura, R., Lu, L. and Hurley, J.B. (1995) Cloning and expression of a second photoreceptor-specific membrane retina guanyl cyclase (RetGC), RetGC-2. *Proc. Natl. Acad. Sci. U.S.A* **92**, 5535-5539.

Maier, E., Hoheisel, J.D., McCarthy, L., Mott, R., Grigoriev, A.V., Monaco, A.P., Larin, Z. and Lehrach, H. (1992) Complete coverage of the *Schizosacharomyces pombe* genome in yeast artificial chromosomes. *Nat. Genet.ics* **1**, 231-300.

Magenis, R.E., Maslen, C.L., Smith, L., Allen, L., Sakai, L.Y. (1991) Localisation of the fibrillin (FBN) gene to chromosome 15, band q21.1. *Genomics* **11**:346-351.

Manhant S, Levin A (1995). Retinal dystrophy in 18q- (de Grouchy) syndrome. *Am. J. Hum. Genet.* **57**:A96.

Mansour, AM. Long-term follow-up of dominant macular dystrophy with flecks (Stargardt). *Ophthalmologica*.1992;**205**:138-143.

Margulis, A., Goraczniak, R.M., Duda, T., Sharma, R.K. and Sitaramayya, A. (1993) Structural and biochemical identity of retinal rod outer segment membrane guanylate cyclase. *Biochem. Biophys. Res. Commun.* **194**, 855-861.

Marquardt, A., Stöhr, H., Passmore, L.A., Krämer, F., Rivera, A., Weber, B.H.F. (1998). Mutations in a novel gene, VMD2, encoding a protein of unknown properties cause juvenile-onset vitelliform macular dystrophy (Best's disease). *Hum. Mol. Genet.* **7**:1517-1525.

Marra, M.A., Hillier, L. and Waterston, R.H. (1998) Expressed sequence tags- ESTablishing bridges between genomes. *Tren. in Genet.* **14**, 4-7.

Marrs, J.A., Andersson-Fisone, C., Jeong, M.C., Cohen-Gould,L., Zurzulo, C., Nabi, I. R., Rodriguez-Boulan, E. and Nelson, W.J.(1995) Plasticity in epithelial cell phenotype: modulation by expression of different cadherin cell adhesion molecules. *J. Cell Biol.*, **129**, 507-519.

Martinez-Mir A, Paloma E, Allikmets R, Ayuso C, Tdel Rio, Dean M, Vilageliu L, Gonzàlez-Duarte R, Balcells S (1998). Retinitis pigmentosa caused by a homozygous mutation in the Stargardt disease gene ABCR. *Nat. Genet.* **18**:11-12.

Matthews, R., Murphy, R.L.W., Fain, G.L. and Lamb, T.D. (1988) Photoreceptor light adaptation is mediated by calcium concentration. *Nature* **334**, 67-69.

McConkey, D.J., Hartzell, P., Nicotera, P. and Orrenius, S. (1989) Calcium-activated DNA fragmentation kills immature thymocytes. *FASEB J.* **3**, 1843-1849.

McGinnis, J.F., Austin, B., Bateman, B., Heinzman, C., Kojis, T., Sparkes, R.S., Bateman, J.B. and Lerious, V. (1995) Chromosomal assignment for the human gene for the cancer-associated retinopathy protein (recoverin) to chromosome 17p13.1. *J. Neuroscience res.* **40**, 165-168.

McKusick, V.A. (ed.): Mendelian inheritance in man. Baltimore: John Hopkins University Press, 1992.

McKusick, V.A.; Abbey, H.; Bartalos, M.; Bowen, P.; Boyer, S. H., Cohen, B. H.; Danks, D. M.; Duchastel, Y.; Emery, A. E. H.; Epstein, E. J.; Fainer, D. C.; Finn, R.; and 18 others : Medical genetics 1962. *J. Chronic Dis.* **16**: 457-634, 1963.

McLauglin, M.E., Sandberg, M.A., Berson, E.L. and Dryja, T.P (1993) Recessive mutations in the gene encoding the β-subunit of rod phosphodiesterase in patients with retinitis pigmentosa . *Nature Genet.*, **4**, 130-134.

McNally, N., Kenna, P., Humphries, M.M., Hobson, A.H., Khan N.W., Bush, R.A., Sieving, P.A., Humphries, P. and Farrar, J. (1999) Structural and functional rescue of murine rod photoreceptors by human rhodopsin transgene. *Hum Mol. Genet*, **8**(7): 1309-1312.

McPherson, D., Hickie, R.A., Wasmuth, J.J., Mayskens, F.L., Perham, R.N., Strhler, E.E. and Graham, M.T. (1991) Chromosomal localisation of multiple genes encoding calmodulin. *Cytogenet. Cell Genet* **58**:1951

Meindel, A., Dry, K., Herrmann, K., Manson, F., Ciccodicola, A., Edgar, A., Carvalho, M.R.S and others (1996) A gene (RPGR) with homology to the RCC1 guanine nucleotide exchange factor is mutated in X-linked retinitis pigmentosa (RP3). *Nat. Genet.* **13**, 35-42.

Milam, A.H., Dacey, D.M. and Dizhoor, A.M. (1993) Recoverin immunoreactivity in mammalian cone bipolar cells. *Visual Neurosci.* **10**, 1-12.

Millington-Ward, S., O'Neill, B., Tuohy, G., Al-Jandal, N., Kiang, A.S., Kenna, P.F., Palfi, A., Hayden, P., Mansergh, F., Kennan, A., Humphries, P. and Farrar, G.J. (1997) Strategems *in vitro* for gene therapies directed to dominant mutations. *Hum Mol Genet* Sep;6(9):1415-26.

Mizukami, T. and 11 others (1993) A 13 kb resolution cosmid map of the 14 Mb fission yeast genome by non random sequence tagged site mapping. *Cell* **73**, 121-132.

Molday, L.L., Cook, N.J., Kaupp, U.B. and Molday, R. S. (1990) The cGMP-gated cation channel of bovine rod photoreceptor cells is associated with a 240 kDa protein exhibiting immunochemical cross reactivity with spectrin. *J. Biol. Chem.* **265**, 18690-18695.

Monaco, A.P. and Larin Z. (1994) YACs, BACs, and PACs, and MACs: artificial chromosomes as research tools. *Trends in Biotechnology* **12**, 280-286.

Monaco, A.P., Neve, R.L., Colletti-Feener, C., Bertlson, C.J., Kurnit, D.M. and Kunkel, L.M. (1986) Isolation of candidate cDNAs portions of Duchenne Muscular Dystrophy gene. *Nature* **323**, 646-650.

Moore, A.T. (1992) Cone and cone-rod dystrophies. *J. Med. Genet.* **29**, 289-290.

Morrow, D.M., Tagle, D.A., Shilh, Y., Collins, F.S and Hieter, P. (1995) An *S. cerevisiae* homologue of the human gene mutated in ataxia telangiectasia, is functionally related to the yeast checkpoint gene *MEC1*. *Cell* **82**, 831-840.

Morton, N.E. (1955) Sequential tests for the detection of linkage. *Am. J. Hum. Genet.* **7**, 277-318.

Morton, N.E. (1991) Parameters of the human genome *Proc Natl Acad Sci* **88**(17):7474-6.

Morton, N.E. (1991) Gene maps and location databases *Am J Hum Genet* **55** (Pt3):235-41.

Muller, B., Orth, U., van Nouhuys, C.E., Duvigneau, C., Fuhrmann, C., Schwinger, E., Laqua, H., Gal, A. (1994). Mapping of the autosomal dominant exudative vitreoretinopathy locus (EVR1) by multipoint linkage analysis in four families. *Genomics* **15**;20(2):317-9.

Muenke, M., Schell, U., Weinberg, J., Bray-Ward,P., Hehr, A., Kao, F.T. and Ward, D.C. (1994) Physical mapping of the holoprosencephaly minimal critical region in 2p21. *Cytogenet. Cell Genet.*, **67**, 242-243.

Murray, N. (1986) Phage lambda and molecular cloning. In *Lambda II* (ed. Hendrix, R., Roberts, J., Stahl, F. and Weisberg, R.), pp. 395-432. Cold Spring Harbour Laboratory, Cold Spring Harbour, NY.

Nagao, S., Yamazaki, A. and Bitenski, K.M. (1987) Calmodulin and calmodulin binding proteins in amphibian rod outer segments. *Biochemistry* **26**, 1659-1665.

Nakazawa, M., Kikawa, E., Chida, Y. and Tamai, M. (1994) Asn244His mutation of the peripherin/RDS gene causing autosomal dominant cone-rod degeneration. *Human. Mol. Genet.*, **3**, 1195-1196.

Nakazawa, M., Kikawa, E., Chida, Y., Wada, Y., Shiono, T. and Tamai, M. (1996) Autosomal dominant cone-rod dystrophy associated with mutations in codon 244 (Asn244His) and codon 184 (Tyr184Ser) of the peripherin/RDS gene. *Arch. Ophthalmol.* **114**, 72-78.

Nasonkin I, Illing M, Koehler MR, Schmid M, Molday RS, Weber BH (1998). Mapping of the rod photoreceptor ABC transporter (ABCR) to 1p21-p22.1 and identification of novel mutations in Stargardt's disease. *Hum Genet Jan*;102(1):21-6.

Nathans, J., Merbs, S.L., Sung, C-H, Weitz, C.J., and Wang, Y. (1992) Molecular genetics of human visual pigments. *Annu. Rev. Genet.* 403-424.

Neetens A., Burvenich H., Hendrata Y., Van Rampay J and Hofhens R.(1980). Goldman-Favre hyaloid-tapeto-retinal degeneration. *Bull. Mem. Soc. Fr. Ophthal.* **92**:185-90.

Nelson, D.L., Ledbetter, S.A., Corbo, L., Victoria, M.F., Ramirez-Solis, R., Webster, T.D., Ledbetter, D.H. and Caskey, T.C. (1989) Alu polymerase chain reaction: a method for rapid isolation of human-specific sequences from complex sources. *Proc Natl Acad Sci U S A*. 1989 Sep;86(17):6686-90.

Nelson, W.J., Veshnock, P.J., Ankyrin binding to (Na+ + K+)ATPase and implications for the organization of membrane domains in polarized cells. 1987 Aug 62;328(6130):533-6.

Nichols, BE., Drack, A.V., Vandenburgh, K., Kimura, A. E., Sheffield, V.C. and Stone, E. M. (1993) A 2 base pair deletion in the RDS gene associated with the butterfly-shaped pigment dystrophy of the fovea. *Hum. Mol. Genet.*, **2**, 601-603.

Nichols B.E., Bascom, R., Litt, M., McInnes, R., Sheffield, V.C., Stone, E.M. (1994). Refining the locus for Best vitelliform macular dystrophy and mutation analysis of the candidate gene ROM1. *Am. J. Hum. Genet.* 54:95-103.

Jacobson, S., Cideciyan, A.V., Regunath, G., Rodriguez, F.J., Vandenburgh, K., Sheffield, V.C. and Stone, E.M. (1995) Nightblindness in Sorsby's fundus dystrophy reversed by vitamin A. *Nature Genet.,* 11, 27-32.

Nichols, B.E., Sheffield V.C., Vanderburgh K., Drack A.V., Kimura, A.E. and Stone, E.M. Butterfly-shaped pigment dystrophy of the fovea caused by a point mutation in codon 167 of the RDS gene. March1993;*Nature Genet;*202-207.

Noble, K.G., Carr, R.E., Stargardt's disease and fundus flavimaculatus. *Arch Ophthalmol.* (1979) 97: 1281-1285.

Noble, K.J. Hereditary macular dystrophies. In: Renie, W.A. (Ed) Goldberg's genetic and metabolic eye diseases. *Littele Brown and Co. Boston/Toronto* (1986): pp 439-464.

Nojima, H. (1989) Structural organisation of multiple rat calmodulin genes *J. Mol. Biol.* 208:269-282.

Ohishi, K., Inoue, N., Endo, Y., Fujita, T., Takeda, J., and Kinoshita T. (1995) Structure and chromosomal localisation of the GPI-anchor gene PIGF and its pseudogene psi PIGF. *Genomics* 10; 29(3):804-7.

Olson, M., Hood, L., Cantor, C., Botstein, D. (1989). A common language for physical mapping of the human genome. Science;245(4925):1434-5.

Olson, M.V., Dutchik, J.E., Graham, M.Y., Brodeur, G. M., Helms, C., Frank, M., MacCollin, M., Scheinman, R. and Frank, T. (1986) A random-clone strategy for restriction mapping in yeast. *Proc. Natl .Acad. Sci. USA* 83, 7826-7830.

Palczewski, K., Subbaraya, I., Gorczyca, W.A., Helekar, B.S., Ruiz, C.C., Ohguro, H., Huang, J., Zhao, X., Crabb, J.W., Johnson, R.S., et al (1994). Molecular cloning and characterization of retinal photoreceptor guanylyl cyclase-activating protein. *Neuron;*13(2):395-404.

Papadopoulos, N. (1995) Mutations of GTBP in genetically unstable cells. *Science* June 268(5219):1915-7.

Parimoo, S., Patanjali, S.R., Shukle, H., Chaplin, D.D. and Weisman, S.M. (1991) cDNA selection: efficient PCR approach for the selection of cDNA encoded in large chromosomal DNA fragments. *Proc. Natl .Acad. Sci. USA* 88, 9623-9627.

Parra, I. and Windle, B. (1993) High resolution visual mapping of stretched DNA by fluorescent hybridisation. *Nat. Genet.* 5, 17-21.

Payne, A.M., Downes, S.M., Bessant, D.A.R., Taylor, R.,Holder, G.E., Warren, M.J., Bird, A.C. and Bhattacharya, S.S. (1998) A mutation in guanylate cyclase activator 1A (GUCA1A) in an autosomal dominant cone dystrophy pedigree mapping to a new locus on chromosome 6p21.1. *Hum Mol. Genet.* 7, 273-277.

Pearce, W.G. (1968) Doyne's honeycomb retinal degeneration: clinical and genetic features. *Br. J. Ophthalmol.*, **52**, 73-78.

Pearson, W.R. and Lipman, D.J. (1988) Improved tools for biological sequence comparison. *Proc. Natl .Acad. Sci. U.S.A* **89**, 10882-10886.

Pepose, J.S. and Leib, D.A. (1994) Herpes simplex viral vectors for therapeutic gene delivery to ocular tissues. *Invest. Ophthalmol. Vis. Sci.* **35**, 2662-2666.

Peters A, Greenberg J (1995). Sorsby's fundus dystrophy: a South African family with a point mutation in the tissue inhibitor of metalloproteinases-3 gene on chromomeom 3. *Retina* **15**:480-485.

Perrault, I., Rozet, J.M., Calvas, P., Gerber, S., Camuzat, A., Dollfus, H., Chatelin, S., Petrukhin, K., Koisti, M.J.., Bakal, B., Li, W., Xie, G., Marknell, T., Sandgren, O., Forsman, K., Holmgren, G., Andresson, S., Vujic, M., Bergen, A. A., McGarty-Dugan, V., Figueroa, D., Austin C. P., Metzker, M. L., Caskey, C. T., and Wadelius, C. (1998). Identification of the gene responsible for Best macular dustrophy. *Nat Genet.***19**: 241-247.

Perrault, I., Rozet, J.M., Calvas, P., Gerber, S., Camuzat, A., Dollfus, H., Chatelin, S., Souied, E., Ghazi, I., Leowski, C., Bonnemaison, M., Le Paslier, D., Frezal, J., Dufier, J.L., Pittler, S., Munnich, A., Kaplan, J.(1996). Retinal-specific guanylate cyclase gene mutations in Leber's congenital amaurosis. *Nat. Genet.*, **14**(4):461-4.

Pierce, J.C., Sauer, B. and Sternberg, N. (1992) A positive selection vector for cloning high molecular weight DNA by the bacteriophage P1 system: improved cloning efficiency. *Proc. Natl. Acad. Sci. USA:* **89**, 2056-2060.

Piguet, B., Wells, J.A., Palmvang, I. B., Wormald, R., Chisholm, I.H. and Bird, A.C. (1993) Age-related bruch's membrane chnage: a clinical study of the relative role of heredity and environment . *Br. J. Ophthamol.*, **77**, 400-403.

Piguet, P., Haimovici, R. and Bird A. C. (1995) Dominantly inherited drusen represent more than one disorder: a historical review. *Eye*, **9**, 34-41.

Pinkel, D., Straume, T. and Grey, J.M. (1986) Cytogenetic analysis using quantitative high sensitivity fluorescent hybridisation. *Proc. Natl. Acad. Sci. USA:* **83**, 2934-2938.

Pittler, S.J. and Baehr, W. (1991) Identification of a nonsense mutation in the rod photoreceptor of cGMP phosphodiesterase beta subunit gene of the *rd* mouse. *Proc. Natl.Acad.Sci.***88**,8322-8326.

Pochet, R., Pesteels, B., Seto-Ohshima, A., Bastianelli, E., Kitajima, S., and van Eldik, L. J., (1991) Calmodulin and calbindin localisation in retina from six vertebrate species. *J. Comp. Neurol.*, **314**, 750-762.

Polans, A.S., Baehr, W. and Palczewski, K. (1996) Turned on by Ca2+. The physiology and pathology of Ca2+ binding proteins in the retina. *Trends in Neurosci.* **19**, 547-554.

Polans, A.S., Burton, M.D., Haley, T.L., Crabb, J.W. and Palczewski, K. (1993) Recoverin, but not visinin, is an autoantigen in the human retina identified with a cancer-associated retinopathy. *Invest. Ophthalmol. Vis. Sci.* **34**, 81-90.

Polymeropoulos, M.H., Xiao, H., Glodek, A., Gorski, M., Adams, M.D., Moreno. R.F., Fitzgerald, M.G., Venter, J.C. and Merril, C.R.(1992) Chromosomal assignment of 46 brain cDNAs. *Genomics* **12**, 492-496.

Polymeropoulos, M.H., Xiao, H., Sikela, J.M., Adams, M., Venter, J.C. and Merril, C.R. (1993) Chromosomal distribution of 320 genes from a brain cDNA library. *Nat. Genet.* **4**, 381-386.

Portera-Cailliau, C., Sung, C.H., Nathans, J. and Adler, R. (1994) Apoptotic photoreceptor cell death in mouse models of retinitis pigmentosa. *Proc. Natl. Acad. Sci. USA* **91**, 974-978.

Ragoussis, J., Monaco, A., Mockridge, I., Kendall, E., Campbell, R.D. and Trowsdale, J. (1991) Cloning of the HLA class II region in yeast artificial chromosomes. *Proc. Natl. Acad. Sci. USA* **88**, 3753-3757.

Reig, C., Alicia, S., Gean, E., Vidal, M., Arumi, J., De la Calzada , M. D., Antich, J. and Carballo, M. (1995) A point mutation in the *RDS*-peripherin gene in the Spanish family with central areolar choroidal dystrophy. *Ophthalmic Genet.,* **16**, 39-44.

Reuter, JH., and Sanyal, S. (1984) Development and degeneration of the retina in *rds* mutant mouse:the electroretinogram. *Nerosci. Letts.* **46**,231.

Ribeaudeau, F., Abitbol, M., Finiels, F., Roustan, P., Revah, F., Dufier, J.L., Mallet, J. In vivo adenovirus-mediated gene transfer to newborn rat retinal pigment epithelial cells. *C R Acad Sci III* 1997 Jul;**320**(7):523-32.

Roof, D.J., Adamian, M. and Hayes, A. (1994) Rhodopsin accumulation at abnormal sites of mice with a human P23H rhodopsin transgene. *Invest. Ophthalmol. Vis. Sci.***35**, 4049-4062.

Rousseau-Merck, M.F., Atger M, Loosfelt H, Milgrom E, and Berger R. (1993) The chromosomal localisation of the human follicle-stimulating hormone receptor gene (FSHR) on 2p21-p16 is similar to that of the luteinising hormone receptor gene. *Genomics* **15**(1): 222-4.

Rozet, J.M., Gerber, S., Souied, E., Perrault, I., Chatelin, S., Ghazi, I., Leowski, C., Dufier, J.L., Munnich, A., Kaplan, J. (1998). Spectrum of ABCR gene mutations in autosomal recessive macular dystrophies. *Eur J Hum Genet*;**6**(3):291-5.

Sanger, F., Nicklen, S. and Coulson, A.R. (1977) DNA sequencing with chain terminating inhibitors. *Proc. Natl. Acad. Sci. U.S.A* **74**, 5463-5467.

Sanyal, S. (1987) Cellular site of expression and genetic interaction of the *rd* and *rds* loci in the retina of the mouse. In degenerative retinal disorders: clinical and laboratory investigations (JG Hollyfield, RE Anderson and MM LaVail, eds.) Alan R.Liss, New York p175-194.

Sarfarazi, M., Akarsu, A.N., Hossain, Turacli, M.E., Aktan, S, G., Barsoum-Homsy, M., Chevrette, L. and Sayli, B.S. (1995) Assignment of a locus (GLC3A) for primary congenital

glaucoma (buphthalamos) to 2p21 and evidence for genetic heterogeneity. *Genomics* **30**: 171-177.

Sauer CG Gehrig, A, Warneke-Wittstock R, Marquardt A, Ewing CC, Gibson A, Lorenz, Jurklies B B, BHF Weber (1997). Positional cloning of the gene associated with X-linked juvenile retinoschisis. *Nat. Genet.* **17**:164-170.

Sauer CG, Schworm HD, Ulbig M, Blankenagel A, Rohrschneider K, Pauleikhoff D, Grimm T and Weber BH (1997a). An ancestral core haplotype defines the critical region harbouring the North Carolina macular dystrophy gene (MCDR1). *J.Med. Genet.* **34**:961-966.

Saxon, P.J., Srivatsan, E.J., Leipzig, V., Sameshima, J.H. and Stanbridge, E.J. (1985) Selective transfer of individual human chromosomes to recipient cells. *Mol. Cell. Biol.* **5**, 140-146.

Schuler, G.D. (1997) Pieces of the puzzle: expressed sequence tags and the catalogue of human genes. *J. Mol. Med.* **75**, 694-698.

Schuler, G.D. and 103 others (1996) A gene map of the human genome. *Science* **274**, 540-546.

Schwartz, D.C. and Cantor, C.R. (1984) Preparation of yeast chromosome-sized DNAs by pulse field gel electrophoresis. *Cell* **37**, 67-75.

Screaton, G.R., Bell, M.V., Bell J.I. and Jackson, D.G. (1993) The identification of a new alternative exon with highly restricted tissue expression in transcripts encoding the mouse Pgp-1 (CD44) homing receptor. Comparison of all 10 variable exons between mouses, human, and rat. *J Biol Chem* **268**, 12235-12238.

Sedlacek, Z., Konecki, D.S., Siebenhaar, R., Kioschis, P., Poustka, A. (1993). Direct selection of DNA sequences conserved between species. *Nucleic Acids Res* 25;21(15):3419-25.

Shastry, B.S. and Trese M.T. (1999) Evaluation of the peripherin/RDS gene as a candidate gene in families with age-related macular degeneration. *Ophthalmologica* 213(3):165-70.

Sheffield, V.C., Carmi, R., Kwitek-Black, A., Rokhlina, T., Nishimura, D., Duyk, G.M., Elbedour,K., Sunden, S.L. and Stone, E.M. (1994) Identification of a Bardet-Biedel syndrome locus on chromosome 3 and evaluation of an efficient approach to homozygosity mapping. *Hum Mol. Genet.* **3**, 1331-1335.

Shichi, H. and Somers, R.L. (1978). Light dependent phosphorylation of rhodopsin. Purification and properties of rhodopsin kinase. *J. Biol. Chem.* **253**, 7040-7046.

Shizuya, H., Birren , B., Kim, U-J., Mancino, V.,Slepak, T., Tachiiri, Y. and Simon, M. (1992) Cloning and stable maintenance of 300- kilobase-pair fragments of human DNA in E coli using an F-factor based vector. *Proc. Natl. Acad. Sci. USA* **89**, 8794-8797.

Shyjan, A.W., de Sauvage, F.J., Gillet, N.A., Goeddel, D.V. and Lowe, D.G. (1992) Molecular cloning of a retina-specific membrane guanylyl cyclase. *Neuron* **9**, 727-737.

Sieving PA, Bingham EL, Roth MS, Young MR, Boehnke M, Kuo C-Y, Ginsburg D(1990). Linkage relationship of X-linked juvenile retinoschisis with Xp22.1-p22.3 probes *Am. J. Hum. Genet.* **47**:616-621.

Silvestri, G., Johnston, P.B. and Hughes, A.E. (1994) Is genetic predisposition an important risk factor in age-related macular degeneration? *Eye,* **8**, 564-568.

Small, K.W., Weber, J. L., Roses, A., Lennon, F., Vance, J.M. and PericakVance, P. (1992). North Carolina macular dystrophy is assigned to chromosome 6. *Genomics,* 13, 681 -685.

Small, K.W., Syrquin, M., Mullen, L. and Gehrs, K. (1996). Mapping autosomal dominant cone degeneration to chromosome 17p. *Am. J. Ophthalmol.* **121**, 13-18.

Small, K.W., Puech, B., Mullen, L., Yelchits, S. (1997). North Carolina macular dystrophy phenotype in France maps to the MCDR1 locus. *Mol. Vis.* **3**:1

Smith, M.W., Holmsen, A.L., Wei, Y.H., Peterson, M. and Evans, G.A. (1994) Genomic sequence sampling: a strategy for high-resolution sequence-based physical mapping of complex genomes. *Nat. Genet.* **7**, 40-47.

Sohocki, M.M., Sullivan, L.S., Mintz-Hittner, H.A., Small, K., Ferrell, R.E., Daiger, S.P. (1997). Exclusion of atypical vitelliform macular dystrophy from 8q24.3 and from other known macular degenerative loci. *Am. J. Hum. Genet.* **61**:239-241.

Sohocki, M.M., Sullivan S.L., Mintz-Hittner, H.A, Birch, D., Heckenlively, JR., Freund, C. L., McInnes, R.R. and Stephen, D. (1998) A range of clinical phenotypes associated with mutations in CRX, a photoreceptor transcription-factor gene. *Am J. Hum Genet* Nov; **63**(5): 1307-15.

Souied, E., Ghazi, I., Leowski, C., Bonnemaison, M., Le Paslier, D., Frezal, J., Dufier, J-L., Pittler, S., Munnich, A. and Kaplan, J. (1996) Retinal specific guanylate cyclase gene mutations in Leber's congenital amaurosis. *Nat. Genet.* **14**, 461-464.

Southern, E.M. (1975) Detection of specific sequences among DNA fragments separated by gel electrophoresis. *J. Mol. Biol.* **98**, 503-517.

Stargardt, K., Uber familiare, progressive degeneration in der Maculagegend des Auges, *Albrecht von Graefes Arch Klin Exp Ophthalmol,* 1909; **71**:534-550.

Sternberg, N. (1990). Bacteriophage P1 cloning system for the isolation, amplification and recovery of DNA fragments as large as 100 kilo base pairs. *Proc. Natl .Acad. Sci. USA* **87**, 103-107.

Sternberg, N. (1994). The P1 cloning system-past and future. *Mammalian Genome* **5**, 397- 404.

Stockton, D.W., Lewis, R.A., Abboud, E.B., Al-Rajhi, A., Jabak, M., Anderson, K.L., Lupski, J.R. (1998). A novel locus for Leber congenital amaurosis on chromosome 14q24. *Hum. Genet.* **103**:328-333.

Stöhr, H., Roomp, K., Felbor, U., Weber, B.H.F. (1995). Genomic organization of the human tissue inhibitor of metalloproteinases-3 (TIMP3). *Genome Res.* **5**:483-487.

Stone, E.M., Nichols, B.E., Kimura, A.E., Weingeist, T.A., Drack A. and Sheffield, V.C. (1994) Clinical features of a Stargardt-like dominant progressive macular dystrophy with genetic linkage to chromosome 6q. *Arch. Ophthalmol.,* **112**, 765 -772.

Stone, E. M., Nichols, B. E., Streb, L. M., Kimura, A.E. and Sheffield, V.C. (1992) Genetic linkage of vitelliform macular degeneration (Best's disease) to chromosome 11q13. *Nature Genet.*, **1**, 246 -250.

Stone, E.M., Webster, A.R., Vandenburgh, K., Streb, L.M., Hockey, R.R., Lotery, A.J., Sheffield, V.C. (1998). Allelic variation in ABCR associated with Stargardt disease but not age-related macular degeneration. *Nat. Genet.* **20**:328-329.

Strachan, T., Abitol, M., Davidson, D and Beckmann, J.S. (1997) A new dimension for the human genome project: towards comprehensive expression maps. *Nat. Genet.* 16, 126-132.

Stratakis, C.A., Jenkins, R.B., Pras, E., Mitsiadis, C.S., Raff, S.B., Stalboerger, P.G., Tsigos, C., Carney, J.A., and Chrousos, G.P. (1996). Cytogenetic and microsatellite alterations in tumours from patients with the syndrome of myxomas, spotty skin pigmentation and endocrine overactivity (Carney complex). *J Clin Endocrinol Metab*.81(10):3607-14.

Stryer, L. (1986) Cyclic GMP cascade of vision. *Annu. Rev. Neurosci*. 9, 87-119.

Stryer, L. (1988) Cold Spring Harb Symp Molecular basis of visual excitation.Quant Biol;**53** Pt 1:283-94.

Subbaraya, I., Ruiz, C.C., Helekar, B.S., Zhao, X., Gorczyca, W.A., Pettenati, M.J., Rao, P.N., Palczewski, K., Baehr, W. (1994). Molecular characterization of human and mouse photoreceptor guanylate cyclase-activating protein (GCAP) and chromosomal localization of the human gene. *J Biol Chem* 9;**269**(49):31080-9.

Suber, M.L., Pittler, S.J., Qin, N., Wright, G.C., Holcomber, V., Lee, R.H., Craft, C.M., Lolley, R.N., Baehr, W. and Hurwitz, R.L (1993) Irish setter dogs affected with rod/cone dysplasia contain a nonsense mutation in the rod cGMP phosphodiesterase beta subunit gene. *Proc. Natl.Acad.Sci. USA*. **90**, 3968-3979.

Sun, H., Nathans, J. (1997). Stargardt's ABCR is localized to the disc membrane of retinal rod outer segments. *Nat. Genet.* **17**:15-16.

Sung, C.H., Mackino, C., Baylor, D., and Nathans, J. (1994) A rhodopsin gene mutation responsible for autosomal dominant retinitis pigmentosa results in a protein that is defective in localisation to the photoreceptor outer segment. *J. Neurosci.* 14, 5818-5833.

Swain, P.K., Chen S, Wang QL, Affatigato LM, Coats CL, Brady KD, Fishman GA, Jacobson SG, Swaroop A, Stone E, Sieving PA, Zack DJ (1997) Mutations in the cone-rod homeobox gene are associated with the cone-rod dystrophy photoreceptor degeneration. *Neuron*. 1997 Dec; **19** (6): 1329-36.

Swaroop, A., Wang, Q., Wu, W., Cook, J., Coats, C., Xu, S., Zack, D.J. and Seiving, P.A. Leber congenital amurosis caused by a homozygous mutation (R90W) in the homeodomain of the retinal transcription factor CRX: direct evidence for the involvement of CRX in the development of phooreceptor function. *Hum. Mol. Genet.* 1999 Feb; 8(2): 299-305.

Tartellin, E.E., Krschner, S.L., Bellingham, J., Baffi, J., Taymans, S.E., Gregory-Evans, K., Cskay, K., Stratakis, C.A., and Grogory-Evans, C.Y. (1999) Cloning and characterisation of a

novel orphan G-protein-coupled receptor localised to human chromosome 2p16. *Biochem and Biophys Res Com* **260**:174-180.

Taymans, S.E., Kirschner, L.S., Giatzakis,C. and Stratakis, C.A. (1999) Radiation hybrid mapping of chromosomal region 2p15-p16: integration of expressed and polymorphic sequences maps at the Carney complex (CNC) and Doyne honeycomb retinal dystrophy (DHRD) loci. *Genomics* 15;**56**(3):344-9.

The Utah Marker Development Group (1995) A collection of ordered tetranucleotide-repeat markers from the human genome. *Am. J. Hum. Genet.* **57**,619-628.

Thiselton, D., *et al* (1995) Genetic and physical mapping of five microsatellite markers on human Xp21.1-p11.22.;**25**(1):279-81.

Trask, B.J., Massa, H., Kenwrick, S. and Gitschier, J. (1991) Mapping of human chromosome Xq28 by two-colour fluorescence in situ hybridisation of DNA sequences to interphase cell nuclei. *Am. J. Hum. Genet.* **48**, 1-15.

Trask, B.J., Pinkel, D. and Van den Engh, G. (1989) The proximity of DNA sequences in interphase nuclei is correlated to genomic distance and permits ordering of cosmids spanning 250 kilobase pairs. *Genomics* **5**, 710-717.

Travis, G.H., Brennan, M.B., Danielson, P.E., Kozak, C.A., and Sutcliffe, J.G. (1989) Identofication of a photoreceptor-specific mRNA encoded by the gene responsible for retinal degeneration slow (*rds*). *Nature* **338**, 70-73.

Travis, G.H., Christerson, L., Danielson, P., Klisak, I., Sparkes, R., Hahn, L., Dryja, T., Sutcliffe, J. (1991). The human retinal degeneration slow (RDS) gene: chromosome assignment and structure of the mRNA. *Genomics* **10**:733-739.

Travis, G.H., Sutcliffe, J.G., Bok, D. (1991a). The retinal degeneration slow (rds) gene product is a photoreceptor disc membrane-associated glycoprotein. *Neuron* **6**:61-790.

Tripathy, R.C. and Tripathy, B.J. (1984) The eye (ed. Davson, H.), Academic press.

Tunnacliffe, A., Parker, M., Povey, S., Bengtsson, B.O., Stanley, K., Solomon, E. and Goodfellow, P. (1983) Integration of Eco-gt and SV40 early region sequences into human chromosome 17: a dominant selection system in whole cell and microcell human-mouse hybrids. *EMBO J.* **2**, 1577-1584.

Maghtheh, M., Vithana, E.N., Bhattacharya, S.S., and Inglehearn, C. (1999) Positional cloning of the RP11 gene : exclusion of 3 candidate genes and a mutation in PRKCG. *Invest. Ophthalmol. Vis. Sci.* **39**:1353.

Van Nie, R., Ivani, D., and Demant, P. (1978) A new H-2 linked mutation, rds, causing retinal degeneration slow in mouse. *Tissue Antigens.* **12**, 106-108.

Vollrath, D. and Davies, R. W. Resolution of DNA molecules greater than 5 megabases by contour-clamped homogeneous electric fields. (1987) *Nucleic Acids Res.* **18**(8):1951-6.

235

Wadeilus, C., Graff, C., Foresman, K., Lind, L., Westermark, E., Larsson, C., Sandgren, O., Gustavson, K.H, Holmgren, G. (1993). Detailed mapping of hereditary vitelliform macular dystrophy. *Am. J. Hum. Genet.* **53**:1718.

Wald, G. (1968) The molecular basis of visual excitation. *Nature* **219**, 800-807.

Walter, M.A., Spillet, D.J., Thomas, P., Weissenbach, J. and Goodfellow, P.N. (1994) A method for constructing radiation hybrid maps of whole genomes. *Nat. Genet.* **7**, 22-28.

Wang, M.G., Yi, H., Guerini, D., Klee, C.B. and McBride, O.W.(1996) Calcineurin A alpha (PPP3CA), calcineurin A beta (PPP3CB) and calcineurin B (PPP3R1) are located on human chromosomes 4, 10q21→q22 and 2p16→p15 respectively. *Cytogenet Cell Genet* **72** (2-3):236-41.

Warburg, M., Sjo, O. and Fledelius, H.C. (1991) Deletion mapping of a retinal cone-rod dystrophy: assignment to 18q21.1. *Am. J. Med. Genet.* **39**, 288-293.

Warburton, D., Gersend, s., Yu, M.T., Jackson, C., Handelin, B. and Housman, D. (1990) Monochromosomal rodent-human hybrids from microcell fusion of human lymphoblastoid cells containing an inserted dominant selectable marker. *Genomics* **6**, 358-366.

Watkins, P.C., Eddy, R., Forget, B.G., Chang, J.G., Rochelle, R., and Shows T.B. (1988) Assignment of non-erythroid spectrin to gene to human chromosome 2. *Am. J. Hum Genet.* *(abstract)*

Weber B, Walker D, Mar L, Müller B (1993). Refined localization of the gene causing Best's macular dystrophy (BMD). *Am. J. Hum. Genet.* **53**:1099.

Weber, B.H.F., Vogt, G., Pruett, R.C., Stohr, H. and Felbor, U. (1994) Mutations in the tissue inhibitor of metalloproteinases-3 (TIMP3) in patients with Sorsby's fundus dystrophy . *Nature Genet.*, **8**, 352-355.

Weber B.H.F., Vogt, G., Stöhr, H., Sander, S., Walker, D., Jones, C. (1994a). High-resolution meiotic and physical mapping of the Best vitelliform macular dystrophy (VMD2) locus pericentromeric to chromosome 11. *Am. J. Hum. Genet.* **5**:1182-1187.

Weber, B.H.F., Vogt, G., Wolz, W., Ives, E.J., Ewing, C.C. (1994b). Sorsby's fundus dystrophy is genetically linked to chromosome 22q13-qter. *Nat. Genet.* **7**:158-161.

Weber, B.H., Walker, D., Müller, B., Mar, L. (1994c). Best's vitelliform dystrophy (VMD2) maps between D11S903 and PYGM: no evidence for locus heterogeneity. *Genomics* **20**:267-274.

Weber, J.L. (1990) Informativeness of human (dC-dA)n. (dG-dT)n polymorphisms. *Genomics* **7**, 524-530.

Weber, J.L. and May, P.E. (1989) Abundant class of human DNA polymorphisms which can be typed using polymerase chain reaction. *Am. J. Hum. Genet.* **44**, 388-396.

Weissenbach, J., Gyapay, G., Dib, C., Vignal, A., Morissette, J., Millasseau, P., Vaysseix, G. and Lathrop, M. (1992) A second-generation linkage map of the human genome. *Nature* **359**, 794-801.

he gene responsible for autosomal dominant oyne's honeycomb retinal dystrophy (DHRD) maps chromosome 2p16

eryl Y. Gregory[1,*], Kevin Evans[1,2], Sujeewa D. Wijesuriya[1], Sana Kermani[1], rcelle R. Jay[2], Catherine Plant[2], Nigel Cox[3], Alan C. Bird[2] and omi S. Bhattacharya[1]

artments of [1]Molecular Genetics and [2]Clinical Ophthalmology, Institute of Ophthalmology, 11–43 Bath Street, don EC1V 9EL, UK and [3]Department of Ophthalmology, Wycombe General Hospital, Queen Alexandra d, High Wycombe, Bucks HP11 2TT, UK

eneration in the macula region of the retina is a ure of a heterogeneous group of inherited, gressive disorders, causing blinding visual airment. Autosomal dominant Doyne's honeycomb nal dystrophy (DHRD) is characterised by the sence of drusen deposits at the level of Bruch's mbrane in the macula and around the edge of the ic nerve head. We have studied 63 members of a e, nine-generation British pedigree by linkage lysis. Two-point analysis showed significant linkage nine markers on the short arm of chromosome 2, a ion overlapping that recently reported to be linked to attia leventinese. A maximum lod score (Z_{max}) of 9 ($\theta = 0.0$) was obtained at marker locus D2S2251. lotype analysis of recombination events localised disease to a 5 cM region between marker loci S2316 and D2S378. Striking clinical similarities ween DHRD and the more common condition -related macular degeneration (ARMD) suggest that disease gene at this locus could be considered as most likely candidate in future studies on ARMD.

RODUCTION

inal degeneration focused on the macular region of the human na is a feature of a number of different disorders, all of which lt in colour blindness and loss of central vision sufficiently ere for blind registration. Morphological defects in the rosensory retina, retinal pigment epithelium (RPE) and/or ich's membrane may be observed. Despite the large number of omic loci which have been linked to specific retinal trophies that principally affect the macula (1–6), mutations in y two genes peripherin/RDS (7–15) and TIMP3 (6,16–18) e so far been identified in this important group of disorders.

Doyne's honeycomb retinal dystrophy (DHRD) (19–21) is a disease that leads to 'drusen' deposits in the macula. Malattia leventinese is also characterised by drusen but is considered distinct from DHRD because of differences in drusen composition and distribution (22,23). Malattia leventinese has recently been localised to the short arm of chromosome 2 (24). These two conditions together with Hutchinson-Tay choroiditis (25) and Holthouse-Batten chorioretinitis (26) have been denoted by the collective term dominantly inherited drusen (23), although it is unknown how many different nosological entities they may represent. Members of the original families expressing the DHRD phenotype that were studied by Doyne (19) and Pearce (21) were contacted (Fig. 1) and a molecular genetic linkage study was undertaken. Our findings demonstrate that the DHRD gene maps to chromosome 2p16.

RESULTS

Loci implicated in previous studies on autosomal dominant macular dystrophy were excluded in this family as part of a total genome search comprising 228 markers, before linkage was obtained to chromosome 2 at marker locus D2S378. Linkage of the DHRD locus to chromosome 2p was established by genotyping nine other marker loci in the region, of which significant linkage was obtained at eight. Two-point lodscores with marker loci mapping to chromosome 2p are presented in Table 1. The highest lodscore calculated (9.49 at $\theta = 0.06$) was obtained with marker locus D2S378.

Haplotypes across the linked region were constructed for all family members and analysis of recombinants (Fig. 2) localised the DHRD gene to a 5 cM interval between D2S2316 (one recombination event) and D2S378 (two recombinant events). This establishes a more precise mapping of the disease gene to chromosome 2p16 (27). Three affected individuals (VII-33, VII-34 and VII-36) were recombinant at marker locus D2S2316. All of these patients had the same recombinant allele at this locus and were descended from one branch of the pedigree [originally described as family A2 (21)], suggesting that a single
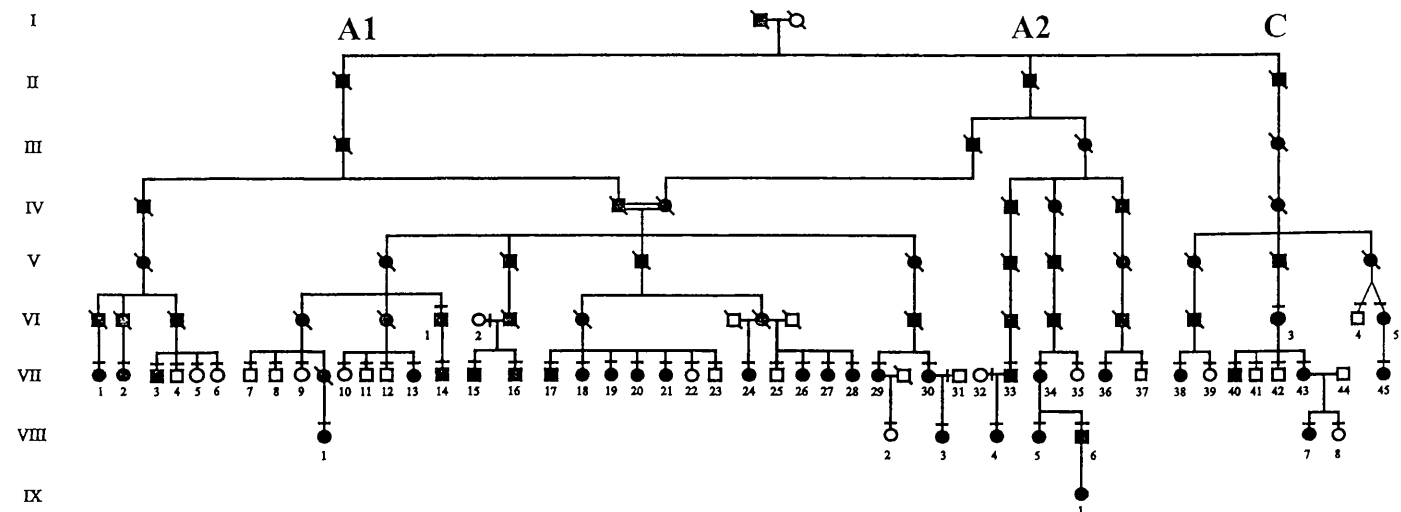
whom correspondence should be addressed

Figure 1. Autosomal dominant inheritance of Doyne's honeycomb retinal dystrophy in a large kindred. Open symbols indicate unaffected individuals and filled symbols indicate affected individuals. A bar above the symbols indicates individuals that were clinically examined. Symbols with a slash indicate deceased family members. A double line between symbols indicates a consanguinity. Branches of the family which were published originally by Pearce (21) are denoted by the letters A1, A2 and C.

recombination event had occurred in a common ancestor (III-3). Four other affected individuals (VII-24, VII-26, VII-27 and VII-28) were recombinant at marker locus *D2S378*. Inspection of the haplotypes again suggested a single recombination event in a common ancestor (VI-11). In addition, one unaffected individual (VII-8) was recombinant at locus *D2S378*.

Table 1. Two-point lod scores for markers linked to *DHRD*

Locus	0.0	0.01	0.05	0.1	0.2	Z_{max}	0
D2S119	$-\infty$	−0.86	4.49	5.96	5.99	6.24	0.18
D2S391	$-\infty$	5.62	8.73	9.12	7.89	9.12	0.10
D2S2227	$-\infty$	0.34	2.92	3.63	3.39	3.67	0.09
D2S2316	$-\infty$	8.23	8.25	7.62	5.92	8.38	0.03
D2S2739	6.56	6.45	5.97	5.29	3.78	6.65	0.00
D2S2251	7.29	7.04	6.32	5.13	3.27	7.29	0.00
D2S2352	4.14	3.98	3.37	2.16	1.09	4.14	0.00
D2S378	$-\infty$	7.64	9.43	9.32	7.71	9.49	0.06
D2S370	$-\infty$	2.58	3.92	3.86	2.80	3.98	0.08
D2S147	$-\infty$	−6.45	−1.85	−0.96	0.81	−2.0*	0.04

*Marker locus *D2S147* is not linked to the *DHRD* locus giving a −2.0 lodscore at θ = 0.04

DISCUSSION

We have demonstrated by linkage analysis that the *DHRD* disease-gene is localised to a 5 cM interval on the short arm of chromosome 2 in the region 2p16. Of the genes which map to this region centromeric to marker locus *D2S119* (28,29), calmodulin-2 (*CALM2*) is the best potential candidate gene. Calmodulin is known to be expressed in the retina (30) and interacts with calcium to modulate phototransduction (31). Mutations in other phototransduction genes such as *rhodopsin* (32) and *cGMP-phosphodiesterase* (33) have previously been associated with retinal dystrophies in humans. That a disease

thought to affect primarily the retinal pigment epithelium (RPE) should be due to a mutation in a gene expressed in the photoreceptor cells would be unexpected. However, the example of *peripherin/RDS* giving rise to pattern dystrophy of the RPE exists (12,34). One RPE-expressed gene (35,36), the non-erythrocyte form of β-spectrin, β-fodrin (*SPTBN1*) (37) maps close to this region, but may be excluded as a candidate gene for *DHRD* by the recombination events with marker loci *D2S391*, *D2S2227* and *D2S2316*, which convincingly map the *DHRD* locus centromeric to the locus assigned to this gene. Human 2p16 is syntenic with a region of mouse chromosome 11 (The Mouse Genome database, 1995); however, no mouse genes in the syntenic region between *Mor2* (malate dehydrogenase) and *Rel* (reticuloendotheliosis oncogene) could be considered as good candidates for *DHRD*.

Four other disorders map close to the region assigned to *DHRD*. Congenital glaucoma (*GLC3A*) (38), holoprosencephaly type 2 (*HPE2*) (39), hereditary nonpolyposis colorectal cancer (*COCA1*) (40) and Malattia leventinese (24). The genetic map of this region can be summarised as tel-*D2S367*-GLC3A-*D2S119*-HPE2- *D2S391*-COCA1-*D2S2316*-DHRD-*D2S378*-*D2S444*-cen. The Malattia leventinese locus has been assigned to a 14 cM region flanked by *D2S1761* (between *D2S119* and *D2S391*) and *D2S444* (24), encompassing the loci *COCA1* and *DHRD*. Mapping data and some clinical similarities between *DHRD* and Malattia leventinese might suggest that they could be allelic. However, important differences at present make this suggestion premature. Clinical studies of these conditions have described differences in the form and distribution of drusen deposits (26). In Malattia leventinese there are small discrete drusen seen radiating into the peripheral retina, with the later development of confluent soft drusen at macula. These ophthalmoscopic features have been consistently and invariably reported in patients affected with the condition (22,23,26), and histopathological studies (41,42) have established that the radial deposits are continuous with or internal to the basement membrane of the retinal pigment epithelium (RPE). In contrast large, soft drusen deposits affecting the macula and peridiscal areas are seen in DHRD (19,21) which have been
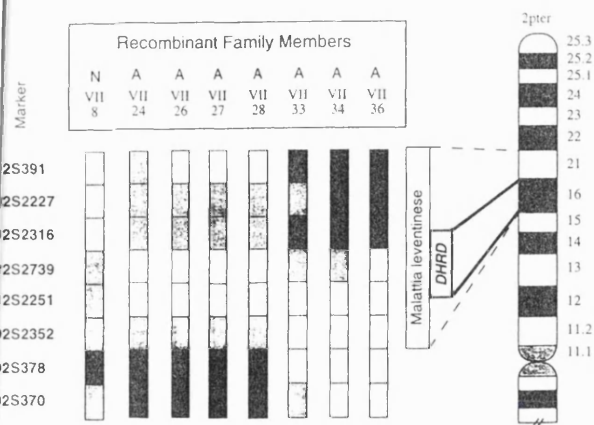
Figure 2. Recombinant analysis occurring between disease and chromosome markers. Eight genetic markers mapping to chromosome 2p are listed to the left of the figure with genetic distances (53) between markers denoted (marker locus D2S2739 has not been mapped to a genetic distance relative to D2S2316 and D2S2251). Recombinant individuals are listed by status (A = affected or N normal), generation and pedigree number at the top of the figure. The boxes below each individual represents the haplotype data for each marker. A black box indicates an informative recombination event between disease and marker. A grey box indicates that the meiosis was uninformative. The white box indicates that no recombination had occurred between the disease and that marker. The relative position of the DRHD locus (between D2S2316 and D2S378) compared to the Malattia leventinese localisation is depicted on the right side of the figure.

described histologically (20) as external to the basement membrane of the RPE, occupying the entire thickness of Bruch's membrane. Radial drusen extending into the periphery have not been described in DHRD. These morphological studies suggest that the deposits seen in the two conditions are different in both localisation and composition and may result from different biochemical abnormalities. In view of these differences future linkage studies and physical mapping projects on the region should not assume that one dominant drusen disease-gene exists in the region.

Macular drusen are also an important feature of age-related macular degeneration (ARMD) (43). The importance of dominant drusen disorders is their potential homology with ARMD (43,44), a complex genetic disorder (45–47) which accounts for 50% of blind registration in the developed world (48,49). No genomic locus or genetic mutation has yet been identified in ARMD. The present study strengthens the importance of chromosome 2p21-p16 in the development of dominant drusen phenotypes and the locus should now be considered the best candidate region for disease susceptibility genes in ARMD. Assessment of the CALM2 gene as the defective gene in this DHRD family is currently underway and a YAC contig of the region is under construction, to facilitate the cloning of the DHRD gene. Additionally, we are screening other dominant drusen families from the Moorfields Register to determine whether genetic heterogeneity is associated with this phenotype.

MATERIALS AND METHODS

Clinical studies

Information from living descendants and genealogical techniques (50) were used to construct a single, nine-generation pedigree consisting of over 400 individuals derived from Buckinghamshire in the United Kingdom (Fig. 1). One hundred and nineteen members of the DHRD family were examined by two ophthalmologists (KE and ACB). Each patient had standard diagnostic ocular examinations including indirect ophthalmoscopy and fluorescein angiography. The results of clinical evaluations and ophthalmological examinations are described in detail elsewhere (21 and K. Evans et al., in preparation).

Affected status was assigned by the observation of soft drusen deposits at the macula and more importantly the appearance of drusen around the optic nerve head, a feature considered pathonomonic for DHRD. Allocation of unaffected status was more difficult since it could not be assumed that a normal clinical examination at <30 years of age indicated that the patient was unaffected and drusen deposits can be a common sign of other conditions. Unaffected status was therefore reserved for individuals over 45 years of age who had no deposits, on critical clinical examination. Many individuals failed to satisfy these criteria and were excluded from the linkage analysis. An abbreviated pedigree illustrating the relationships between the individuals enrolled into the molecular genetic study is given in Figure 1, which clearly demonstrates autosomal dominant inheritance of the disease. The branches of the pedigree reported by Pearce (21) are identified using his original classification (A1, A2 and C). Difficulties in disease allocation as described above meant that the linkage panel of family members originated mostly from one generation and were linked genealogically through a number of unsampled generations. A total of 35 affected individuals, 20 unaffected individuals and eight spouses were enrolled into the study. Local ethical committee approval and informed consent from each patient was obtained prior to the molecular genetic study.

Genotyping

Peripheral blood samples were taken from patients and genomic DNA was extracted with a Nucleon II DNA extraction kit (Scotlab, Bioscience). Genotyping was performed across the entire genome at 10–20 cM intervals as previously described (51), with 228 microsatellite markers that were selected from Généthon (52,53), the Collaborative Human Linkage Center (CHLC) and from the published literature.

Linkage analysis

Data were prepared for linkage analysis using the LINKSYS (version 3.1) data management package (54). Two-point linkage analysis was performed with the MLINK programme (version 5.10) of the LINKAGE package (55). Allele frequencies were calculated from eight spouses in the family.

ACKNOWLEDGEMENTS

REFERENCES

1. Small, K.W., Weber, J.L., Roses, A., Lennon, F., Vance, J.M. and Pericak-Vance, P. (1992) North Carolina macular dystrophy is assigned to chromosome 6. *Genomics*, 13, 681–685.
2. Stone, E.M., Nichols, B.E., Streb, L.M., Kimura, A.E. and Sheffield, V.C. (1992) Genetic linkage of vitelliform macular degeneration (Best's disease) to chromosome 11q13. *Nature Genet.*, 1, 246–250.
3. Stone, E.M., Nichols, B.E., Kimura, A.E., Weingeist, T.A., Drack, A. and Sheffield, V.C. (1994) Clinical features of a Stargardt-like dominant progressive macular dystrophy with genetic linkage to chromosome 6q. *Arch. Ophthalmol.*, 112, 765–772.
4. Evans, K., Fryer, A., Ingleheam, C., Duvall-Young, J., Whittaker, J.L., Gregory, C.Y., Butler, R., Ebenezer, N., Hunt, D.M. and Bhattacharya S. (1994) Genetic linkage of cone-rod retinal dystrophy to chromosome 19q and evidence for segregation distortion. *Nature Genet.*, 6, 210–213.
5. Small, K.W., Syrquin, M., Mullen, L. and Gehrs, K. (1996) Mapping autosomal dominant cone degeneration to chromosome 17p. *Am. J. Ophthalmol.*, 121, 13–18.
6. Weber, B.H.F., Vogt, G., Pruett, R.C., Stohr, H. and Felbor, U. (1994) Mutations in the tissue inhibitor of metalloproteinases-3 (*TIMP3*) in patients with Sorsby's fundus dystrophy. *Nature Genet.*, 8, 352–355.
7. Apfelstedt-Sylla, E., Theischen, M., Ruther, K., Wedemann, H., Gal, A. and Zrenner, E. (1995) Extensive intrafamilial and interfamilial phenotypic variation among patients with autosomal dominant retinal dystrophy and mutations in the human peripherin/RDS gene. *Br. J. Ophthalmol.*, 79, 28–34.
8. Keen, T.J., Ingleheam, C.F., Kim, R., Bird, A.C. and Bhattacharya, S. (1994) Retinal pattern dystrophy associated with a 4 bp insertion at codon 140 in the RDS-peripherin gene. *Hum. Mol. Genet.*, 3, 367–368.
9. Weleber, R.G., Carr, R.E., Murphey, W.H., Sheffield, V.C. and Stone, E.M. (1993) Phenotypic variation including retinitis pigmentosa, pattern dystrophy, and fundus flavimaculatus in a single family with a deletion of codon 153 or 154 of the peripherin/RDS gene. *Arch. Ophthalmol.*, 111, 1531–1542.
10. Hoyng, C.B., Heutink, P., Deutman, A.F. and Oostra, B.A. (1995) A mutation in codon 142 in central areolar choroidal dystrophy. *Invest. Ophthalmol. Vis. Sci.*, 36(Suppl), 3817.
11. Nichols, B.E., Sheffield, V.C., Vandenburgh, K., Drack, A.V., Kimura, A.E. and Stone, E.M. (1993) Butterfly-shaped pigment dystrophy of the fovea caused by a point mutation in codon 167 of the RDS gene. *Nature Genet.*, 3, 202–206.
12. Wells, J., Wroblewski, J., Keen, J., Ingleheam, C., Jubb, C., Eckstein, C., Jay, M., Arden, G., Bhattacharya, S.S., Fitzke, F. and Bird A.C. (1993) Mutations in the human retinal degeneration slow (*RDS*) gene can cause either retinitis pigmentosa or macular dystrophy. *Nature Genet.*, 3, 213–218.
13. Reig, C., Alicia, S., Gean, E., Vidal, M., Arumi, J., De la Calzada, M.D., Antich, J. and Carballo, M. (1995) A point mutation in the RDS-peripherin gene in a Spanish family with central areolar choroidal dystrophy. *Ophthalmic Genet.*, 16, 39–44.
14. Nakazawa, M., Kikawa, E., Chida, Y. and Tamai, M. (1994) Asn244His mutation of the peripherin/*RDS* gene causing autosomal dominant cone-rod degeneration. *Hum. Mol. Genet.*, 3, 1195–1196.
15. Nichols, B.E., Drack, A.V., Vandenburgh, K., Kimura, A.E., Sheffield, V.C. and Stone, E.M. (1993) A 2 base pair deletion in the RDS gene associated with butterfly-shaped pigment dystrophy of the fovea. *Hum. Mol. Genet.*, 2, 601–603.
16. Jacobson, S., Cideciyan, A.V., Regunath, G., Rodriguez, F.J., Vandenburgh, K., Sheffield, V.C. and Stone, E.M. (1995) Night blindness in Sorsby's fundus dystrophy reversed by vitamin A. *Nature Genet.*, 11, 27–32.
17. Felbor, U., Stöhr, H., Amann, T., Schönherr, U. and Weber, B.H.F. (1995) A novel Ser156Cys mutation in the tissue inhibitor of metalloproteinase-3 (TIMP3) in Sorsby's fundus dystrophy with unusual clinical features. *Hum. Mol. Genet.*, 4, 2415–2416.
18. Wijesuriya, S.D., Evans, K., Jay, M.R., Davison, C., Weber, B.H.F., Bird, A.C., Bhattacharya, S.S. and Gregory, C.Y. (1996) Sorsby's fundus dystrophy in the British Isles: demonstration of a striking founder effect by microsatellite- generated haplotypes. *Genome Res.*, 6, 92–101.
19. Doyne, R.W. (1910) A note on family choroiditis. *Trans. Ophthalmol. Soc. UK*, 30, 93–95.
20. Collins, T. (1913) A pathological report on a case of Doyne's choroiditis ('honeycomb' or 'family choroiditis'). *Ophthalmoscope*, 11, 537–538.

21. Pearce, W.G. (1968) Doyne's honeycomb retinal degeneration: clinical and genetic features. *Br. J. Ophthalmol.*, 52, 73–78.
22. Klainguti, R. (1932) Die tapeto-retinal degeneration im Kanton Tessin. *Klin. Monatsbl. Augenheilkd.*, 107, 361–372.
23. Piguet, P., Haimovici, R. and Bird A.C. (1995) Dominantly inherited drusen represent more than one disorder: a historical review. *Eye.* 9, 34–41.
24. Héon, E., Piguet, B., Munier, F., Sneed, S.R., Morgan, C.M., Forni, S., Pescia, G., Schorderet, D., Taylor. C.M., Streb, L.M., Wiles, C.D., Nishimura, D.Y., Sheffield, V.C. and Stone, E.M. (1996) Linkage of autosomal dominant radial drusen (malattia leventinese) to chromosome 2p16-21. *Arch. Ophthalmol.*, 114, 193–198.
25. Hutchinson, J. and Tay, W. (1875) Symmetrical central chorioretinal disease occurring in senile persons. *R. London Ophthalmol. Hosp. Rep.*, 8, 231–244.
26. Holthouse, E.H. and Batten, R.D. (1897) A case of superficial chorioretinitis of peculiar form and doubtful causation. *Trans. Ophthalmol. Soc. UK*, 17, 62–63.
27. Chumakov, I.M., Rigault, P., Le Gall, I., Bellanné-Chantelot, C., Billault, A., Gillou, S., Soularue, P., Guasconi, G., Poullier, E., Gros, I., Belova, M., Sambucy, J.-L., Susini, L., Gervy, P., Glibert, F., Beaufils, S., Bui, H., Massart, C., De Tand, M.-F., Dukasz, F., Lecoulant, S., Ougen, P., Perrot, V., Saumier, M., Soravito, C., Bahouayila, R., Cohen-Akenine, A., Barillot, E., Bertrand, S., Codani, J.-J., Caterina, D., Georges, I., Lacroix, B., Lucotte, G., Sahbatou, M., Schmit, C., Sangouard, M., Tubacher, E., Dib, C., Fauré S., Fizames, C., Gyapay, G., Millasseau, P., Nguyen, S., Muselet, D., Vignal, A., Morissette, J., Menninger, J., Lieman, J., Desai, T., Banks, A., Bray-Ward, P., Ward, D., Hudson, T., Gerety, S., Foote, S., Stein, L., Page, D.C., Lander, E.S., Weissenbach, J., Pasleir, D. and Cohen, D. (1995) A YAC contig map of the human genome. *Nature*, 377 (Suppl), 175–297.
28. Fasman, K.H., Cuticchia, A.J. and Kinsbury, D.T. (1994) The GDB (TM) human genome data base anno 1994. *Nucleic Acids Res.* 22, 3462–3469.
29. Cox, S., Bryant, S.P., Collins, A., Weissenbach, J., Donis-Keller, H., Koeleman, B.P.C., Steinkasserer, A. and Spurr, N.K. (1995) Integrated genetic map of human chromosome 2. *Ann. Hum. Genet.*, 59, 413–434.
30. Pochet, R., Pasteels, B., Seto-Ohshima, A., Bastianelli, E., Kitajima, S. and van Eldik, L.J. (1991) Calmodulin and calbindin localisation in retina from six vertebrate species. *J. Comp. Neurol.*, 314, 750–762.
31. Hsu, Y-T. and Molday, R.S. (1993) Modulation of the cGMP-gated channel of rod photoreceptor cells by calmodulin. *Nature*, 361, 76–79.
32. Al-Maghtheh, A., Gregory, C., Ingleheam, C., Hardcastle, A. and Bhattacharya, S.S. (1993) Rhodopsin mutations in autosomal dominant retinitis pigmentosa. *Hum. Mutat.*, 2, 249–255.
33. McLaughlin, M.E., Sandberg, M.A., Berson, E.L. and Dryja, T.P. (1993) Recessive mutations in the gene encoding the β-subunit of rod phosphodiesterase in patients with retinitis pigmentosa. *Nature Genet.*, 4, 130–134.
34. Kim, R.Y., Dollfus, H., Keen, T.J., Fitzke, F.W., Arden, G.B., Bhattacharya, S.S. and Bird, A.C. (1995) Autosomal dominant pattern dystrophy of the retina associated with a 4 bp insertion at codon 140 in the *RDS/peripherin* gene. *Arch. Ophthalmol.*, 113, 451–455.
35. Gundersen, D., Orlowski, J. and Rodriguez-Boulan, E. (1991) Apical polarity of Na+ K+-ATPase in retinal pigment epithelium is linked to a reversal of the ankyrin fodrin submembrane cytoskeleton. *Invest. Ophthalmol. Vis. Sci.*, 29, 814–817.
36. Marrs, J.A., Andersson-Fisone, C., Jeong, M.C., Cohen-Gould, L., Zurzolo, C., Nabi, I.R., Rodriguez-Boulan, E. and Nelson, W.J. (1995) Plasticity in epithelial cell phenotype: modulation by expression of different cadherin cell adhesion molecules. *J. Cell Biol.*, 129, 507–519.
37. Chang, J.G., Scarpa, A., Eddy, R.L., Byers, M.G., Harris, A.S., Morrow, J.S., Watkins, P., Shows, T.B. and Forget, B.G. (1993) Cloning of a portion of the chromosomal gene and cDNA for human β-fodrin, the non-erythroid form of β-spectrin. *Genomics*, 17, 287–293.
38. Sarfarazi, M., Akarsu, A.N., Hossain, A., Turacli, M.E., Aktan,S.g., Barsoum- Homsy, M., Chevrette, L. and Sayli, B.S. (1995) Assignment of a locus (GLC3A) for primary congenital glaucoma (buphthalmos) to 2p21 and evidence for genetic heterogeneity. *Genomics*, 30, 171–177.
39. Muenke, M., Schell, U., Wienberg, J., Bray-Ward, P., Hehr, A., Kao, F.T. and Ward, D.C. (1994) Physical mapping of the holoprosencephaly minimal critical region in 2p21. *Cytogenet. Cell Genet.*, 67, 242–243.
40. Green, R.C., Narod, S.A., Morasse, J., Young, T-L., Cox, J., Fitzgerald, G.W.N., Tonin, P., Ginsburg, O., Miller, S., Jothy, S., Poitras, P., Laframboise, R., Routhier, G., Plante, M., Morissette, J., Weissenbach, J., Khandjian, E.W. and Rousseau, F. (1994) Hereditary nonpolyposis colon cancer: analysis of linkage to 2p15-16 places the COCA1 locus telomeric to D2S123 and reveals genetic heterogeneity in seven Canadian families. *Am. J. Hum. Genet.*, 54, 1067–1077.

icher, T., Schmidt, T. and Dusek, J. (1982) Hereditäre drusen der chschen membran I. Klinische und lichtmikroskopische beobachtungen. . *Monatsbl. Augenheilkd.*, **181**, 27–31.

ek, J., Streicher, T. and Schmidt, T. (1982) Hereditäre drusen der chschen membran II. Untersuchung von semidünnschnitten und electro-roskopischen ergebnissen. *Klin. Monatsbl. Augenheilkd.*, **181**, 79–83.

z, F.G., Wolfensberger, T.J., Piguet, B., Gross-Jendroska, M., Wells, J.A., hassian, D.C., Chisholm, I.H. and Bird, A.C. (1994) Bilateral macular sen in age-related macular degeneration. *Ophthalmology*, **101**, 2–1528.

ssler, N.M., Bressler, S.B. and Fine, S.L. (1988) Age-related macular eneration. *Surv. Ophthalmol.*, **32**, 375–413.

uet, B., Wells, J.A., Palmvang, I.B., Wormald, R., Chisholm, I.H. and Bird, C. (1993) Age-related Bruch's membrane change: a clinical study of the tive role of heredity and environment. *Br. J. Ophthalmol.*, **77**, 400–403.

ba, I.M., Elston, R.C., Klein, B.E.K. and Klein, R. (1994) Sibling relations and segregation analysis of age-related maculopathy: The ver Dam Eye Study. *Gen. Epidemiol.*, **11**, 51–67.

estri, G., Johnston, P.B. and Hughes, A.E. (1995) Is genetic predisposition important risk factor in age-related macular degeneration? *Eye*, **8**, –568.

bowitz, H.M., Krueger, D.E., Maunder, L.R., Milton, R.C., Kini, M.M., nn, H.A., Nickerson, R.J., Pool, J., Cotton, T.L., Ganley, J.P., Loewenstein, nd Dawber, T.R. (1980) The Framingham eye study monograph. *Surv. hthalmol.*, **24** (Suppl), 335–610.

49. Evans, J. and Wormald, R. (1996) Is the incidence of registrable age-related macular degeneration increasing? *Br. J. Ophthalmol.*, **80**, 9–14.
50. Jay, M. (1995) Ophthalmic genetics: a genealogical guide to sources in England and Wales. *J. Med. Genet.*, **32**, 946–950.
51. Evans, K., Fryer, A., Ingleheam, I., Duvall-Young, J., Whittaker, J.L., Gregory, C.Y., Butler, R., Ebenezer, N., Hunt, D.M. and Bhattacharya, S.S. (1994) Genetic linkage analysis of cone-rod retinal dystrophy to chromosome 19q and evidence for segregation distortion. *Nature Genet.*, **6**, 210–213.
52. Gyapay, G., Morissette, J., Vignal, A., Dib, C., Fizames, C., Millasseau, P., Marc, S., Bernardi, G., Lathrop, M. and Weissenbach, J. (1994) The 1993–1994 Généthon human genetic linkage map. *Nature Genet.*, **7**, 246–335.
53. Dib, C., Fauré, S., Fizames, C., Samson, D., Drouot, N., Vignal, A., Millasseau, P., Marc, AS., Hazan, J., Seboun, E., Lathrop, M., Gyapay, G., Morissette, J. and Weissenbach, J. (1996) The Généthon human genetic linkage map. *Nature*. In press.
54. Attwood, J. and Bryant, S. (1988) A computer programme to make analysis with LIPED and LINKAGE easier to perform and less prone to imput errors. *Ann. Hum. Genet.*, **52**, 259.
55. Lathrop, G.M., Lalouel, J.M., Julier, C. and Ott, J. (1984) Strategies for multipoint linkage analysis in humans. *Proc. Natl Acad. Sci. USA*, **81**, 3443–3446.

OPHTHALMIC MOLECULAR GENETICS

ssessment of the Phenotypic Range Seen Doyne Honeycomb Retinal Dystrophy

n Evans, MD; Cheryl Y. Gregory, PhD; Sujeewa D. Wijesuriya, PhD; Sana Kermani; celle R. Jay, PhD; Catherine Plant; Alan C. Bird, MD

ective: Using molecular genetics as the basis for di- osis, to assess the phenotype in the family originally cribed as having dominantly inherited Doyne hon- omb retinal dystrophy (DHRD) linked to chromo- e 2p16.

ign: Clinical examination including fluorescein an- raphy was undertaken in 107 family members. Nine cted patients underwent electroretinography, perim- , dark adaptometry, color-contrast sensitivity mea- ement, and autofluorescent fundus imaging.

ients: The disease-associated haplotype used to al- te disease status was based on our further refine- t of the DHRD locus to between loci D2S2739 and 378. The study identified 50 affected patients. In ad- on, previously published information on a further 8 ividuals was used. The study population represented enerations of a 9-generation pedigree.

sults: Three types of deposits were seen: large, soft sen at the macula and abutting the optic nerve head; small, hard deposits that in some patients radi- ated from the macula; and autofluorescent deposits. Most younger affected individuals exhibited small hard drusen only at the macula and had normal visual function. Information on 2 patients suggested that DHRD can be a cause of childhood-onset blindness. Advanced disease was associated with severe visual loss and posterior pole atrophy without signs of dru- sen. Advanced age was not invariably associated with severe visual loss.

Conclusions: Previously identified characteristics of DHRD were confirmed and new features identified. Contrary to previous reports, the constancy and sever- ity of radial (basal laminar) drusen seen clinically are the only features that can be used to differentiate between DHRD and malattia leventinese. The highly variable phenotype suggests that the influence of the DHRD-mutant gene may be modulated by other genetic and/or environmental factors.

Arch Ophthalmol. 1997;115:904-910

T HE DOMINANT drusen pheno- type represents an unknown number of genetically dis- tinct entities, some of which have been labeled as epony- mous diseases.[1] The first of these to convinc- ingly demonstrate autosomal dominant in- heritance was Doyne honeycomb retinal dys- trophy (DHRD), described by Robert W. Doyne in 1899.[2] Further studies have con- firmed and extended this initial work.[3-9]

Recently, DHRD has been mapped to chromosome 2p16,[10] overlapping the re- gion previously ascribed to contain the ge- netic mutation causing malattia leventi- nese,[11] another autosomal dominant drusen phenotype. This has raised the pos- sibility that these 2 conditions may de- rive from allelic mutations of the same gene. It has also been suggested that the 2 conditions may in fact be clinically in- distinguishable.[11]

Genealogy has established that 4 of the originally described DHRD families[9] are in fact branches of 1 large pedigree.[12] Working with this extended pedigree, a 2-part study was undertaken. First, using molecular genetic haplotype data as the ba- sis for disease-status allocation, the range of phenotypic expression was assessed. Second, detailed clinical information was compared with published data on the clini- cal characteristics of malattia leventinese to determine whether these 2 epony- mous phenotypes are actually clinically distinct. The importance of these disor- ders lies in their potential homology with age-related macular degeneration.

RESULTS

Fifty individuals who carried the disease- associated haplotype between marker loci D2S2739 and D2S378 were allocated as

m the Departments of ical Ophthalmology s Evans, Jay, and Bird and Plant) and Molecular etics (Drs Gregory and esuriya and Ms Kermani), itute of Ophthalmology and rfields Eye Hospital, don, England.

PATIENTS AND METHODS

PATIENTS

Members of the extended DHRD pedigree (**Figure 1**) were contacted and enrolled in the study. Informed consent for clinical and molecular genetic assessment was obtained from 107 members of the DHRD pedigree. Sufficient clinical information, including fundus photographs, was available on 8 additional individuals from previously published work[4,6,9] to allow for inclusion in our study. Patient IV-9 in Figure 1 was studied histologically by Treacher-Collins[4] and clinically by Tree, who documented the patient as case 4 in his series.[6] Patients V-17, V-22, and V-36 in Figure 1 represent cases 3, 6, and 7, respectively, in Tree's study.[6] Patients represented by Figure 1, a, b, c, and e in the study by Pearce[9] correspond with patients VI-14, VI-15, VI-47, and VII-82, respectively, in our Figure 1. The patient represented in Figure 1, d, in the work by Pearce[9] is depicted as patient VI-58 in our Figure 1. This patient was also available to us and underwent clinical reexamination and molecular genetic study.

GENOTYPING

Peripheral blood samples (10 mL) were taken from each patient and genomic DNA was extracted using standard techniques. All DNA samples were genotyped using 6 highly polymorphic microsatellite marker loci. Previous studies had localized the DHRD mutation to a 5-cM region bounded by marker loci *D2S2316* and *D2S378*.[10] As part of this study, molecular genetic analysis has refined this to a 4-cM region between *D2S2739* and *D2S378*. In the present study, patients were haplotyped at marker loci, *D2S2739*, *D2S2251*, *D2S2352*, and *D2S378*. Clinically classic cases were allocated as affected if they carried the disease-associated haplotype at 3 or more of these loci. Clinically mild cases were allocated as affected only if they carried the disease-associated haplotype at all 4 marker loci.

CLINICAL AND FUNCTIONAL INVESTIGATIONS

An extensive ophthalmic history was recorded. Full ophthalmic examinations that included assessment of visual acuity and detailed examination of the anterior segment and fundus were performed. To assess whether a systemic abnormality might be segregating with ocular disease, a detailed general medical history and a brief physical examination were performed.

Selected subjects underwent standardized electrophysiological investigation.[13-15] Electro-oculographic responses and dark-adapted electroretinography, including blue flash (rod-dominated responses), red flash (cone-dominated responses), white flash (mixed photoreceptor responses), 30-Hz flicker responses, and oscillatory potentials, were recorded. Color-contrast sensitivity was undertaken using a system based on broken rings of different diameters.[16,17]

For psychophysical studies, pupils were dilated with 1% cyclopentolate hydrochloride and 2.5% phenylephrine hydrochloride, and subjects were dark adapted for 40 minutes. Dark-adapted static perimetry was performed with a modified Humphrey automated perimeter (Allergan Humphrey, San Leandro, Calif).[18-20] Cone and rod sensitivities were assessed by using a standard Humphrey 30-2 program with the background illumination turned off. Size 5 red and blue test stimuli were used. In each case, the eye with better visual acuity was tested. For dark adaptometry, prebleach thresholds were determined at selected positions. Patients were exposed to bright white light for 2 minutes, which is sufficient to bleach 95% of rhodopsin. Recovery of sensitivity with time was assessed with size 5 blue test stimuli.[21-23]

Fundus autofluorescent images were obtained by means of a confocal laser scanning ophthalmoscope (prototype SM 30-4024). An argon laser (488 nm, 250 μW) was used for illumination. A wide-band pass filter with a cutoff at 521 nm inserted in front of the detector was used to detect autofluorescence and images were recorded on videotape.[24]

---

affected. A further 30 individuals were found not to carry this haplotype and were assigned as unaffected. Twenty-seven individuals carried part of the disease-associated haplotype between the disease-flanking loci. None of these 27 patients had fundus features suggestive of the disease phenotype, and for the purposes of this study were therefore assigned as unaffected (Figure 1) and not included in the reassessment of the DHRD phenotype.

The **Table** documents clinical characteristics of the 50 affected and genotyped individuals. Information on 4 individuals studied by Tree[6] and a further 4 studied by Pearce[9] who were unavailable to us (see above) is also included. Ages ranged from 22 to 90 years. No systemic disease was seen more commonly among the disease haplotype carriers than among unaffected family members.

ELECTRODIAGNOSTIC STUDY

Five individuals (VII-10, VII-34, VII-48, VII-52, and VII-54) underwent electrodiagnostic investigation. Electro-oculographic responses were within the normal range

(160%-400%) in each patient. Electroretinographic responses to blue and red flash were also normal in each patient studied. Oscillatory potentials were diminished in 2 subjects (VII-10 and VII-52). The 30-Hz flicker responses were delayed in 1 patient (VII-10) and absent in another (VII-52).

PSYCHOPHYSICAL ASSESSMENT

Only minor abnormalities were seen on photopic and scotopic dark-adapted static perimetry in most individuals tested (VII-1, VII-34, VII-50, and VII-54). In these cases, abnormalities were confined to the central 10° of visual field and were within 19 dB of expected values based on patient age and location within the visual field. Two individuals (VII-10 and VII-52) exhibited more profound scotopic and photopic field losses with greater than 30-dB loss of sensitivity involving more than 15% of central visual field. Dark adaptometry was normal in 3 affected individuals (VII-1, VII-34, and VII-54). Delayed focal dark adaptation at a macular locus was seen in 3 individuals
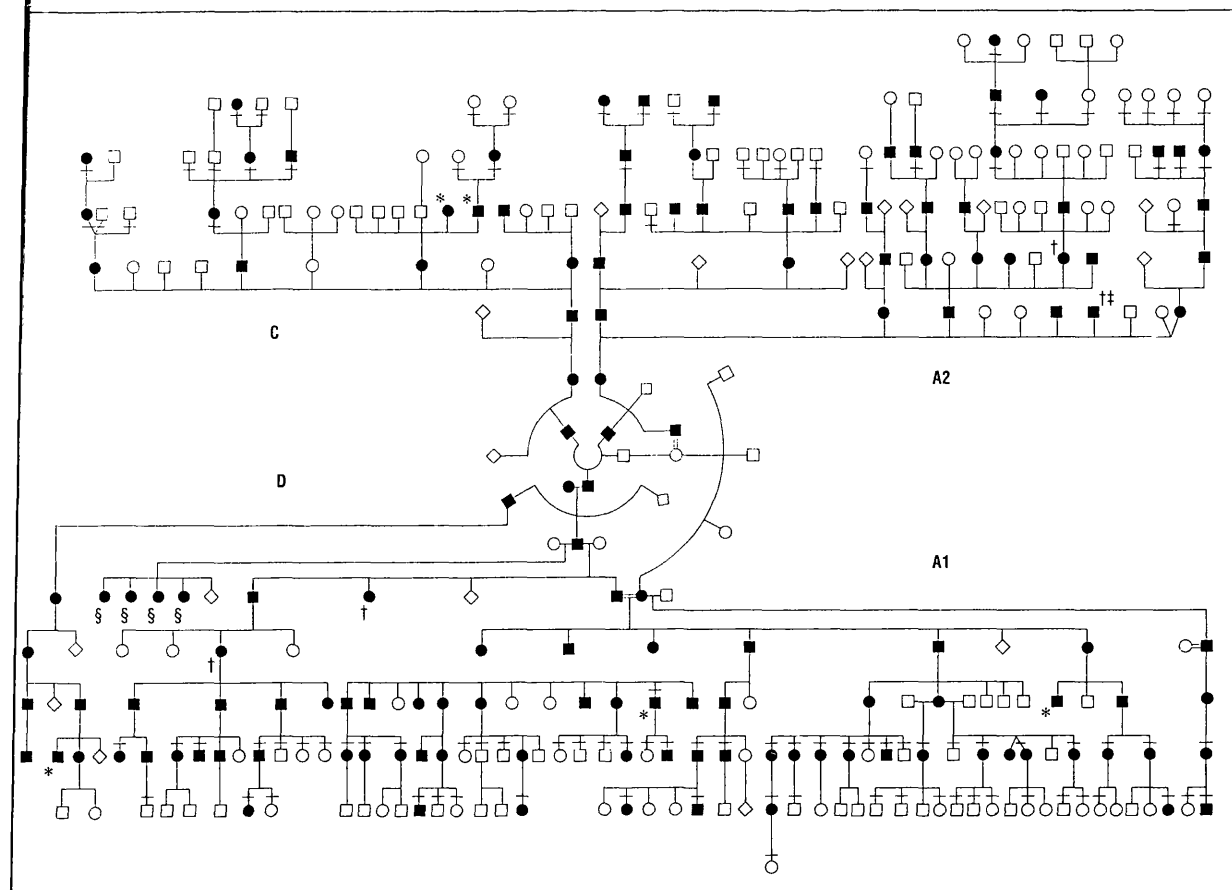
1. *Autosomal dominant Doyne honeycomb retinal dystrophy pedigree. Position in the pedigree is numbered clockwise from the top left-hand corner. Major [branch]es are named A1, A2, C, and D, as originally allocated by Pearce.[9] Open symbols indicate unaffected individuals and solid symbols indicate affected [individ]uals. A double line between symbols indicates consanguinity. A bar above or below the symbols indicates individuals who were clinically examined by us [fro]m whom molecular genetic haplotypes were available. Family member V-27 was the illegitimate daughter of member III-8. Asterisk indicates patients [studied] by Pearce[9]; dagger, patients studied by Tree[6]; double dagger, patients studied by Treacher-Collins[4]; and section mark, patients studied by Doyne.[2,3]*

[50, VII-52, and VIII-2). In 1 of these patients (VII-
there was an associated delay in the time to rod-
break. Minor abnormalities of color-contrast sen-
[sitivi]ty were seen in severely affected individuals only.

AUTOFLUORESCENT IMAGING

[A]ffected patients underwent autofluorescent imag-
[ing.] Normal background autofluorescence for patient age
[was] seen in all individuals tested. Abnormal focal auto-
[fluor]escence was seen at the macula in all 6 affected pa-
[tient]s examined. These deposits were located close to but
[not e]xactly coincidental to soft drusen seen ophthalmo-
[scop]ically. No abnormal autofluorescence was seen
[arou]nd the optic nerve head (**Figure 2**).

PHENOTYPE RANGE

[Over]all evaluation of the 50 affected individuals exam-
[ined] in this study, the 4 studied by Tree,[6] and the 4 stud-
[ied b]y Pearce[9] suggested that disease severity could be
[class]ified into 3 categories: mild, moderate, and severe.
[Mild] disease (5 individuals) was characterized by nor-
[mal] visual acuity with patients reporting no visual defi-
[cit.] Minimal fundus abnormalities were identified. A few
[smal]l, discrete drusen were found at the macula, but no

peripapillary drusen were seen (**Figure 3**, A). *Moder-
ate disease* (36 individuals) was characterized by evi-
dence of some loss of visual acuity. In 21 affected pa-
tients, the macular abnormalities seen in mild disease were
associated with large, soft drusenoid deposits abutting
the optic nerve head (peripapillary drusen) (Figure 3, B).
Patients still reported normal visual function, with vi-
sual acuities recorded as 20/30 or better. Minor abnor-
malities on dark-adapted static perimetry and dark-
adaptometry localized to the macula region were
detectable. In 15 individuals, large soft drusen were also
seen at the macula (Figure 3, C). Small drusen radiating
in a centrifugal pattern from the macula were seen in 9
of these 15 cases. These deposits had an appearance simi-
lar to those seen in malattia leventinese (Figure 3, C-E).
The best recorded visual acuities were 20/40 to 20/80.
For *severe disease* (17 individuals), profound visual acu-
ity loss (20/100 to counting fingers only) was seen usu-
ally in the most elderly, affected family members. Two
types of fundus appearance were identified. In 10 cases,
macular drusen were seen in association with abnormal
macular pigmentation and hypertrophic tissue, suggest-
ing that visual loss was secondary to submacular neo-
vascularization (Figure 3, F). This neovascular compli-
cation was associated with signs of radial drusen in only
2 of these 10 cases. In 4 cases, signs suggestive of sub-

Clinical Assessment of 58 Affected Individuals*

Pedigree No./ Age, y	Visual Acuity OD	Visual Acuity OS	Fundus Features
IV-9†‡/60	20/80	20/100	SD, MA, PA
V-17†/80	CF	CF	SD, SRN
V-22†/49	20/200	20/60	SD, SRN
V-36†/55	20/40	20/200	SD, SRN
VI-1/69	20/30	20/30	SD, RD, SRN
VI-4/83	20/200	CF	MA, PA
VI-14§/64	CF	CF	SD, SRN
VI-15§/65	20/30	20/30	SD
VI-47§/90	CF	CF	SD, MA, PA
VI-58/65	20/20	20/20	HD, SD
VII-1/40	20/15	20/15	HD, SD
VII-5/58	CF	20/30	SD, RD, SRN
VII-6/61	20/200	20/30	SD, SRN, PA
VII-9/71	20/30	20/200	SD, RD, SRN
VII-10/76	CF	20/200	SRN, PA
VII-20/73	20/60	20/60	SD
VII-24/84	CF	CF	SD, MA, PA
VII-31/60	20/30	20/30	HD, SD
VII-32/48	20/30	20/30	HD, SD
VII-33/60	20/60	20/60	HD, SD
VII-34/64	20/100	20/60	SD
VII-35/63	20/30	20/60	SD, RD
VII-36/67	20/30	20/30	SD, RD
VII-37/51	20/40	20/20	HD, SD
VII-39/54	20/30	20/60	SD, RD
VII-41/57	20/20	20/20	HD, SD
VII-43/73	20/400	20/400	SD, SRN, MA
VII-45/76	20/30	20/30	MA, PA
VII-48/69	20/200	20/100	SD, SRN, MA, PA
VII-49/64	20/30	20/30	SD, RD
VII-50/66	20/20	20/20	SD, RD
VII-52/49	20/200	20/200	SD, MA, PA
VII-53/55	CF	CF	SD, MA, PA
VII-54/55	20/15	20/15	HD, SD
VII-56/49	20/80	20/100	HD, SD
VII-67/75	20/30	20/20	HD, SD
VII-68/66	20/30	20/20	HD, SD
VII-69/78	20/30	20/30	HD, SD
VII-73/62	20/30	20/20	SD
VII-76/60	20/30	20/30	HD, SD
VII-77/55	20/30	20/30	SD, RD
VII-79/72	20/400	20/200	SD, MA, PA
VII-82§/31	20/20	20/20	HD, SD
VIII-2/34	20/15	20/15	SD
VIII-7/48	20/15	20/15	HD, SD, RD
VIII-8/43	20/15	20/15	HD
VIII-10/36	20/15	20/15	HD, SD
VIII-13/65	20/15	HM	SD
VIII-14/60	20/15	20/15	SD
VIII-20/28	20/15	20/15	HD
VIII-22/44	20/60	20/40	SD, RD
VIII-43/47	20/30	20/30	HD, SD
VIII-46/22	20/15	20/15	HD
VIII-49/29	20/15	20/15	HD
VIII-51/35	20/15	20/15	HD, SD
VIII-56/60	20/40	20/40	SD
VIII-62/23	20/15	20/15	HD
IX-2/36	20/15	20/15	SD

*CF indicates counting fingers acuity; HM, hand motions; HD, hard drusen; SD, soft drusen; RD, radial drusen; SRN, subretinal neovascularization; MA, macular atrophy; and PA, peripapillary atrophy.
†Studied by Tree.[6]
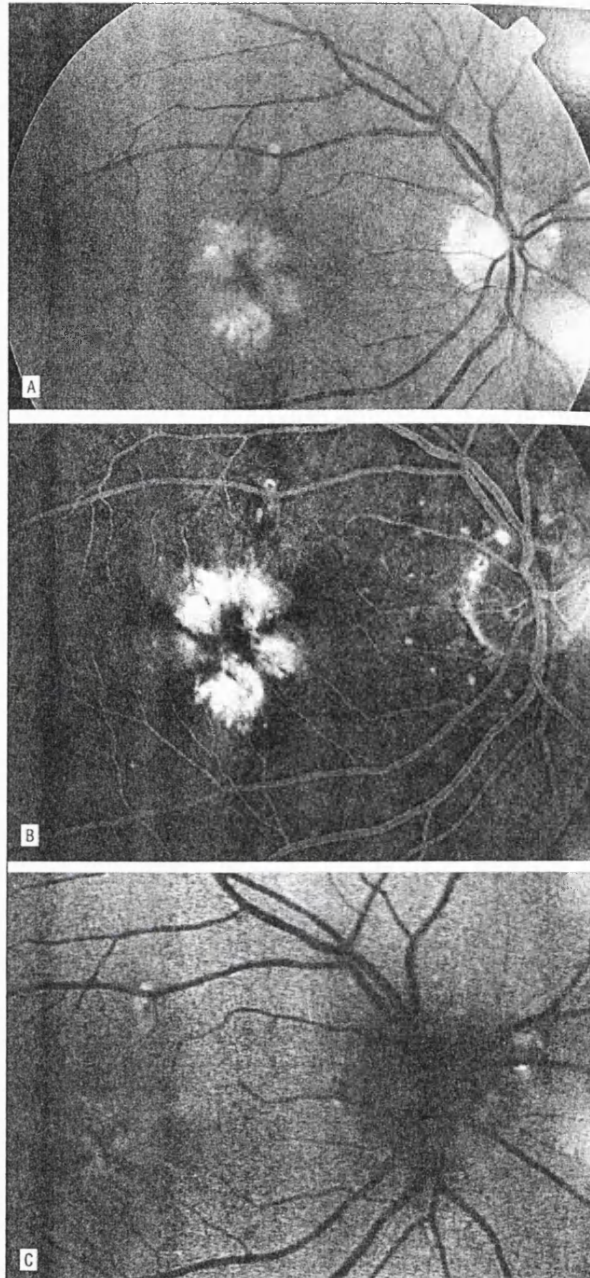‡Studied by Treacher-Collins.[4]
§Studied by Pearce.[9]

Figure 2. Patient VII-34. Color fundus photograph (A), fluorescein angiogram (B), and autofluorescent image (C) showing different deposits.

macular neovascularization were seen in association with macular or peridiscal atrophy. In 7 patients, marked peripapillary and macular atrophy was seen with little or no associated drusen deposits (Figure 3, G). Significant psychophysical and electrophysiological abnormalities localized to the macular region only were recorded in patients with severe disease.

Disease severity was to some extent associated with age. Mild disease was seen in patients aged 22 to 43 years; moderate disease, 31 to 78 years; and severe disease, 49 to 90 years. However, this was not a consistent finding, and notable exceptions to this were seen at the extremes of disease severity. Four affected patients 65 years or older
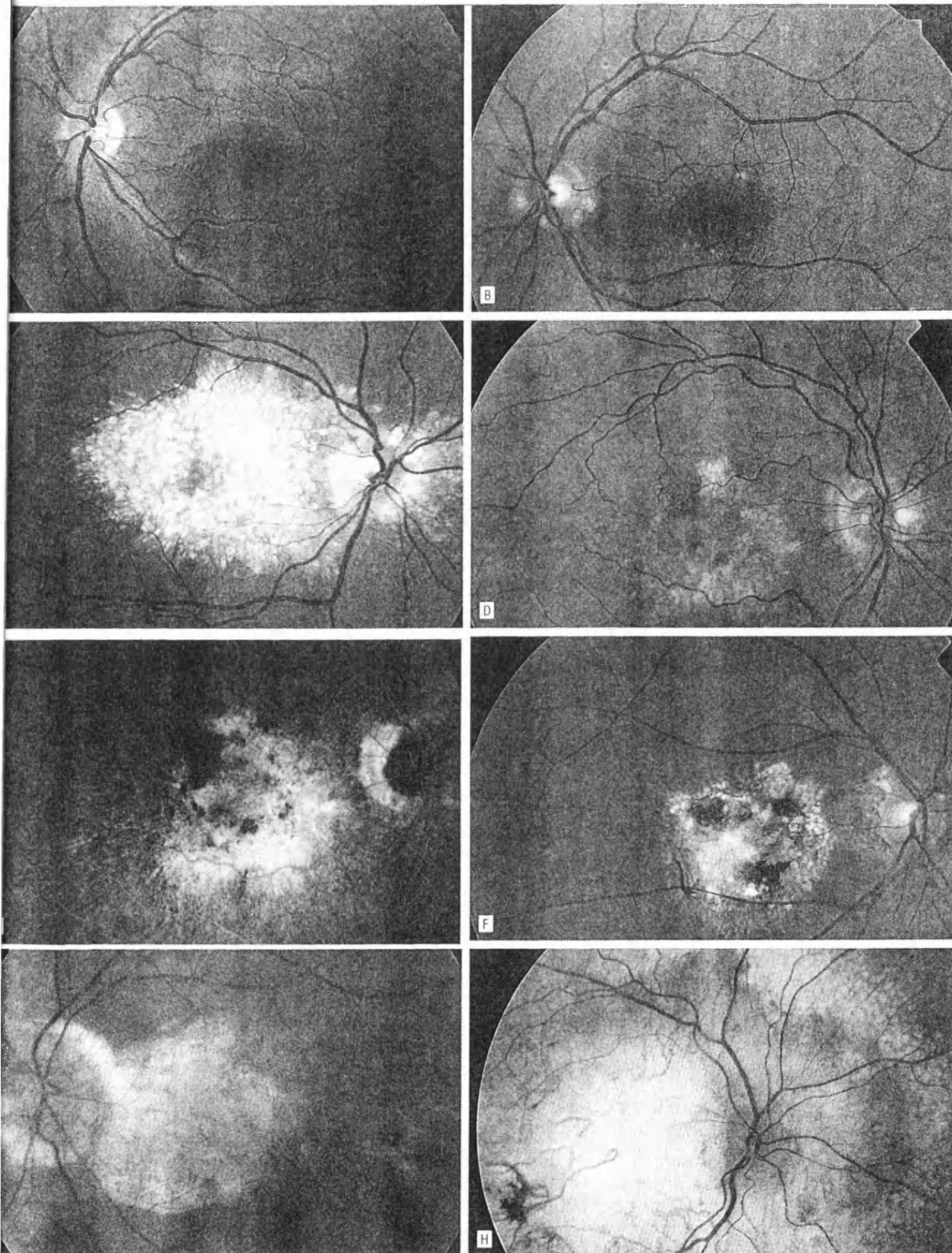
Figure 3. Color fundus photographs and fluorescein angiographic images of affected patients demonstrating the phenotypic range seen in Doyne honeycomb retinal dystrophy. A, Patient VIII-46; B, patient VIII-10; C, patient VIII-22; D and E, patient VII-50; F, patient VII-5; G, patient VI-4; and H, patient VII-52. For patient numbers, see Figure 1.

ll retained visual acuities of 20/60 or better. In addition, contrary to the adult-onset loss of vision reported all other affected family members, patients VII-52 and VII-53 recounted severe visual loss since early childhood. Clinical examination at just 49 and 55 years of age, respectively, revealed extensive posterior pole chorio-

retinal atrophy encircled by a ring of soft drusen in both cases. This clinical appearance was the most severe that was encountered (Figure 3, H). Both patients carried the DHRD-associated disease haplotype. Neither was homozygous across the chromosome 2p16-linked region, so neither had a "double dose" of the DHRD mutation. It was considered that perhaps both carried a second genetic mutation for another childhood-onset macular dystrophy. This seems unlikely, however, since such a disease was not identified from the clinical histories of either of their parents (a nonconsanguineous union). Their mother was available for examination and reported normal vision up to 3 years previously, when she had experienced a left central retinal vein occlusion. No maculopathy that might explain her sons' childhood-onset blindness could be identified on her clinical examination.

<div style="text-align:center">**COMMENT**</div>

Features previously described in DHRD were confirmed in this study. All investigative modalities suggested that the disease is localized to the macular region only and that it is fully penetrant, although there is variation in severity. Fundus abnormalities were identified in all disease haplotype carriers older than 22 years. With the advantage of allocating disease status on the basis of genetic haplotype, new clinical features have come to light.

The mildest fundus feature evident in affected patients (in the third decade of life) was the appearance of fine, hard drusen at the macula. Large soft drusen, especially around the optic disc, previously thought to be the earliest fundus features, were not identified until the fourth decade of life. Most striking, the severest maculopathy was reported as having its onset in childhood with little subsequent progression, suggesting that DHRD can cause childhood-onset visual loss.

It has previously been suggested that severe visual acuity loss in DHRD relates to 1 of 2 final outcomes—submacular neovascularization (as suggested in this study by the observation of hypertrophic macular tissue) or posterior pole atrophy.[9] Both outcomes were observed in this study. The most severe manifestation of disease in elderly patients was seen as peripapillary and macular atrophy. Most of these severe cases were without associated signs of drusen deposits, which we assume had resolved with the onset of outer retinal atrophy—a phenomenon well recorded in age-related macular degeneration.[25,26] Doyne honeycomb retinal dystrophy should therefore be considered in the differential diagnosis of atrophy of the posterior pole in elderly patients, even when there is no evidence of drusen deposits.

Previous reports have stated that small, hard drusen centered on the macula and radiating into the peripheral retina are not a feature of DHRD.[1] Eleven patients in the present study had fundic deposits with clinical and angiographic features that fulfilled the criteria for this phenomenon, which has also been termed *basal laminar drusen*.[27] All of these patients had the DHRD-associated disease haplotype. Although this was not a prominent feature of the retinopathy seen in DHRD, the present study establishes that this is one feature of the phenotype. Radial drusen were observed mainly in moderate disease and were associated with minimal loss of visual acuity even in older family members. It was interesting to observe that in the most elderly individuals with retention of good macular function, no large soft drusen were seen at the macula but rather small hard drusen and radial drusen (basal laminar drusen) were seen. This agrees with the conclusions of Gass et al,[27] who found that persons with small hard radial drusen deposits often have a relatively good prognosis in the absence of confluent deposits at the fovea. The appearance of small hard drusen only may still be consistent with a good long-term prognosis, supporting the conclusion that the DHRD-mutation does not invariably lead to severe visual loss even in advanced age.

Similar radial drusen have been said to be a consistent ophthalmoscopic finding and a prominent feature of malattia leventinese, another dominant drusen phenotype known to map within a genomic region overlapping that ascribed to DHRD. This statement was made on the basis of reappraisal of published fundus images of affected individuals.[1] Although this feature was not highlighted in original descriptions of affected individuals from the Leventine Valley in Switzerland,[28,29] it was clearly illustrated, and one author did comment on streaks of abnormal pigmentation radiating into the peripheral retina.[30] The present study and previous reports on the malattia leventinese phenotype now suggest that the only feature differentiating between these 2 eponymous diagnoses are the constancy and quantity of radial drusen seen. In DHRD, they are an infrequent finding and, even when present, are only a minor feature. In malattia leventinese, they are said to be an invariable and abundant feature.

One striking feature in the family presented here is the variability of severity in the phenotype and the presence of deposits that appear different one from another. This degree of variability is seen in many dominantly inherited disorders, and is generally ascribed to the modifying effects of other genetic attributes. From studies of age-related macular degeneration there is good evidence of a genetic influence on metabolic function of the retina.[31-34] The high prevalence of macular disease in the elderly implies that genetic abnormalities in the genes involved are common in Western communities.[35-37] Different genetic backgrounds in individual patients may therefore modify the effects of the mutation of interest. This may explain the presence of radial drusen in some subjects but not in others, and most severe disease occurring in siblings. Environmental factors may also play a role in modifying the DHRD phenotype, as has been postulated in age-related macular degeneration.[38-40] Although there may be little variation in extraneous risk factors within the United Kingdom,[31] observed differences in the phenotype between communities might be explained on this basis. Thus, any differences between malattia leventinese and DHRD may reflect different genetic backgrounds and/or environmental influences between southern England and the Leventine Valley.

REFERENCES

iguet B, Haimovici R, Bird AC. Dominantly inherited drusen represent more than
ne disorder: a historical review. *Eye*. 1995;9:34-41.

oyne RW. Peculiar condition of choroiditis occurring in several members of
e same family. *Trans Ophthalmol Soc U K*. 1899;19:71.

oyne RW. A note on family choroiditis. *Trans Ophthalmol Soc U K*. 1910;30:
3-95.

reacher-Collins T. A pathological report on a case of Doyne's choroiditis ('hon-
ycomb' or 'family choroiditis'). *Ophthalmoscope*. 1913;11:537-538.

ould GT. Family choroiditis. *Trans Ophthalmol Soc U K*. 1910;30:189-190.

ree M. Familial hyaline dystrophy in the fundus oculi or Doyne's family honey-
comb choroiditis. *Br J Ophthalmol*. 1937;21:65-91.

lper MG, Alfano JA. Honeycomb colloid degeneration of the retina. *Arch Oph-
thalmol*. 1953;49:392-399.

ranceceschetti A, François J, Babel J. *Les Hérédo-dégénérescence chorio-
rétiennes*. Paris, France: Mason; 1963;1:494-515.

Pearce WG. Doyne's honeycomb retinal degeneration: clinical and genetic fea-
tures. *Br J Ophthalmol*. 1968;52:73-78.

Gregory CY, Evans K, Wijesuriya S, et al. The gene responsible for autosomal
dominant Doyne's honeycomb retinal dystrophy (DHRD) maps to chromosome
2p16. *Hum Mol Genet*. 1996;5:1055-1059.

Héon E, Piguet B, Munier F, et al. Linkage of autosomal dominant radial drusen
(malattia leventinese) to chromosome 2p16-21. *Arch Ophthalmol*. 1996;114:
193-198.

Jay M, Plant C, Evans K, Gregory CY. Doyne's revisited. *Eye*. 1996;10:469-472.

Arden GB, Carter RM, Hogg CR, et al. A modified ERG technique and the results
obtained in X-linked retinitis pigmentosa. *Br J Ophthalmol*. 1981;67:419-430.

International Standardization Committee. Standard for clinical electroretinogra-
phy. *Arch Ophthalmol*. 1989;107:816-819.

Arden GB, Barrada A, Kelsey JH. New clinical test of retinal function based upon
the standing potential of the eye. *Br J Ophthalmol*. 1962;46:449-467.

Arden GB, Gunduz K, Perry S. Colour vision testing with a computer graphics
system. *Clin Vis Sci*. 1988;2:303-320.

Yu TC, Falcao-Reis F, Spileers W, Arden GB. A new screening test for preglau-
comatous visual loss. *Invest Ophthalmol Vis Sci*. 1991;32:2779-2789.

Massof RW, Finklestein D. Rod sensitivity relative to cone sensitivity in retinitis
pigmentosa. *Invest Ophthalmol Vis Sci*. 1979;18:263-272.

19. Jacobson SG, Voigt W, Parel J, et al. Automated light- and dark-adapted perim-
etry for evaluating retinitis pigmentosa. *Ophthalmology*. 1986;93:1604-1611.

20. Chen JC, Fitzke FW, Pauleikhoff D, Bird AC. Functional loss in age-related Bruch's
membrane change with choroidal perfusion defect. *Invest Ophthalmol Vis Sci*.
1992;33:334-340.

21. Ernst W, Faulkner DJ, Hogg CR, Powell DJ, Arden GB. An automated static pe-
rimeter/adaptometer using light emitting diodes. *Br J Ophthalmol*. 1983;67:431-
442.

22. Steinmetz RL, Polkinghorne PC, Fitzke FW, Kemp CM, Bird AC. Abnormal dark
adaptation and rhodopsin kinetics in Sorsby's fundus dystrophy. *Invest Oph-
thalmol Vis Sci*. 1992;33:1633-1636.

23. Moore AT, Fitzke FW, Kemp CM, et al. Abnormal dark adaption kinetics in auto-
somal dominant sector retinitis pigmentosa due to rod opsin mutation. *Br J Oph-
thalmol*. 1992;76:465-469.

24. von Rückmann A, Fitzke FW, Bird AC. Imaging and quantifying fundus autofluo-
rescence in normal subjects, macular dystrophy and age-related macular de-
generation with a scanning laser ophthalmoscope. *Br J Ophthalmol*. 1995;79:
407-412.

25. Bressler NM, Munoz B, Maguire MG, et al. Five-year incidence and disappear-
ance of drusen and retinal pigment epithelium abnormalities: Waterman Study.
Arch Ophthalmol. 1995;113:301-308.

26. Schatz H, MacDonald HR. Atrophic macular degeneration: rate of spread of geo-
graphic atrophy and visual loss. *Ophthalmology*. 1989;96:1541-1551.

27. Gass JDM, Jallow S, Davis B. Adult vitelliform macular detachment occurring in
patients with basal laminar drusen. *Am J Ophthalmol*. 1985;99:445-459.

28. Klainguti R. Die tapeto-retinal degeneration im katon Tessin. *Klin Monatsbl Au-
genheilkd*. 1932;89:253-254.

29. Forni S, Babel J. Etude clinique et histologique de la Malattia Leventinese: affec-
tion appartenant au groupe des dégénérescences hyalines du pole posterieur.
Ophthalmologica. 1962;143:313-322.

30. Wagner H, Klainguti R. Heredodegeneration der Papillen und Maculagegend, beo-
bachtet im Katon Tessin (Malattia levantinese): (Ges der Äerzte in Zurich, 21-
01-1943.) *Schweiz Med Wochenschr*. 1994;74:197.

31. Piguet B, Wells JA, Palmvang IB, Wormald R, Chisholm IH, Bird AC. Age-related
Bruch's membrane change: a clinical study of the relative role of heredity and
environment. *Br J Ophthalmol*. 1993;77:400-403.

32. Heiba IM, Elston RC, Klein BEK, Klein R. Sibling correlations and segration analy-
sis of age-related maculopathy: the Beaver Dam Eye Study. *Genet Epidemiol*. 1994;
11:51-67.

33. Silvestri TG, Johnson PB, Hughes AE. Is genetic predisposition an important risk
factor in age-related macular disease? *Eye*. 1994;8:564-568.

34. Klein ML, Mauldin WM, Stoumbos VD. Heredity and age-related macular degen-
eration: observations in monozygotic twins. *Arch Ophthalmol*. 1994;112:932-
937.

35. Klein R, Klein BEK, Linton KLP. Prevalence of age-related maculopathy: the Bea-
ver Dam Eye Study. *Ophthalmology*. 1992;99:933-943.

36. Mitchell P, Smith W, Attebo K, Wang JJ. Prevalence of age-related maculopathy
in Australia: the Blue Mountains Eye Study. *Ophthalmology*. 1995;102:1450-
1460.

37. Vingerling JR, Dielemans I, Hofman A, et al. The prevalence of age-related macu-
lopathy in the Rotterdam Study. *Ophthalmology*. 1995;102:205-210.

38. Tsang NC, Penfold PL, Snitch PJ, Billson F. Serum levels of antioxidants and age-
related macular degeneration. *Doc Ophthalmol*. 1992;81:387-400.

39. Seddon JM, Ajani UA, Sperduto RD, et al. Dietary carotenoids, vitamins A, C,
and E, and advanced age-related macular degeneration. *JAMA*. 1994;272:1413-
1420.

40. Mares-Perlman JA, Brady WE, Klein R, et al. Serum antioxidants and age-
related macular degeneration in a population-based case-control study. *Arch Oph-
thalmol*. 1995;113:1518-1523.

ORIGINAL INVESTIGATION

Ina Kermani · Kevin Gregory-Evans
Emma E. Tarttelin · James Bellingham
Catherine Plant · Alan C. Bird · Margaret Fox
Shomi S. Bhattacharya · Cheryl Y. Gregory-Evans

Refined genetic and physical positioning of the gene for Doyne honeycomb retinal dystrophy (DHRD)

Abstract Doyne honeycomb retinal dystrophy (DHRD) is a late-onset autosomal dominant disorder that causes degeneration of the retina and can lead to blindness. We have previously assigned *DHRD* to a 5-cM region of chromosome 2p16 between marker loci *D2S2739* and *D2S378*. Using sequence-tagged sites (STSs), expressed sequence tags (ESTs) and polymorphic markers within the *DHRD* region, we have identified 18 yeast artificial chromosomes (YACs) encompassing the *DHRD* locus, spanning approximately 3 Mb. The YAC contig was constructed by STS content mapping of these YACs and incorporates 13 STSs, including four genes and six polymorphic marker loci. We also report the genetic mapping of two families with a dominant drusen phenotype to the *DHRD* locus, and genetic refinement of the disease locus to a critical interval flanked by microsatellite marker loci *D2S2352* and *D2S2251*, a distance of approximately 700 kb. These studies exclude a number of candidate genes and provide a resource for construction of a transcriptional map of the region, as a prerequisite to identification of the *DHRD* disease-causing gene and genes for other diseases mapping in the region, such as Malattia leventinese and Carney complex.

I. Kermani · S. S. Bhattacharya
Department of Molecular Genetics, Institute of Ophthalmology,
London EC1V 9EL, UK

K. Gregory-Evans
Academic Unit of Ophthalmology, The Western Eye Hospital,
London NW1 5YE, UK

E. E. Tarttelin · J. Bellingham · C. Y. Gregory-Evans (✉)
Department of Molecular Genetics, Division of Biomedical Science,
Imperial College School of Medicine, Sir Alexander Fleming
Building, South Kensington, London SW7 2AZ, UK
e-mail: c.gregory-evans@ic.ac.uk, Tel: +44-171-594-3007,
Fax: +44-171-594-3100

C. Plant · A. C. Bird
Moorfields Eye Hospital, London, EC1V 2PD, UK

M. Fox
MRC Human Biochemical Genetics Unit, University College
London, NW1 2HE, UK

Introduction

Macular dystrophies are a heterogeneous group of disorders ranging from childhood to late-onset phenotypes and to date 12 loci have been mapped (Small et al. 1992; Stone et al. 1992; Kaplan et al. 1993; Wells et al. 1993; Kremer et al. 1994; Stone et al. 1994; Weber et al. 1994a; Zhang et al. 1994; Kelsell et al. 1995; Gregory et al. 1996; Héon et al. 1996; Lotery et al. 1996), although only four of the disease-causing genes have been identified (*RDS*/peripherin, Wells et al. 1993; *TIMP3*, Weber et al. 1994b; *ABCR*, Allikmets et al. 1997a; *VMD2*, Petrukhin et al. 1998). Macular dystrophies are characterised by loss of central vision associated with morphological changes at the macula region of the retina and underlying retinal pigment epithelium (RPE), and can include soft drusen, abnormal pigmentation, geographic atrophy and subretinal neovascularisation with sub-retinal scarring. Autosomal dominant Doyne honeycomb retinal dystrophy (DHRD) is an example of this class of diseases and was recently mapped to chromosome 2p16 by our group (Gregory et al. 1996).

There are striking clinical similarities of DHRD to the more common condition age-related macular degeneration (ARMD), which accounts for 50% of registrable blindness in the developed world (Evans and Wormald 1996). ARMD is a complex genetic trait that could be influenced by a number of different genes and environmental factors (Evans and Bird 1996). One gene that was shown to be mutated in Stargardt macular dystrophy and then subsequently implicated in ARMD is the *ABCR* gene, which accounts for 16% of cases of ARMD in North America (Allikmets et al. 1997b). Thus, elucidation of the disease-causing gene for other macular dystrophies such as DHRD may provide more clues to the molecular aetiology of ARMD.

In the original linkage study (Gregory et al. 1996) we mapped *DHRD* to a 5-cM region flanked by *D2S2316* and *D2S378*, which overlapped with another macular dystrophy locus, Malattia leventinese (*D2S1761-D2S444*, Héon et al. 1996) as well as Carney complex (*CA2-D2S378*, Vottero et al. 1996), a multiple neoplasia syndrome. We have used

microsatellite markers, sequence-tagged sites (STSs) and expressed sequence tags (ESTs) to screen the ICRF yeast artificial chromosome (YAC) library (Larin et al. 1991) and the ICI YAC library (Anand et al. 1990) in order to construct a YAC contig spanning the *DHRD* region. Furthermore, we have taken advantage of STS-positive YAC clones available from the Whitehead Institute's Human Genome Mapping Project (Whitehead Institute 1996) in construction of the contig. In addition we have now genotyped new branches of the original DHRD family and have mapped to the region two other dominant drusen families. This has allowed us to search for further recombination events to narrow the disease interval.

Materials and methods

Screening of YAC libraries

YAC clones were identified by screening hierarchical pools of genomic YAC libraries from ICI or ICRF with five microsatellite markers (*D2S2379, D2S2352. D2S2251. D2S2153* and *D2S378*), two STSs (*D2S1285* and *D2S2663*) and three ESTs (*D2S1981E, D19S1848E* and *SPTBN1*), using polymerase chain reaction (PCR) amplification of YAC DNA embedded in agarose plugs. Additional YACs positive for these markers, STSs or ESTs were identified from the Whitehead database (1996) and obtained from the Human Genome Mapping Project (HGMP) Resource Centre. Cambridge, UK. To size the YAC inserts, the YAC DNA was separated from yeast chromosomes by pulse-field gel electrophoresis (PFGE) through a 1% agarose gel in 0.5% TBE using a CHEF DRII apparatus (Biorad, Hercules, Calif.,USA) under the following conditions: 175 V for 20 h with a linear ramp from 60 s to 90 s. YAC sizes were determined by comparison with yeast chromosome size standards by Southern blot hybridisation using ^{32}P-labelled Cot-1 DNA as the probe. For STS content mapping YAC colonies were inoculated into 100 ml of YEPD medium and grown for 24 h at 30°C. Yeast cells were pelleted in SEM buffer (0.9 M sorbitol, 20 mM EDTA, 14 mM 2-mercaptoethanol) and treated with 10 mg/ml zymolase for 1 h at 37°C. Cells were resuspended in lysis solution (4.5 M guanidinium HCl, pH 8.0, 0.1 M EDTA, 0.15 M NaCl, 0.05% Sarkosyl) for 10 min at 65°C and then extracted with ethanol. The DNA was treated with RNase A (100 µg/ml) for 30 min at 37°C followed by proteinase K (200 µg/ml) for 60 min at 65°C, before phenol-chloroform extraction and ethanol precipitation. For preparation of high molecular weight intact yeast chromosomes (YAC plugs), the yeast cells were embedded in 1% low melting point agarose before spheroplasting, lysis and deproteination (Chandrasekharappa et al. 1992).

Characterisation of YAC insert termini

STSs were developed from YAC insert terminal sequences by isolation of pYAC4-*Alu* PCR products (Tagle and Collins 1992). For amplification of DNA between pYAC4 vector arms and nearby *Alu* sequences a combination of vector arm and *Alu* primers was used: left arm primer (5′-CACCCGTTCTCGGAGCACTGTCCGACCGC-3′); right arm primer (5′-ATATAGGCGCCAGCAACCGCACCTGTGGC-3′); Ale 1 primer (5′-GCCTCCCAAAGTGCTGGGATTACAG-3′); Ale 3 primer (5′-CCAT/CTGCACTCCAGCCTGGG-3′). Unique PCR products were purified through S-400 HR MicroSpin columns (Pharmacia Biotech) and then sequenced by fluorescent dye termination sequencing on an ABI373A DNA Sequencer using internal vector arm primers (left arm, 5′-GTTGGTTTAAGGCGCAAG-3′; right arm, 5′-GTCGAACGCCCGATCTCAAG-3′). Sequences obtained from *Alu*-vector PCR were analysed for homology to known DNA sequences in Genbank using the BLAST/BLASTN programs (Altschul et al. 1990) before STSs were designed. The chromosomal origins of

these STSs were tested in the Genebridge4 radiation hybrid mapping panel (Gyapay et al. 1996). The STSs were then tested in individual YAC clones to identify the STS content and overlapping YACs.
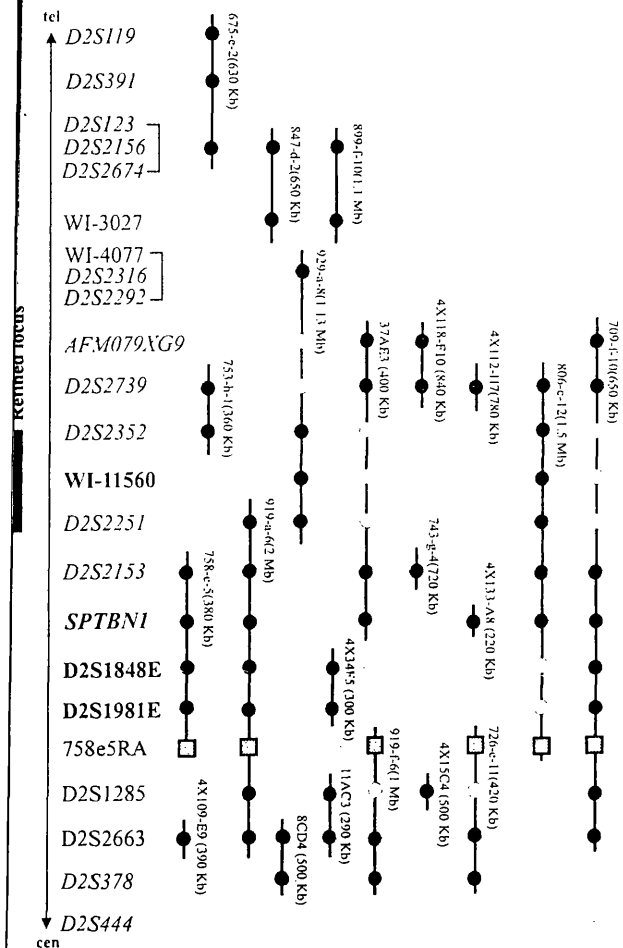
Genetic refinement

The clinical features of DHRD have been previously described (Pearce 1968; Evans et al. 1997). We were able to ascertain new branches of the original Doyne family. which have been clinically examined (by K. Gregory-Evans) and now genetically examined. In addition two small families (family A-RP4180 and family B-RP3890) diagnosed as having a dominant drusen phenotype were investigated. Informed consent for the clinical and genetic assessment was obtained prior to the study. For the purpose of linkage analysis, subjects were classified as affected if they had soft drusen at the macula or around the optic nerve head before the age of 45 years. Unaffected status was assigned if they had a normal ophthalmological examination over the age of 45 years. In family A, the three individuals in generation IV were all under 45 years of age. They were not included in the linkage calculations initially, but were included in the haplotype analysis. In family B, only family members over the age of 45 years were included in this study. Genomic DNA (100 ng) from patients was genotyped using microsatellites from the region (*D2S2739, D2S2352, D2S2251, D2S2153, D2S378, D2S370*) by PCR amplification (35 cycles of 94°C for 30 s, 55°C for 30 s and 72°C for 30 s) with end-labelling of the forward primer of each microsatellite marker with [γ-^{32}P]ATP (Amersham, Little Chalfont, UK). The PCR products were fractionated on 6% polyacrylamide denaturing gels and visualised by autoradiography. Data were prepared for linkage analysis using the LINKSYS (version 3.1) data management package (Attwood and Bryant 1988). Two-point linkage analysis was performed with the MLINK program (version 5.10) of the LINKAGE package (Lathrop et al. 1984). Allele frequencies were calculated from spouses in the families.
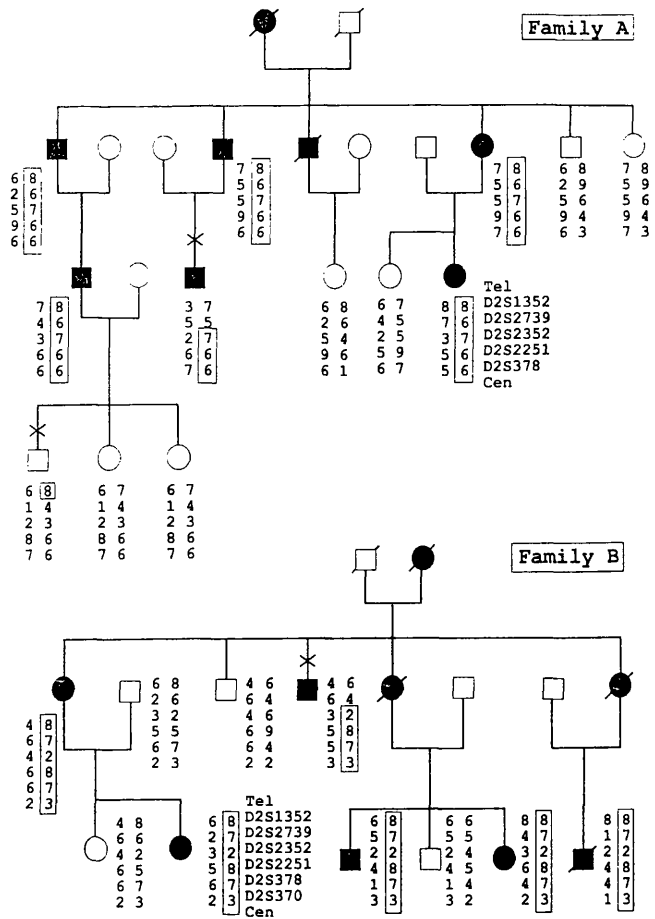
Results

Physical mapping of the *DHRD* locus

When this work was initiated, the *DHRD* critical region extended between *D2S2739* and *D2S378* (Evans et al. 1997). CEPH YACs containing microsatellite markers and STSs within this region were selected from the Whitehead WC2.4 contig as a starting point for analysis of the *DHRD* physical map. We found inconsistencies in the STS content of a number of these YACs and some chimaerism consistent with previous findings for the YAC library (Todd et al. 1995), thus we screened two other YAC libraries (ICRF and ICI) with markers and STSs in the region and isolated nine new YACs (Fig. 1). Two of these YACs (8CD4, 500 kb, and 37AE3, 400 kb) in addition to two CEPH YACs (758-e-5, 380 kb, and 929-a-8, 1.13 Mb) were hybridised to metaphase spreads of normal human chromosomes and none were found to be chimaeric (data not shown). The size and integrity of the YACs was determined by PFGE followed by Southern hybridisation using Cot-1 DNA as the hybridisation probe. The insert terminal sequence for YAC 758-e-5 was determined by *Alu*-vector PCR. The 73-bp YAC end fragment (758e5RA) was PCR amplified in a mouse/human monochromosomal hybrid panel (from HGMP) and was found to be present only in the chromosome 2 hybrid panel (forward primer 5′-ACACAGTACA-AAAACATAGAGTAA-3′ and reverse primer 5′-TTTCT-

Fig. 2 Haplotype analysis of 2p16 markers in two dominant drusen families. *Filled symbols* represent affected individuals, *open symbols* represent unaffected individuals. A *cross* indicates a recombinant individual. The disease haplotypes are *boxed*. The order of the markers tested in each family is denoted

1 Schematic diagram of a yeast artificial chromosome (YAC) tig encompassing the Doyne honeycomb retinal dystrophy *HRD*) region and adjacent markers. The *vertical line with bidirecal arrows* represents the chromosome, with the *DHRD* locus internext to it (published and refined in this study) denoted by *thick ck lines*. Sequence-tagged sites (STSs) are listed in order as detered by YAC content. The *bold vertical lines* represent YACs, with s denoted in *parentheses* next to the YAC identification number. Cs 675-e-2, 847-d-2, 899-f-10, 753-h-1, 758-e-5, 929-a-8, 919-ar43-g-4, 919-f-6, 726-e-11, 806-c-12 and 709-f-10 are from the PH library; YACS 37AE3, 8CD4 and 11AC3 are from the ICI liry; YACs 4X118-F10, 4X112-H7, 4X15-C4, 4X34-F5 and 4X133- are from the ICRF library. A *solid circle* indicates a verified STS sence in a YAC, an *open circle* denotes an internal deletion, and a *ded square* depicts the presence of a terminal sequence STS. The is that are also genes are shown in *bold* and those that are also ymorphic markers are in *italics*

ATAGTTGGCAAGACCA-3′). This was confirmed in Genebridge RH mapping panel. This STS was found to present in five other YACs (see Fig. 1) and when comed with sequences deposited in EMBL/Genbank, failed eveal significant homology to any previously described uence. The YAC contig was assembled from a total of YACs by an STS content mapping strategy. Most clones re shown to contain more than one STS and several nes did not contain the expected STS. YACs 709-f-10 37AE3 did not contain *D2S2352*, *WI-11560* and *S2251*. Also, YAC 929-a-8 did not contain *AFM079XG9*

and *D2S2739*. One interpretation of these data is that if *AFM079XG9* and *D2S2739* were placed below *D2S2251*, this would effectively remove the deletions in the three YACs. However, the meiotic mapping data in this paper and in previous publications (Gregory et al. 1996; Evans et al. 1997) show that *AFM079XG9* and *D2S2739* are recombinant and thus cannot be below *D2S2251* or *D2S2352* and *D2S2153* because all three markers are non-recombinant and fully informative in the three families tested. Thus, the deletions we have observed are most likely correct.

We also determined the STS content of three YACs telomeric to the *DHRD* locus, which would encompass the Malattia leventinese locus (below *D2S119-D2S444*). We found a gap between *WI-3027* and *WI-4077/D2S2316/D2S2292*, which we tried to close by screening the ICI and ICRF YAC libraries for new YACs. However, we were unable to identify any YACs in this gap, which lies outside the *DHRD* critical region. The minimum tiling path across the *DHRD* region is approximately 3 Mb based on the published flanking marker loci. However, genetic refinement described in this paper (see below) has localised the *DHRD* gene to between marker loci *D2S2352* and *D2S2251*, a ge-

Table 1 Two-point LOD scores between the *DHRD* locus and 2p16 markers

Marker	Lod score at recombination fraction					
	0	0.05	0.1	0.2	0.3	0.4
Family A						
D2S2379	–inf	–1.14	–0.63	–0.2	–0.03	0.03
D2S2352	2.58	2.37	2.14	1.62	1.02	0.4
D2S2251	1.24	1.14	1.12	1.01	0.74	0.35
D2S378	1.03	0.93	0.83	0.39	0.22	0.07
Family B						
D2S2379	–inf	1.42	1.2	0.98	0.66	0.48
D2S2352	2.11	1.88	1.65	1.15	0.61	0.16
D2S378	1.21	0.98	0.91	0.86	0.59	0.26
D2S370	0.87	0.78	0.7	0.52	0.35	0.17

netic distance of about 1 cM (Dib et al. 1996) and it is estimated to be about 700 kb. We have been able to resolve the order of three polymorphic markers (*D2S2352*, *D2S2251* and *D2S2153*) based on YAC STS content and meiotic mapping to be Tel-*D2S2739-D2S2352-D2S2251-D2S2153-D2S378*-Cen. We were not able to resolve the order of *D2S123/D2S2156/D2S2674* as these markers must be present in the overlap of YACs 675-e-2, 847-d-2 and 899-f-10, nor the order of *WI-4077/D2S2316/D2S2292* as they were all present on YAC 929-a-8, but not in any other YAC (Fig. 1). In addition we have placed an STS designed to match the β-fodrin gene (*SPTBN1*) in the contig between *D2S2153* and *D2S1848E*, an EST (*WI-11560*) between *D2S2352* and *D2S2251* and an STS (*WI-3027*) centromeric to *D2S123/D2S2156/D2S2674*. Another STS (*WI-4077*) was present only in YAC 929-a-8, placing it telomeric to *AFM079XG9* (Fig. 1).

Genetic refinement of *DHRD*

Two dominant drusen pedigrees of British descent analysed in this study are shown in Fig. 2. Both families exhibited characteristic features of drusen deposits. Loci implicated in previous studies on either autosomal dominant macular dystrophy or cone dystrophy, namely *STGD1*, *RDS*, *GUCA1A*, *STGD3*, *NCMD/PBCRA*, *CYMD*, *VMD2*, *STGD2*, *RCD2*, *CACD*, *RETGC1*, *CORD6*, *CORD7*, *CORD2* and *SFD* (RetNet 1997) were excluded in the families (data not shown). Linkage to chromosome 2p16 in these families was established by genotyping six marker loci previously linked to *DHRD*. In family A (Fig. 2), marker *D2S2352* gave a maximum LOD score of 2.58 without recombination (see Table 1). In family B (Fig. 2), marker *D2S2352* gave a maximum LOD score of 2.11 without recombination (see Table 1).

A LOD score of 2 is accepted as sufficient (although not significant) evidence for linkage of a disease to a previously known locus of similar phenotype (Terwilliger and Ott 1994) and is referred to as 'posterior probability' (Mueller and Young 1998). In addition, linkage to 2p16 is also sup-

ported by exclusion of other disease loci by linkage analysis in these families. The haplotypes that define the chromosomal interval containing the disease-causing gene are indicated in Fig. 2. In family A affected individual III-3 and unaffected individual IV-1 are recombinant for *D2S1352*. However, since unaffected individual IV-1 was under the age of 45 years, his phenotypic status could not be guaranteed. However, individual III-3 is also recombinant for *D2S2739*, placing the disease locus centromeric to *D2S2739*, confirming our previous telomeric flanking marker (Evans et al. 1997). In family B affected individual II-4 is recombinant for *D2S1352* as well as the more centromeric marker *D2S2739*, placing the dominant drusen gene centromeric to *D2S2739*, again confirming the published flanking marker. Thus, neither of these two families were able to refine the *DHRD* locus. However, importantly, the haplotypes in these two families differ from each other and from the original *DHRD* haplotype, indicating that three independent mutational events have occurred (Table 2).

The genetic and clinical analysis of new members of the original DHRD pedigree has highlighted two new recombination events (Table 2). Affected individual I is recombinant for *D2S1352*, *D2S2379* and *D2S2352*, placing the disease centromeric to *D2S2352*. Affected individual II is recombinant for *D2S2251*, *D2S378* and *D2S370*, placing the disease telomeric to *D2S2251*. Thus, the disease gene now resides in a genetic interval of about 1 cM (Dib et al. 1996) between *D2S2352* and *D2S2251*. These meiotic breakpoints have also resolved the order of *D2S2352* and *D2S2251* with respect to each other (tel-*D2S2352-D2S2251*-cen), which is also confirmed by the STS content of YACs 753-h-1 and 919-a-6 (Fig. 1).

Discussion

The identification of a mutant gene involved in a specific human disease, for which no obvious candidate genes are known, usually involves establishing a physical map of the chromosomal region previously linked to the disease. We

ble 2 Disease haplotypes of different families with dominant drusen mapping to 2p16. The alleles in bold type of affected recombinant in-
viduals I and II denote haplotype in common with the main DHRD family disease haplotype. Thus the disease locus lies between *D2S2352*
d *D2S2251*. Families A and B show disease haplotypes that are different from each other and from the original DHRD disease haplotype

mily or individual	Marker loci and *DHRD* locus haplotypes					
	Tel					Cen
	D2S1352	*D2S2379*	*D2S2352*	*D2S2251*	*D2S378*	*D2S370*
mily A	8	6	7	6	6	2
mily B	8	7	2	8	7	3
HRD family	6	7	4	9	2	5
ffected I	6	4	2	9	2	5
ffected II	6	7	4	8	1	5

ve applied this strategy to the 2p16 region containing the HRD gene. We have assembled a YAC contig that extends om *AFM079XG9* to *D2S378*, encompassing the *DHRD* cus. This physical map comprises 18 YACs from three fferent sources, ordered according to STS content, incor- rating 13 STSs, of which 4 are genes and 6 are polymor- ic markers spanning a distance of approximately 3 Mb. ine of these YACs have not been previously reported, thus e ICI and ICRF libraries are a useful, alternative resource r detailed analysis of this region of chromosome 2p as in her areas of the genome (Thiselton et al. 1996). We have sted a number of large YACs for chimaerism and found em to be non-chimaeric, and the remaining YACs were amined for physical overlap by comparison of inter-*Alu* CR fingerprints (data not shown). Additionally, the pres- ice of contiguous STSs in overlapping YACs makes chi- aerism in these YACs unlikely. Furthermore, we tried to tablish continuity of the contig by generating a number of AC end fragments by *Alu*-vector PCR. However, upon se- encing, only the end of one YAC (758-e-5) was found to useful as an STS owing to high GC content in a number other ends. We have been able to resolve the genetic or- r of three polymorphic marker loci by the STS content of ACs in the region of these markers to Tel-*D2S2352*- 2S2251-D2S2153-Cen. In addition we have localised four STs (*D2S1848E*, *D2S1981E*, *SPTNB1* and *WI-11560*) to e physical map.

DHRD is characterised by drusen deposits in the macu- and optic nerve head region causing progressive retinop- hy due to damage to the retina at the level of the RPE. The ne *SPTBN1* was considered as a candidate for DHRD be- use it has been shown to be expressed in the RPE underson et al. 1991); however STS content analysis of ACs places *SPTBN1* between *D2S2153* and *D2S1848E*, cluding this gene as a candidate for DHRD. *D2S1848E* d *D2S1981E* both originate from a pancreatic cDNA li- ary, were not found to be present in retinal mRNA by re- rse transcription (RT)-PCR, map outside the refined dis- se region and thus are not considered as candidates for disease gene. We mapped the EST *WI-11560* (Acces- on no. R08151) to the refined *DHRD* critical interval. is EST was originally identified from a fetal liver/spleen NA library and thus seems an unlikely candidate for a inal disease. However, ubiquitously expressed genes are

known to cause retinal diseases. such as the *TIMP3* gene in Sorsby's fundus dystrophy (Weber at al. 1994b) and the *RPGR* gene in X-linked retinitis pigmentosa (Meindl et al. 1996). Consequently. we are currently assessing *WI-11560* by Northern analysis and RT-PCR to determine whether it is expressed in the eye.

Many retinal diseases are clinically and genetically het- erogeneous, which reflects the limited repertoire of re- sponses of the eye to a variety of genetic lesions. In addition allelic heterogeneity, in which different mutations in the same disease gene can cause clinically distinct ocular phe- notypes, is an emerging concept in retinal dystrophies (Wells et al. 1993; Cremers et al. 1998). The dominant drusen phenotype (including a number of eponymous dis- eases) is thought to represent an unknown number of genet- ically distinct entities based on specific clinical differences. However, the genetic analysis of two dominant drusen fam- ilies in this study has established their linkage to the same chromosomal region as DHRD, which shows at least two phenotypes mapping to the same region. This implies that either different mutations in the same gene or microheterogeneity in the region due to the presence of an- other gene(s) causes a variation in phenotype. This will be- come evident once the disease gene is cloned for one of these phenotypes. Moreover, haplotype analysis from the two dominant drusen families and from the Doyne family eliminates the possibility of a founder effect, which has been observed in other retinal dystrophies such as Sorsby fundus dystrophy (Wijesuriya et al. 1996) and North Caro- lina macular dystrophy (Small et al. 1997). Furthermore, we have been able to refine the genetic region in which the gene must lie by analysis of additional members of the orig- inal Doyne pedigree. These data place the disease gene be- tween *D2S2352* and *D2S2251*.

In summary we present genetic refinement and a physi- cal map of the critical region for *DHRD*. This should facil- itate the identification of the defective gene causing DHRD at this locus, as well as providing candidates for other dis- eases mapping to the region such as dominant drusen and Carney complex.

References

Allikmets R, Singh N, Sun H, Shroyer NF, Hutchinson A, Chidambaram A. Gerrard B (1997a) A photoreceptor cell-specific ATP-binding transporter gene (ABCR) is mutated in recessive Stargardt macular dystrophy. Nat Genet 15:236–246

Allikmets R, Shroyer NF, Singh N, Seddon JM, Lewis RA, Bernstein PS, Peiffer A (1997b) Mutation of the Stargardt Disease gene (ABCR) in age-related macular degeneration. Science 277:1805–1807

Altschul SF, Gish W, Miller W, Myers EW, Lipman DJ (1990) Basic local alignment search tool. J Mol Biol 215:403–410

Anand R, Riley JH, Butler R, Smith JC, Markham AF (1990) A 3.5 genome equivalent multi access YAC library: construction, characterisation, screening and storage. Nucleic Acids Res 18:1951–1956

Attwood J, Bryant S (1988) A computer programme to make analysis with LIPED and LINKAGE easier to perform and less prone to input errors. Ann Hum Genet 52:259

Chandrasekharappa SC, Marchuk DA, Collins FS (1992) In: Burmeister M, Ulanovsky I (eds) Methods in molecular biology. Humana Press, Totowa, NJ, pp 235–257

Cremers FPM, Pol DJR van de, Driel M van, Hollander AI den, Haren FJJ van, Knoers NVAM, Tijmes N (1998) Autosomal recessive retinitis pigmentosa and cone-rod dystrophy caused by splice site mutations in the Stargardt's disease gene ABCR. Hum Mol Genet 7:355–362

Dib C, Faure S, Fizames C, Samson D, Drouot N, Vignal A, Millasseau P (1996) A comprehensive genetic map of the human genome based on 5,264 microsatellites. Nature 380:152–154

Evans J, Wormald R (1996) Is the incidence of registrable age-related macular degeneration increasing? Br J Ophthalmol 80:9–14

Evans K, Bird AC (1996) The genetics of complex ophthalmic disorders. Br J Ophthalmol 80:763–768

Evans K, Gregory CY, Wijesuriya SD, Kermani S, Jay MR, Plant C, Bird AC (1997) Assessment of the phenotypic range seen in Doyne honeycomb retinal dystrophy. Arch Ophthalmol 115:904–910

Gregory CY, Evans K, Wijesuriya SD, Kermani S, Jay MR, Plant C, Cox N (1996) The gene responsible for autosomal dominant Doyne's honeycomb retinal dystrophy (DHRD) maps to chromosome 2p16. Hum Mol Genet 5:1055–1059

Gundersen D, Orlowski J, Rodriguez-Boulan E (1991) Apial polarity of Na-K+-ATPase in retinal pigment epithelium is linked to a reversal of the ankyrin fodrin submembrane cytoskeleton. Invest Ophthalmol Vis Sci 29:814–817

Gyapay G, Schmitt K, Fizames C, Jones H, Vega-Czarny N, Spillett D, Muselet D (1996) A radiation hybrid map of the human genome. Hum Mol Genet 5:339–346

Héon E, Piguet B, Munier F, Sneed SR, Morgan CM, Forni S, Pescia G (1996) Linkage of autosomal dominant radial drusen (malattia leventinese) to chromosome 2p16–21. Arch Ophthalmol 114:193–198

Kaplan J, Gerber S, Larget-Piet D, Rozet JM, Dollfus H, Dufier JL, Odent S (1993) A gene for Stargardt's disease (fundus flavimaculatus) maps to the short arm of chromosome 1. Nat Genet 5:308–311

Kelsell RE, Godley BF, Evans K, Tiffen PAC, Gregory CY, Plant C, Moore AT (1995) Localisation of the gene for progressive bifocal chorioretinal atrophy (PBCRA) to chromosome 6q. Hum Mol Genet 4:1653–1656

Kremer H, Pinckers A, Helm B van den, Deutman AF, Ropers H-H, Mariman ECM (1994) Localisation of the gene for dominant cystoid macular dystrophy on chromosome 7p. Hum Mol Genet 3:299–302

Larin Z, Monaco AP, Lehrach H (1991) Yeast artificial chromosome libraries containing large inserts from mouse and human DNA. Proc Natl Acad Sci USA 88:4123–4127

Lathrop GM, Lalouel JM, Julier C, Ott J (1984) Strategies for multipoint linkage analysis in humans. Proc Natl Acad Sci USA 81:3443–3446

Lotery AJ, Hughes AE, Silvestri G, Ennis KT, Nicholl S, McGibbon D, Archer DB (1996) Localisation of a gene for central areolar choroidal dystrophy to chromosome 17p. Hum Mol Genet 5:705–708

Meindl A, Dry K, Herrmann K, Manson F, Ciccodicola A, Edgar A, Carvalho MRS (1996) A gene (RPGR) with homology to the RCC1 guanine nucleotide exchange factor is mutated in X-linked retinitis pigmentosa (RP3). Nat Genet 13:35–42

Mueller RF, Young ID (1998) Emery's elements of medical genetics, 10th edn. Churchill Livingstone, Edinburgh, pp 292–293

Pearce WG (1968) Doyne's honeycomb retinal degeneration: clinical and genetic features. Br J Ophthalmol 52:73–78

Petrukhin K, Koisti MJ, Bakall B, Li W, Xie G, Marknell T, Sandren O (1998) Identification of the gene responsible for Best macular dystrophy. Nat Genet 19:241–247

RetNet (1997) http://www.sph.uth.tmc.edu/Retnet/

Small KW, Weber JL, Roses A, Lennon F, Vance JM, Pericak-Vance MA (1992) North Carolina macular dystrophy is assigned to chromosome 6. Genomics 13:681–685

Small KW, Mullen L, Svetlana Y, Udar N, Klein R, Garcia C, Saperstein D (1997) North Carolina macular dystrophy (MCDR1) locus: a fine resolution genetic map and haplotype analysis. Am J Hum Genet 61:1722

Stone EM, Nichols BE, Streb LM, Kimura AE, Sheffield VC (1992) Genetic linkage of vitelliform macular degeneration (Best's disease) to chromosome 11q13. Nat Genet 1:246–250

Stone EM, Nichols BE, Kimura AE, Weingeist TA, Drack AV, Sheffield VC (1994) Clinical features of a Stargardt-like dominant progressive macular dystrophy with genetic linkage to chromosome 6q. Arch Ophthalmol 112:765–772

Tagle DA, Collins FS (1992) An optimized Alu-PCR primer pair for human-specific amplification of YACs and somatic cell hybrids. Hum Mol Genet 1:121–122

Terwilliger JD, Ott J (1994) Handbook of human genetic linkage, 1st edn. Johns Hopkins University Press, Baltimore

Thiselton DL, Hampson RM, Nayudu M, Maldergem L van, Wolf ML, Saha BK, Bhattacharya SS (1996) Mapping the RP2 locus for X-linked retinitis pigmentosa on proximal Xp: a genetically defined 5 cM critical region and exclusion of candidate genes by physical mapping. Genome Res 6:1093–1102

Todd S, Roche J, Hahner L, Bolin R, Drabbin HA, Gremmil RM (1995) YAC contigs covering an 8-megabase region of 3p deleted in the small cell lung cancer cell line U2020. Genomics 25:19–28

Vottero A, Lin J-P, Aksentijevich I, Kastner DL, Carney JA, Chrousos GP, Stratakis CA (1996) Carney complex segregates with markers from the chromosome 2p16 CNC locus in two new kindreds: placement of new markers and integration of genetic and physical mapping of the region. Am J Hum Genet 59:A240

Weber BHF, Vogt G, Wolz W, Ives EJ, Ewing CC (1994a) Sorsby's fundus dystrophy is genetically linked to chromosome 22q13–qter. Nat Genet 7:158–161

Weber BHF, Vogt G, Pruett RC, Stohr H, Felbor U (1994b) Mutations in the tissue inhibitor of metalloproteinases-3 (TIMP3) in patients with Sorsby's fundus dystrophy. Nat Genet 8:352–356

Wells J, Wroblewski J, Keen J, Inglehearn C, Jubb C, Eckstein C, Jay M (1993) Mutations in the human retinal degeneration slow (RDS) gene can cause either retinitis pigmentosa or macular dystrophy. Nat Genet 3:213–218

Whitehead Institute/MIT Center for Genome Research, Human Genetic Mapping Project, Data Release 10 (1996) http://www-genome.wi.mit.edu/

Wijesuriya SD, Evans K, Jay MR, Davison C, Weber BMF, Bird AC, Bhattacharya SS, et al. (1996) Sorsky's fundus dystrophy in the British Isles: demonstration of a striking founder effect by microsatellite-generated haplotypes. Genome Res 6:92–101

Zhang K, Bither PP, Park R, Donoso LA, Seidman JG, Seidman CE (1994) A dominant Stargardt's macular dystrophy locus maps to chromosome 13q34. Arch Ophthalmol 112:759–764